Superpave In-Situ Stress/Strain Investigation – Phase II

FINAL REPORT
Vol. III: Field Data Collection and Summary

May 2009

By Mansour Solaimanian, Shelley M. Stoffels, Hao Yin, Abraham Bae, and Suri Sadasivam

The Thomas D. Larson
Pennsylvania Transportation Institute

COMMONWEALTH OF PENNSYLVANIA
DEPARTMENT OF TRANSPORTATION

CONTRACT No. 999012
PROJECT No. HA2006-02

1. Report No. FHWA-PA-2009-009-999012 HA 2006-02	2. Government Accession No.	3. Recipient's Catalog No.	
4. Title and Subtitle SuperPave In-Situ Stress/Strain Investigation, Phase II Volume III: Field Data Collection and Summary		**5. Report Date** May 2009	
		6. Performing Organization Code	
7. Author(s) Mansour Solaimanian, Shelley M. Stoffels, Hao Yin, Abraham Bae and Suri Sadasivam		**8. Performing Organization Report No.** PTI 2009-18	
9. Performing Organization Name and Address The Thomas D. Larson Pennsylvania Transportation Institute Transportation Research Building The Pennsylvania State University University Park, PA 16802-4710		**10. Work Unit No. (TRAIS)**	
		11. Contract or Grant No. 999012 Project HA2006-02	
12. Sponsoring Agency Name and Address The Pennsylvania Department of Transportation Bureau of Planning and Research Commonwealth Keystone Building 400 North Street, 6th Floor Harrisburg, PA 17120-0064		**13. Type of Report and Period Covered** Final Report 6/23/2006 – 11/30/2008	
		14. Sponsoring Agency Code	

15. Supplementary Notes
COTR: Mr. Michael Long, johlong@state.pa.us

16. Abstract
Phase II of the PennDOT-sponsored project Superpave In-Situ Stress/Strain Investigation (SISSI) was initiated in June 2006 and completed in November 2008. This phase of the project was focused on extensive analysis of the collected data during Phase I and implementation of results from Phase I. Field-focused efforts during Phase II consisted of collection of pavement condition data, dynamic data, falling weight deflectometer data, traffic data, in-situ modulus data, and environmental data. All SISSI sites appeared to be in good shape except for the two overlaid pavement sections at the Warren and Delaware sites. At these two sites, a significant number of the longitudinal cracks at the lane-lane and lane-shoulder joints were probably due to poor construction. Transverse cracks on the pavement surface may be induced by underlying concrete slabs. Durability of Superpave mixes was of concern at two of these sites, Warren and Mercer. The project's last pavement condition survey at the Warren site indicated no cracking of the pavement mat at the site even though minor to moderate raveling and loss of fine was evident at the vicinity of the longitudinal joint. The minor to moderate raveling observed at the Mercer site is probably an indication of insufficient binder content for the mix used at this site. In general, some Superpave mixes have demonstrated that they are highly resistant to rutting, and this excellent rut resistance has come at the cost of lower durability in some cases. In general, the field-measured rutting, after 5 to 8 years of service, ranged from 2.5 to 8.5 millimeters, indicating excellent rut resistance of SISSI mixtures at all of the sites. Dynamic data collected during Phase II indicated significantly larger strain levels induced in the pavement during warmer times and lower speeds compared to colder seasons and higher speeds. Backcalculated moduli of asphalt concrete from FWD measurements were compared with the laboratory-obtained elastic moduli. The comparisons indicated that the backcalculated moduli were always higher than the laboratory-determined values. The present report is one of four volumes, Volume I: Summary Report; Volume II, Materials Characterization; Volume III: Field Data Collection and Summary; Volume IV: Mechanistic Analysis and Implementation.

17. Key Words SISSI, asphalt, data collection, instrumentation, rutting, raveling, durability, modulus, FWD, backcalculation, traffic, environmental data		**18. Distribution Statement** No restrictions. This document is available from the National Technical Information Service, Springfield, VA 22161	
19. Security Classif. (of this report) Unclassified	**20. Security Classif. (of this page)** Unclassified	**21. No. of Pages** 311	**22. Price**

Form DOT F 1700.7   **(8-72)**   **Reproduction of completed page authorized**

TABLE OF CONTENTS

LIST OF FIGURES

LIST OF TABLES

EXECUTIVE SUMMARY

The PennDOT-sponsored project Superpave In-Situ Stress/Strain Investigation (SISSI) was conducted in two phases. Phase I lasted five years, having started in May 2001 and ended in June 2006. Phase II of the project was initiated in June 2006 and was completed in November 2008. Phase I of this project was focused on completion of instrumentation and collection of various types of data required for validation of the Superpave mix design system as well as pavement performance prediction models. Phase II of SISSI was focused on extensive analysis of the collected data during Phase I and implementation of results from Phase I. The major objective achieved during Phase II of the program included utilization of SISSI data with the Mechanistic Empirical Pavement Design Guide (MEPDG) and comparing predicted performance versus observed field measurements. Phase II also included continuation of the data collection efforts of Phase I.

Phase I included an extensive effort toward instrumenting eight pavement sites throughout the Commonwealth of Pennsylvania. Instrumentation included dynamic (load associated) sensors and environmental (non-load) sensors. Upon completion of the instrumentation, a vast amount of effort was applied to testing, measurements, and data collection. In general, these efforts fell into two major categories: field activities and laboratory activities. The field activities included measurement of traffic, pavement performance, and pavement response to both load and environmental factors. Laboratory activities were conducted with the goal of characterizing all asphalt binders and mixtures used in the pavements of the SISSI project and determining the required engineering properties for use with performance prediction models. Dynamic data were collected during several visits to the sites at different times to capture seasonal effects on pavement response. Environmental data were collected remotely every half-hour for temperature and moisture content and every hour for frost. The major tests conducted in the laboratory on the procured binders included the Superpave grading tests (short- and long-term aging, rotational viscometer, dynamic shear rheometer, and bending beam rheometer). The mixture testing included the tests required for verification of mix design, as well as dynamic modulus testing at a range of temperatures and frequencies to capture properties required for input to performance prediction models.

Part of the Phase II work included all field data collection activities, as was conducted during Phase I, with the exception that the pavement condition survey and dynamic data collection were conducted at a significantly lower frequency. A major challenge during Phase II was the need for an extensive level of effort to maintain sensors and data acquisition systems as functional. Continuity of environmental data collection was not able to be maintained at all times, and this resulted in gaps and discontinuity in the collected data. Some of the sensors did not provide reasonable responses because of malfunctioning or damage, specifically frost and moisture content gages. In regard to dynamic sensors, the best results were obtained from strain gages, and the most serious problems were noticed with multidepth deflectometers (MDD). In spite of all data collection problems. The data collected at SISSI sites is an extremely valuable resource considering that multiple sites were available and collection of data was continued for such an extended time period.

An additional field activity during Phase II included determination of in-situ modulus using the Portable Seismic Pavement Analyzer (PSPA). In summary, field-focused efforts during Phase II consisted of collection of pavement condition data, dynamic data, falling weight deflectometer (FWD) data, traffic data, in-situ modulus data, and environmental data. The current report provides details of these data collection efforts and the corresponding analysis and interpretation of such data.

All SISSI sites appeared to be in good shape except for the two overlaid pavement sections at the Warren and Delaware sites. At these two sites, a significant number of the longitudinal cracks at the lane-lane and lane-shoulder joints were probably due to poor construction. Transverse cracks on the pavement surface may be induced by underlying concrete slabs. Durability of Superpave mixes was of concern at two of these sites, Warren and Mercer, based on observations of PennDOT personnel. The Warren site was finally milled and overlaid during spring 2007. For the Mercer site, only a small section of the road prior to the SISSI site was milled and overlaid. Our last pavement condition survey at this site, during November 2007, indicated no cracking of the pavement mat at the site even though minor to moderate raveling and loss of fines was evident at the vicinity of the longitudinal joint. The pavement had also experienced longitudinal cracking both at the joint between the two lanes as well as the joint between the travel lane and the shoulder. These cracks appear to be construction related rather than mix related. However, the minor to moderate raveling observed at the Mercer site is probably an indication of insufficient binder content at this site. In general, some Superpave mixes have demonstrated that they are highly resistant to rutting, and this excellent rut resistance has sometimes come at the cost of lower durability. The field-measured rutting, after 5 to 8 years of service, ranged from 2.5 to 8.5 millimeters, indicating excellent rut resistance of SISSI mixtures at all the sites.

Collection of dynamic data during Phase II was conducted at a significantly lower frequency compared with Phase I. During Phase II, dynamic data collection was conducted at specific sites to complement the data collected during Phase I. More repeated measurements were conducted at the same speed, and lower speeds were included in Phase II. At a few sites, collection of such data was not possible because of loss or corrosion of gages. Dynamic data collected during Phase II indicated significantly larger strain levels induced in the pavement during warmer times and lower speeds compared to colder seasons and higher speeds. Backcalculated moduli of asphalt concrete from FWD measurements were compared with the laboratory-obtained elastic moduli. The comparisons indicated that the backcalculated moduli are always higher than the laboratory-determined values. The observation is in general agreement with the suggestion by the 1993 AASHTO Design Guide that the FWD backcalculated moduli are typically higher than the laboratory determined moduli.

The moduli of asphalt concrete determined from laboratory complex modulus tests were also compared with the moduli from in-situ nondestructive tests using PSPA. Statistical analysis indicated an excellent PSPA measurement repeatability. Comparison between seismic and dynamic moduli indicated about 30 percent difference in these two moduli. When making such comparisons, it is important to consider the impact of air void content because the in-situ seismic modulus is very sensitive to the air void of the asphalt concrete. For the SISSI project, pavement cores obtained one to two years after construction revealed air voids very similar to those of the laboratory specimens tested for dynamic modulus. The second important point in making such comparison regards the aging of the asphalt binders. Aging increases binder stiffness and

therefore results in a higher mixture modulus. In this study, no attempts were made to determine the aging level of the binder and base layers. However, it is expected that since these layers are not exposed to solar radiation and also experience the moderate temperatures of the Pennsylvania climate, there is not a significant aging level for the binder and base layers. Significant aging is expected for the wearing course binder, but modulus of this layer is not measured by PSPA. Most of the successful environmental data during Phase II consists of pavement temperature and solar radiation. Frost and moisture content data were limited due to gage malfunctioning. Environmental data from Phase I and the first year of phase II were analyzed in regard to frost depth and the freezing index. Different approaches were utilized in the determination of the freezing index, and the impact of the freezing index on the computed frost depth was evaluated as part of the Phase-II SISSI research. The freezing index was calculated based on a major freeze cycle as well as multiple shorter freeze-thaw cycles. It was observed that there is rarely a freeze-thaw cycle that is over 40 days in Pennsylvania. Most freeze-thaw cycles have periods less than 10 days. For a freezing index difference of less than 150 °C-days, variation of computed frost depth, in most cases, does not exceed 0.20 m. However, for a freezing index difference of approximately 200 °C-days, computed values vary from 0.15 to 0.25 m. Frost data from the Blair site was analyzed to determine the depth and rate of frost penetration. The data indicate that as freezing period lasts longer, frost severity increases at various depths. Overall, at deeper pavement layers, more time is required to reach a specific freezing condition.

In summary, a considerable amount of valuable data was collected from the SISSI sites during Phases I and II of this project. The data were extensively used with the AASHTO Mechanistic Empirical Pavement Design Guide (MEPDG) as well as for independent mechanistic analysis, documented in a separate report. The data were also analyzed to provide overall assessment of the condition of SISSI pavements and Superpave mixtures and to provide freezing conditions of Pennsylvania pavements. This data provide a very useful source for local calibration of the MEPDG and Enhanced Integrated Climatic Models (EICM) used in MEPDG.

CHAPTER 1: INTRODUCTION

In 2001, the Pennsylvania Department of Transportation (PennDOT) sponsored a 5-year research project for the full evaluation of Superpave called the Superpave In-Situ Stress/Strain Investigation (SISSI) to produce data needed for calibration and validation of asphalt pavement performance prediction models. The first phase (Phase I) of the SISSI project was completed in May 2006. A second phase (Phase II) was then initiated to continue data collection from the installed instrumentation, monitoring of pavement condition, laboratory and field testing for materials characterization, and analysis of the data.

This report is one of four volumes of the final report for Phase II of the SISSI project. Separate volumes have been prepared for an overall summary, materials characterization, and comprehensive mechanistic analyses for the SISSI sites. This volume documents the field data collected, including the pavement condition (distress survey and transverse profile), dynamic, deflection, seismic, traffic, and environmental data. These data elements were collected on the dates shown in Table 1. This volume also includes the data collected from the environmental and traffic instrumentation on a more continuous basis.

The following sections provide summaries for field data collection for all SISSI sites except the Somerset site. Because of traffic and scheduling difficulties, field data could not be collected at the Somerset site. The final section provides an overall summary. In addition, the appendices provide detail on the collected field data.

Table 1. Summary of field data collection

SISSI Site	Date	Field Data				
		Distress Survey	Transverse Profile	Dynamic	Deflection	Seismic
Tioga	11/6/2007	X	X			X
Mercer East	11/1/2007	X	X			X
Mercer West	11/1/2007	X	X			X
Warren	3/26/2007	X	X			
Perry	7/17/2008	X	X	X		
Delaware	10/07/2008	X	X			
Blair	3/13/2008			X		
	3/27/2008			X		
	4/29/2008		X	X	X	X
	6/24/2008			X		X

CHAPTER 2: CONDITION DATA

Distress Survey

Manual distress surveys were conducted in accordance with Long-Term Pavement Performance protocols. The distress definitions utilized for this project were detailed in the *Performance, Traffic and Weather Data Collection and Reporting Manual* since some of the distress definitions have changed over time. Distress surveys were conducted over one-thousand-foot sections, including both instrumentation sections. Detailed crack maps were prepared for each instrumentation section. Photographs were taken in conjunction with the manual distress surveys.

As shown in Table 2, all SISSI sites appeared to be in good shape except for the two overlaid pavement sections at the Warren and Delaware sites. At these two sites, a significant amount of the longitudinal cracks at the lane-lane and lane-shoulder joints were probably due to poor construction. Transverse cracks on the pavement surface may have been induced by underlying concrete slabs. Representative photographs for the last distress surveys conducted at each site have been included in Figures 1 through 7. Additional photographs are included in Appendix A.

Table 2. Summary of most recent distress surveys

SISSI site	Survey Date	Distress and Units	Quantity
Tioga	11/6/2007	Longitudinal Cracking (m/km)	0
		Alligator Cracking (%)	0
		Transverse Cracking (m/km)	0
Mercer East	11/1/2007	Longitudinal Cracking (m/km)	0
		Alligator Cracking (%)	0
		Transverse Cracking (m/km)	0
Mercer West	11/1/2007	Longitudinal Cracking (m/km)	0
		Alligator Cracking (%)	0
		Transverse Cracking (m/km)	0
Warren	3/26/2007	Longitudinal Cracking (m/km)	2340*
		Alligator Cracking (%)	0
		Transverse Cracking (m/km)	103
Perry	7/17/2008	Longitudinal Cracking (m/km)	0
		Alligator Cracking (%)	0
		Transverse Cracking (m/km)	0
Delaware	10/7/2008	Longitudinal Cracking (m/km)	213**
		Alligator Cracking (%)	10
		Transverse Cracking (m/km)	240
Blair	4/29/2008	Longitudinal Cracking (m/km)	0
		Alligator Cracking (%)	0
		Transverse Cracking (m/km)	0

Notes: * Most longitudinal cracks were observed at the lane-lane
and lane-shoulder joints.
** A significant amount of the longitudinal cracks
which were recorded during Phase I had been sealed.

Figure 1. Pavement condition at Tioga site, 11/6/2007
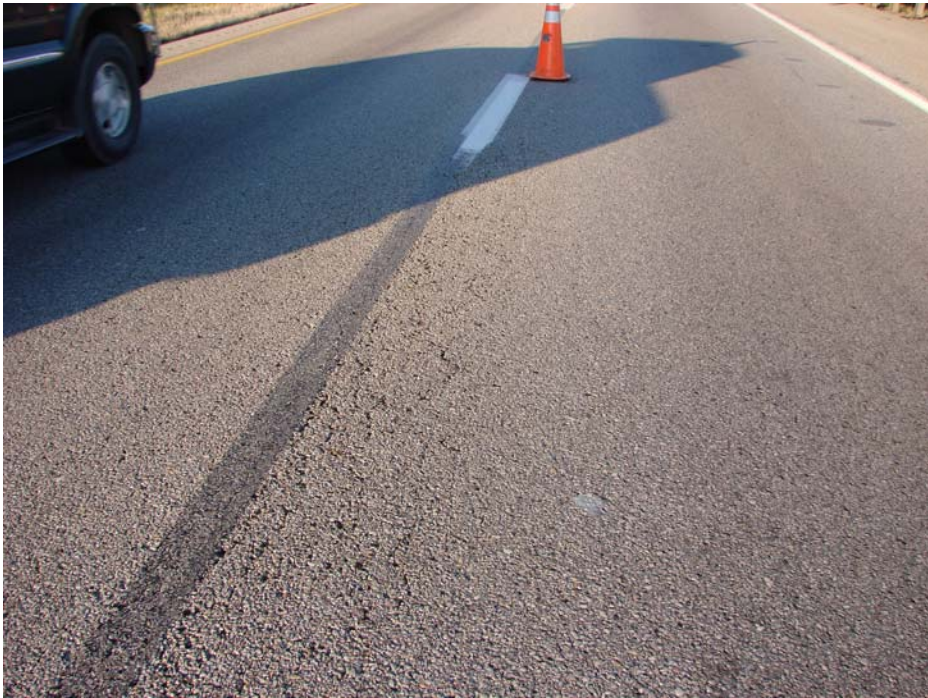
Figure 2. Pavement condition at Mercer East site, 11/1/2007

Figure 3. Pavement condition at Mercer West site, 11/1/2007

Figure 4. Pavement condition at Warren site, 3/26/2007

Figure 5. Pavement condition at Perry site, 7/17/2008

Figure 6. Pavement condition at Delaware site, 10/7/2008

Figure 7. Pavement condition at Blair site, 4/29/2008

Transverse Profile (rutting)

Transverse profiles were collected with a Mitutyo Digimatic Absolute Depth Gage. This digital depth meter is aligned vertically adjacent to the beam and connects to a laptop computer. Every time the triggering button on the meter is activated, the measured depth is transferred to the spreadsheet file developed on the laptop computer. Measurements with this system were conducted at 5-cm intervals along the beam. The rut depths were determined by the differences between the maximum peak and minimum valley measurements from the profiles. As rut depths progressed, transverse profiles were plotted and shapes evaluated as appropriate. A summary of average rut-depth measurements is included in Table 3. It can be seen that the rut depths in the left wheelpath are smaller than those in the right wheelpath at some SISSI sites, and vice versa at other sites. In addition, bar charts of rut depth with time (Figures 8 to 14) for each SISSI site appear to show a slight increase in rut depth with time for both left and right wheelpaths.

Table 3. Summary of transverse profile data

SISSI Site	Location	Date	Rut Depth, mm	
			Left Wheelpath	**Right Wheelpath**
Tioga	1	11/6/2007	3.7	6.0
		8/25/2005	3.3	5.7
		10/26/2004	2.8	5.0
		8/17/2004	2.3	5.2
	2	11/6/2007	5.7	6.9
		8/25/2005	4.5	6.6
		10/26/2004	-	-
		8/17/2004	-	-
Mercer East	1	10/30/2007	3.4	3.1
		3/22/2005	3.1	3.4
		8/3/2004	3.1	3.4
		4/6/2004	2.7	3.0
	2	10/30/2007	5.0	4.2
		3/22/2005	3.8	2.7
		8/3/2004	3.8	3.5
		4/6/2004	3.1	3.2
Mercer West	1	10/30/2007	4.3	3.0
		12/1/2005	5.0	2.5
		8/4/2004	3.2	3.0
		4/7/2004	-	-
	2	10/30/2007	4.0	3.3
		12/1/2005	-	-
		8/4/2004	2.8	3.0
		4/7/2004	2.7	2.9
Warren	1	3/26/2007	5.6	2.4
		3/17/2005	4.3	1.7
		11/5/2004	4.5	2.1
		8/24/2004	4.5	1.8
	2	3/26/2007	4.8	4.5
		3/17/2005	4.3	2.4
		11/5/2004	4.2	2.4
		8/24/2004	3.9	2.0

Table 3. Summary of transverse profile data (cont'd)

SISSI Site	Location	Date	Rut Depth, mm	
			Left Wheelpath	**Right Wheelpath**
Delaware	1	10/7/2008	2.4	8.6
		3/15/2007	4.8	9.1
		3/30/2005	4.1	6.7
		11/10/2004	4.1	4.4
		3/22/2004	3.3	6.5
	2	10/7/2008	-	-
		3/15/2007	5.2	4.4
		3/30/2005	4.9	4.1
		11/10/2004	4.7	3.7
		3/22/2004	-	-
Perry	1	7/17/2008	-	-
		2/23/2005	3.3	2.5
		10/28/2004	4.0	2.6
		7/27/2004	3.6	2.5
	2	7/17/2008	5.5	2.9
		2/23/2005	3.8	2.1
		10/28/2004	-	-
		7/27/2004	3.2	2.1
Blair	1	4/29/2008	3.5	5.2
		8/23/2005	2.8	3.5
		10/22/2004	1.9	3.2
		7/20/2004	1.6	2.2
	2	4/29/2008	3.8	5.6
		8/23/2005	2.8	4.3
		10/22/2004	2.0	3.0
		7/20/2004	1.6	2.3
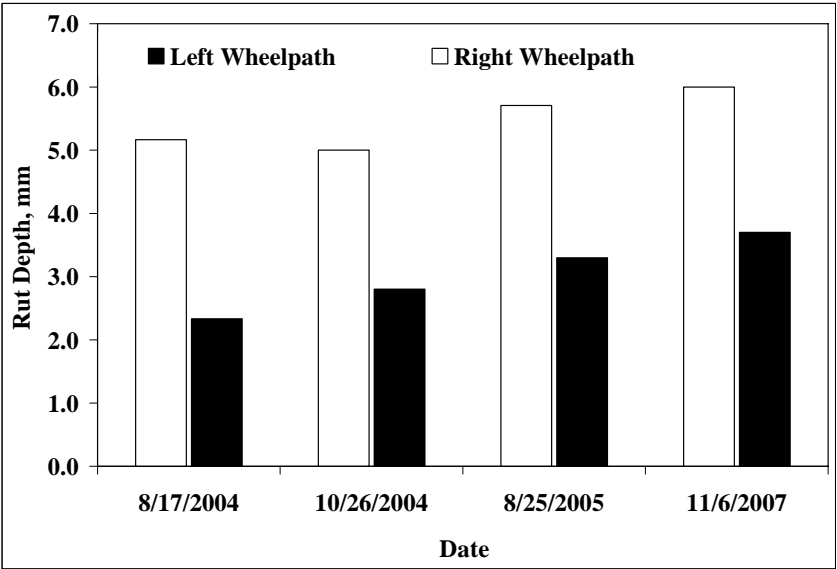
(a) location 1
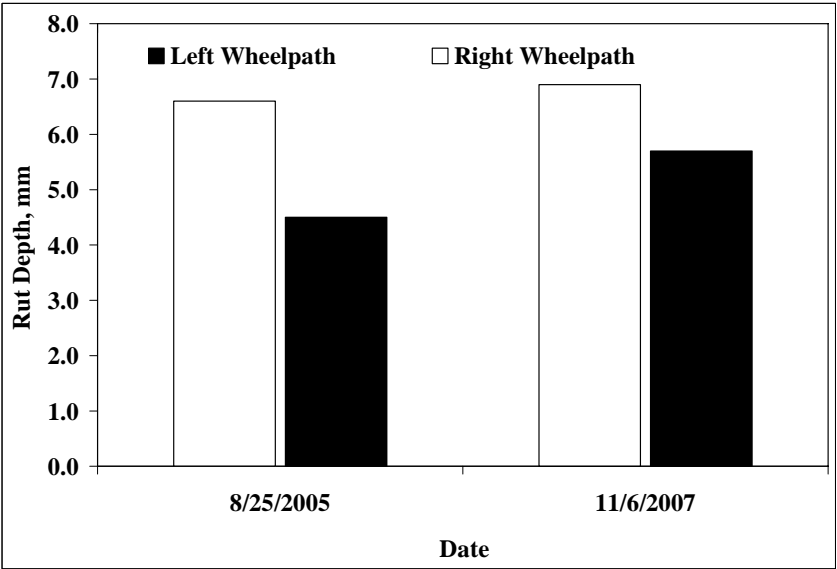
(b) location 2

Figure 8. Rut depths at Tioga site
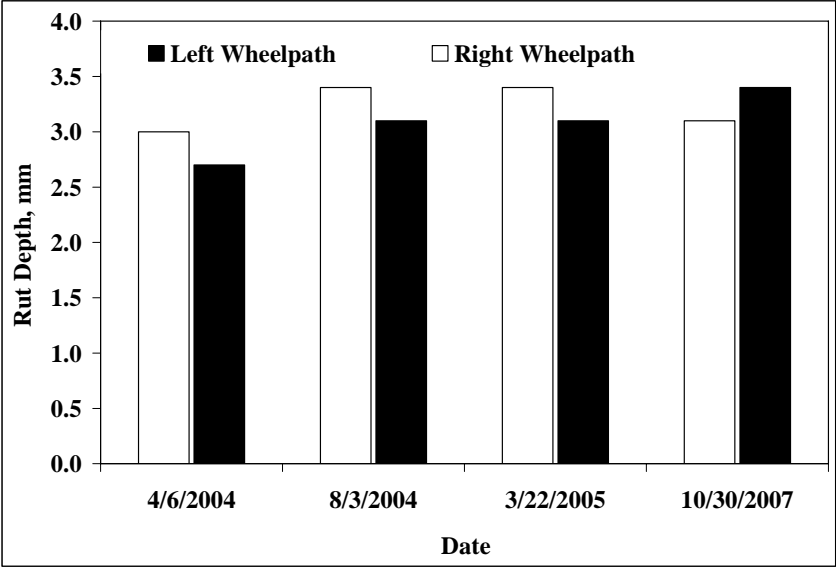
(a) location 1
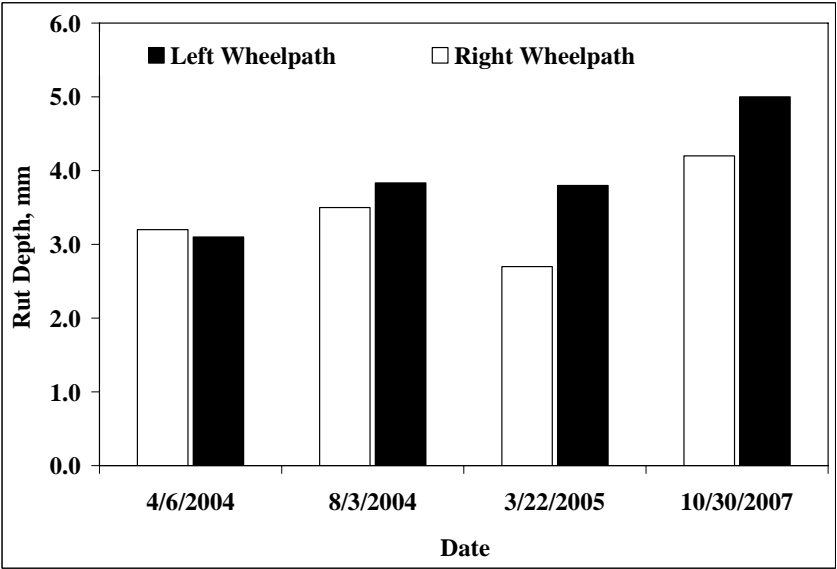
(b) location 2

Figure 9. Rut depths at Mercer East site
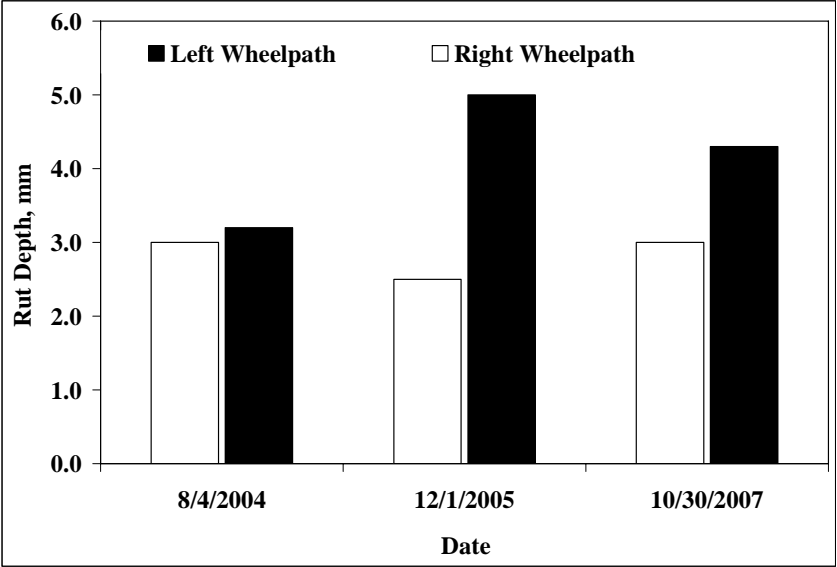
(a) location 1
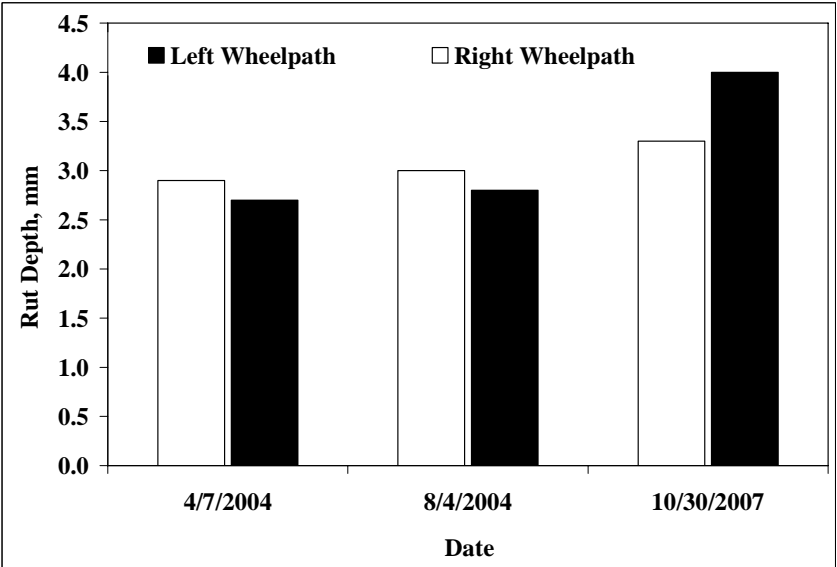
(b) location 2

Figure 10. Rut depths at Mercer West site

16
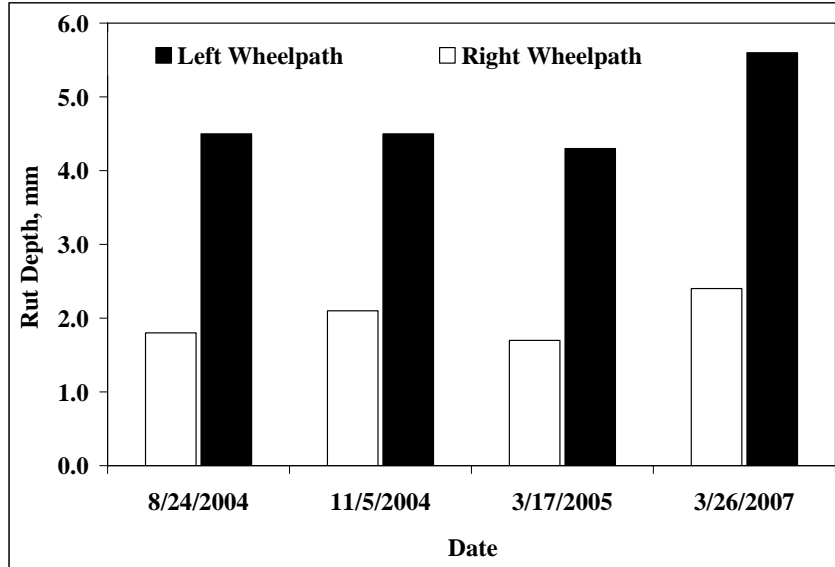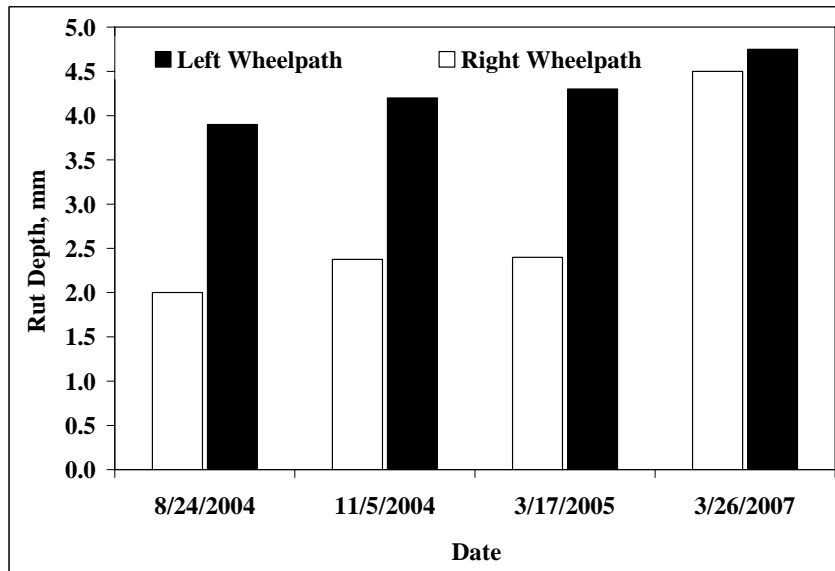
(a) location 1

(b) location 2

(c) Figure 11. Rut depths at Warren site
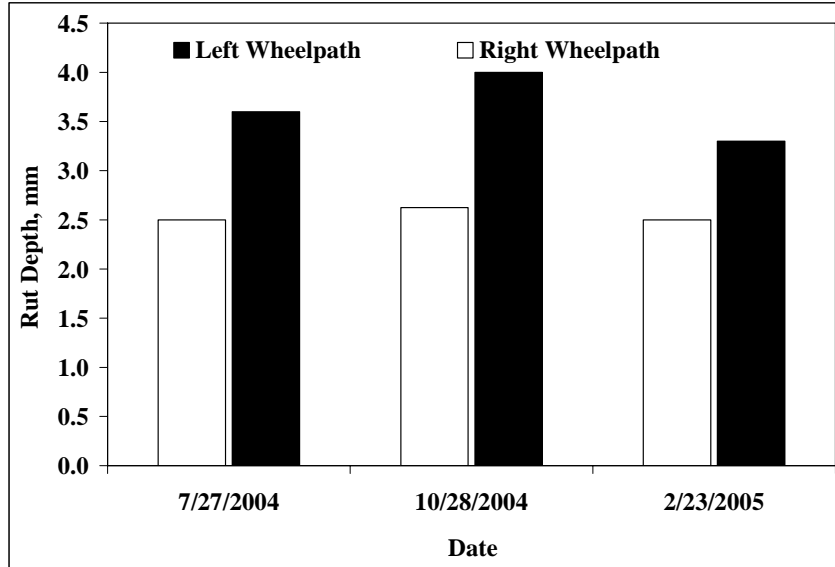
(a) location 1
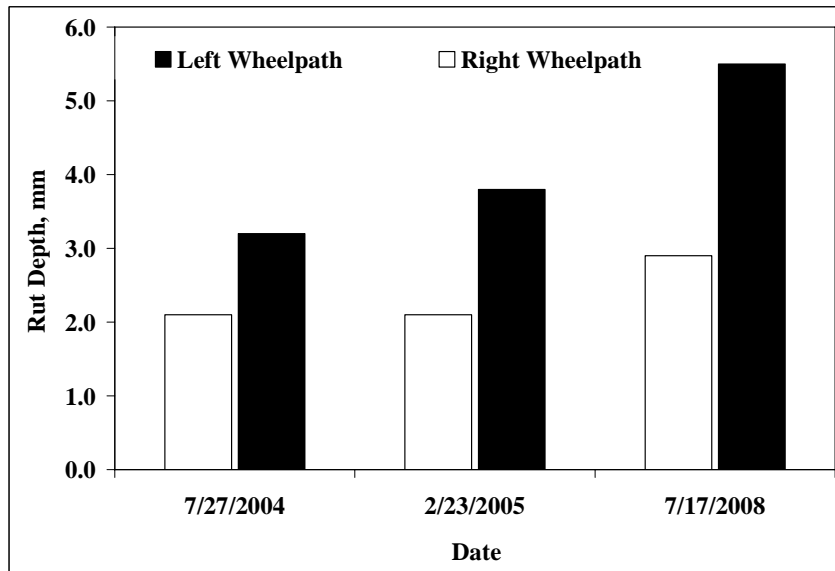
(b) location 2

Figure 12. Rut depths at Perry site
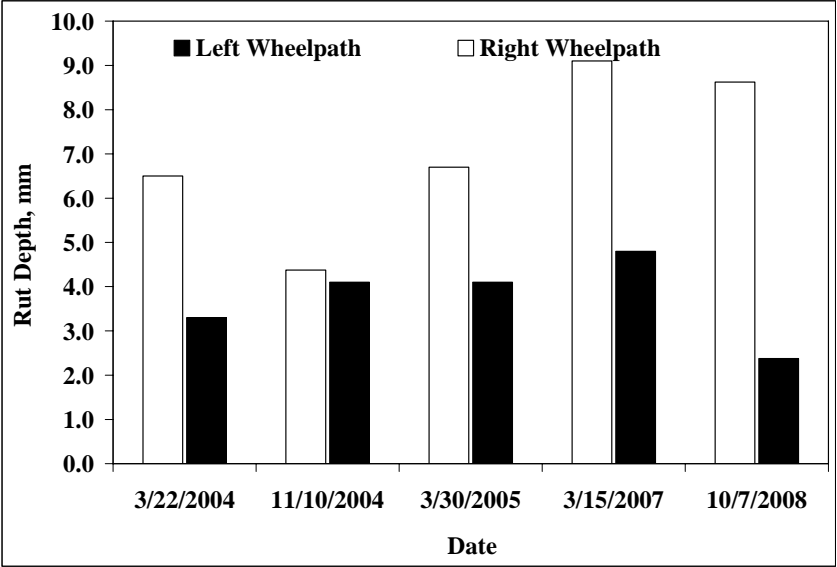
(a) location 1
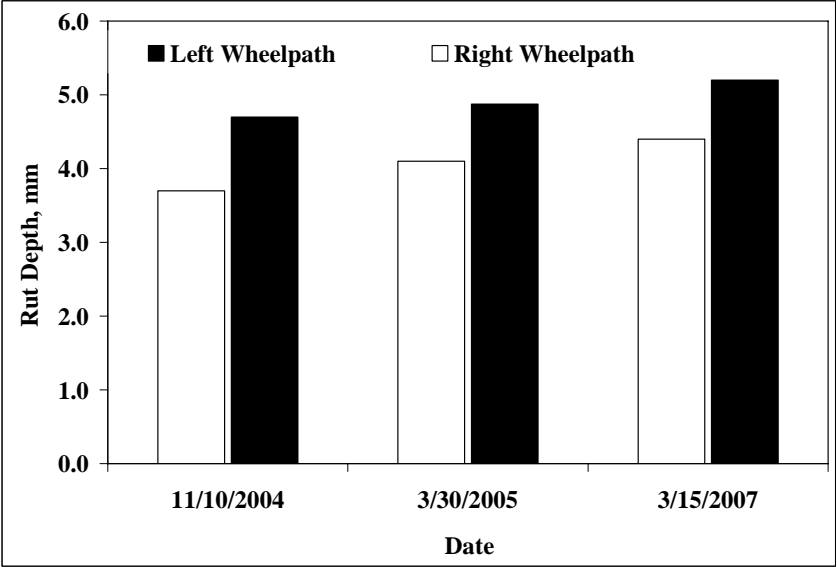
(b) location 2

Figure 13. Rut depths at Delaware site
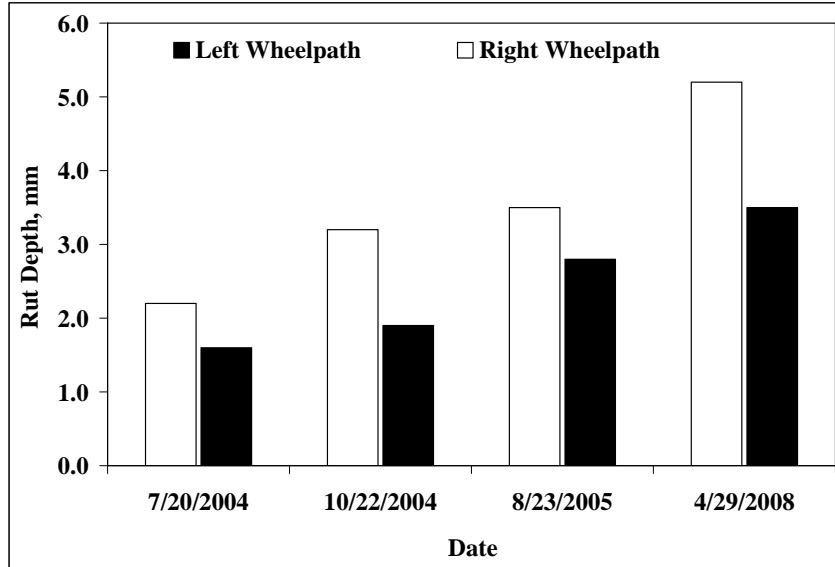
(a) location 1
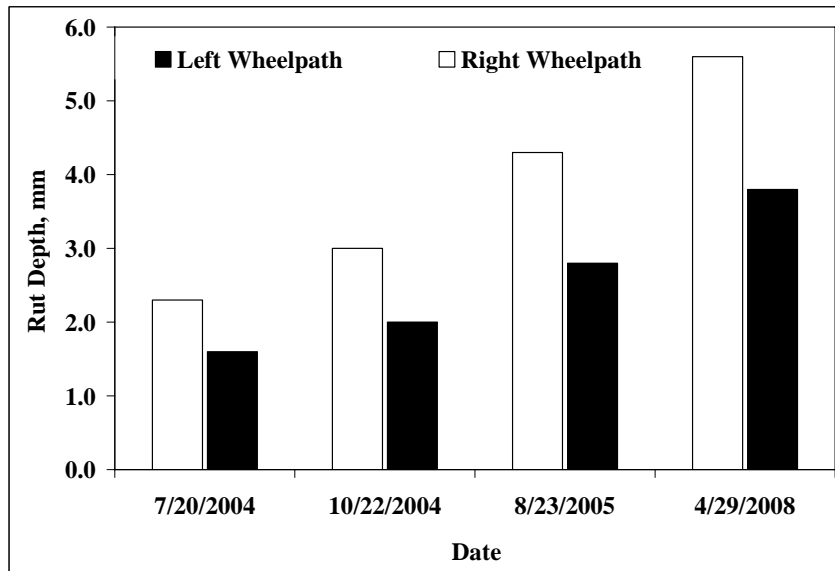
(b) location 2

Figure 14. Rut depths at Blair site

CHAPTER 3: DYNAMIC DATA

Dynamic data collected from the Blair and Perry sites during Phase II of the SISSI project were collected and processed, as shown in Figure 15. The first step was overall evaluation of the quality of each data set. This step was followed by investigating the effects of various factors on pavement responses.

Figure 15. Dynamic data collection apparatus

The processed dynamic data were from the Dynatest Past-II strain gages and the RST pressure cells. The Dynatest Past-II strain gages were installed at the bottom of asphalt concrete (AC) layers, while the RST pressure cells were installed on the top of the subbase and subgrade layers.

The first stage of analysis was focused on determining whether the Phase II dynamic data were consistent with the Phase I data under similar loading and environmental conditions. Details of the load configurations and protocols were presented in the Phase I report. Dynamic data from Location 1 of Blair site with back load configuration (when concrete blocks are in back of the trailer) are presented here as an example. Since maximum pavement responses were always observed when the fourth axle of the loading truck passed the gage, these peak responses were selected to check the consistency of the Phase II dynamic data. As shown in Figures 16 through 20, a good agreement was observed between the dynamic data collected from both phases. The difference was usually smaller than 20%.
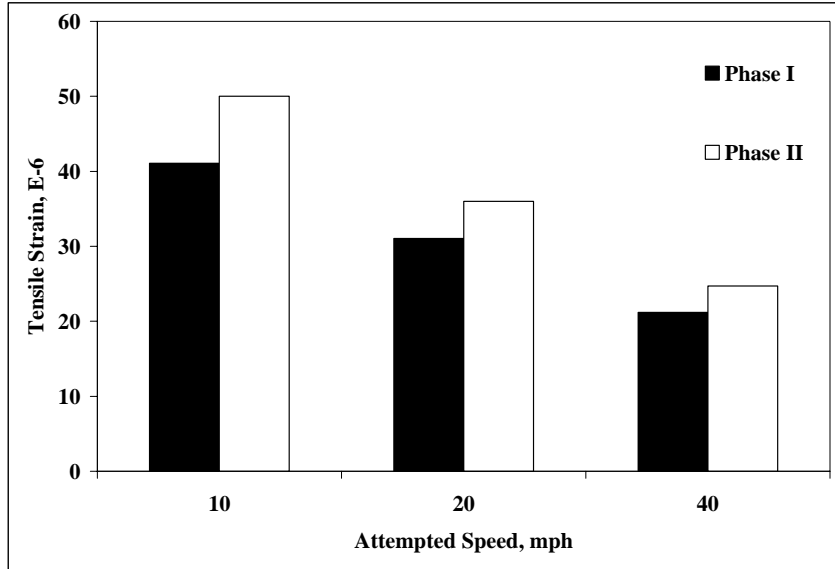
Figure 16. Tensile strain at the bottom of wearing layer (Blair, location 1, 3/7/2005 and 3/27/2008)
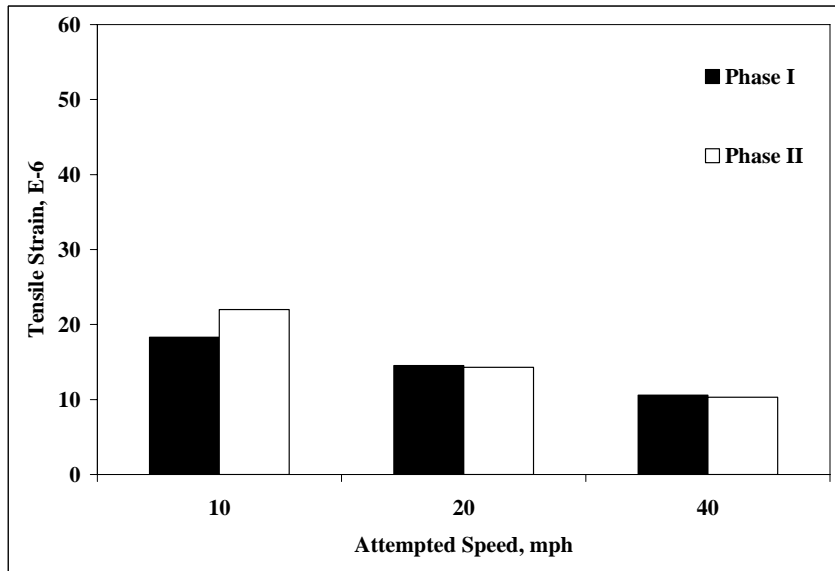
Figure 17. Tensile strain at the bottom of binder layer (Blair, location 1, 3/7/2005 and 3/27/2008)
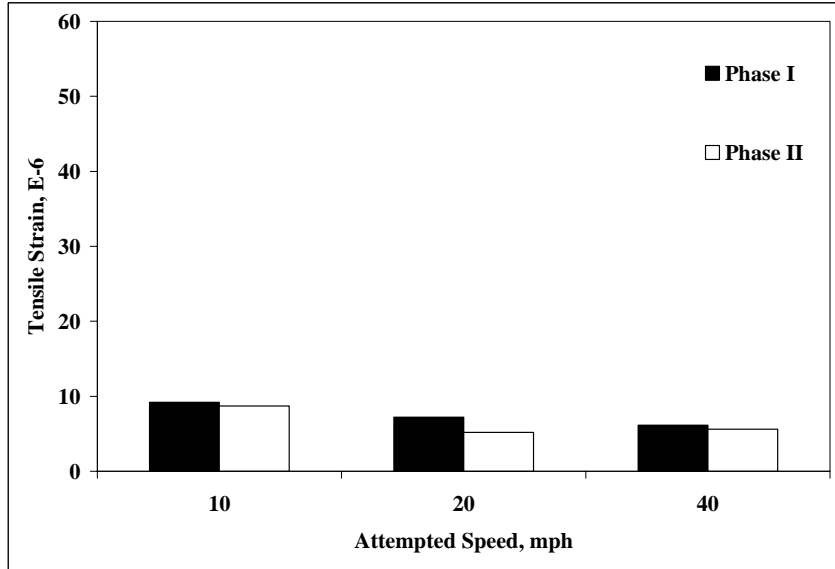
Figure 18. Tensile strain at the bottom of BCBC layer (Blair, location 1, 3/7/2005 and 3/27/2008)
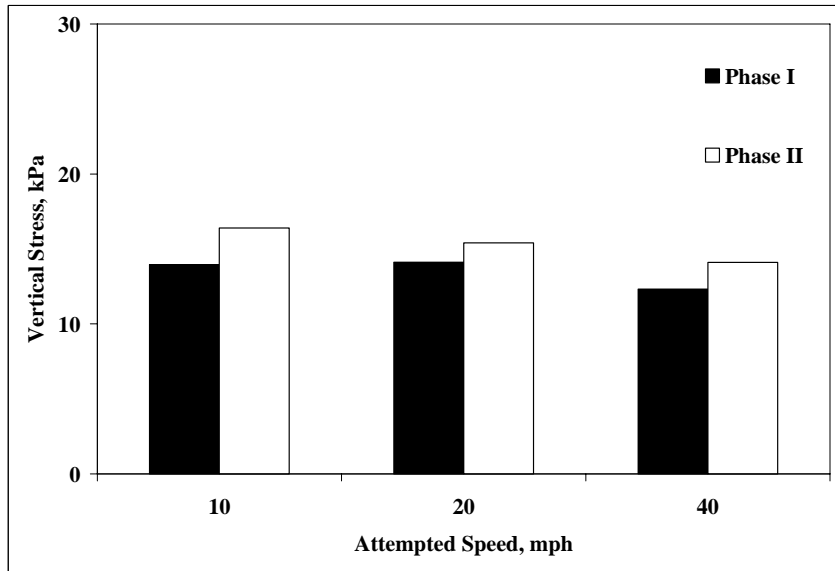
Figure 19. Vertical stress at the top of subbase (Blair, location 1, 3/7/2005 and 3/27/2008)
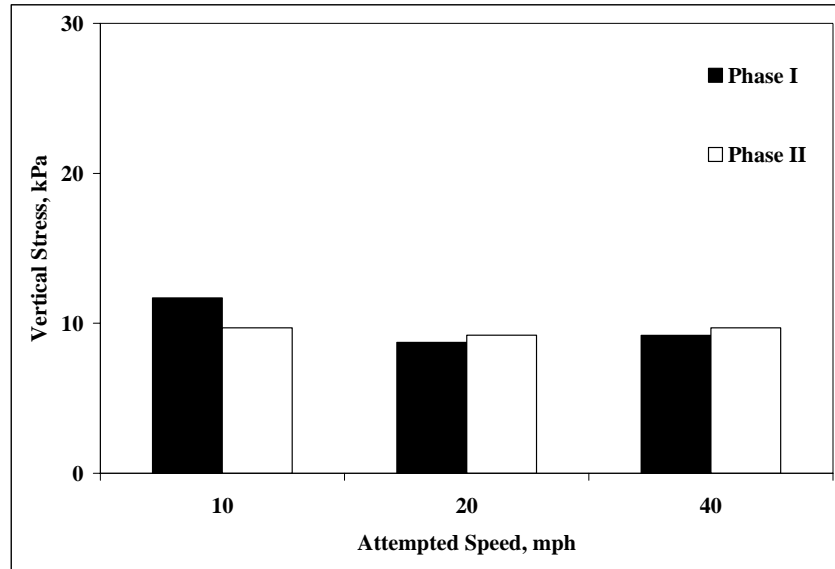
Figure 20. Vertical stress at the top of subgrade (Blair, location 1, 3/7/2005 and 3/27/2008)

To the extent possible and applicable, the collected data were further analyzed in both of the following ways: 1) Responses from similar gages from different layers at the same site and location were compared and 2) Responses from a specific gage at a specific layer were analyzed at various speeds. Examples of these measurements are provided in this section, and details of all dynamic measurements are provided in Appendix B.

Horizontal Strains at Different Layers

This part of the analysis was concentrated on the magnitude of the responses from these gages and how these responses were affected by position in the pavement and the speed of the loading vehicle. Attempts were made to maintain the speed of the truck at 5, 10, 20, 40, and 60 mph at the time of loading the pavement sensors. However, exact speeds deviated from the intended speeds during operation. Actual speed was determined based on the available data from the triggering system as well as from the gage responses.

Generally, it is expected that the magnitude of tensile strain would be decreased at deeper pavement layers. An example of the tensile strain variation with depth is presented in Figures 21 through 26 for the measurements at the Blair and Perry sites. Strain at the bottom of the wearing, binder, and BCBC layers are in a decreasing trend because the layers are deeper in the pavement.

Because of the viscoelastic nature of asphalt, higher strain is expected as the vehicle speed is increased. The effect of speed is clear from Figures 21 through 26, especially at lower speeds. Strain is decreased as the speed is increased from 5 to 10 and then to 20 mph. However, there is not a significant change in response when the speed is increased beyond this level. Measurements at lower speeds, such as 5 mph, resulted in considerably higher strain levels compared to the values at 20 mph. The data indicate the significance of loading at lower speeds, as the deformations in pavement layers increase with reduced speed, thus increasing the potential for developing distresses at pavement layers.

24

Vertical Pressure

Vertical pressure in unbound layers at the Blair site has been captured by pressure cells. These cells have been typically installed inside the subgrade at a depth of approximately 1 to 2 inches below the bottom of the subbase layer, or inside the subbase at a depth of approximately 1 to 2 inches below the bottom of the BCBC layer.

Figures 27 through 30 show the results for the measurements at Blair SR 1001 in 2008. The results also indicate that the induced vertical stress is considerably higher at the top of the subbase than at the top of the subgrade. Generally, as shown in figures for the vertical stresses at the top of the subbase layer, the vertical pressure is reduced at higher speeds even though in a few cases, the stresses induced by the 5 mph speed does not follow this trend. However, the speed effect on stress responses is not as pronounced as on strain responses. It can be seen that for the subgrade layer, as the magnitude of stresses is considerably reduced compared to the subbase layer, the effect of speed becomes less important and no significant difference is observed among stress levels from different speeds.
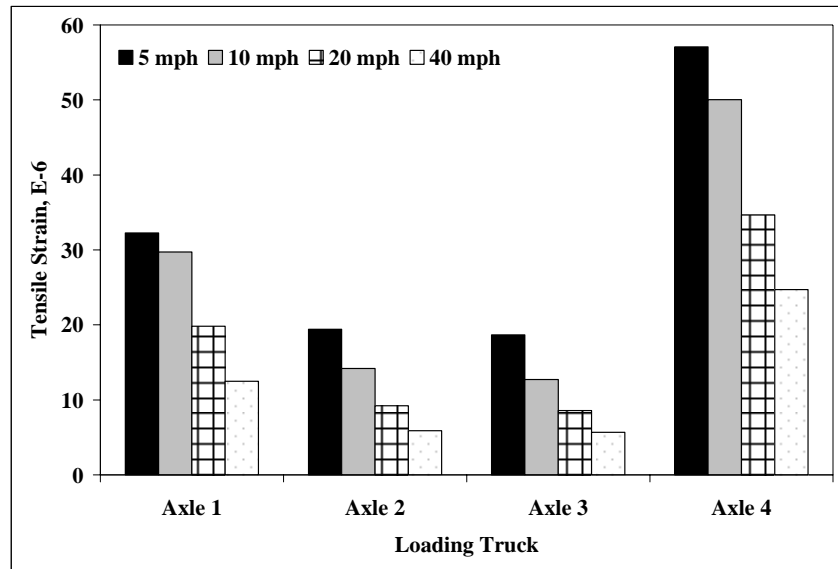
(a) tensile strain at the bottom of wearing layer
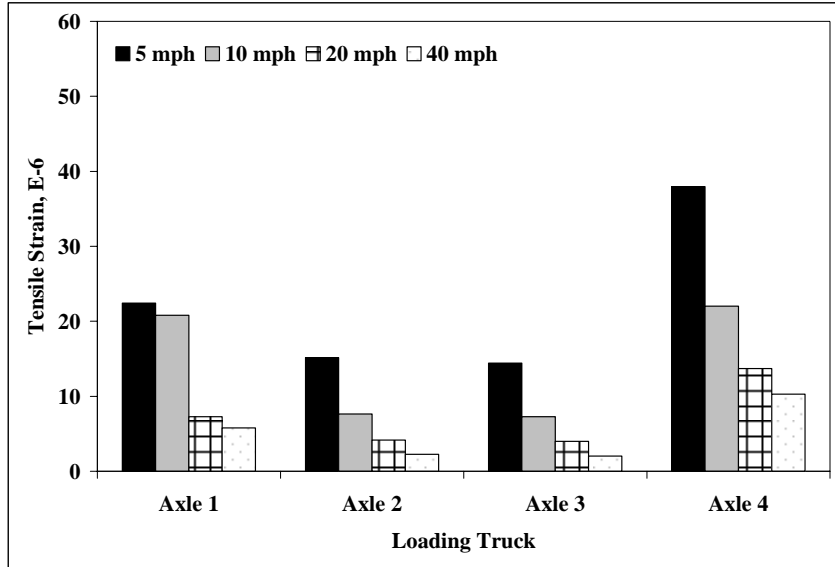
(b) tensile strain at the bottom of binder layer
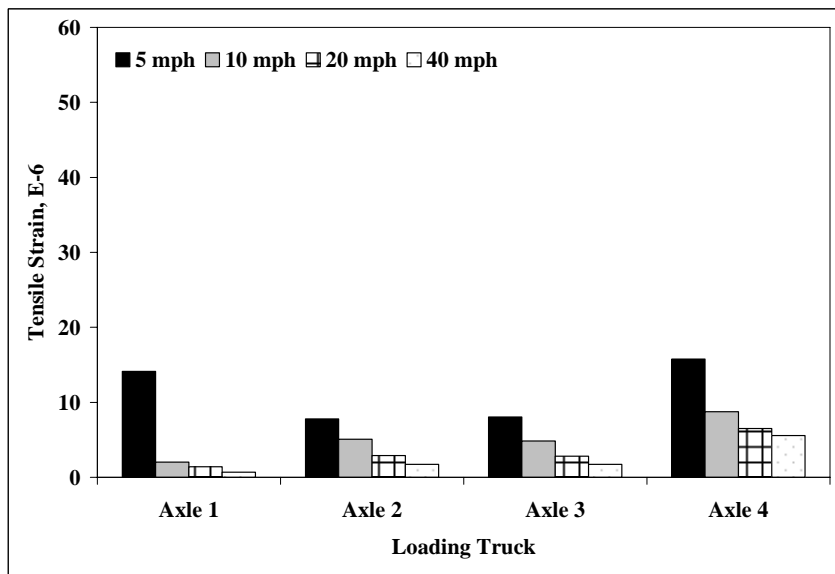
(c) tensile strain at the bottom of BCBC layer

Figure 21. Strain response of pavement layers at Blair location 1 (measured on 03/27/2008, back load configuration)
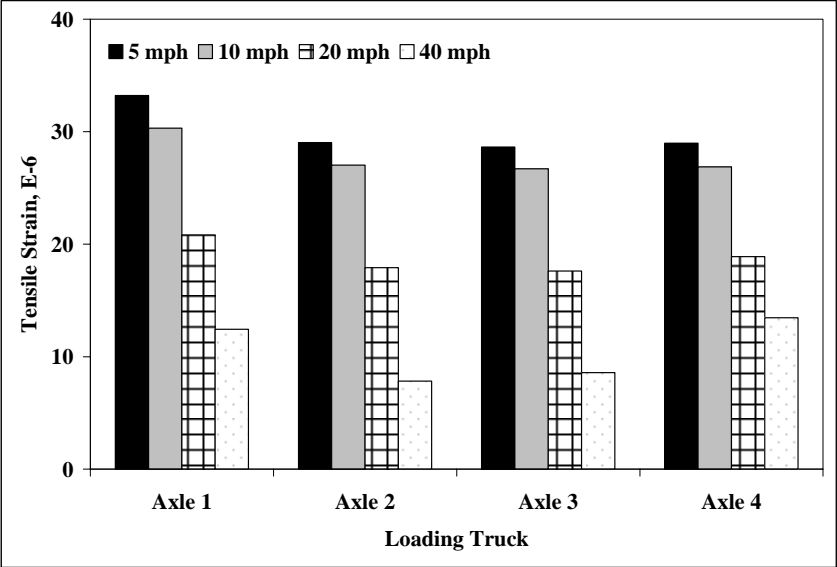
(a) tensile strain at the bottom of wearing layer
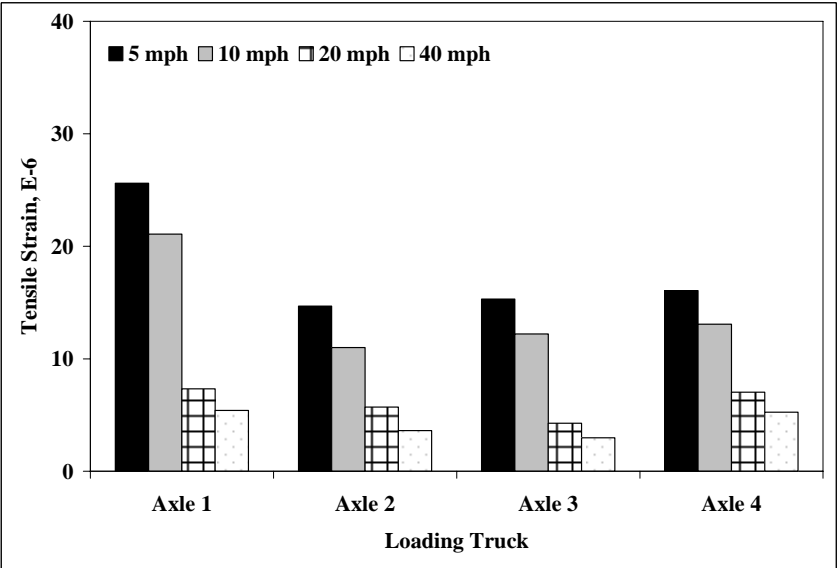
(b) tensile strain at the bottom of binder layer
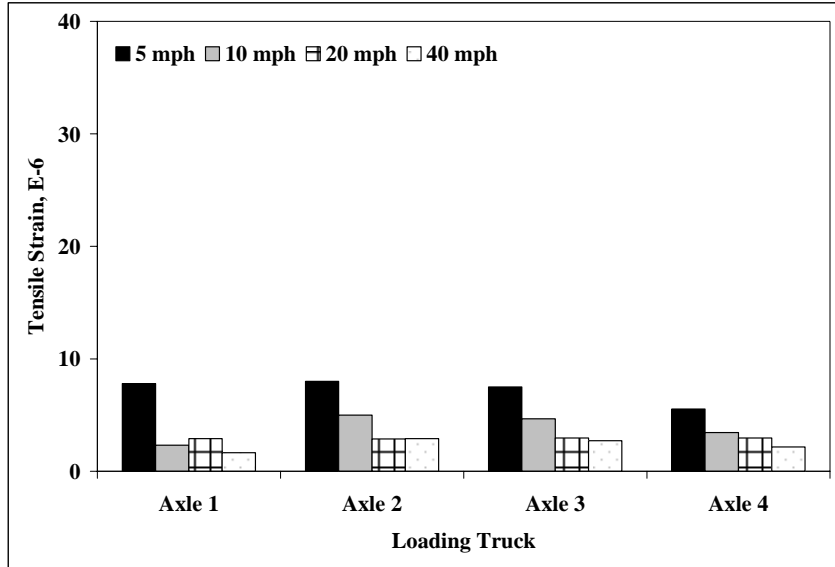
(c) tensile strain at the bottom of BCBC layer

Figure 22. Strain response of pavement layers at Blair location 1 (measured on 03/27/2008, front load configuration)
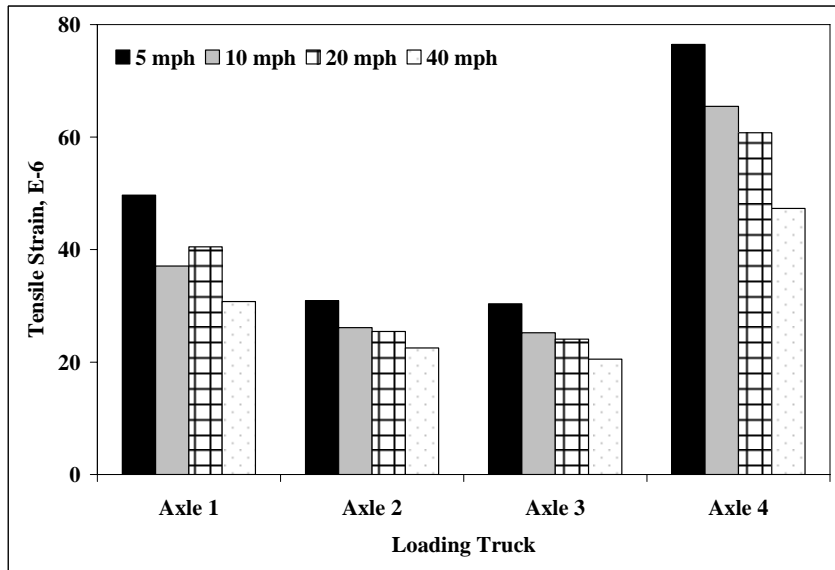
(a) tensile strain at the bottom of wearing layer
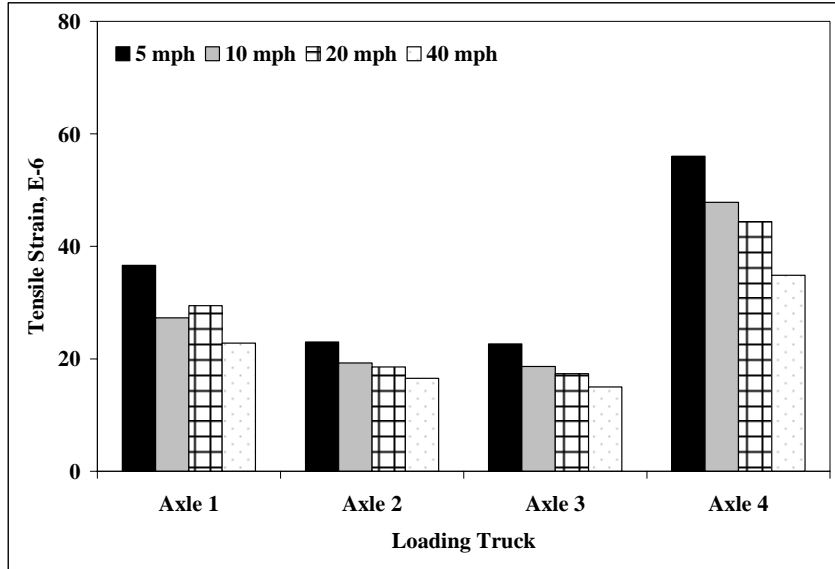
(b) tensile strain at the bottom of binder layer
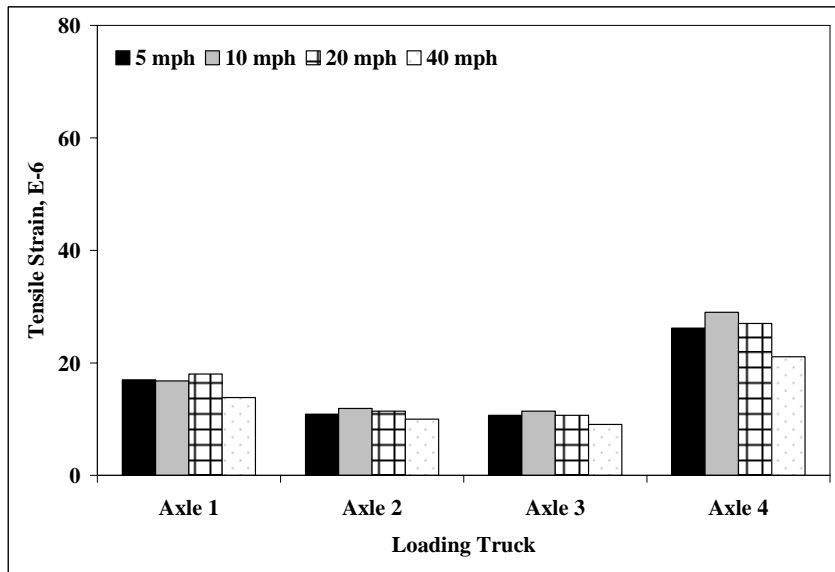
(c) tensile strain at the bottom of BCBC layer

Figure 23. Strain response of pavement layers at Blair location 2 (measured on 06/24/2008, back load configuration)
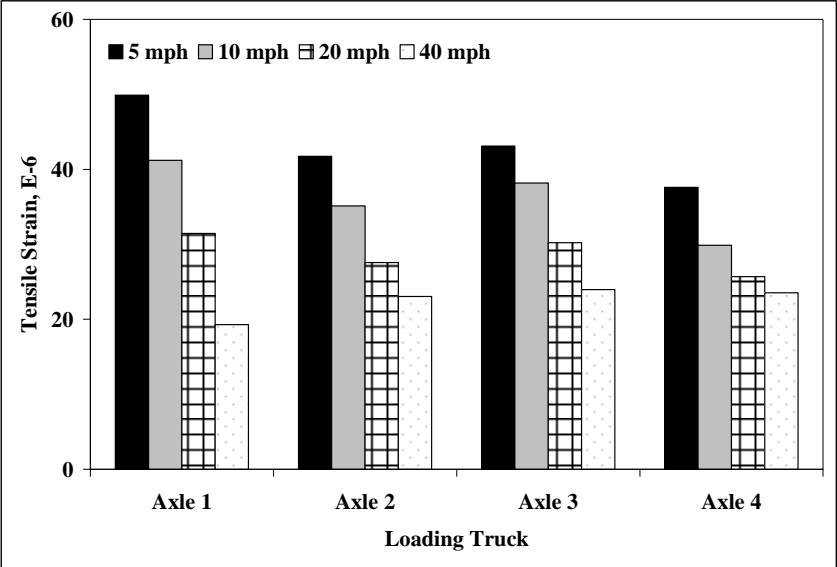
(a) tensile strain at the bottom of wearing layer
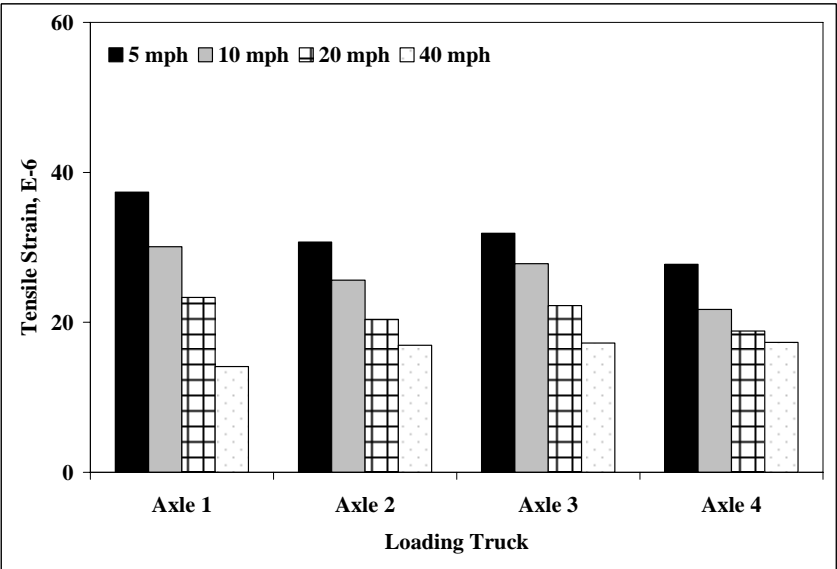
(b) tensile strain at the bottom of binder layer
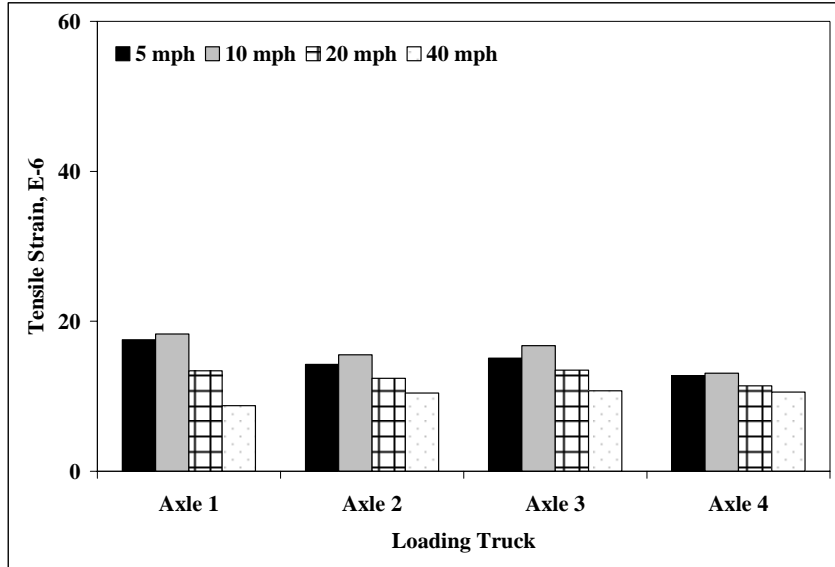
(c) tensile strain at the bottom of BCBC layer

Figure 24. Strain response of pavement layers at Blair location 2 (measured on 06/24/2008, front load configuration)
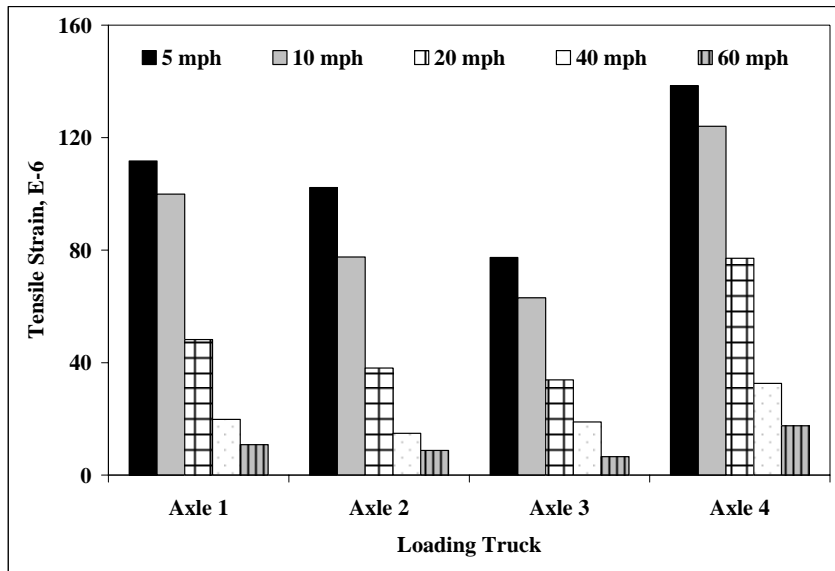
(a) tensile strain at the bottom of wearing layer
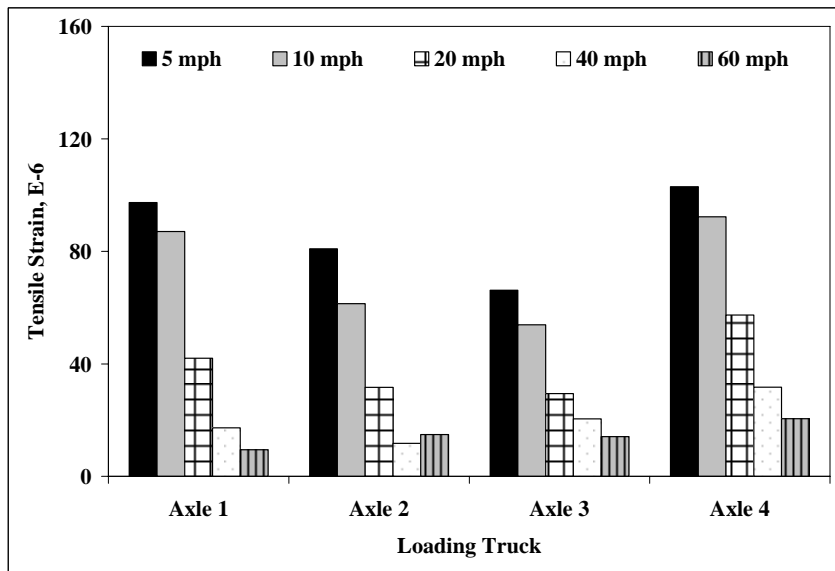
(b) tensile strain at the bottom of binder layer

Figure 25. Strain response of pavement layers at Perry location 2 (measured on 07/17/2008, back load configuration)
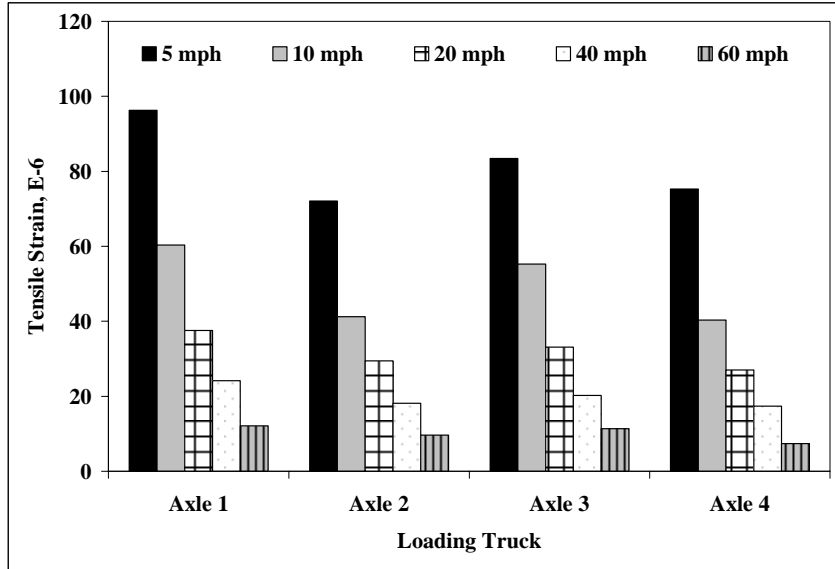
(a) tensile strain at the bottom of wearing layer
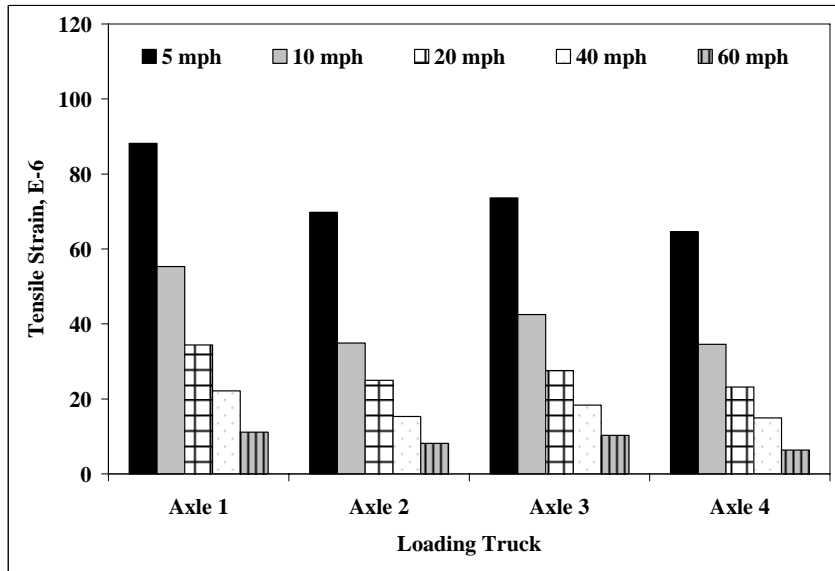
(b) tensile strain at the bottom of binder layer

Figure 26. Strain response of pavement layers at Perry location 2 (measured on 07/17/2008, front load configuration)
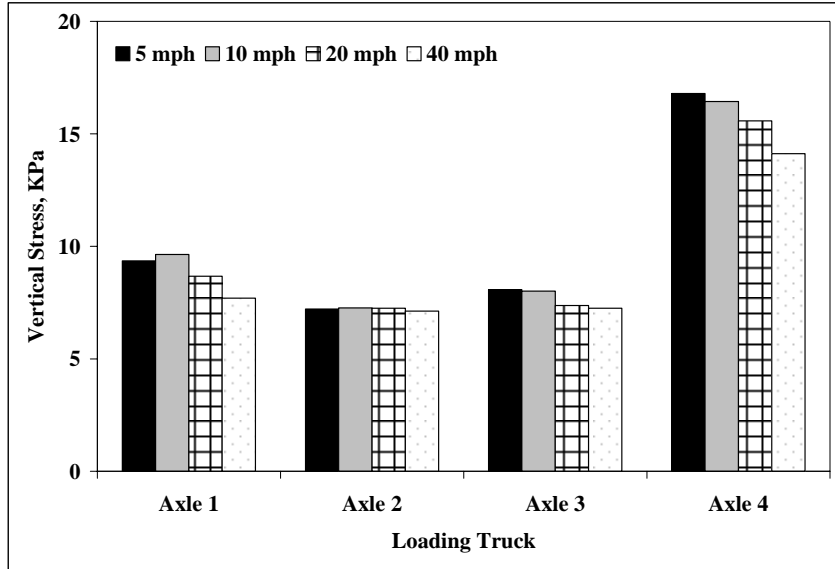
(a) vertical stress at the top of subbase layer
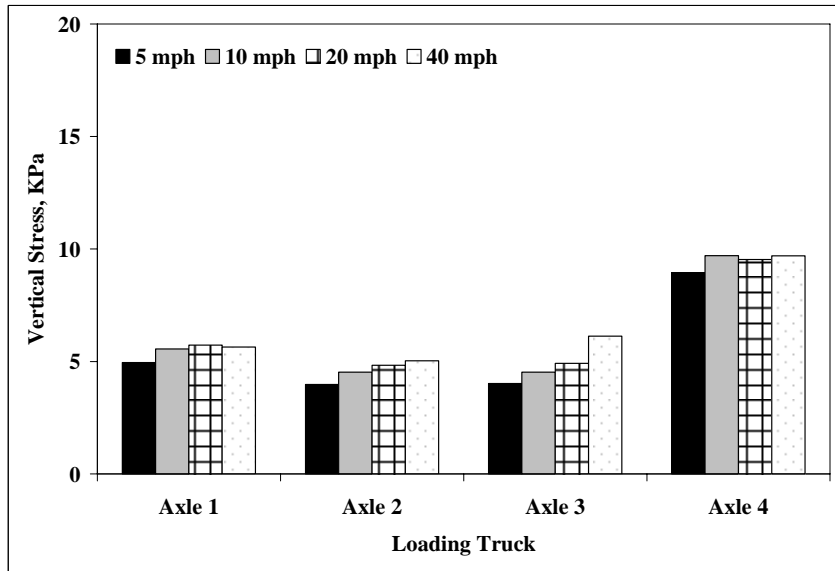
(b) vertical stress at the top of subgrade layer

Figure 27. Stress response of pavement layers at Blair location 1 (measured on 03/27/2008, back load configuration)
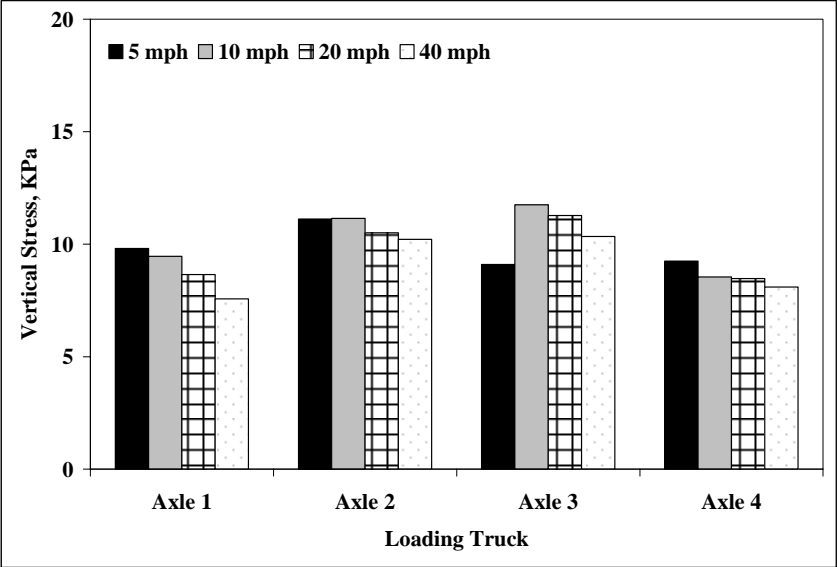
(a) vertical stress at the top of subbase layer
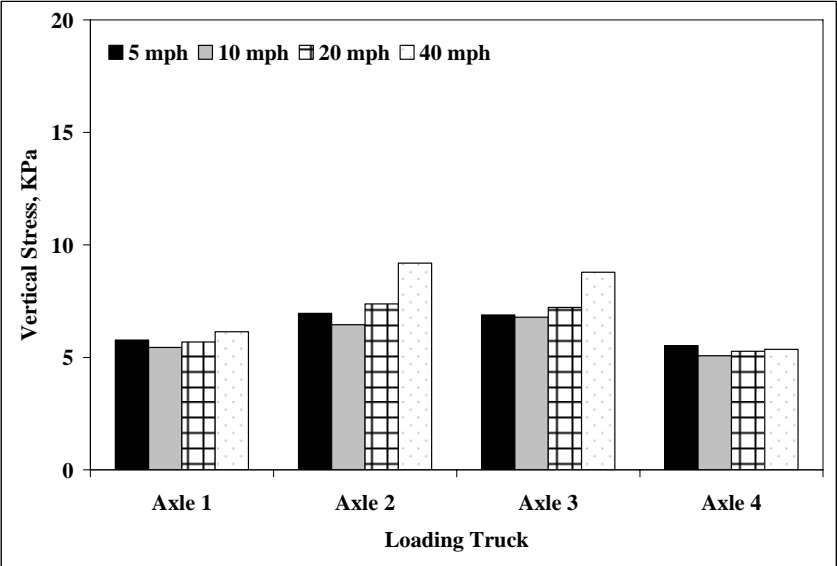
(b) vertical stress at the top of subgrade layer

Figure 28. Stress response of pavement layers at Blair location 1 (measured on 03/27/2008, front load configuration)
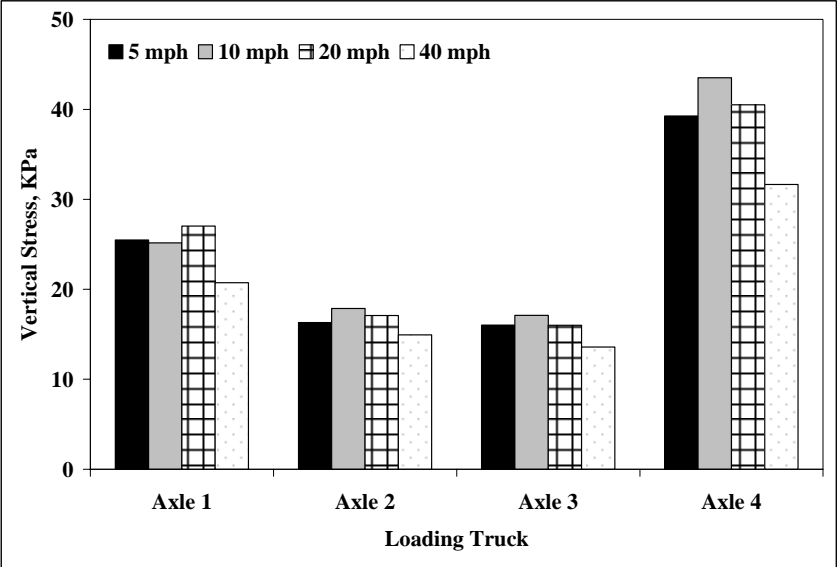
(a) vertical stress at the top of subbase layer
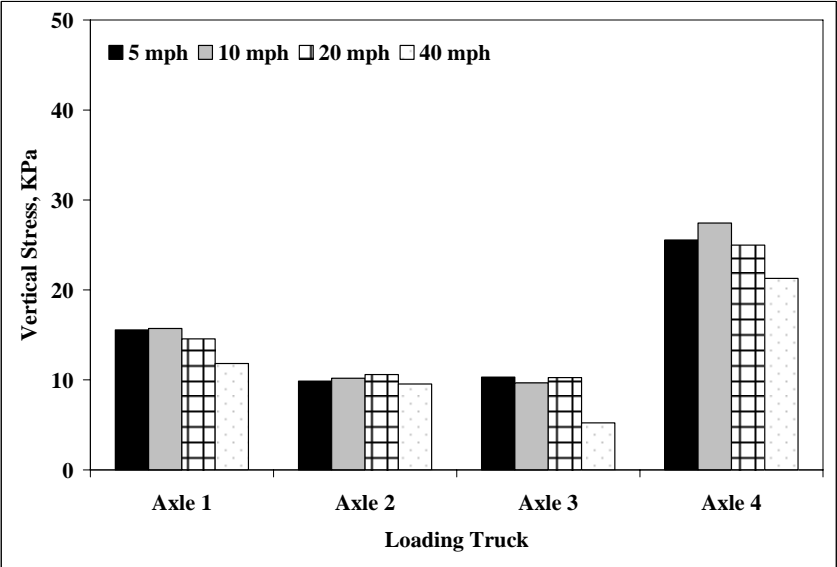
(b) vertical stress at the top of subgrade layer

Figure 29. Stress response of pavement layers at Blair location 2 (measured on 06/24/2008, back load configuration)
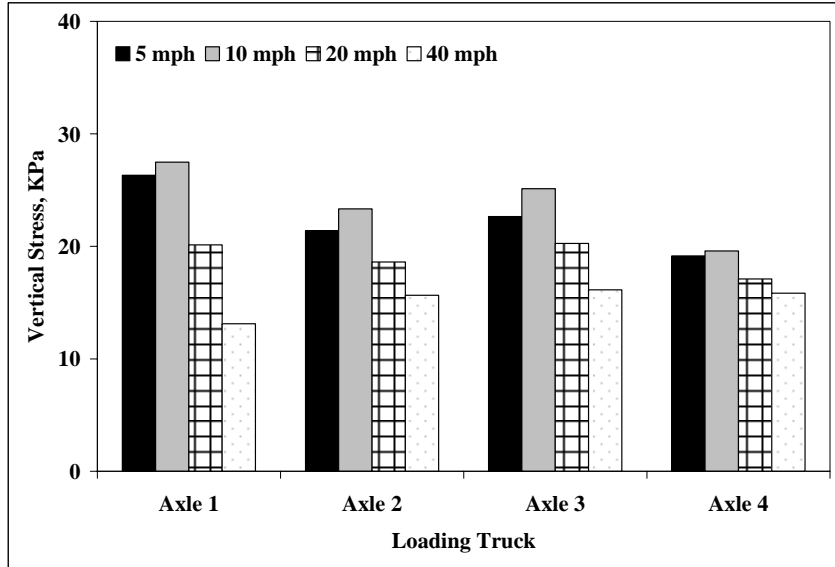
(a) vertical stress at the top of subbase layer
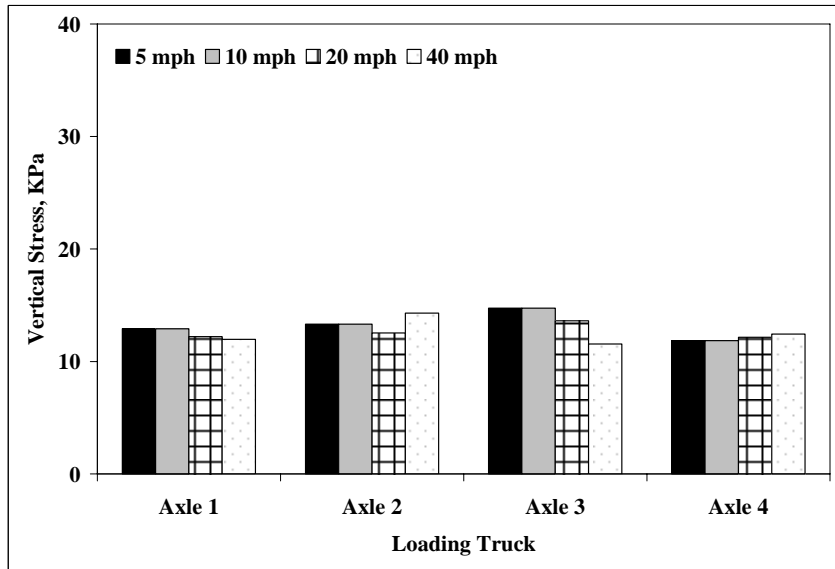
(b) vertical stress at the top of subgrade layer

Figure 30.   Stress response of pavement layers at Blair location 2 (measured on 06/24/2008, front load configuration)

CHAPTER 4: DEFLECTION DATA

During Phase II, falling weight deflectometer testing was conducted at the Blair site. The Blair site was selected for a number of reasons, including its age and condition, but the primary reason was that backcalculation efforts using the Phase I data were only marginally successful. Therefore, it was desirable to collect data at additional load levels and to collect the load-deflection history data during testing. Finally, it provided an opportunity to collect simultaneous data from the embedded instrumentation and the FWD.

All falling weight deflectometer testing was performed by the Pennsylvania Department of Transportation (PennDOT) with their Dynatest falling weight deflectometer (Figure 31). The Dynatest FWD, as utilized during Phase II, is configured with a 150-mm (5.91-in) radius load plate, with sensors spaced at 305-mm (12-in) intervals from the center of the load. One sensor is behind the load, one is centered under the load plate, and the remaining sensors are in front of the load. FWD testing was performed at four load levels (LLs): 2 drops at 33.36 kN (7,500 lb), 2 drops at 46.71 kN (10,500 lb), 2 drops at 64.50 kN (14,500 lb), and 2 drops at 84.52 kN (19,000 lb). A total of three instrumentation locations were included in this study. At each instrumentation location, FWD testing was repeated three times to ensure data quality. The load-deflection history data were collected for all FWD drops.

Figure 31. FWD data collection

Layer Moduli from Backcalculations

It is the nature of FWD analysis that extensive user input and judgment is required. Batch processing of FWD data may be suitable for pavement management purposes, but as discovered during the Long-Term Pavement Performance (LTPP) efforts, it is typically not adequate for research usage. The analysis steps conducted in this study were similar to those utilized for the

LTPP data analysis. The MODCOMP5 computer program was used for backcalculations because of its program features, including nonlinear analysis (Irwin 2000).

The deflections are first normalized to the approximate (rounded) mean load for each load level. The mean and standard deviation of deflection for each sensor is computed, and any outliers noted and removed from averaging. The normalized deflections for each specific drop height at each test point location are averaged. For a test location, this results in two basins being averaged. This assists in minimizing the effect of random measurement error. This is especially important for thick, stiff pavement sections, where the magnitude of deflections is small, and the impact of measurement error is therefore larger. The normalized deflection basins are examined for shape. Deflection basins with a significant decrease in measured deflections between two adjacent sensors are noted, but are not included in the analysis. An example of FWD load and deflection data is given in Figure 32.

Material Characterization

Viscoelastic materials, such as asphalt concrete (AC), have elements of both elastic and viscous material behaviors and exhibit time-dependent strain when subjected to a stress. This strain occurs such that a part of the strain (elastic part) appears instantaneously, and the remaining part of the strain (viscous part) increases with time at a decreasing rate. Given that FWD testing is a relatively high frequency (short loading time, such as .03 sec) test, the backcalculation is largely simplified if AC layers can be modeled as elastic materials. Figures 33a and 33b plot the load-deflection history (hysteresis loop) for sensor 1. For both low and high temperatures, most or all of the induced deflections are recovered immediately after the FWD load pulse returns to zero. Therefore, characterizing AC layers of the selected pavement structure as elastic materials will not greatly influence the effectiveness of backcalculated layer moduli, because the viscoelastic properties are insignificant in relation to the total measured deflection.
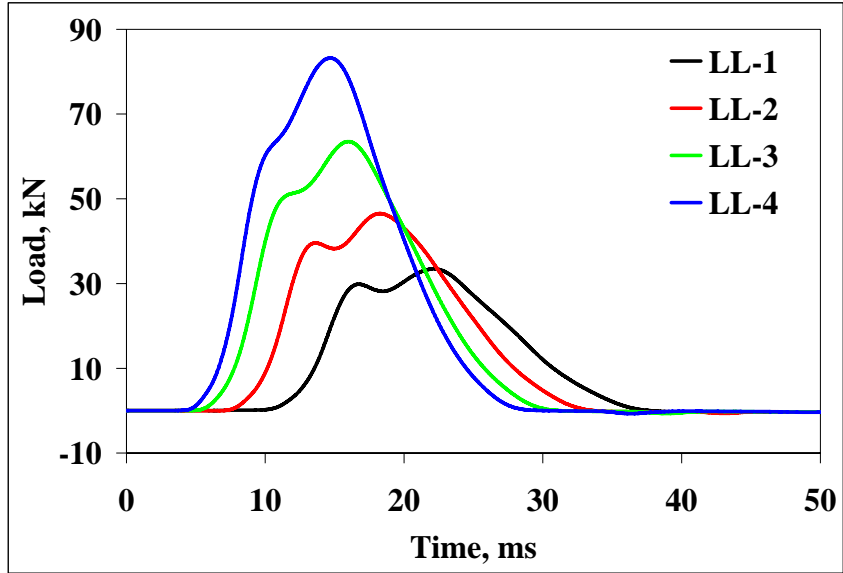
(a) loads
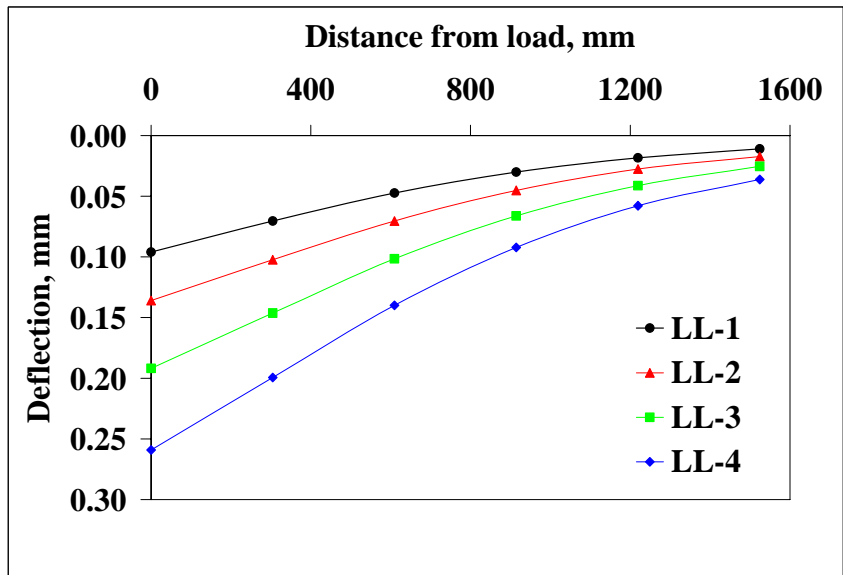
(b) deflections

Figure 32. Example of load and deflection data from FWD testing
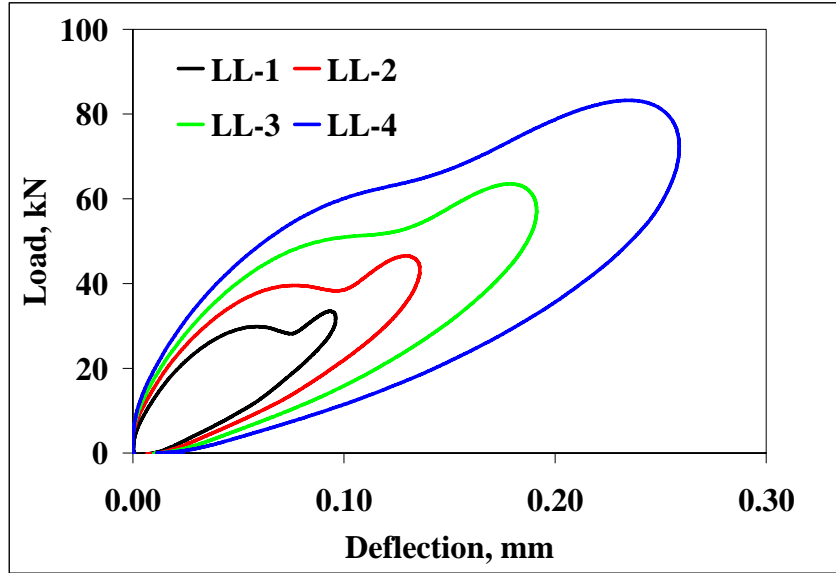
(a) low temperature, 10:30, Location 1
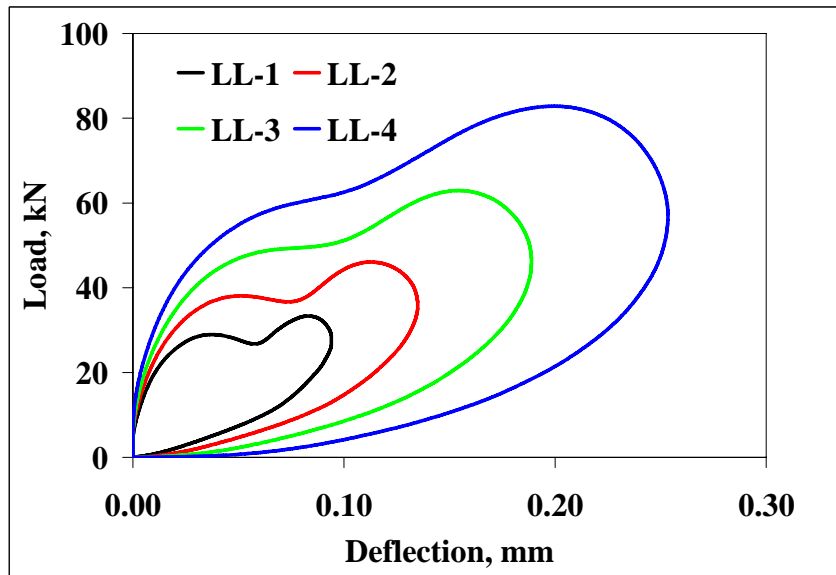
(b) high temperature, 13:00, Location 2

Figure 33. Hysteresis loops of FWD data from sensor 1

In MODCOMP5, pavement materials' responses (stress or strain) to the FWD load can be modeled as either linear or nonlinear. By definition, the linear or nonlinear modes mean that as the load increases or decreases on the pavement surface, the response at a given point will increase or decrease linearly or nonlinearly, respectively. Response data from strain gages and pressure cells were used to examine the linearity of the pavement structure at the Blair site. Average values from multiple FWD testing locations and measurement repetitions are presented

in Figure 34. Figures 34a shows horizontal strains in AC layers, whereas Figure 34b shows vertical stress in granular materials as a function of the FWD load level. All pavement layers, except the subgrade, exhibit linear responses.
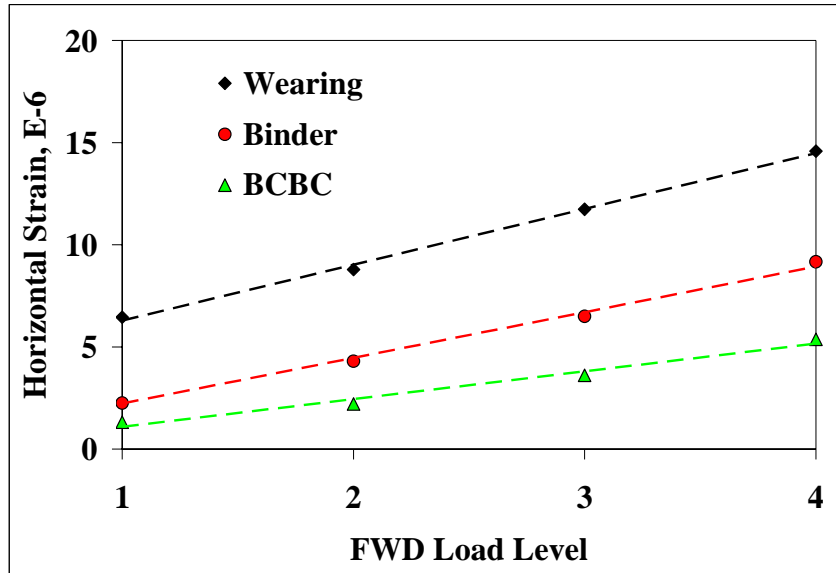
(a) horizontal strain in AC layers
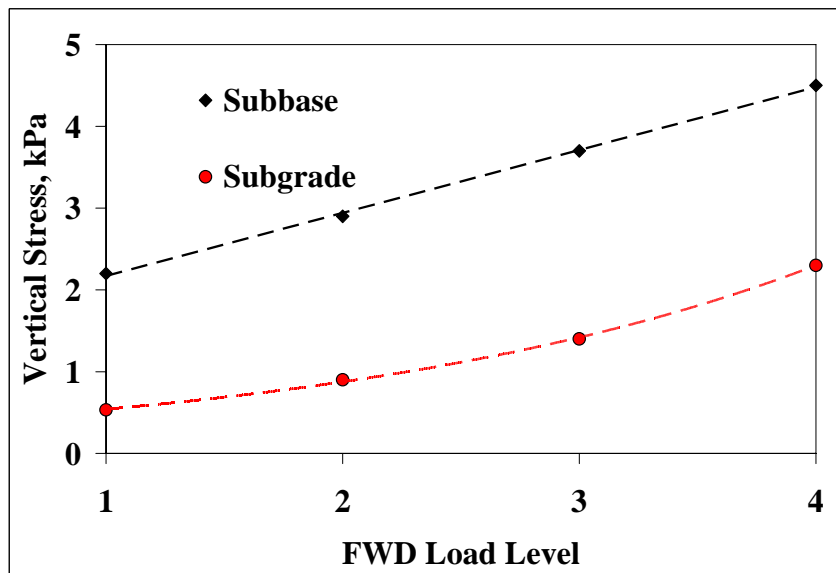
(b) vertical stress in subbase and subgrade

Figure 34. Influence of FWD load level on pavement responses

Granular materials often exhibit stress-dependent elastic moduli. The modulus of a stress-dependent material changes as the overburden pressure changes with depth and as the load stress changes with radial distance from the load. Therefore, the use of nonlinear models is primarily a means of taking into consideration the horizontal effect of the load stress variation in a layer. The nonlinear model used for subbase layer modulus, E, is expressed as:

$$E = K_1 S^{K_2} \tag{1}$$

in which S is the vertical stress that is always compressive, and K_1 and K_2 are model constants. When the stress is zero, then $E = K_1$, and thus K_1 is equal to the initial tangent modulus.

Analysis Results

MODCOMP was executed and strategies revised until a root mean square (RMS) error less than one percent was achieved. The RMS error is a measure of the "goodness of fit" of the deflection basin. The backcalculated layer moduli are used in MODCOMP to compute a set of deflections at the same distance from the FWD load where the deflections were measured. The difference is calculated as a percent error at each sensor. The RMS error is a composite value that is derived from the set of individual errors. MODCOMP also checks the modulus rate of change to help ensure that a wide range of moduli would not produce the same RMS error and that a stable solution has been achieved; one percent was also used for this convergence criterion.

The selected pavement was a traditional flexible pavement structure. It was modeled for backcalculation as a combined AC surface (wearing and binder), BCBC, and granular 2A subbase. A rigid deep layer was introduced at approximately 2000 mm below the surface. The rigid layer was modeled as an unknown layer so that the layer modulus would not remain fixed. The reason for introducing a variable rigid layer was to account for varying depth and quality of the bedrock (Stoffels et al. 2006).

The backcalculated AC, subbase, and subgrade moduli were fairly consistent, as summarized in Table 4. The subbase moduli appear very low but are consistent. During Phase I, FWD testing at three load levels, and without load-deflection histories being recorded, was performed on five different dates in different seasons since construction. Linear elastic backcalculations on all of those data sets also indicated very low subbase moduli.

Laboratory versus Field AC Moduli

Comparisons of elastic moduli obtained from the laboratory and the FWD backcalculations for the upper and lower AC layers are provided in Figures 35a and 35b, respectively. The backcalculated moduli were always higher than the laboratory-determined values. The observation is in general agreement with the suggestion by the 1993 AASHTO design guide (Stolle and Hein 1989) that the FWD backcalculated moduli are typically higher than the laboratory-determined moduli. The maximum divergence between these two moduli, 4349 MPa, occurred when FWD testing was performed at testing location 3. Compared to the other two testing locations, the pavement temperature was significantly higher at 1:00 p.m. In addition, the layer moduli obtained from backcalculations do not decrease as significantly as pavement temperature increases (i.e., from testing location 2 to location 3). The differences

between layer moduli obtained from backcalculations and laboratory complex modulus can be explained in at least three parts. First, laboratory-determined moduli represent intact, and for the most part homogeneous, materials, while the backcalculated moduli represent a kind of effective moduli. All material orientations, thickness variations, confinement, interfaces, and micro- and macro-cracks make the effective moduli backcalculated from in-situ FWD deflections a field characteristic of the entire pavement structure. Second, the uniaxial compression loading mode used in the complex modulus test does not reflect the stress state or load pulse in the field. For example, fatigue cracking usually initiates from the bottom of AC layer because of bending-induced tension; FWD testing also induces a downward deflection or bending. Third, the laboratory specimens were tested at a constant and uniform temperature, whereas the backcalculated moduli represent a composite modulus that has a built-in temperature gradient from the top to the bottom of each AC layer. In addition, the linear interpolation of the mid-depth layer temperature may introduce errors in extracting modulus values from $|E^*|$ master curves. Finally, a variety of other factors not discussed here but found in the literature might also contribute.

Table 4. Summary of layer moduli from backcalculation

Location	Repetition	Time	Surface Modulus (MPa)	BCBC Modulus (MPa)	Subbase Modulus (MPa)	Subgrade K₁ (MPa)	Subgrade K₂	Stiff Layer Modulus (MPa)	RMS (%)
1	1	10:43	10534	9241	34	415	-0.572	428	0.95
1	2	10:44	10457	9103	36	426	-0.597	435	0.92
1	3	10:46	10390	9172	37	441	-0.541	461	0.71
1	*Mean*		*10460*	*9172*	*36*	*427*	*-0.570*	*442*	*0.86*
	Standard Deviation		*72*	*69*	*2*	*13*	*0.028*	*18*	*0.13*
2	1	10:21	11341	9172	36	452	-0.535	439	0.83
2	2	10:24	11310	9034	40	415	-0.516	444	0.98
2	3	10:27	11417	9172	42	428	-0.509	490	0.91
2	*Mean*		*11356*	*9126*	*39*	*432*	*-0.520*	*458*	*0.91*
	Standard Deviation		*55*	*80*	*3*	*19*	*0.013*	*28*	*0.08*
3	1	12:58	10828	8966	35	414	-0.531	406	0.51
3	2	13:00	10672	9093	31	444	-0.555	415	0.63
3	3	13:03	10783	9124	34	408	-0.506	451	0.75
3	*Mean*		*10761*	*9061*	*33*	*422*	*-0.531*	*424*	*0.63*
	Standard Deviation		*80*	*84*	*2*	*20*	*0.025*	*24*	*0.12*
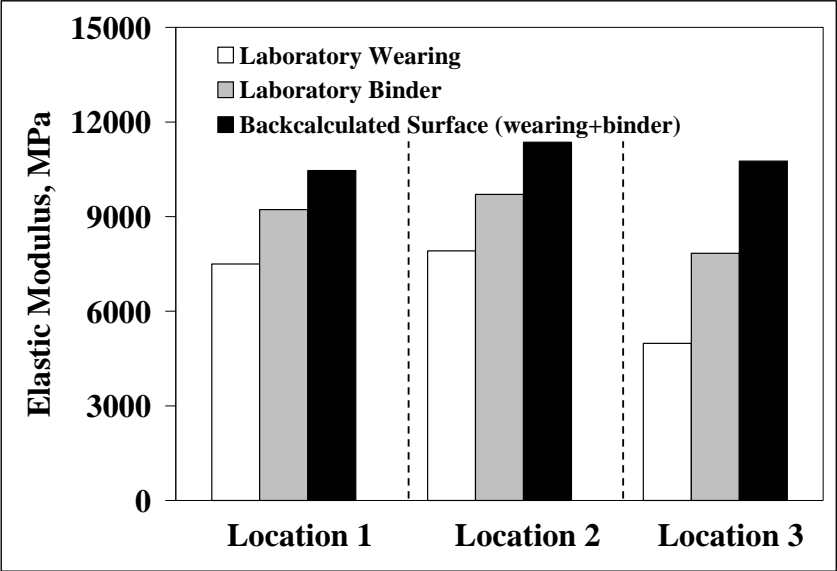
(a) wearing and binder combined layer
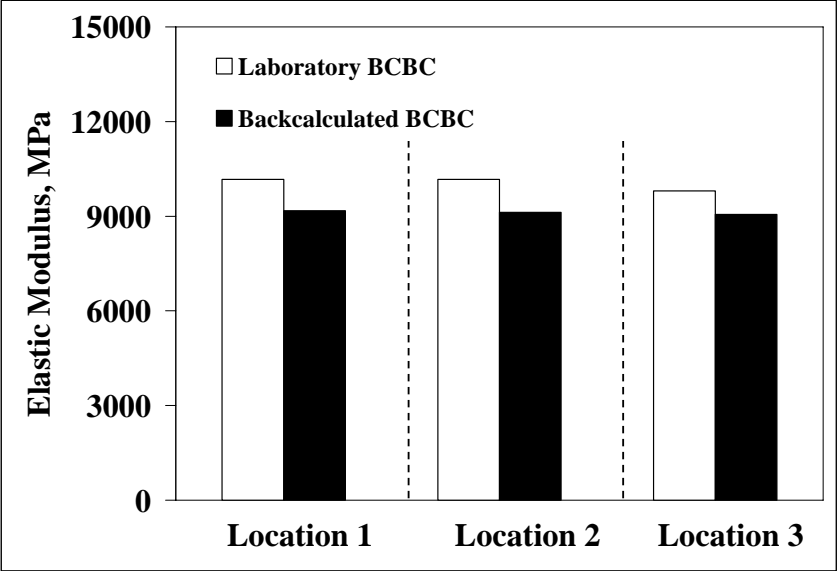
(b) BCBC layer

Figure 35. Comparison of layer elastic moduli

CHAPTER 5: SEISMIC DATA

The research conducted in the NCHRP 10-44A project entitled "Determination of In-situ Material Properties of Asphalt Concrete Pavement Layers" was intended to identify and develop methods for determining the in-situ resilient modulus and thickness of the AC pavement layers in flexible pavements and resurfacing of Portland cement concrete pavements, and to improve the reliability of deflection testing procedures for determining in-situ properties. Falling Weight Deflectometer (FWD), Seismic Pavement Analyzer (SPA), Portable Seismic Pavement Analyzer (PSPA), Ground Penetration Radar (GPR), and Dynamic Cone Penetrometer (DCP) were evaluated and conducted on 10 test sites. The researchers concluded that FWD and GPR were the best current combination of technologies to effectively measure the AC modulus and thickness, respectively. However, seismic methods were also found to provide comparable results to FWD. In addition, a fairly good relationship between the AC modulus from the SPA and that determined from the resilient modulus tests existed. It was noted that different tests evaluated in NCHRP 10-44A had different loading frequencies. Since AC mixtures are viscoelastic and their mechanistic properties are dependent on temperature and loading frequency, a master curve approach (which combines the effect of temperature and loading frequency) was recommended to reconcile the differences in test frequencies and to adjust field-measured moduli to relate to a design vehicle speed.

The objectives of the SISSI Phase II seismic data collection and analysis were to:
- Compare the modulus of AC materials determined from laboratory complex modulus tests and from in-situ nondestructive test (NDT) using the PSPA.
- Evaluate the field performance of SISSI sites using the PSPA.

A total of three SISSI sites, Tioga, Warren, and Delaware, were included.

Spectral Analysis of Surface Waves

If an elastic half-space is disturbed by a vertical impact on the surface, two types of waves will propagate in the medium: body and surface waves. Body waves propagate radially outward in the medium and are composed of two different types: compression and shear waves. These waves are differentiated by the direction of particle motion relative to the direction of wave propagation. Particle motions associated with shear waves are perpendicular to the direction of wave propagation, whereas particle motions associated with compression waves are parallel to the direction of wave propagation. Surface waves resulting from a vertical impact are primarily Rayleigh waves, which propagate away from impact along a cylindrical wavefront near the surface of the medium.

The Spectral Analysis of Surface Wave (SASW) method can be used for in-situ evaluation of elastic moduli and layer thicknesses of layered systems like soils and pavements (Nazarian and Stokoe 1984). The method is based on the phenomenon of Rayleigh wave dispersion in layered systems, i.e., the phenomenon that the velocity of propagation is frequency dependent. Because shear wave velocity and shear modulus are mainly dependent on the effective stress and density, the SASW method is useful in estimating the changes in material strength and density. In layered media, the velocity propagation of surface waves depends on the frequency (or wavelength) of the wave because waves of different wavelengths sample different

parts of the layered medium. The algorithm of the SASW method determines the velocity-frequency relationship described by the dispersion curve, and then, through the process of inversion or backcalculation, obtains the shear wave velocity profile. Elastic moduli profiles can then be easily obtained using simple relationships with the velocity of propagation and measured or approximated values for mass density and Poisson's ratio. The relationship amongst velocity, V, travel time, Δt, and receiver spacing, ΔX, can be written in the following form:

$$V = \frac{\Delta X}{\Delta t}$$

(2)

In this equation, V can be the propagation velocity of any of the three waves (i.e., compression wave, V_P; shear wave, V_S; or surface (Rayleigh) wave, V_R). Knowing wave velocity, the modulus can be determined in several ways. Elastic modulus, E, can be determined from shear modulus, G, through the Poisson's ratio, υ, using:

$$E = 2(1+\upsilon)G$$

(3)

Shear modulus can be determined from shear wave velocity, V_S, and mass density, ρ, using:

$$G = \rho V_S^{\,2}$$

(4)

Portable Seismic Pavement Analyzer

The Portable Seismic Pavement Analyzer (PSPA), as shown in Figure 36, is a device designed to determine the modulus of the top pavement layer in real-time. The PSPA consists of two receivers (accelerometers) and a source packaged into a hand-portable system, which can perform high frequency seismic tests.
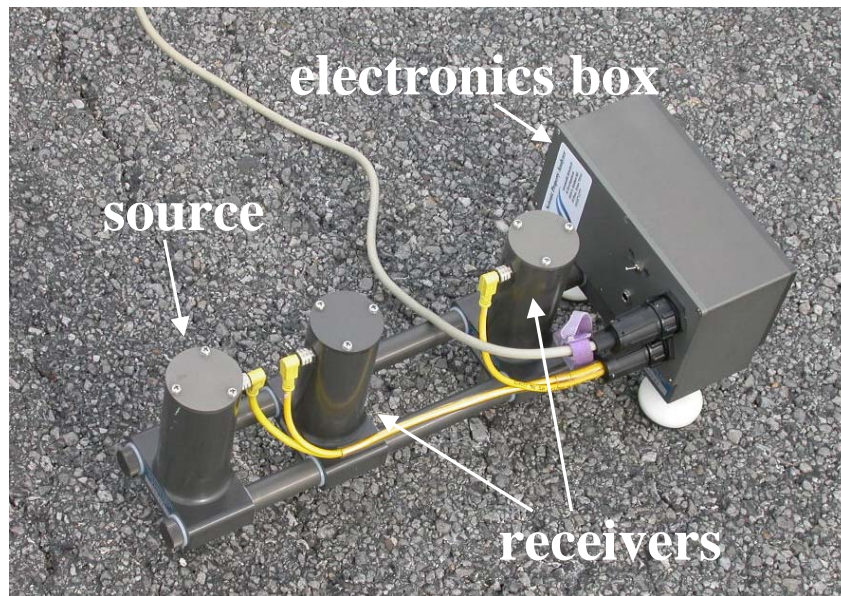
Figure 36. Portable Seismic Pavement Analyzer (PSPA)

The analysis method implemented in the PSPA is called the ultrasonic surface waves (USW) method, which is a simplified version of the SASW method. The major distinction between these two methods is that, in the USW method, the modulus of the top pavement layer can be directly determined without an inversion algorithm (Nazarian et al. 1993). Since surface waves (Rayleigh, R waves) contain most of the seismic energy, the USW method utilizes the surface wave energy to determine the variation in modulus with wavelength. A detailed review of NDT applications using surface wave methods can be found elsewhere (Nazarian et al. 1993, Goel and Das 2006). At wavelengths less than or equal to the thickness of the uppermost layer, the velocity of propagation is independent of wavelength. Therefore, if one simply generates high-frequency (short-wavelength) waves, and if one assumes that the properties of the uppermost layer are uniform, the shear wave velocity of the upper layer, V_S, can be calculated from surface wave velocity, V_R:

$$V_S = V_R(1.13 - 0.16\upsilon)$$

(5)

Then, the elastic modulus of the top layer, E, can be determined:

$$E = 2\rho(1+\upsilon)\left[(1.13 - 0.16\upsilon)V_s\right]^2$$

(6)

PSPA Test

To collect data with a PSPA, the technician initiates the testing sequence through the computer. The high-frequency source is activated four to six times. The output of the two receivers from the last three impacts are saved and averaged (stacked). The other (pre-recording) impacts are used to adjust the gains of the amplifiers. The gains are set in a manner that optimizes the dynamic range.

Typical voltage output of the three accelerometers are shown in Figures 37a and 38a for Delaware and Warren, respectively. In these plots, the red line represents the electronic source, while the black and green lines represent accelerometers 1 and 2. An actual variation in the modulus with wavelength from the time records (data reduction process) is shown in Figures 37b and 38b for Delaware and Warren sites, respectively. For practical reasons, the wavelength is simply relabeled as depth. In that manner, the operator of the PSPA can get a qualitative feel for the variation in modulus with depth. The red solid line represents the average seismic modulus of the total AC layers. It should be noted that the modulus at a depth smaller than 50 mm could not be determined because of the fixed spacing between two accelerometers on the PSPA. The dispersion curve shown in Figures 37b and 38b is developed from the phase spectra shown at the bottom of the same figure. The phase spectrum, which can be considered as an intermediate step between the time records and the dispersion curve (Nazarian et al. 1993), is determined by conducting Fourier transform and spectral analysis on the time records from the two accelerometers. This step makes the determination of the modulus with wavelength much easier. A procedure for conducting PSPA tests was developed during Phase II of the SISSI project. Details on this procedure are included in Appendix D.
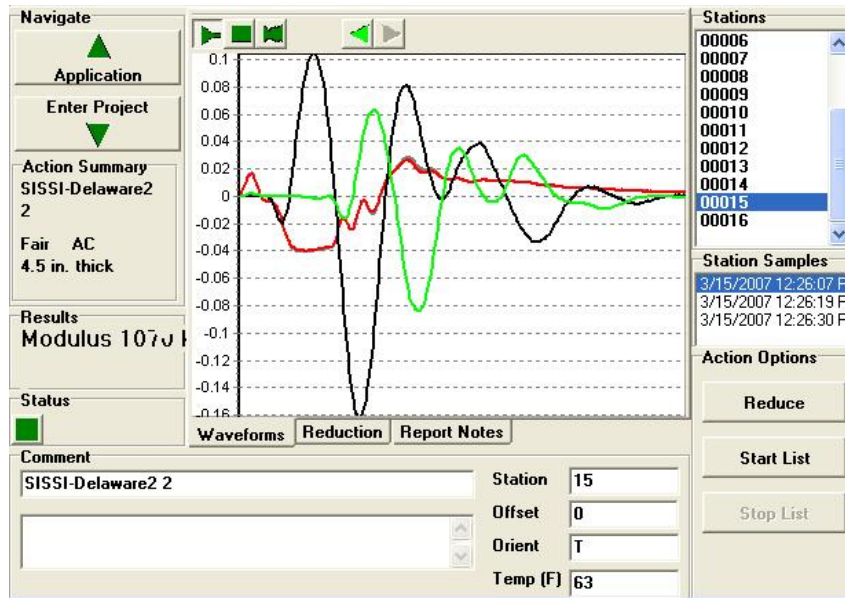
(a) signal
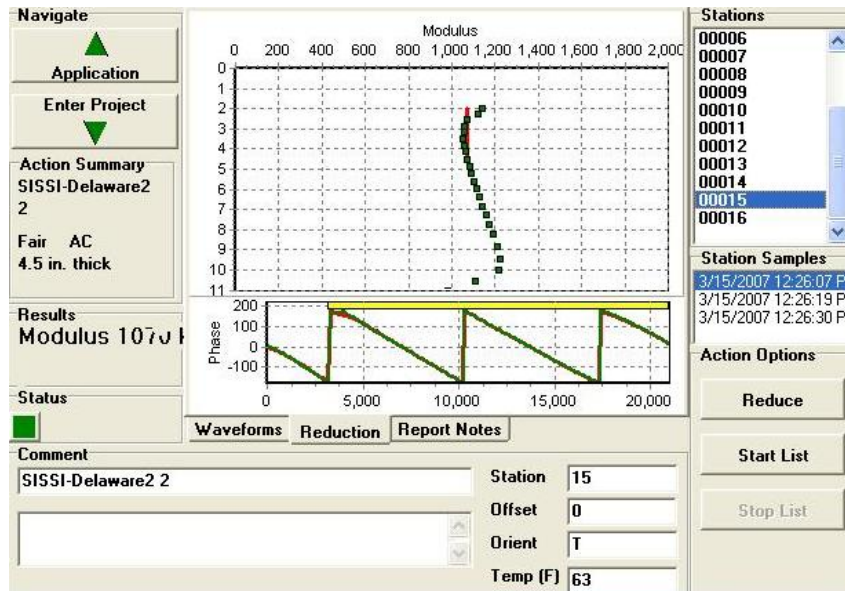
(b) data reduction

Figure 37. Sample PSPA data from Delaware
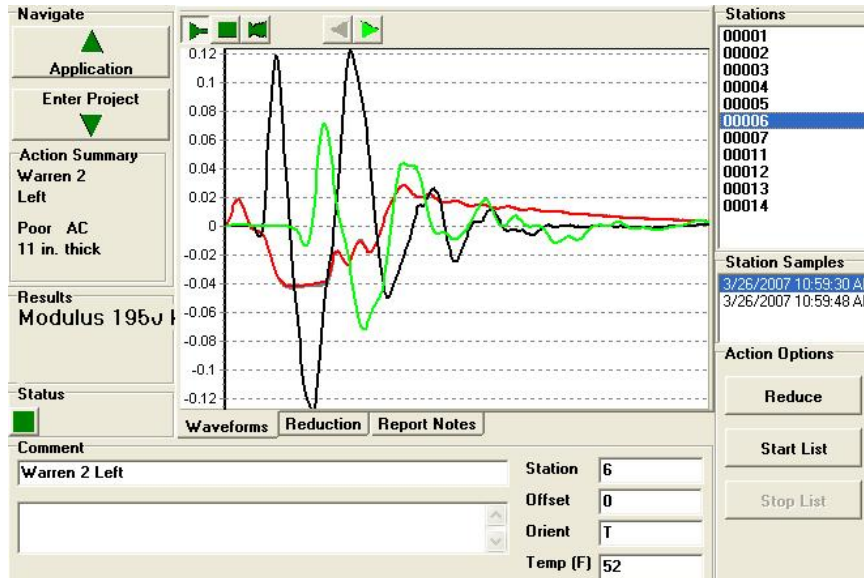
(a) signal
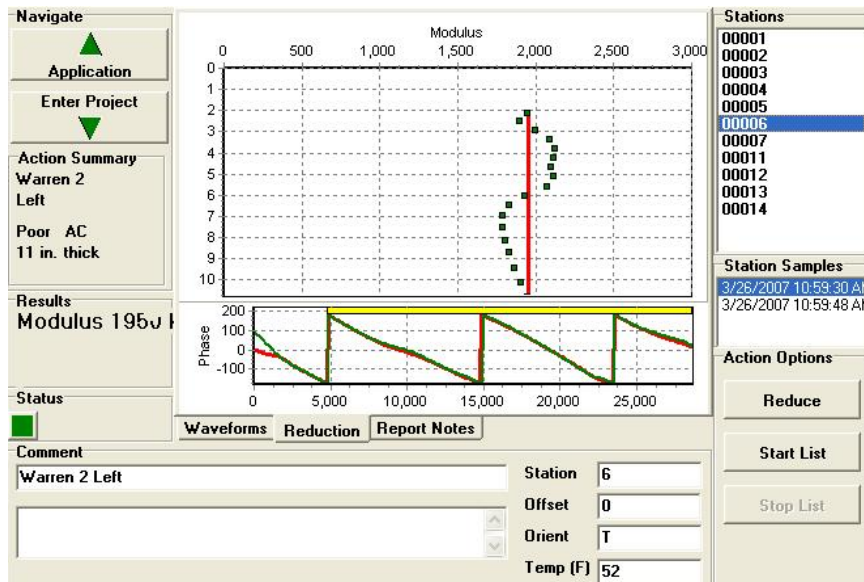
(b) data reduction

Figure 38. Sample PSPA data from Warren

Variability Study of Seismic Data

An experiment was designed to evaluate the variability of seismic moduli collected using PSPA. For each SISSI site and location, six measurements were conducted in two orientations, longitudinal and transverse, before and after the center of the pavement section. The longitudinal orientation is parallel to the traffic direction, while the transverse orientation is perpendicular.

Pavement surface temperatures during PSPA tests were also recorded. The PSPA data collected from the Delaware site are presented in detail in this section.

Total Variability

Two example sets of seismic modulus measurements are presented in Tables 5 and 6. In general, similar grand average seismic modulus values were observed at different locations (E_{L1}=9000MPa vs. E_{L2}=8000MPa) and sections (E_{before}=8200MPa vs. E_{after}=7800MPa). No significant difference was observed between seismic modulus values obtained around longitudinal and transverse strain gages because of the relatively small difference between the coefficients of variation (COV). These observations suggest fairly good construction and instrumentation quality at Delaware.

Variability Due To Measurement and Material Variation

A summary of statistics of all measurements is provided in Table 7. A graphic presentation of Table 4 (Figure 39) suggests two variance components in the total variability: measurement variation and location variation. However, this variability component cannot be separated without a variance component analysis (Yin et al. 2006), which is not within the scope of this study. The combined variability of PSPA data due to measurement and material variation is quite significant when PSPA is moved in a small area, such as from Longitudinal A to Longitudinal B. An averaged COV of 10 percent is expected in the field. This variability level is much higher than the value of 3.5 percent reported by Alexander (1996) but closer to a value of 7 percent from a more recent study (Celaya and Nazarian 2006).

Table 5. In-situ seismic modulus of Delaware location 1 before center line (surface temperature 17°C)

PSPA Orientation	Measurement No.	Date and Time	Average AC Seismic Modulus, MPa
Longitudinal	1	3/15/2007 11:16	8142
Longitudinal	2	3/15/2007 11:17	8142
Longitudinal	3	3/15/2007 11:17	8211
Longitudinal	4	3/15/2007 11:19	8349
Longitudinal	5	3/15/2007 11:19	8211
Longitudinal	6	3/15/2007 11:19	8280
Transverse	1	3/15/2007 11:28	9177
Transverse	2	3/15/2007 11:29	9108
Transverse	3	3/15/2007 11:29	9039
Transverse	4	3/15/2007 11:31	9384
Transverse	5	3/15/2007 11:31	9315
Transverse	6	3/15/2007 11:31	9453

Table 6. In-situ seismic modulus of Delaware location 2 after the center (surface temperature 17°C)

PSPA Orientation	Measurement No.	Date and Time	Average AC Seismic Modulus, MPa
Longitudinal	1	3/15/2007 12:16	8004
Longitudinal	2	3/15/2007 12:16	8073
Longitudinal	3	3/15/2007 12:16	8142
Longitudinal	4	3/15/2007 12:17	8418
Longitudinal	5	3/15/2007 12:18	8280
Longitudinal	6	3/15/2007 12:19	8211
Transverse	1	3/15/2007 12:26	7383
Transverse	2	3/15/2007 12:26	7452
Transverse	3	3/15/2007 12:27	7452
Transverse	4	3/15/2007 12:27	7314
Transverse	5	3/15/2007 12:28	7314
Transverse	6	3/15/2007 12:28	7245

Table 7. Variability due to measurement and location variations

Delaware Location	Relative Location to Center	PSPA Orientation	Statistics		
			Mean, MPa	Standard Deviation, MPa	Coefficient of Variation, %
1	Before	Longitudinal	9396	1457	16
		Transverse	9516	480	5
	After	Longitudinal	9045	767	8
		Transverse	8608	1210	14
2	Before	Longitudinal	8177	727	9
		Transverse	8205	848	10
	After	Longitudinal	7987	343	4
		Transverse	7630	574	8
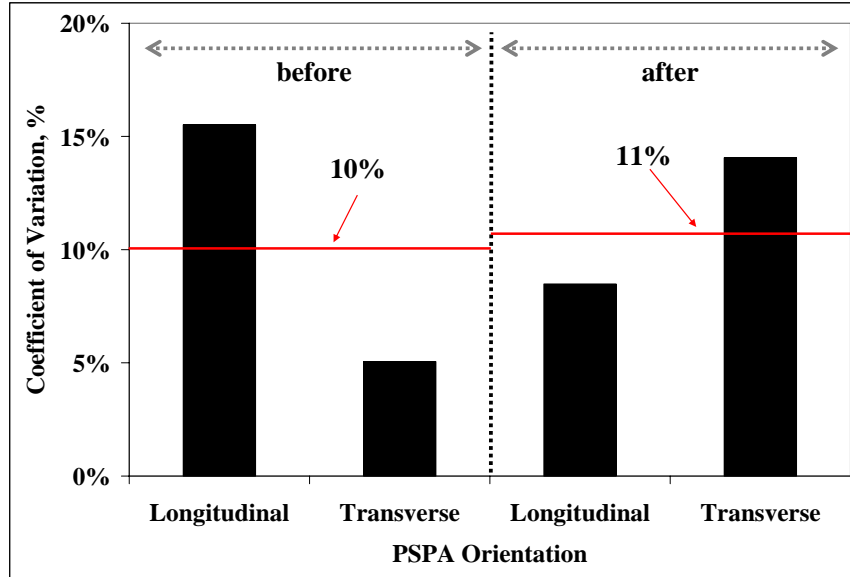
(a) location 1
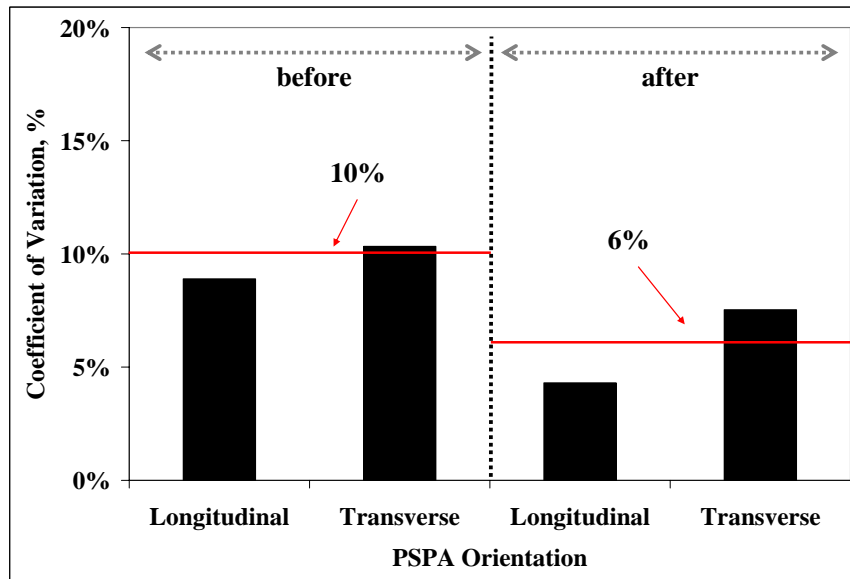
(b) location 2

Figure 39. Variability due to measurement and location variations at Delaware

Variability due to Measurement Variation

Table 8 summarizes the variability of PSPA data due to measurement variation for Delaware locations 1 and 2. Graphic presentations are also provided in Figure 40. The variability within PSPA data is dramatically reduced when only the measurement variation is considered. Overall, excellent agreements are observed among repeated PSPA measurements, which contain an averaged COV of 0.4 percent. This variability level is comparable to a value of 0.5 percent

reported by Alexander (1996) and much lower than a value of 3 percent from Celaya and Nazarian's study (2006). A standard deviation ranging from 50 to 60MPa is expected for in-situ repeated PSPA tests. It is also worth noting that that the variability caused by the measurement variation is dependent upon the magnitude of seismic modulus. Together with the information in the preceding section, it can be concluded that the location variation is mainly caused by the inherent material variability, such as the inhomogeneity induced by aggregates.

Table 8. PSPA measurement variation summary for Delaware (surface temperature 17°C)

Site Location	Relative Location to Center	PSPA Orientation	Statistics		
			Mean, MPa	Standard Deviation, MPa	Coefficient of Variation, %
1	Before	Longitudinal	9361	40	0.4
1	Before	Transverse	9384	69	0.7
1	After	Longitudinal	9660	0	0.0
1	After	Transverse	9637	80	0.8
2	Before	Longitudinal	8050	40	0.5
2	Before	Transverse	8188	40	0.5
2	After	Longitudinal	7314	0	0.0
2	After	Transverse	7291	40	0.5
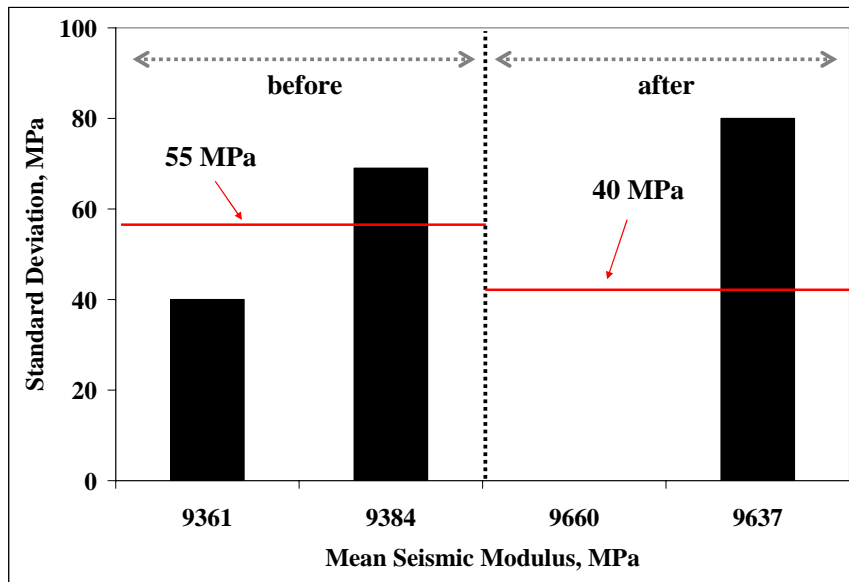
(a) location 1
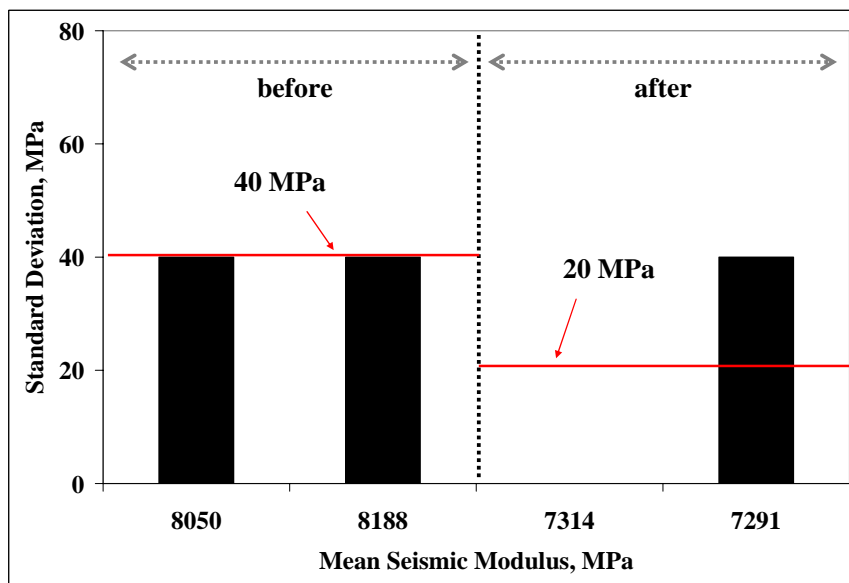
(b) location 2

Figure 40. Measurement variation of seismic modulus at Delaware

Laboratory Dynamic Modulus vs. In-situ Seismic Modulus

Perhaps the most distinct characteristic of AC materials is their temperature and time dependency. Therefore, it is essential to compare the elastic moduli obtained from laboratory complex modulus tests and in-situ PSPA tests at the same temperature and loading frequency. In the following sections, the calculation of pavement temperature and PSPA frequency is first described. Then, comparisons between dynamic and seismic moduli are provided for Warren AC layers. The seismic moduli selected for demonstration purposes were measured at 11:00 a.m. on Mar 26, 2007.

Calculation of Pavement Temperature and PSPA Frequency

At Warren, two thermocouples were placed to monitor pavement temperature. One was at the bottom of the wearing layer (40 mm), and the other was at the bottom of the levelling layer (280 mm). A review of available temperature records on March 26 from 2004 to 2007 indicates that there was generally about -2°C difference between the temperature at the bottom of the wearing and leveling layers. Mid-depth pavement temperatures were approximated from a simple linear interpolation, as shown in Figure 41.

PSPA test frequency is based on AC layer thickness and wave propagation velocity. The velocity of the surface wave can be backcalculated using Equation 6, knowing the seismic modulus for the AC layer from the dispersion curve (Table 9). Then, the representative PSPA test frequency is the velocity of the surface wave divided by half of the AC layer thickness. For the AC layers at Warren, the typical frequencies for binder, BCBC, and leveling layers were 44679, 17623, and 11382 Hz, respectively.
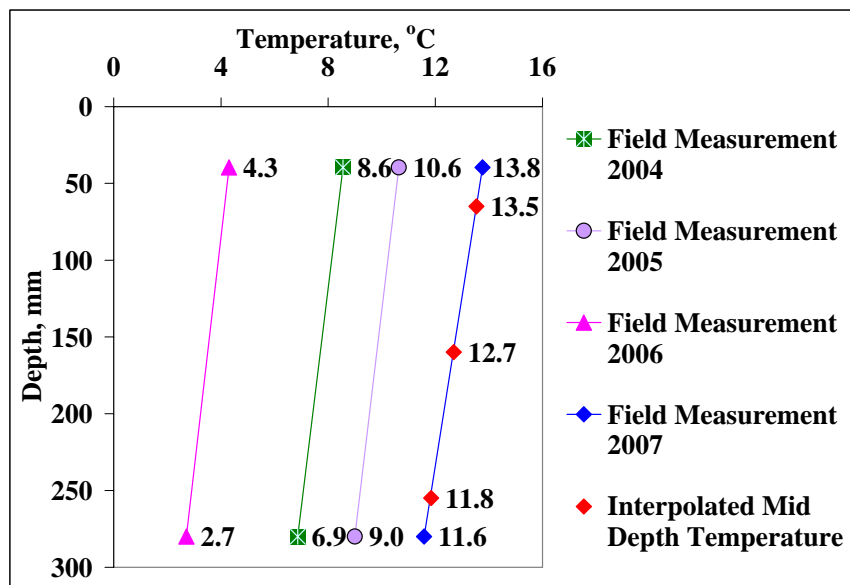
Figure 41. Determination of mid-depth pavement temperature

Table 9. Representative set of seismic modulus values at Warren

Depth, mm	Seismic Modulus, MPa
54	13220
65	13040
75	13810
86	14450
97	14740
107	14480
119	14160
131	14160
142	13730
154	13110
165	12690
178	12490
191	12460
207	12550
222	12720
241	12950
257	13240
275	13550

Comparison at Field and Reference Temperatures

In Figures 42a, 43a, and 44a, the dynamic modulus master curves at field temperatures and seismic modulus are plotted. Since seismic tests provide high-frequency moduli, in all cases the seismic moduli fall on the maximum asymptote of the master curve. As listed in Table 10, exact elastic moduli were extracted from dynamic modulus master curves based upon field temperature and PSPA frequency. It can be concluded that the laboratory complex modulus test always resulted in an elastic modulus about 4000 to 7000MPa higher than the corresponding in-situ seismic modulus.

To compare the dynamic and seismic moduli at the reference temperature of 25°C, an empirical viscoelastic relationship, suggested by Li and Nazarian (1994), for adjusting the AC modulus was used:

$$E_{25} = \frac{E_t}{1.35 - 0.014t} \tag{7}$$

where E_{25} and E_t are seismic moduli at 25°C and t is the mid-depth temperature of the AC layer. Comparisons at 25°C are shown in Figures 42b, 43b, and 44b for the binder, BCBC, and leveling layers, respectively. Similar to the comparison at the field temperature, the laboratory dynamic modulus is higher than in-situ seismic modulus.

58
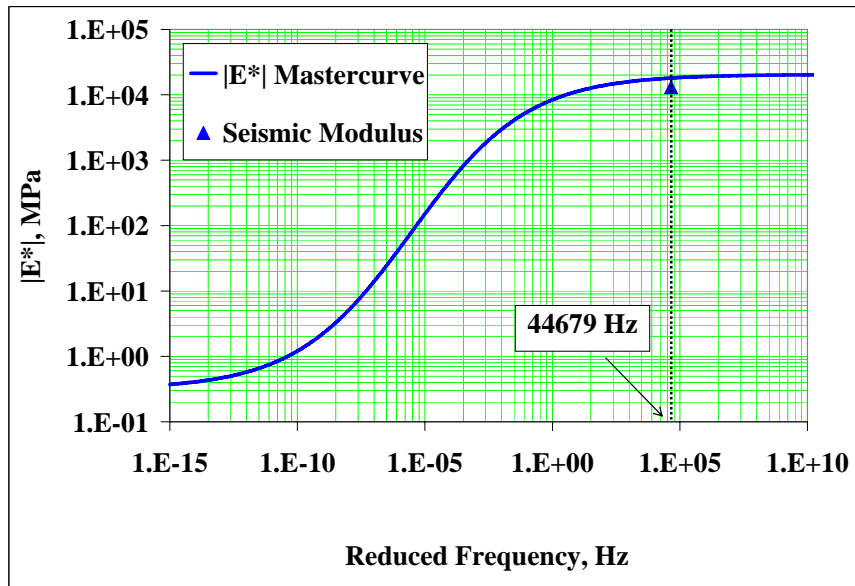
(a) field temperature, 12.4°C
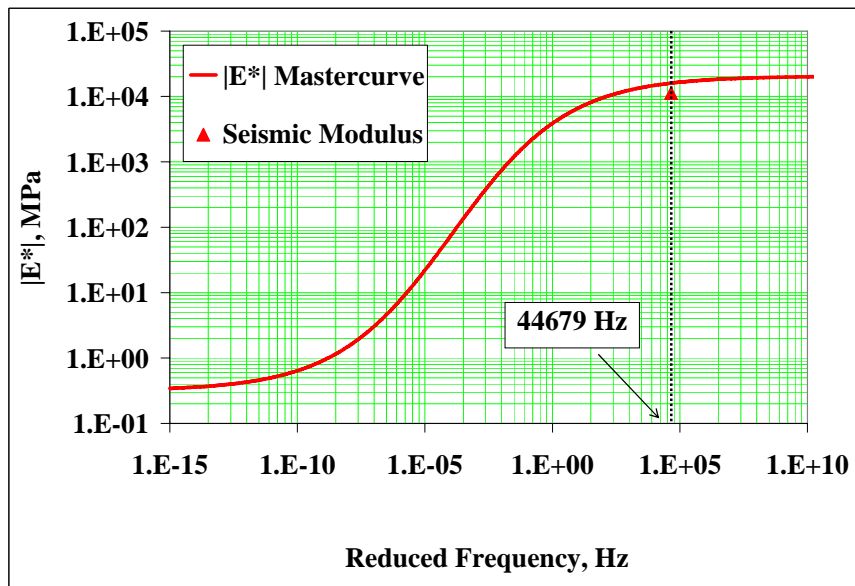
(b) reference temperature, 25.0°C

Figure 42.   Lab dynamic moduli vs. in-situ seismic moduli (Warren binder layer)
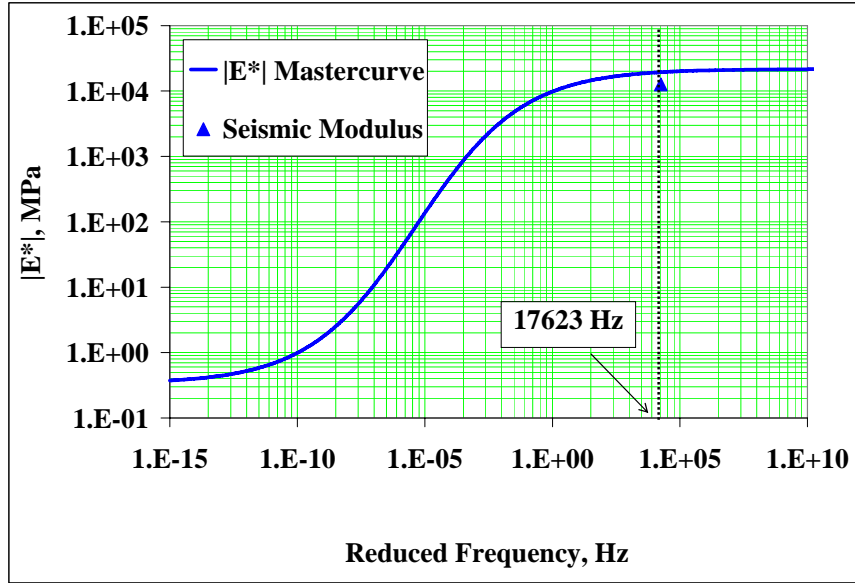
(a) field temperature, 13.5°C
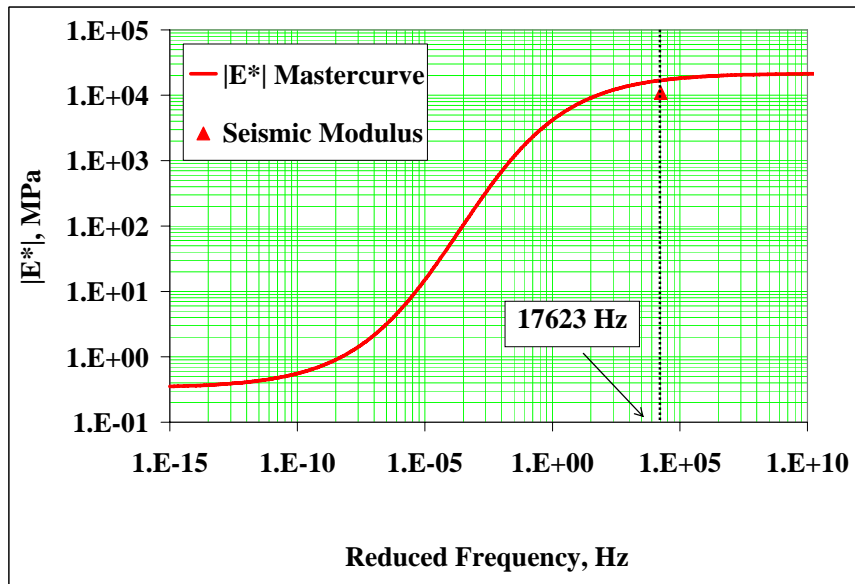
(b) reference temperature, 25.0°C

Figure 43. Lab dynamic moduli vs. in-situ seismic moduli (Warren BCBC layer)
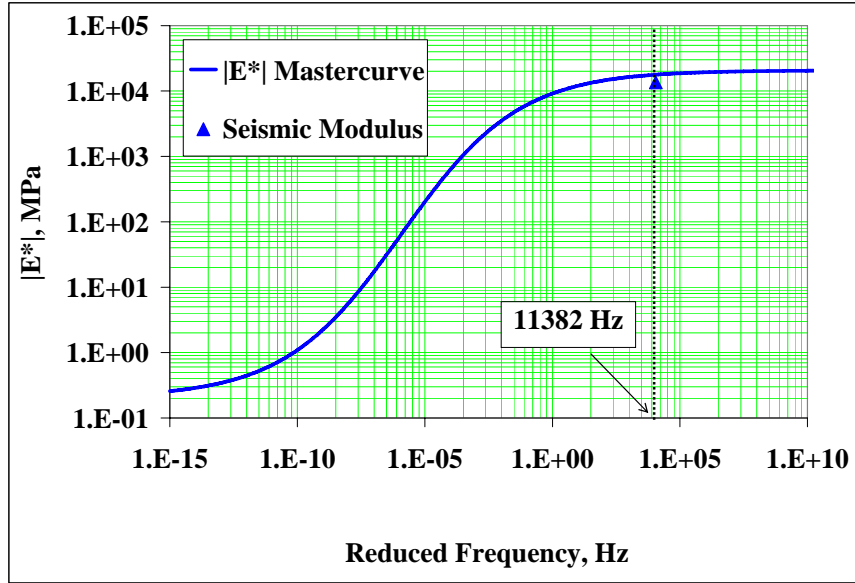
(a) field temperature, 12.7°C
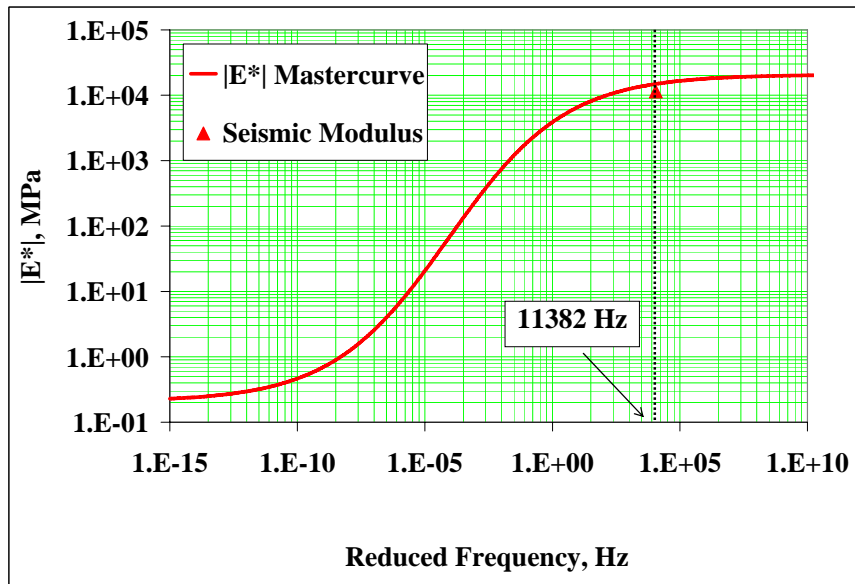
(b) reference temperature, 25.0°C

Figure 44. Lab dynamic moduli vs. in-situ seismic moduli (Warren leveling layer)

Table 10. Comparison summary of dynamic modulus and seismic modulus at Warren

AC Layer	Temperature, °C	Dynamic Modulus, MPa	Seismic Modulus, MPa
Binder	13.5	18091	13050
	25.0	16006	11240
BCBC	12.7	19415	12690
	25.0	16925	10826
Leveling	11.8	17813	13550
	25.0	14921	11437

The Impact of Air Voids and Aging

A number of studies (Saeed and Hall 2003, Tandon et al. 2004) have shown that the seismic modulus and the master curve from complex modulus correlate well; however, when making such comparisons, it is important to consider the impact of air void content and material aging. Celaya and Nazarian (2006) showed that in-situ seismic modulus is very sensitive to the air void of AC mixtures being tested by PSPA. Their study demonstrated that a 1 percent increase of air voids could result in a decrease of 500MPa in seismic modulus measured by PSPA. In this study, pavement cores obtained one to two years after construction revealed air voids very similar to those of the laboratory specimens tested for dynamic modulus. The core air voids were, on average, 0.3 to 0.4 percent higher than the air voids of the dynamic modulus specimens. This lower air void content could have also contributed to the differences observed between the modulus results.

The second important point regards the aging of the asphalt binders. Aging increases binder stiffness and therefore results in a higher mixture modulus. In this study, no attempts were made to determine the aging level of binder and base layers. However, it is expected that since these layers are not exposed to solar radiation and also experience moderate temperatures considering Pennsylvania climate, there is not a significant aging level for the binder and base layers. Significant aging is expected for the wearing course binder, but modulus of this layer is not measured by PSPA.

Evaluation of Field Performance Relative to PSPA Testing

On November 6, 2007, a detailed distress survey was conducted at the Tioga site. The major distresses observed were longitudinal cracks, as shown in Figure 45. Parallel to the distress survey, PSPA data were also collected at a 66-m interval through the pavement section as well as at the locations where distresses were observed. Seismic moduli of the binder layer are plotted in Figure 46. For the entire section, the modulus values range from 7148 to 10446MPa. In addition, much lower seismic moduli were found at 145m north and 188m north. For the low severity longitudinal cracking area (Figure 45a), the representative value of the seismic modulus is 6378MPa. For the high severity longitudinal cracking area (Figure 45b), the representative value of the seismic modulus is 5353MPa.

(a) low severity longitudinal crack along the right edge of the travel lane, 145m north

(b) high severity longitudinal crack along the left edge of the passing lane, 188m north

Figure 45. Distress survey on 11/06/2007
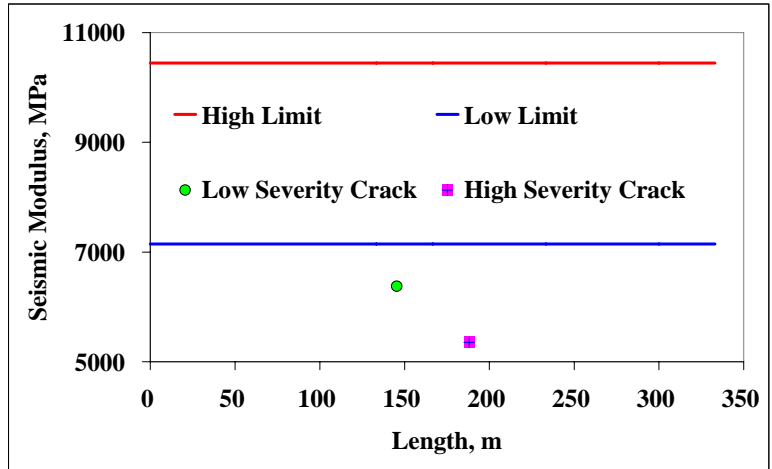
Figure 46. Seismic moduli measured at Tioga on 11/06/2007

CHAPTER 6: TRAFFIC DATA

The Phase II traffic data were collected, processed, and analyzed for the period from January 2006 through May 2008. A full 12 months of data were analyzed for the years 2006 and 2007, whereas only five months of data were analyzed in 2008. Four sites were selected for analysis. The selected sites were Tioga (Site 501), Mercer (Site 502), Perry (Site 505) and Blair (Site 506). The other sites, Warren, Delaware, and Somerset, were not considered because of either pavement reconstruction or instrument maintenance problems at these locations. This report provides the summaries of the analyzed data. Table 11 provides the travel direction and lane designations used in this report for the four sites with reported data.

Table 11. Lane designations

Site	Lane 1	Lane 2	Lane 3	Lane 4
501-Tioga	North - Travel	North - Passing	South - Passing	South -Travel
502-Mercer	West - Travel	West- Passing	East - Passing	East - Travel
505-Perry	West - Travel	West- Passing	East - Passing	East - Travel
506-Blair	South - Travel	South - Passing	North - Passing	North - Travel

The data collected at the selected sites were downloaded remotely every month from an FTP site posted by the PennDOT Bureau of Planning and Statistics. Once downloaded, the raw data files were pre-processed using PAT "Reporter" software to obtain readable "ASCII" files. The daily and monthly records of vehicle counts, classification, and weights were generated and analyzed. These summaries can be used to evaluate trends over time. For instance, as shown in Figure 47, the number of daily truck records collected sequentially over time indicates the seasonal variation of traffic volume. It can be seen that the traffic is higher during the summer months and decreases in the late fall and winter months.
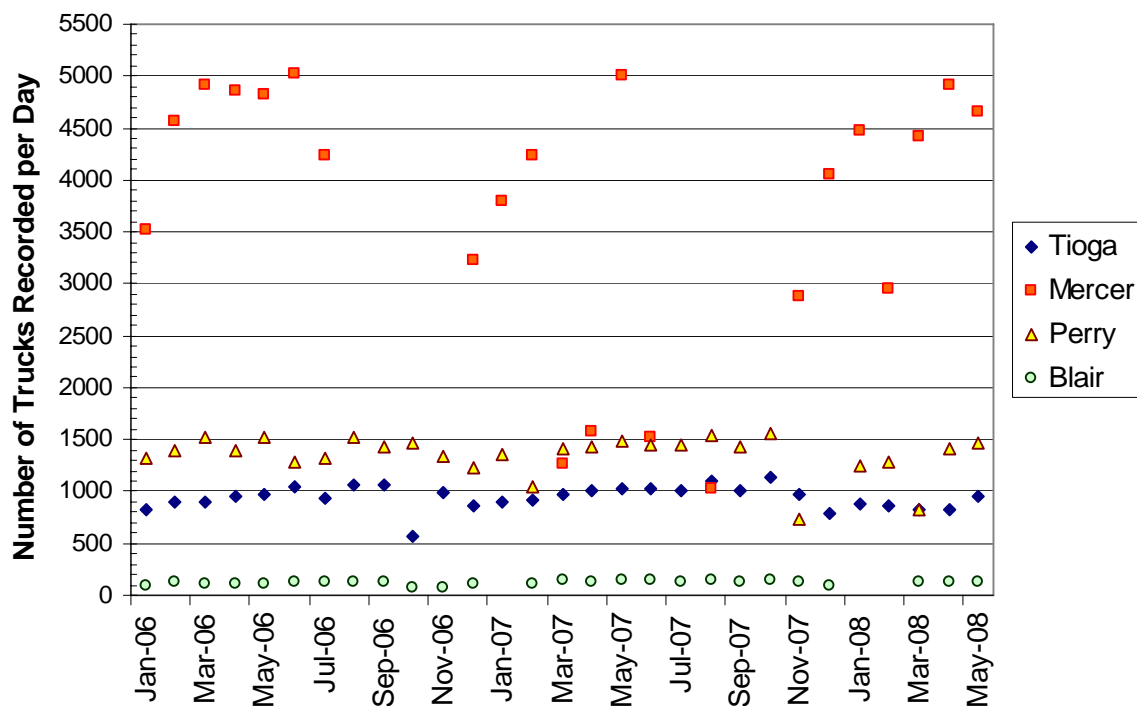
Figure 47. Monthly variation of truck records at SISSI sites

Traffic Volume

Traffic volumes were estimated based on vehicle counts collected at the selected sites. The annual average daily traffic (AADT) values were calculated for the years 2006 and 2007. Average daily traffic values were calculated for 2008 because only five months of data were available. The lane-wise AADT values were calculated for the selected sites and are included in the Appendix E. The AADT values for Lane 1 were calculated and are summarized in Figure 48.

The annual average daily truck traffic (AADTT) values were also calculated based on the truck counts collected at these sites. The 3-year weighted average values of percent truck traffic for the selected sites are provided in Figure 49. Percent trucks is an arithmetic ratio of AADTT over AADT. The detailed estimates of AADT and AADTT for all four lanes at the selected sites are included in Appendix E.

Traffic Variations over Time

Traffic varies by month of the year, by day of the week, and by hour of the day. The magnitudes and patterns of the variations depend upon the type of highway and the social and economic activities of the area served by the highway. Figure 50 shows the hourly distribution of trucks for the selected sites. The hourly distribution factors represent the percentage of the AADTT within each hour of the day. The sum of the percent of daily truck traffic per time increment must add up to 100 percent. The hourly distribution explains the variation of traffic during peak hours and non-peak hours.
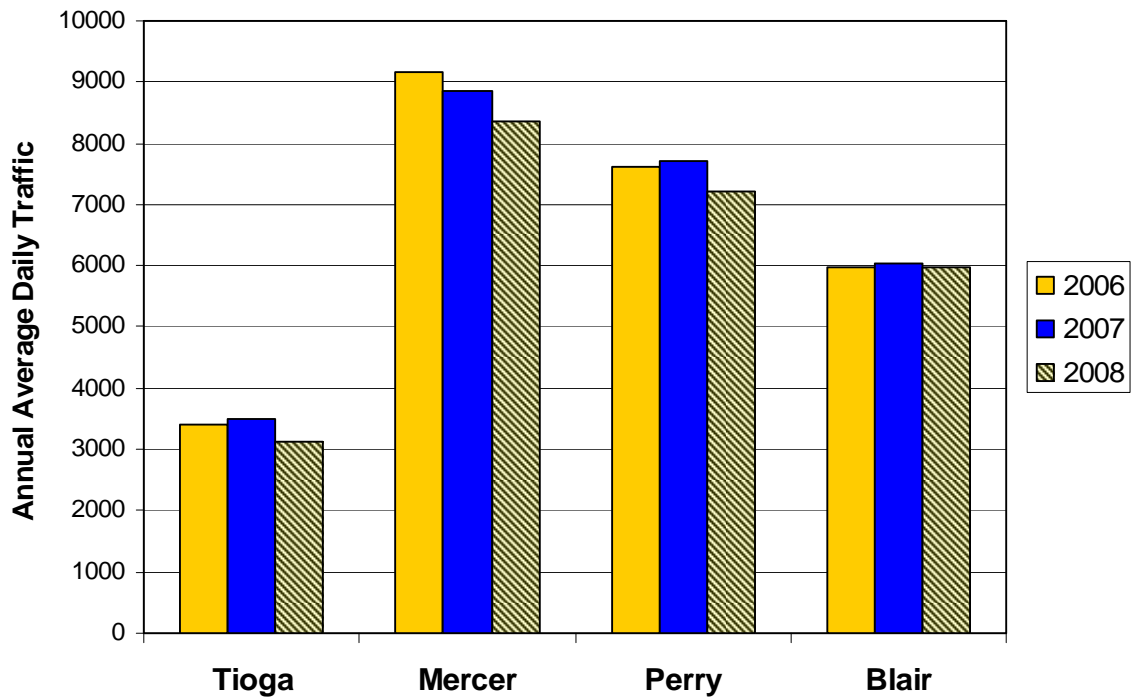
Figure 48. Annual average daily traffic
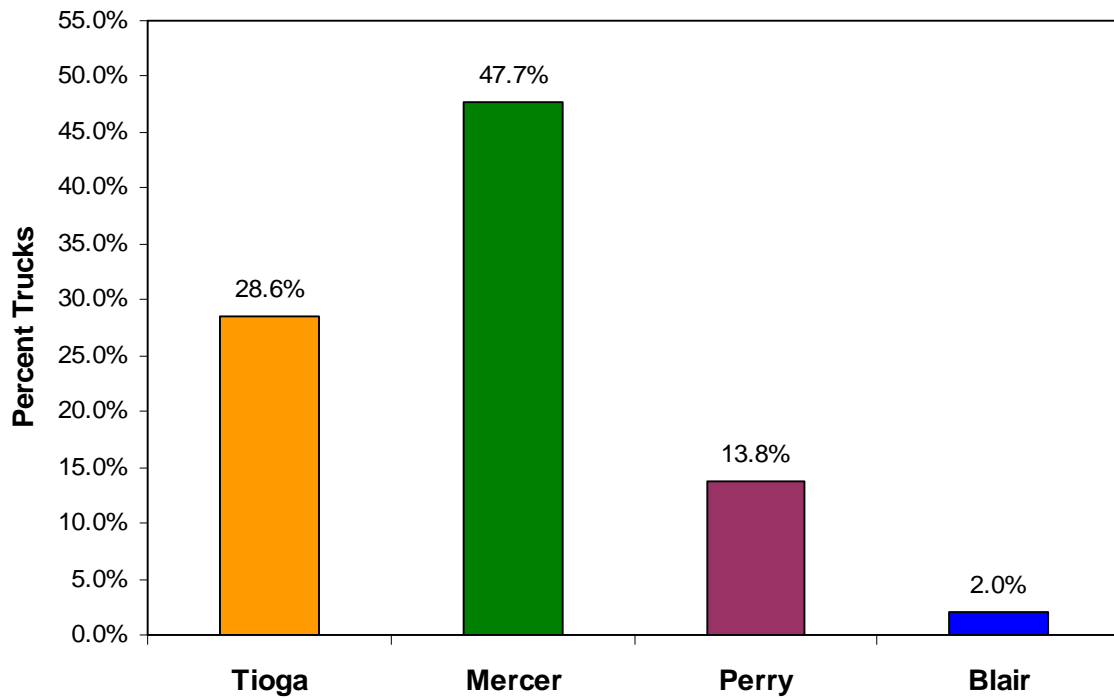
Figure 49. Percent trucks
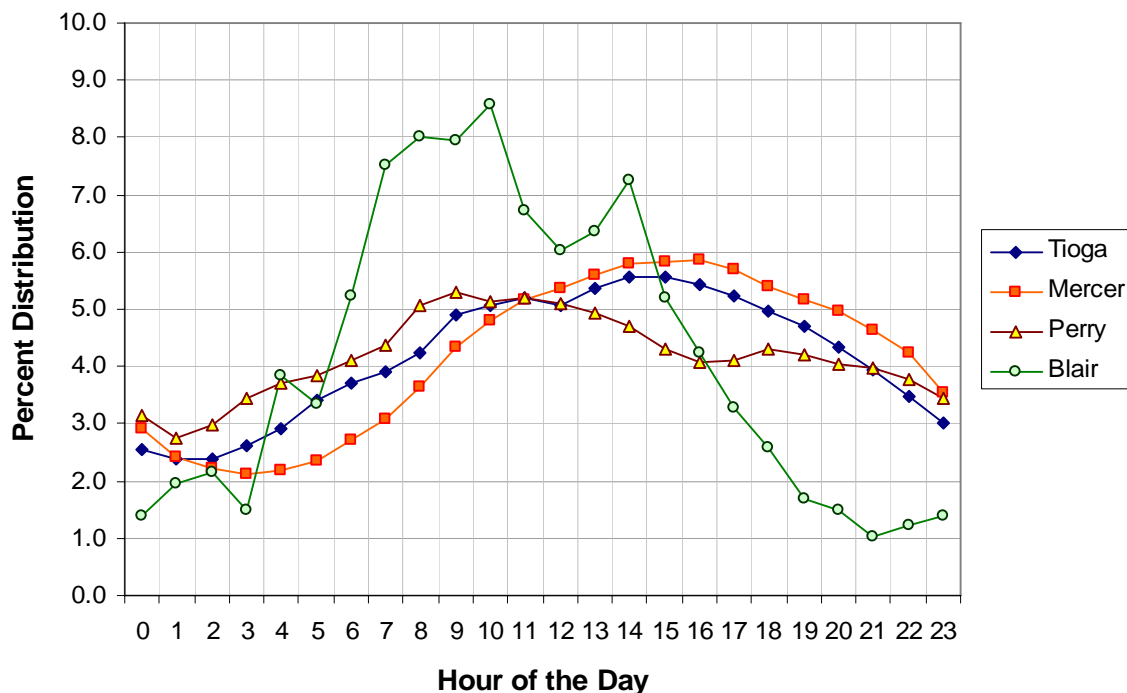
Figure 50. Variation of traffic by hour of the day

Table 12 shows the monthly adjustment factors (MAF) for class 9 vehicles. Similar factors for other vehicle classes are included in Appendix E. The monthly adjustment factors simply represent the proportion of the annual truck traffic for a given truck class that occurs in a specific month. These factors reflect seasonal variation of traffic over a year at each site. For a single site, the sum of these factors must add up to 12. A complete set of monthly adjustment factors and hourly distribution factors for each individual site is included in Appendix E.

Table 12. Monthly adjustment factor for class 9 vehicles

Month	Tioga	Mercer	Perry	Blair
January	0.93	0.96	0.95	0.90
February	0.97	1.00	0.95	1.00
March	0.99	1.02	1.20	1.01
April	1.02	1.03	1.20	1.07
May	1.01	1.02	1.12	0.97
June	1.04	1.03	1.14	1.07
July	0.97	0.96	1.12	0.96
August	1.04	1.06	0.83	1.03
September	1.06	1.02	0.82	1.04
October	1.07	1.03	0.94	1.07
November	0.99	1.00	0.80	0.96
December	0.91	0.89	0.88	0.90

Vehicle Class Distribution

Vehicle class distribution is calculated from vehicle counts and classification data obtained from the WIM system. The vehicle class distribution represents the percentage of each truck class (classes 4 through 13) within the AADTT. Table 13 provides the vehicle class distribution of the selected sites. Table 13 indicates that the distribution of truck classes for each individual site varies greatly from class to class, with class 9 vehicles having the largest percentage, followed by class 5 or class 8 vehicles. The predominant vehicle class types and their percent of distributions for all sites are shown in Table 14.

Table 13. Vehicle class distribution

Class	Tioga	Mercer	Perry	Blair
4	2.0	0.8	4.2	8.0
5	10.1	0.5	7.4	20.5
6	2.8	3.4	5.1	14.6
7	2.0	0.5	1.4	2.1
8	4.1	3.4	15.8	19.7
9	74.2	83.7	63.0	27.4
10	1.2	0.7	0.6	0.5
11	3.1	5.4	1.8	0.1
12	0.4	1.6	0.6	0.1
13	0.2	0.1	0.1	7.1
14	0.0	0.0	0.0	2.0
15	8.1	2.1	8.7	1.7
Total	*352*	*208*	*711*	*6265*
Trucks	*100*	*100*	*100*	*100*

Table 14. Distribution of predominant vehicle classes

Site	Predominant Truck Classes	Percent of Total Truck Traffic		
		Class 5	Class 8	Class 9
Tioga	5, 9	10.1	4.1	74.2
Mercer	9	0.5	3.4	83.7
Perry	8, 9	7.4	15.8	63.0
Blair	5, 8, 9	20.5	19.7	27.4

Axle Load Distribution Factors

The axle load distribution factors represent the percentage of the total axle applications within each load interval for a specific axle type (single, tandem, tridem, and quad) and vehicle class (classes 4 through 13). Figures 51 and 52 provide typical single and tandem axle load distributions, respectively, expressed as percentages of total axles for class 9 vehicles at the Tioga site.
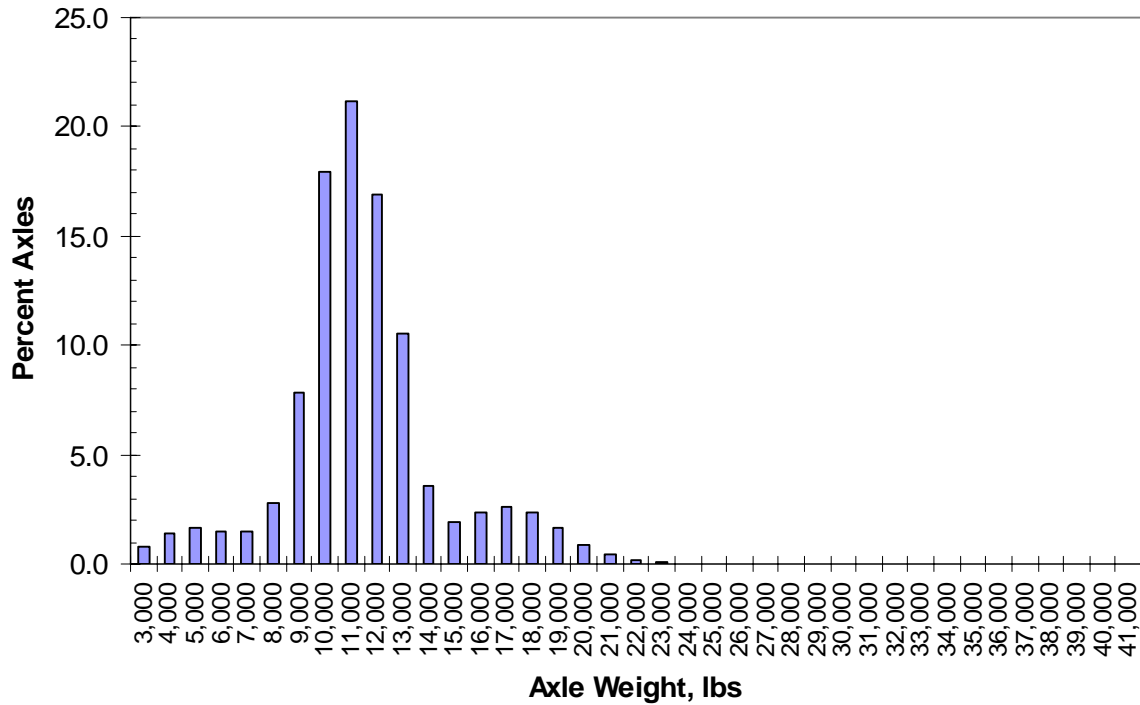
Figure 51. Single axle load distribution at Tioga in 2007
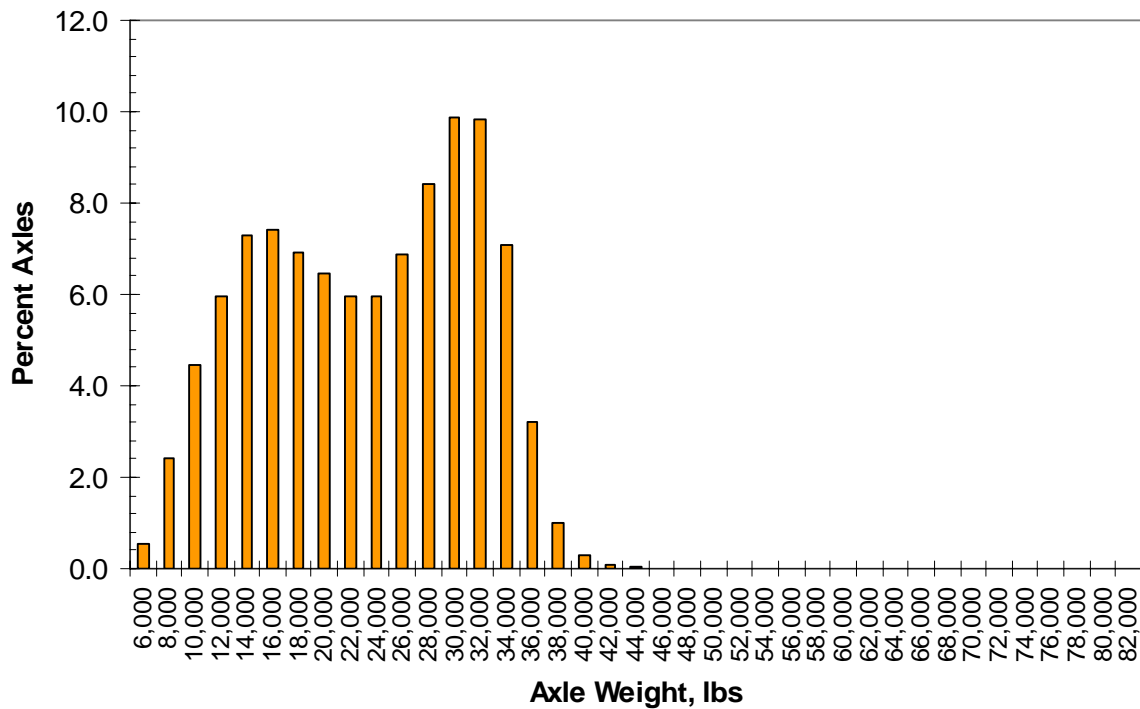
Figure 52. Tandem axle load distribution at Tioga in 2007

Number of Axles per Truck

This input represents the average number of axles for each truck class (classes 4 to 13) for each axle type (single, tandem, tridem, and quad). The average numbers of axles per truck for the selected sites are listed in Tables 15 through 18.

Axle Spacing

Axle spacing is the distance between the two consecutive axle of a tandem, tridem, or quad. The default values of axle spacing recommended by the MEPDG are 51.6 inches for tandem and 49.2 inches for tridem and quad. The average axle spacings are summarized in Table 19 for different axle types.

71

Table 15. Number of axles per truck (single axle)

Class	Tioga	Mercer	Perry	Blair
4	2.0	1.6	1.4	1.8
5	1.0	2.0	2.0	2.0
6	1.0	1.0	1.0	1.0
7	2.2	1.0	1.0	1.0
8	1.3	2.3	2.2	2.4
9	1.1	1.3	1.4	1.1
10	5.0	1.0	1.0	1.0
11	4.0	5.0	5.0	5.0
12	1.3	4.0	4.0	4.0
13	0.0	1.3	1.5	1.8

Table 16. Number of axles per truck (tandem axle)

Class	Tioga	Mercer	Perry	Blair
4	0.1	0.4	0.6	0.2
5	1.0	0.1	0.0	0.0
6	0.0	1.0	1.0	1.0
7	0.8	0.0	0.0	0.0
8	1.8	0.7	0.8	0.6
9	1.0	1.8	1.8	1.9
10	0.0	1.0	1.0	1.0
11	1.0	0.0	0.0	0.0
12	0.6	1.0	1.0	1.0
13	0.0	0.9	0.8	1.2

Table 17. Number of axles per truck (tridem axle)

Class	Tioga	Mercer	Perry	Blair
4	0.0	0.0	0.0	0.0
5	0.0	0.0	0.0	0.0
6	1.0	0.0	0.0	0.0
7	0.0	1.0	1.0	1.0
8	0.0	0.0	0.0	0.0
9	1.0	0.0	0.0	0.0
10	0.0	1.0	1.0	1.0
11	0.0	0.0	0.0	0.0
12	1.0	0.0	0.0	0.0
13	0.0	0.9	1.0	0.8

Table 18. Number of axles per truck (quad axle)

Class	Tioga	Mercer	Perry	Blair
4	0.0	0.0	0.0	0.0
5	0.0	0.0	0.0	0.0
6	0.0	0.0	0.0	0.0
7	0.0	0.0	0.0	0.0
8	0.0	0.0	0.0	0.0
9	0.0	0.0	0.0	0.0
10	0.0	0.0	0.0	0.0
11	0.0	0.0	0.0	0.0
12	0.3	0.0	0.0	0.0
13	0.0	0.3	0.2	0.4

Table 19. Average axle spacing

Site	Average Axle Spacing (in)		
	Tandem	Tridem	Quad
Tioga	50.22	52.74	44.50
Mercer	50.21	51.95	49.90
Perry	50.19	52.54	52.12
Blair	51.03	54.92	61.60

CHAPTER 7: ENVIRONMENTAL DATA

In this section, a summary is provided of temperature data collected during and after 2006, when Phase II of the SISSI project was initiated. Discussion is also provided on solar radiation, and an extensive analysis is presented regarding rate and depth of frost penetration and the freezing index based on SISSI data.

Temperature Data

Detailed temperature data are presented in the SISSI Phase-I detailed final report. Examples of temperature data collected during Phase II of the project are presented in this section, and details of temperature data during Phase II are presented in Appendix F. There were periods of data collection interruption for some of the sites. There were also missing data for some of the thermocouples due to the loss of sensors or connection problems.

Annual, monthly, and daily temperature patterns were similar to what had been previously reported in Phase I and are not reported here for the sake of brevity. However, for each site, examples of weekly temperature during the coldest and hottest months of the year are presented.

The largest variability in weekly temperature is observed for the layers that are closer to the surface. This is because these layers are more influenced by the daily variations of solar radiation and the air temperature, which indicate high temperature fluctuation for the top layers, while such fluctuation is almost non-existent in the deepest layers. Temperature of the pavement surface is influenced by solar radiation, air temperature, wind speed, and to some extent the temperature of the ground. It is the combination of these parameters that results in a different pattern of change for pavement surface temperature during the day and night and also during the cold and warm seasons.

In general, there is a larger variation of temperature at the pavement surface or close to the surface during the summer than the winter. This is basically because the solar radiation is poor during the winter compared to the summer. On a cloudy winter day, the pavement surface temperature is almost equal to the air temperature. During a sunny day in summer, the pavement surface temperature is significantly higher than the air temperature. Before the sun begins to set, the pavement temperature at layers close to the surface begins to drop. This temperature drop continues until the next day at sunrise, when one would expect the pavement surface and the air to reach almost the same temperature. Early in the morning, the temperature of the pavement increases with the depth from the surface until it reaches a maximum level at a certain depth. Further down from this depth, the temperature of the pavement decreases. As the day progresses and the effect of the solar radiation and higher air temperature become dominant, the pavement surface gets warmer. With this, the temperature gradient changes direction as the surface becomes warmer than the deeper layers.

During the winter, in the absence of powerful solar radiation, the temperature increases at depths further down from the surface. In case of solar radiation and higher air temperature, the surface will be warmer than a near-surface depth. Beyond this point, increases in temperature with depth continue.

Figures 53 through 55 show pavement temperature at different depths during winter 2007 and winter 2008. It can be seen that the pavement experienced significantly colder temperatures during winter 2007 compared to winter 2008. This is consistent with weather records, which indicate significantly lower temperatures during February 2007 compared with February 2008. As shown, pavement temperature at a depth of 5 mm varies between -15°C and 5°C during a specific 7-day period in February 2007, while it varies between -3°C and 15°C during the same period in 2008. It is also shown in Figures 56 and 57 that summer pavement temperature for a specific depth varies within a much wider range compared to winter. The graphs indicate that at Blair, the 5-mm depth temperature reaches approximately 50°C during summer.
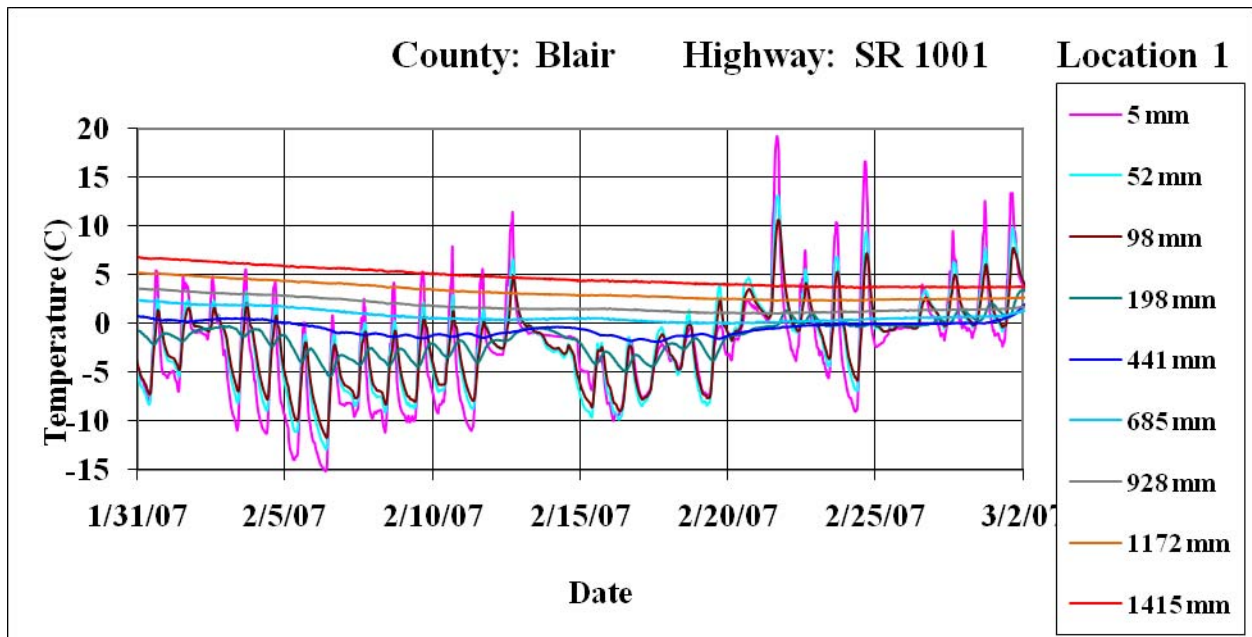
Figure 53. Monthly pavement temperature variation at different depths at SISSI Blair during winter 2007
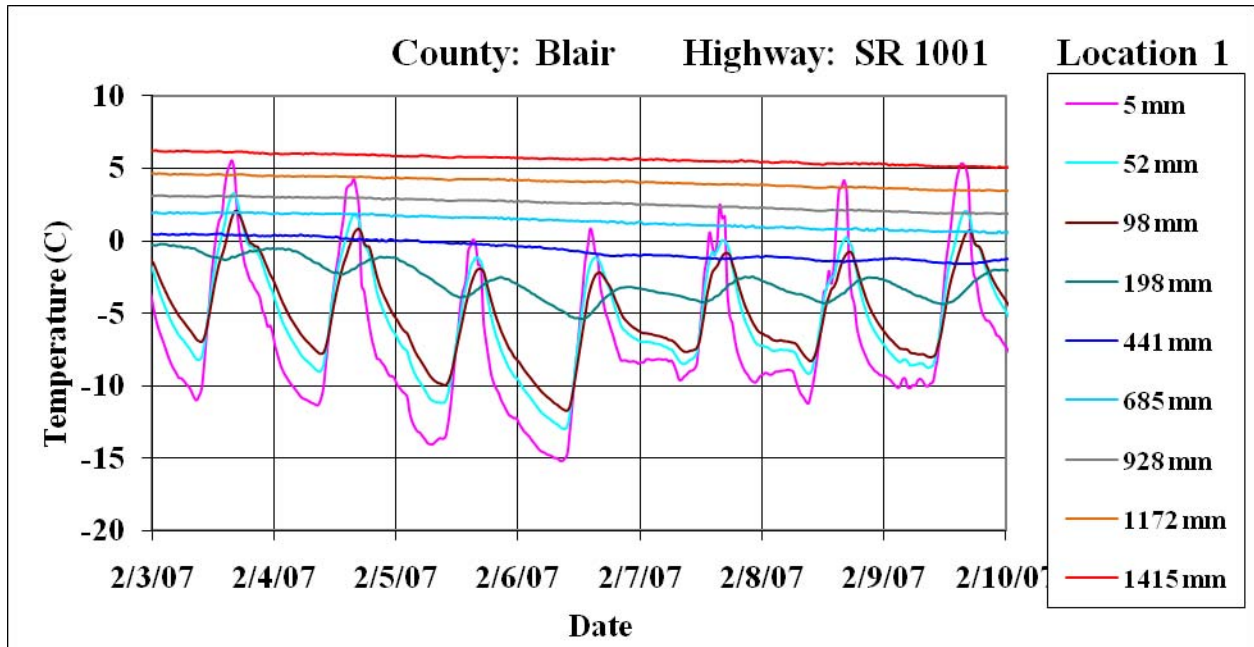
Figure 54. Seven-day pavement temperature variation at different depths at SISSI Blair during winter 2007
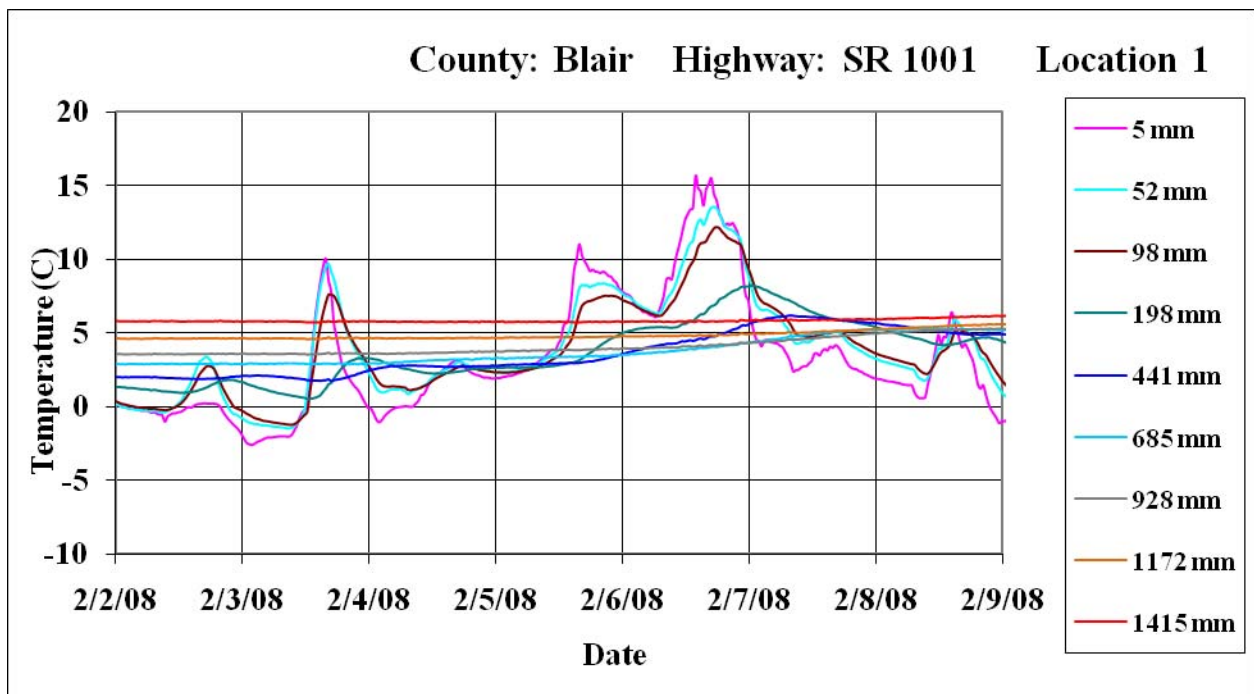
Figure 55. Seven-day pavement temperature variation at different depths at SISSI Blair during winter 2008
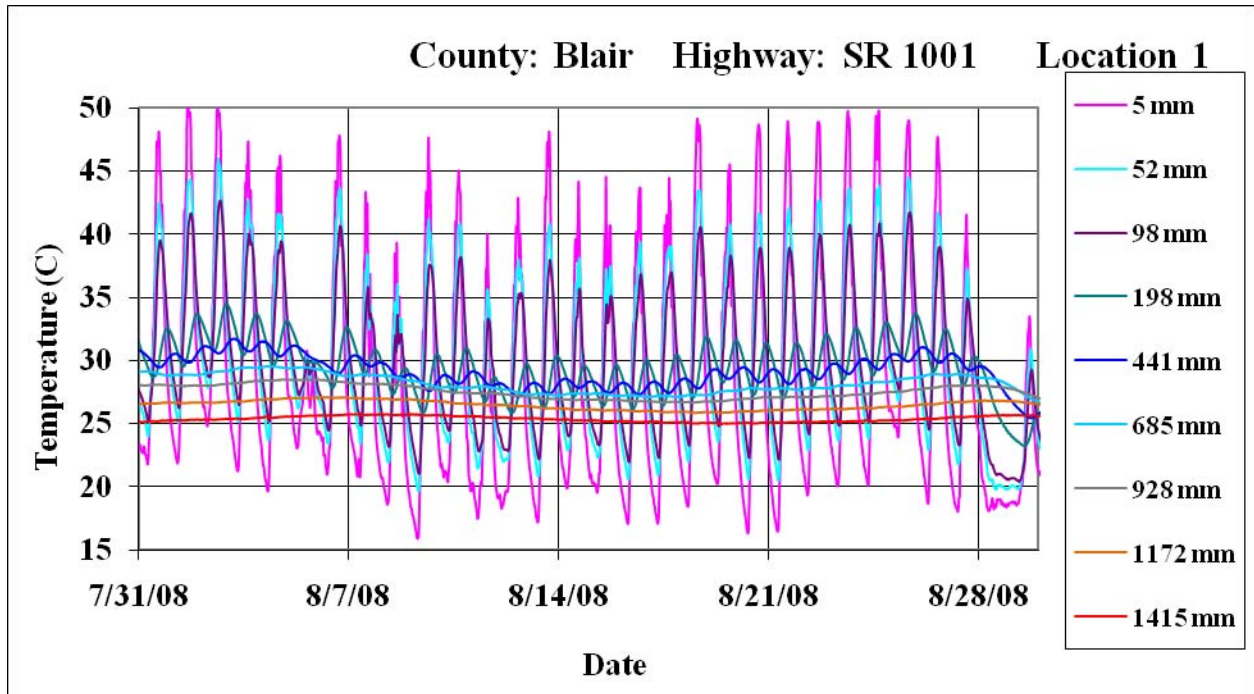
Figure 56. Monthly pavement temperature variation at different depths at SISSI Blair during summer 2008
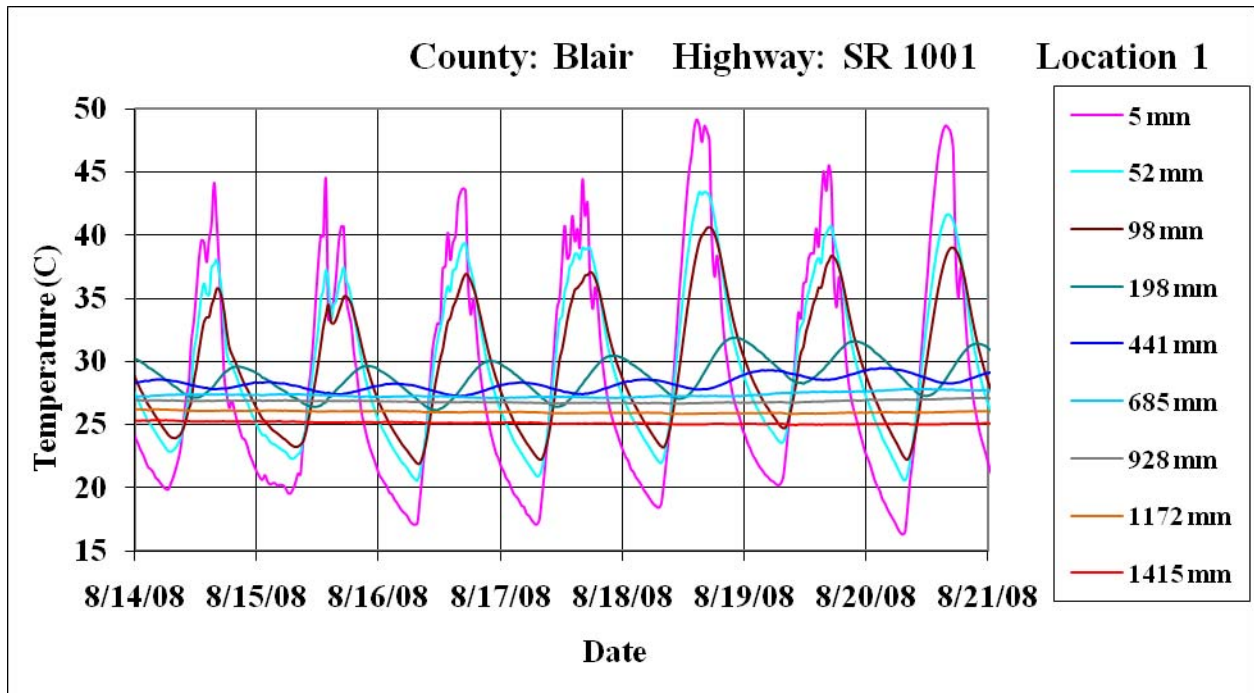
Figure 57. Seven-day pavement temperature variation at different depths at SISSI Blair during summer 2008

Figures 58 through 61 present pavement temperatures at the Perry site. This site is unique regarding pavement temperature data collection because three thermocouples were installed at depths very close to the surface (1, 3, and 6 mm), which was not done at the other sites. The installation was a special addition done several months after original installation. It can be seen that there is not a significant difference between captured temperatures at these depths either during winter or summer. The 1-mm depth temperature is about 1°C to 2°C warmer than the 45-mm depth temperature during winter, whereas it is 5°C to 7°C warmer than the 45-mm depth during summer. Multiple temperature measurements at depths close to the surface are important for calibration and validation of climatic models, which are an important and integral part of mechanistic empirical pavement design guide. From Figures 60 and 61, it can also be observed that the maximum pavement temperature at the Perry site, at depths close to the surface, exceeds those observed at similar depths at the Blair site.
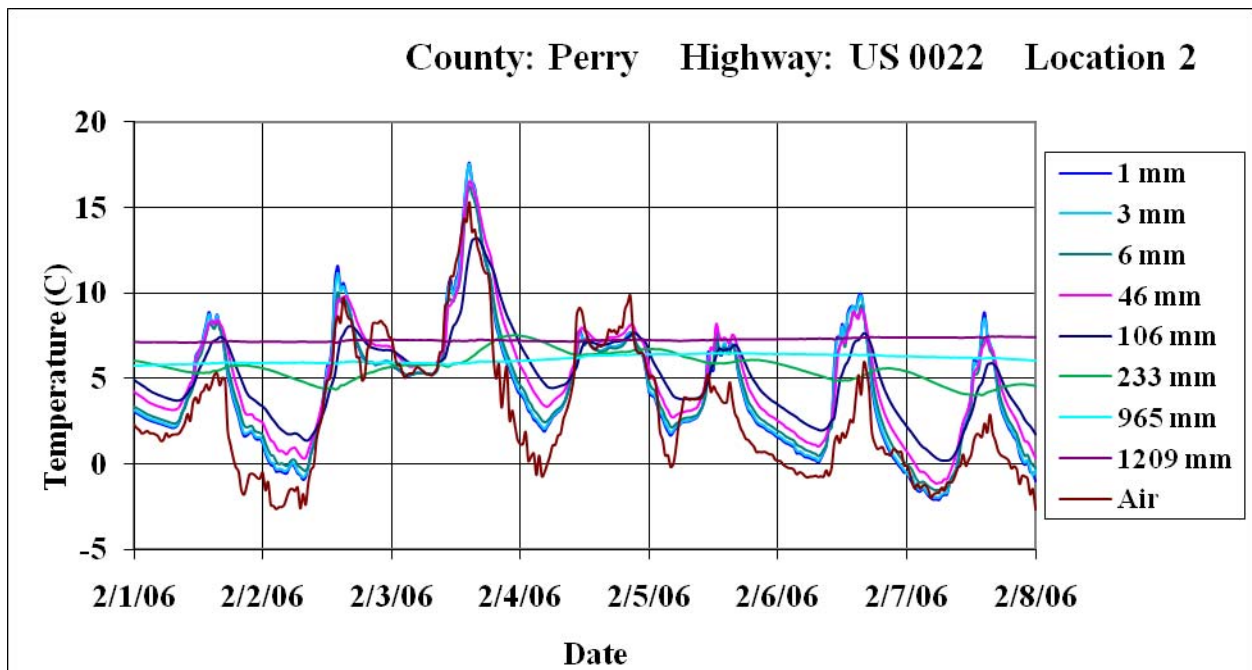
Figure 58. Seven-day pavement temperature variation at different depths at SISSI Perry during winter 2006
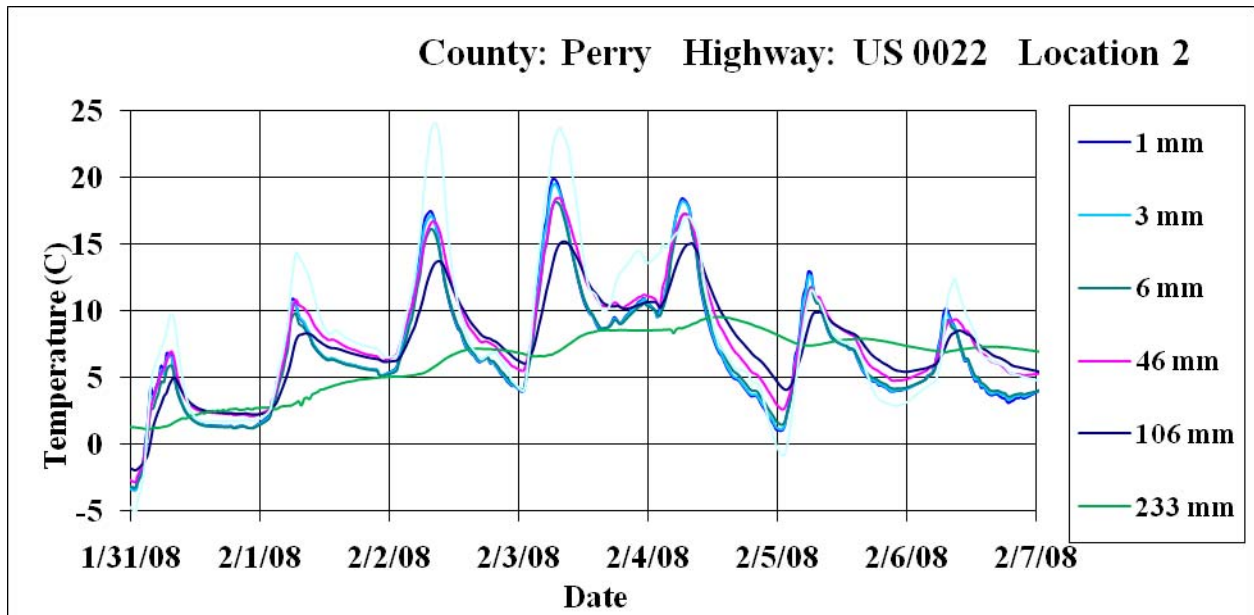
Figure 59. Seven-day pavement temperature variation at different depths at SISSI Perry during winter 2008
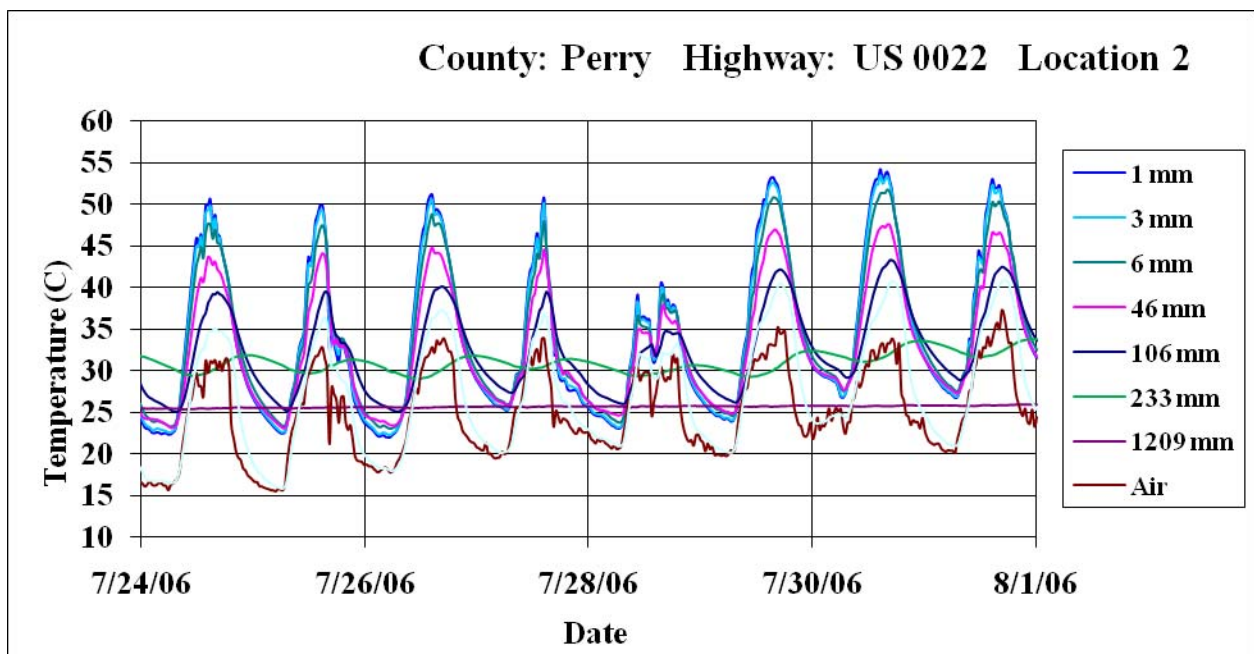
Figure 60. Seven-day pavement temperature variation at different depths at SISSI Perry during summer 2006

79
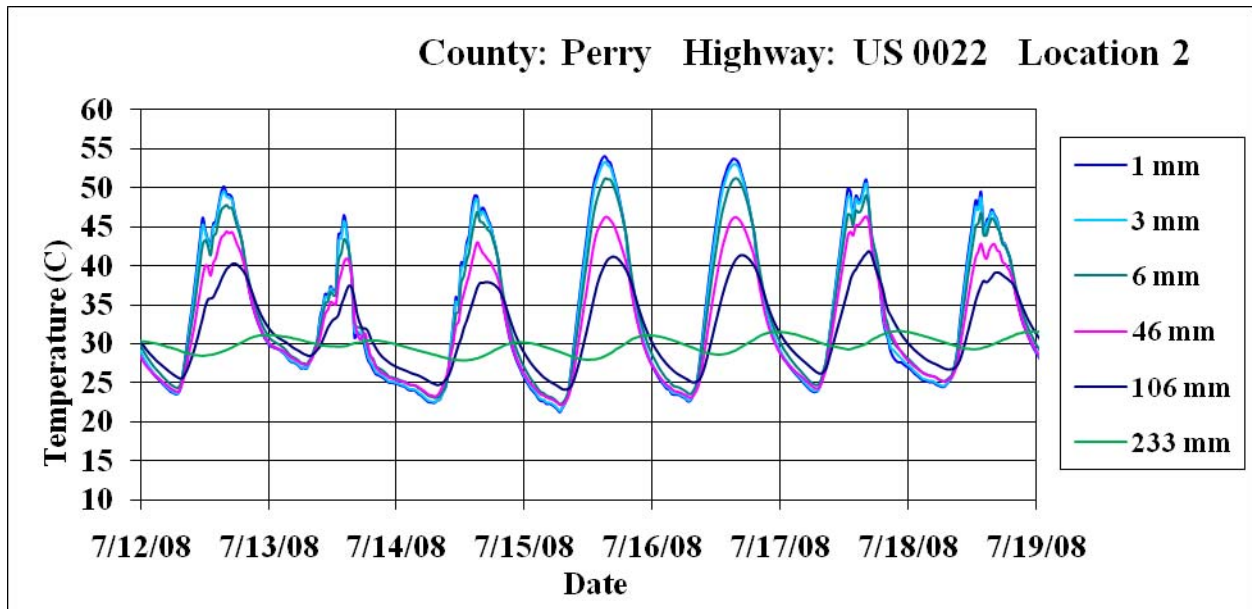
Figure 61. Seven-day pavement temperature variation at different depths at SISSI Perry during summer 2008

Figures 62 and 63 present two examples of pavement temperature at the SISSI site at Somerset County (PA Turnpike) during winter and summer 2007. Extremely cold temperatures at this site show that deeper layers eventually experience freezing conditions, as will be discussed in a later section. During summer, pavement temperature at a 5-mm depth reaches approximately 50°C, similarly to the Blair site.
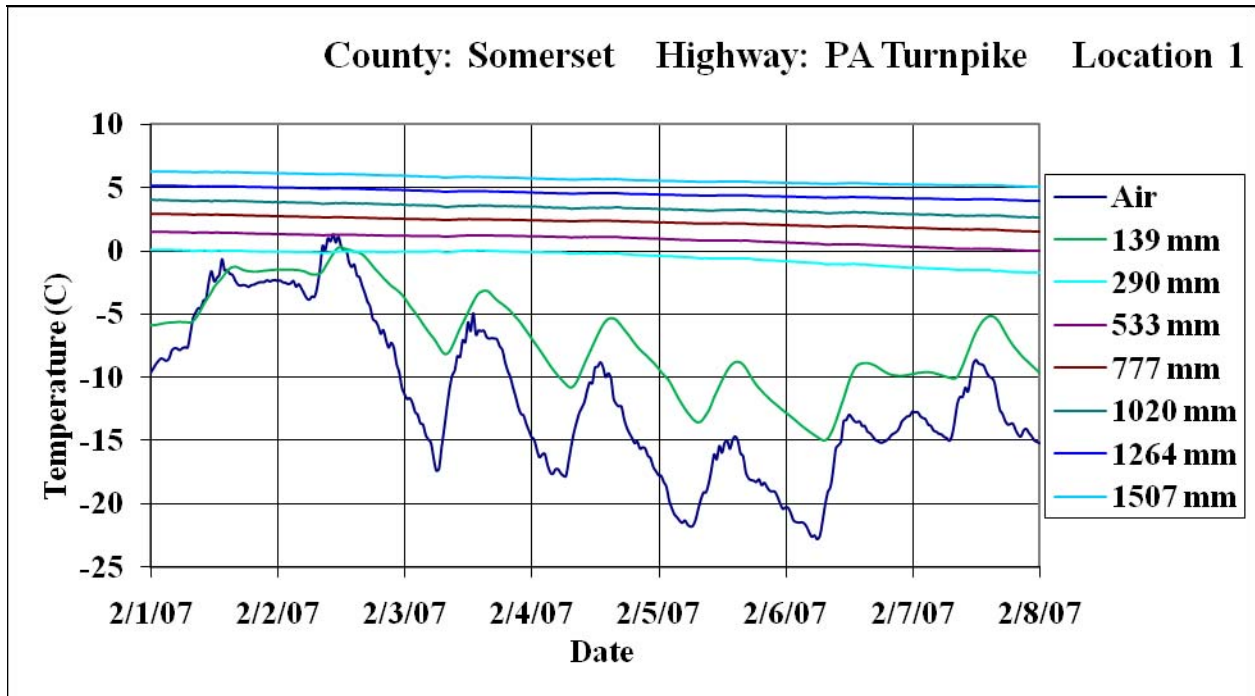
Figure 62. Seven-day pavement temperature variation at different depths at SISSI Somerset during winter 2007
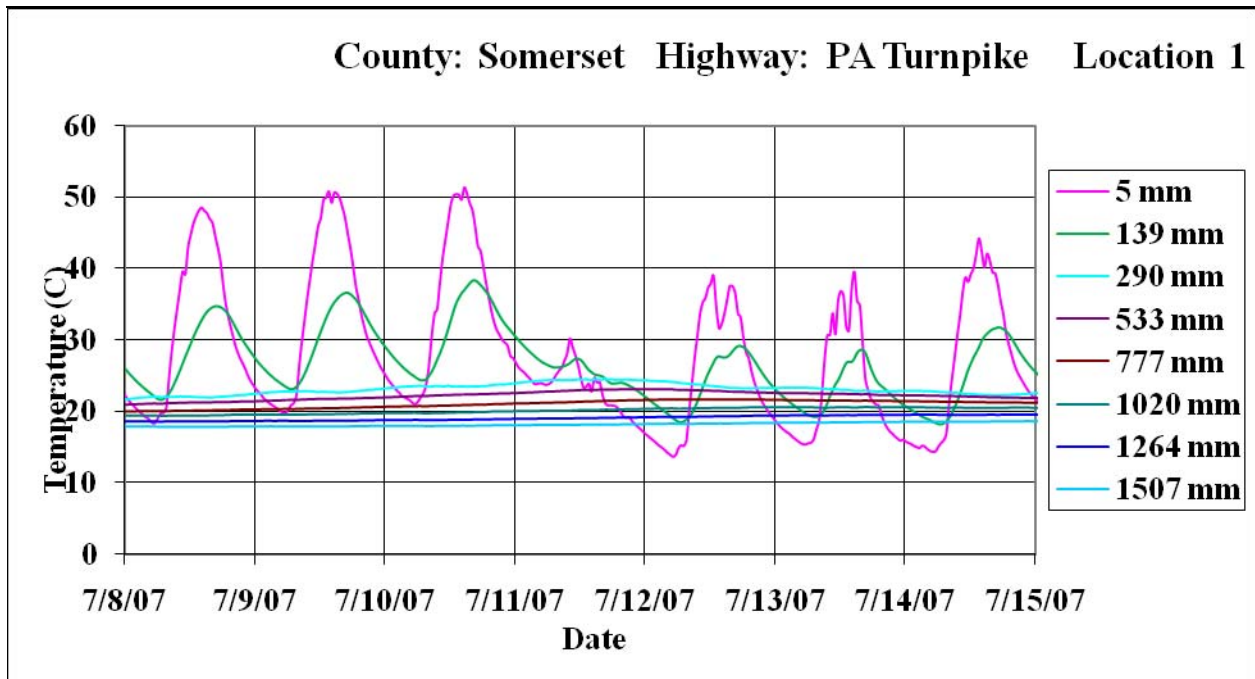
Figure 63. Seven-day pavement temperature variation at different depths at SISSI Somerset during summer 2007

Solar Radiation

A Campbell Scientific LI200X pyranometer was used at the SISSI sites to capture solar radiation. The CR23X datalogger was programmed to deliver average solar flux density in Watts per square meter. This is the total incoming solar radiation (i.e., it includes both direct and diffused radiation). The flux is captured every 30 minutes. Based on this data, the total daily solar radiation (total daily flux density) can be determined.

Figures 64 and 65 show the average flux at the Somerset Site for a typical 7-day collection period during winter and summer 2007, respectively. Significantly lower radiation levels during winter are obvious from these figures. Figures 66 through 68 indicate how radiation varies during a 24-hour period for a typical day in winter, summer, and fall. Figure 68 indicates an almost perfect distribution of solar radiation during a clear, sunny day. Detailed solar radiation data is provided in Appendix F. For SISSI sites, we significance of solar radiation data collection is in regard to its application with pavement temperature prediction models.
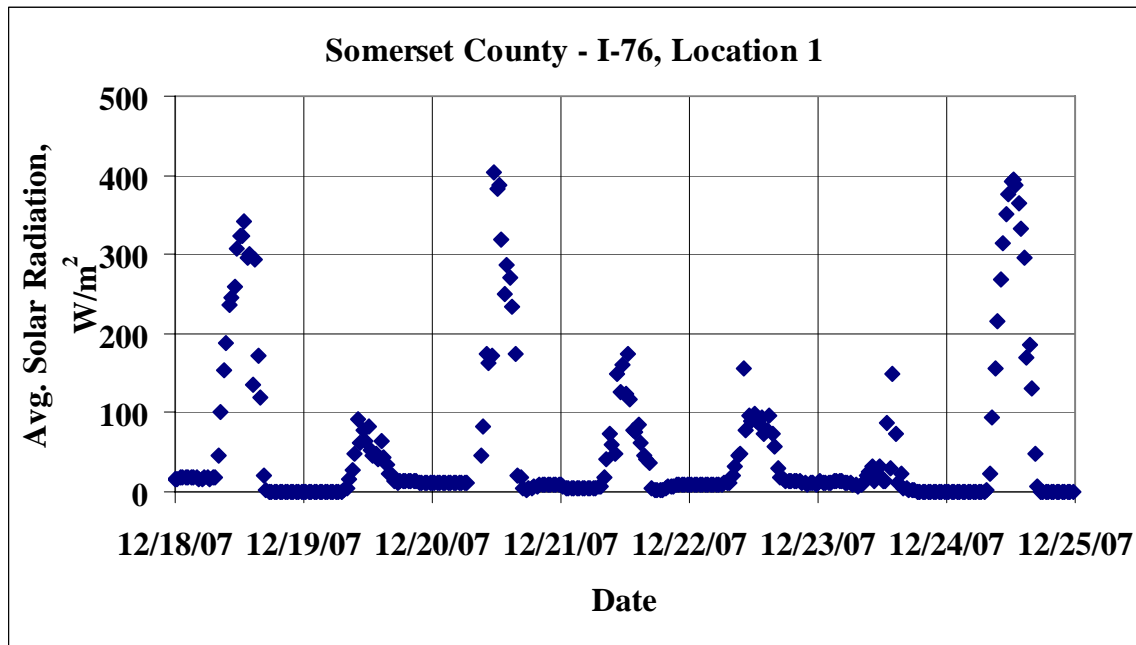
Figure 64. Average solar radiation for a 7-day period during winter at the SISSI Somerset site
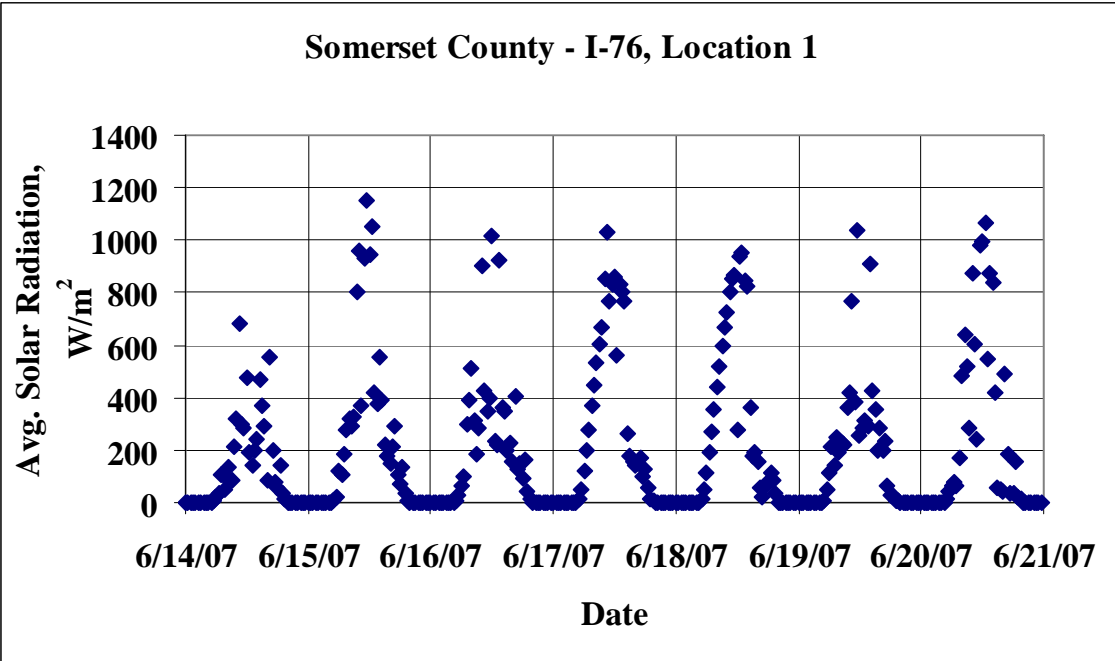
Figure 65. Average solar radiation for a 7-day period during summer at the SISSI Somerset site
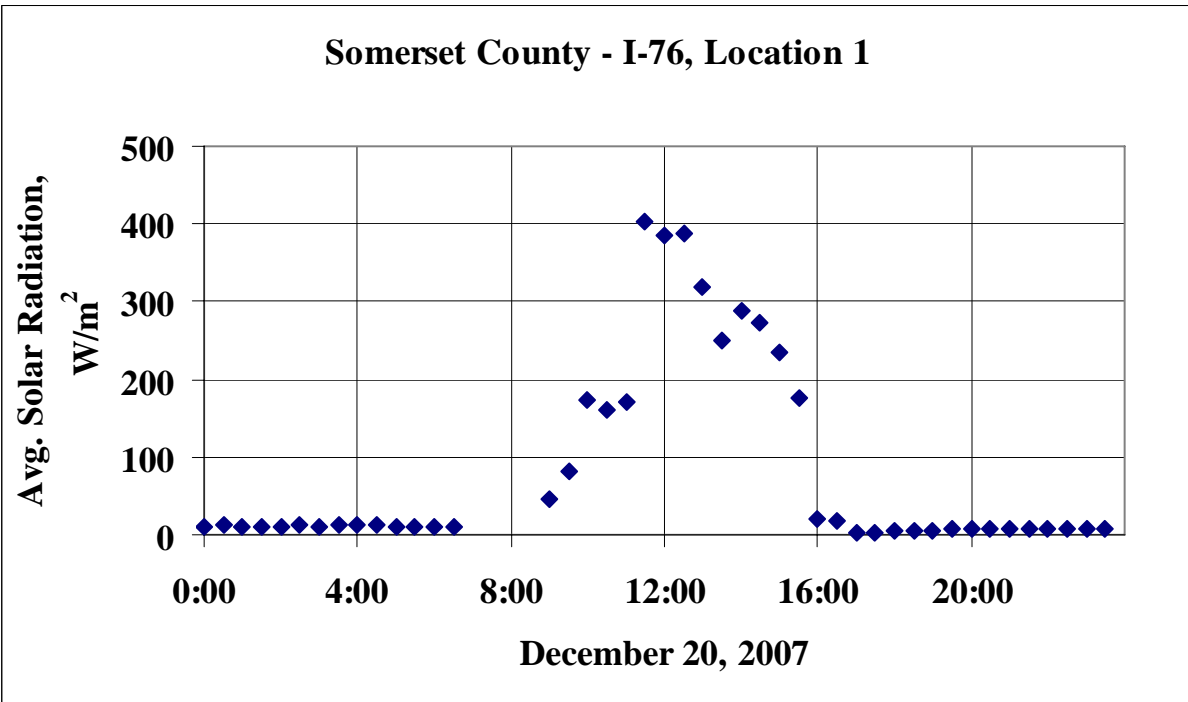
Figure 66. Average solar radiation for a typical winter day at the SISSI Somerset site
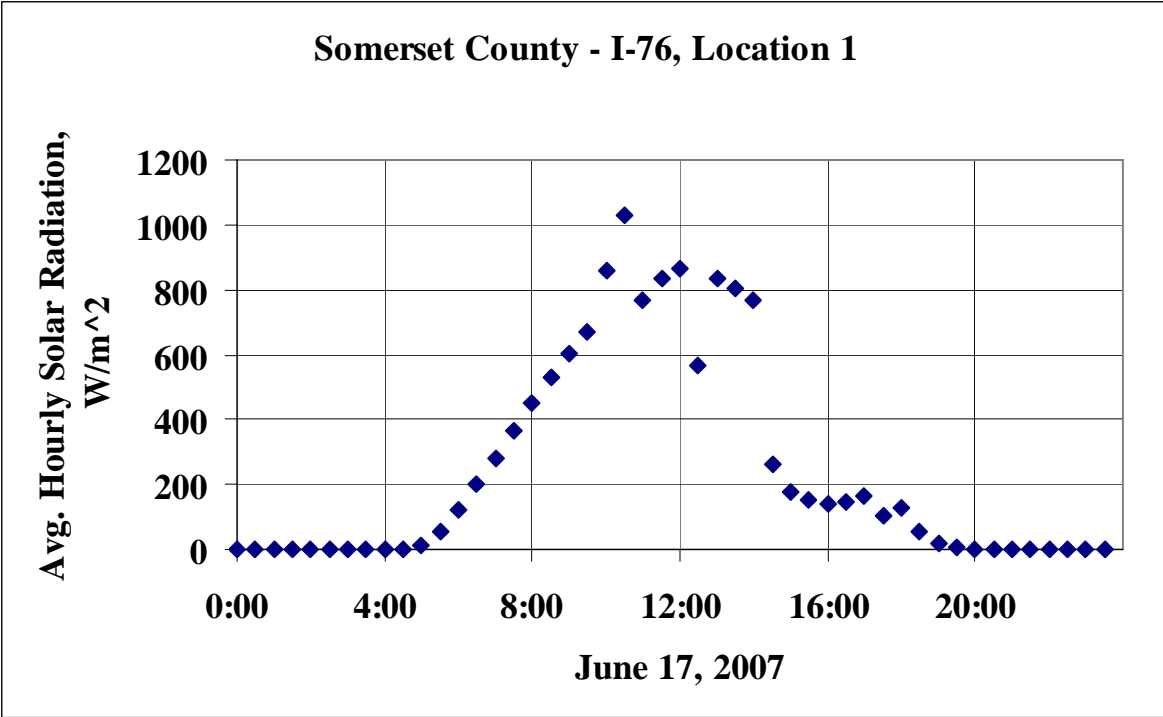
Figure 67. Average solar radiation for a typical summer day at the SISSI Somerset site
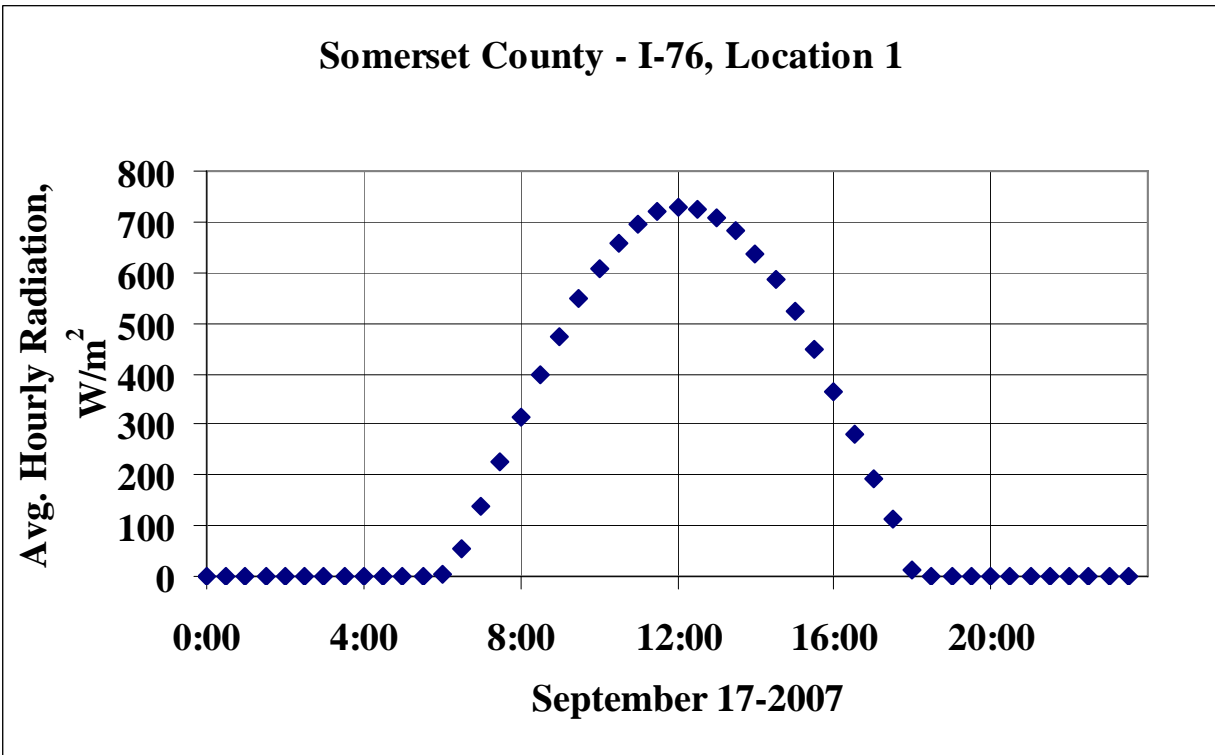
Figure 68. Solar energy measured during a clear day at the SISSI Somerset site

Magnitude and Rate of Frost Penetration at SISSI Sites

There are several reasons that determination and control of depth of frost penetration is important for pavement design and construction. Knowledge of frost depth helps in determining proper depth for installation of a drainage system and underground facilities such as sewer and pipelines. The magnitude of frost depth also affects the pavement potential for frost heave as well as pavement thawing, with the final impact on the period during which spring load limitations must be enforced.

Measurement of frost penetration depth and rate of this penetration can provide valuable information for design of the pavement structure. Based on SISSI data, a method was introduced for interpretation of the measured frost data and determination of frost depth and the rate of penetration. Data from three consecutive winter seasons from 2005 to 2007 were considered in the study.

Temperature and Frost Data Collection

Data Availability

Since February 2004, temperature and frost data have been collected from the Blair site. Temperature data were recorded every 30 minutes, whereas frost data were captured at a rate of one data point per hour for each ring. For the analysis presented here, the data monitored during the 2005 to 2007 winter seasons were used, and daily mean temperature and frost voltage at each depth were utilized for the analysis. The 2004 winter data were not included in the analysis since the available data starts from late February 2004, almost toward the end of the winter season.

2005 to 2007 Winter Temperature Profiles

Figure 69 shows winter temperature data from 2005 through 2007. It is observed that temperature fluctuations follow almost the same trend at depths of 5, 52, and 98 mm (points in HMA layers). Temperature fluctuation is diminished in the deeper layers.

Considering freezing condition (below 0°C) at the depth of 5 mm, the 2007 winter had the longest freezing period and 2006 winter the shortest. In the 2007 temperature data, there were some days when the temperature at 5 mm depth was over 0°C between 1/17/07 and 2/20/07. The days over 0°C were ignored in evaluating the freezing period because those days had minute positive temperature magnitude within mostly a single day.

For this analysis, depths with temperatures at or below 0°C were regarded as being in a frozen condition. With this assumption, frost depth could be estimated from temperature profiles. Maximum frost depths during freezing periods were about 550, 305, and 685 mm from the pavement surface in 2005, 2006, and 2007, respectively. In 2006, freezing temperatures did not penetrate into the subgrade.
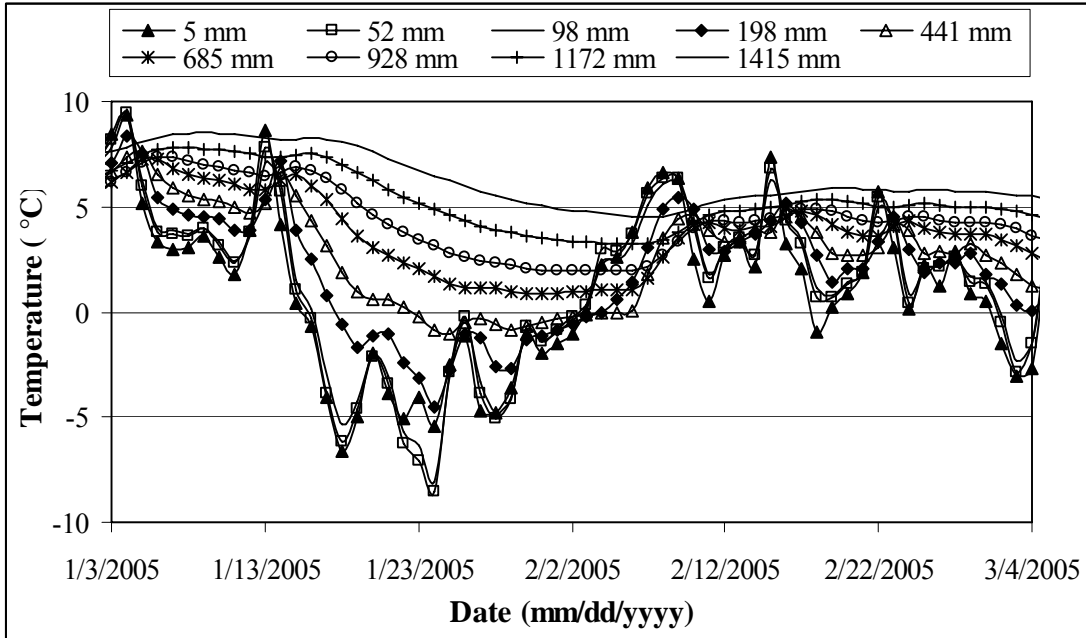
(a) Temperature profiles in the 2005 winter at the SISSI Blair site
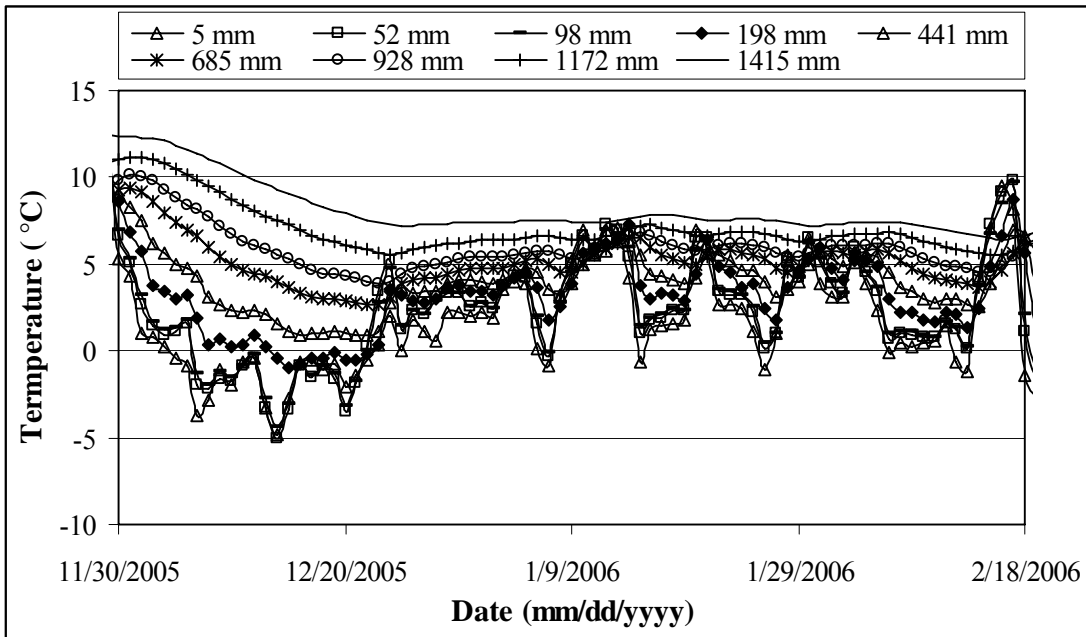
(b) Temperature profiles in the 2006 winter at the SISSI Blair site
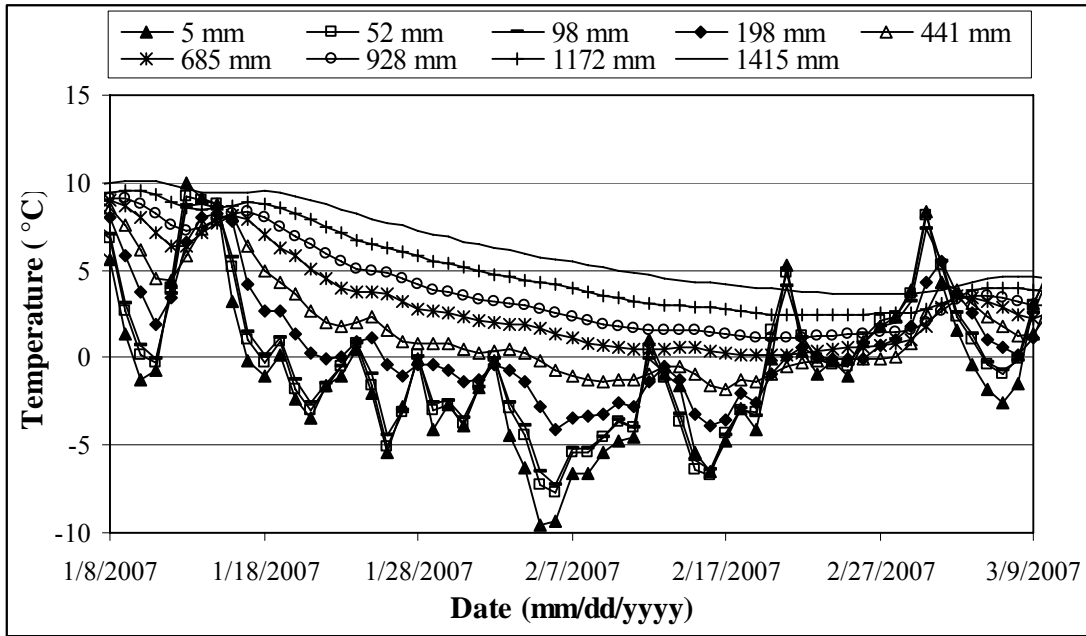
(c) Temperature profiles in the 2007 winter at the SISSI Blair site

Figure 69. Winter temperature profiles from 2005 to 2007 at the Blair site

Table 20 summarizes temperature information from 2005 to 2007. The freezing index was calculated based on temperatures measured at 5 mm beneath pavement surface, and it was defined as the sum of negative daily average temperatures for the period presented in Table 20.

$$\text{Freezing Index} = \sum_{n=1}^{k} (0^{\circ}C - T_n) \tag{8}$$

where k is the number of days when the daily average temperature is below 0°C, and T_n is the daily average temperature on the nth day.

Specifically, freezing intensity is a newly considered parameter in this analysis, defined as the ratio of freezing index over the number of days considered for determination of the freezing index. This parameter was derived to provide a better explanation of the freezing magnitude as measured from frost gages discussed in the following section.

Table 20. Summarized information from the observation of temperature data

Winter Year	Freezing Period	Freezing Index (°C-days)	Frost Depth (mm)	Freezing Intensity (0 °C-days/days)
2007	1/17/07 – 2/20/07 (26 days)	90	685	3.3
2006	12/5/05 – 12/22/05 (18 days)	30	305	1.7
2005	1/16/05 – 2/2/05 (20 days)	59	550	3.3

2005 to 2007 Winter Frost Profiles

The degree of freezing was determined based on the magnitude of electrical voltage measured between consecutive rings on the frost probe. Figure 70 shows the frost data for the same winter periods as used to present the temperature profiles for Figure 69. As the freezing period progressed, it was observed that frost voltage increased at each depth, indicating gradual progress in formation of ice crystals and a move toward freezing. For the given temperature condition, frost sensors installed closer to pavement surface showed greater and sharper peak responses, but the freezing voltage response became weaker in sensors remote from the surface. For example, for the depth of 264 mm, the highest frost voltages were about 510, 200, and 650 mV for 2005, 2006, and 2007, respectively. Higher frost voltage indicates higher freezing level. The magnitude of frost is obviously dependent on the severity of the winter climatic conditions. In addition, frost sensors closer to the pavement surface more quickly respond to the pavement surface temperature fluctuations and can, therefore, be considered more sensitive. The graphs in Figure 70 indicate that the response of deeper positions to pavement surface temperature occurs at a slower rate compared to the response at shallow depths.

It is shown that there are some time delays between peak points in the voltage measured at different depths. The magnitude of the delay for deeper locations to reach the same level of freezing at shallower depths depends upon the magnitude and severity of temperature fluctuations, as well as on the thermal properties of the pavement layers. It is also observed from the sharp voltage drop of most probe sensors that the thawing stage starts very quickly once the temperature rises above 0°C at a specific depth.
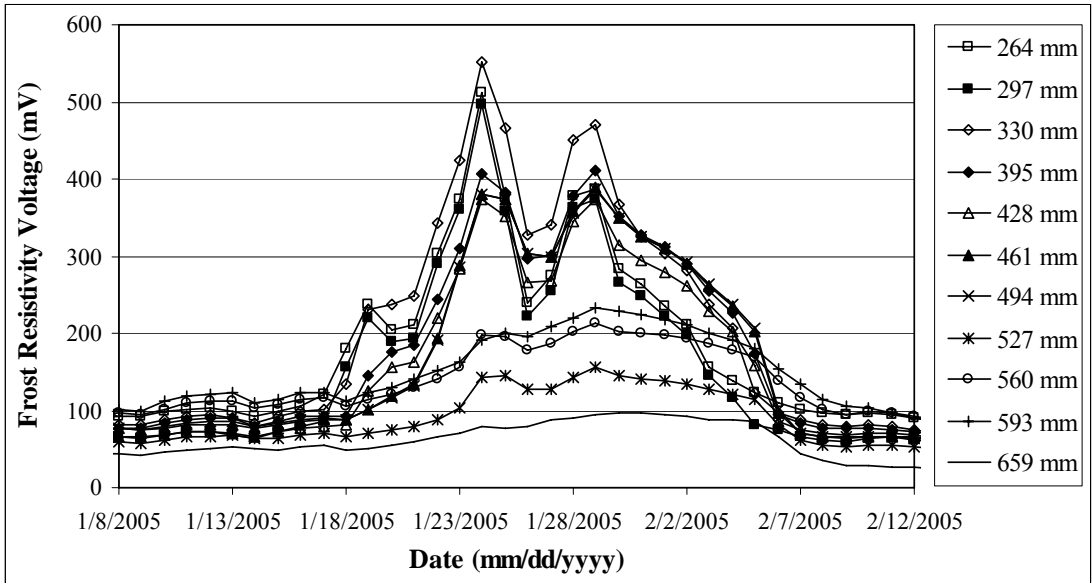
(a) Frost profile in the 2005 winter
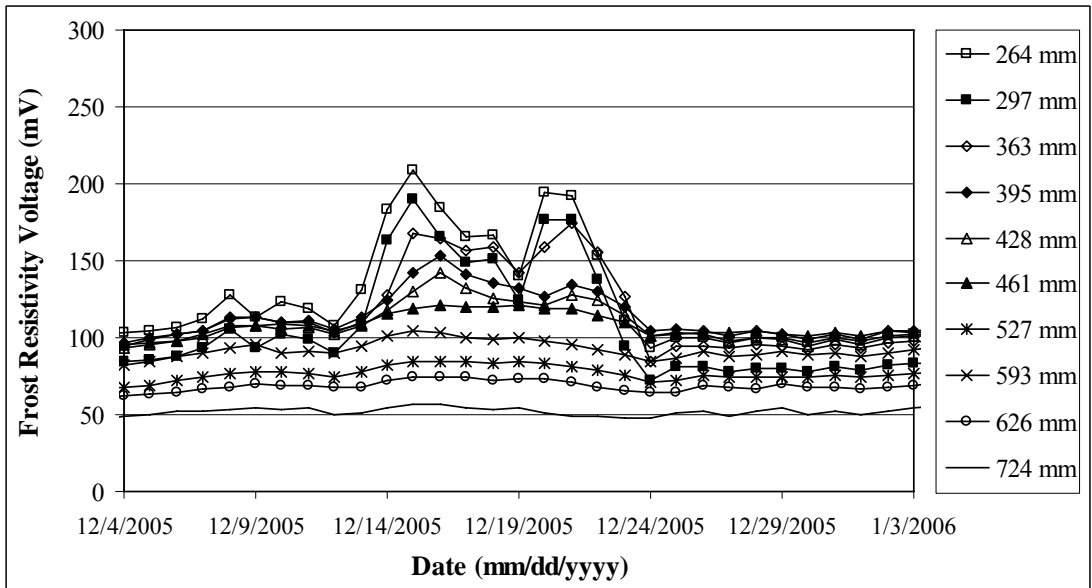
(b) Frost profile in the 2006 winter
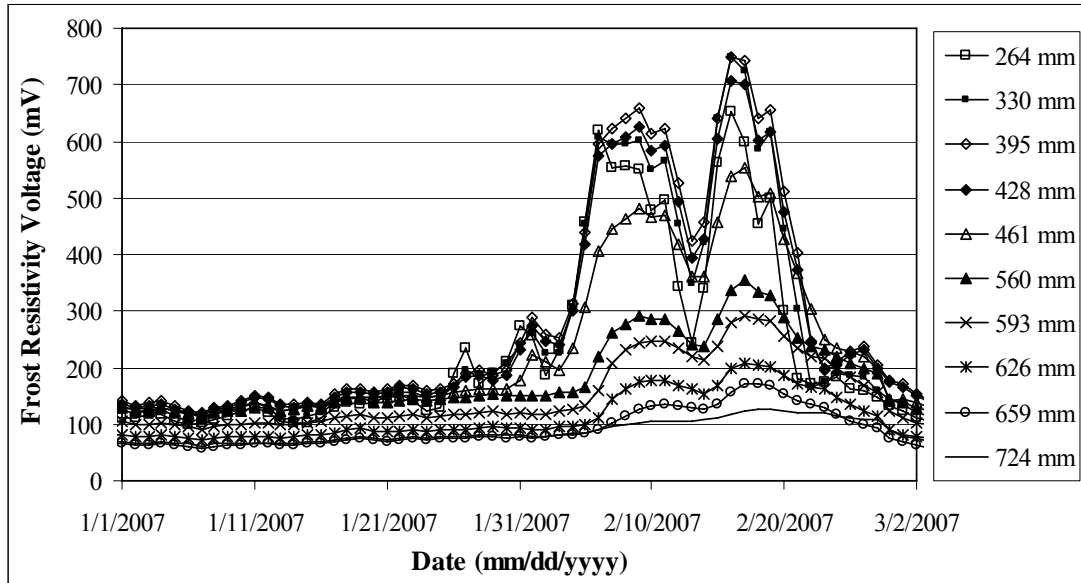
(c) Frost profile in the 2007 winter

Figure 70. Winter temperature profiles from 2005 to 2007 at the Blair site

Frost Depth and Magnitude

Frost depths presented in Table 20 were obtained based on temperature data. The temperature can partially explain soil freezing if moisture is present. On the other hand, the frost resistivity probe can detect actual freezing and the degree of frozen state based on the voltage magnitude. Figure 71 presents the resistivity voltage at each depth, exhibiting the frost impact and its severity, from January 20 to February 20, during 2007.

As shown in Figure 71, high voltages extend to a depth of approximately 500 mm, indicating different levels of freezing conditions. Beyond the 600-mm depth, there is a drastic voltage drop, indicating non-frozen soil. It seems that this significant voltage drop occurs at the vicinity of the boundary between subbase and subgrade layers, probably indicating that the difference in thermal properties between subbase and subgrade might have played a role in observing the difference in the frozen conditions. The 500- to 600-mm range, which covers the subgrade/subbase boundary, indicates the transition range between high voltage (frozen) depth and low voltage depth (not frozen). This area indicates the existence of some freezing, but less than at shallower depths. For determination of frost depth, it becomes important to define the severity of freezing at which the pavement/soil is considered frozen. Depending on the definition, maximum frost penetration depth, for the case observed, can vary between 500 mm and 700 mm. For this study, 200 mV was considered as the threshold value beyond which ice formation begins even though much higher voltage levels should be observed before the soil can be truly considered to be in a state of frost. Similarly, in the case of thawing, voltage dropping below 200 mV is considered to have completely taken the soil out of the frozen state. Accordingly, frost penetration depth for the 2005 and 2007 winter seasons was found to be about 570 mm and 600 mm. Frost depths judged by only temperature profile during the 2005 winter, in Table 20, are almost the same as those determined based on the frost resistivity data. However,

90

frost depths based on 2006 and 2007 temperature data would be considered slightly deeper than those based on resistivity data. For example, on February 16, 2007, the site recorded 0°C at the depth of 685-mm temperature profile in Figure 5 (c), whereas the information by frost resistivity indicated that the freezing phenomenon began at around a 600-mm depth. This result seems to support the fact that actual frost phenomena in unbound layers would not be achieved at 0°C but, rather, even below 0°C (Mitchell 1993). However, the definition for a frozen state based on the resistivity data is somewhat subjective, and, therefore, further work is needed for proper interpretation of the frozen state using the frost gage.
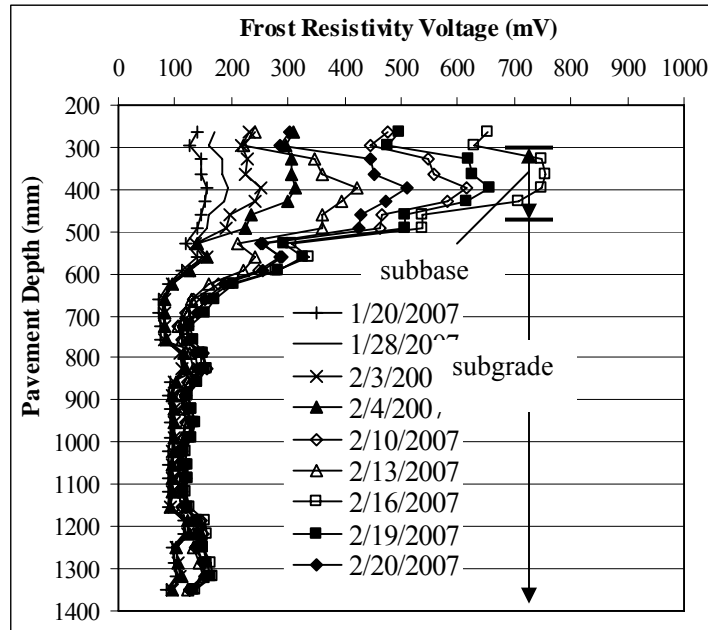
Figure 71. Frost resistivity voltage at each depth from January 20 to February 20, 2007

For examining freezing magnitude (degree of freezing) due to climatic parameters, the peak frost voltage responses shown in Figure 71 were plotted in Figure 72. The peak frost voltage for the 2005 winter is similar to that of 2007 at various depths even though the freezing index and freezing period are both considerably greater for 2007 than 2005. It can be inferred that freezing index and period cannot fully explain freezing magnitude. However, recalling that both years have the same freezing intensity, as shown in Table 20, it can be concluded that the freezing intensity might be better suited to explain the magnitude of freezing at a certain depth.
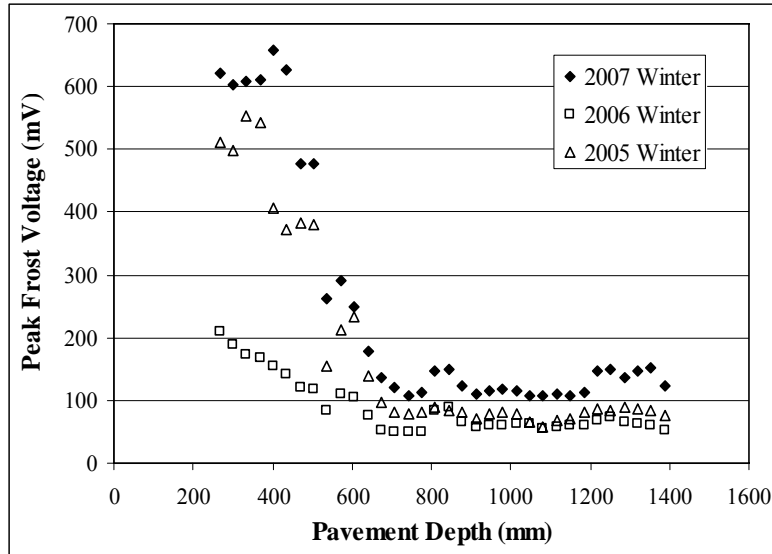
Figure 72. Peak frost resistance for 2005 to 2007 winters at the Blair site

Freezing Rate

Freezing rate is an important factor affecting strength and durability of unbound layers within a pavement structure. Laboratory studies have shown that a lower freezing rate causes lower unconfined compressive strength and higher moisture content in stabilized soils (Dempsey and Thomson 1972). Thus, it is important to monitor and examine how changes in ambient temperature and pavement structure and materials affect the freezing rate and the rate of frost penetration. Freezing rate in this analysis was obtained based on frost resistivity data.

There are many factors that influence frost penetration rate: fluctuations in ambient temperature, thermal properties of materials, and initial temperature condition of materials. In a laboratory, influencing factors can be controlled. In the field, however, temperatures are not constant or controllable. In this study, freezing rate based on field data was evaluated for the period of January 15 to 24, 2005. Pavement temperature was within 5°C before January 15. Afterward, pavement temperature dropped rapidly to subfreezing levels within two days and remained at about -5°C for 8 days.

Figure 73 represents the time needed to reach certain frozen states at each depth for the considered climatic condition for a 10-day period. As illustrated in the previous section, each depth has a different voltage level (the degree of frozen state). Thus, to evaluate freezing penetration time or rate, it should be individually examined for several different voltage levels. The deepest sensors that recorded up to 150 mV, 350 mV, 450 mV, and 550 mV are those embedded at 593 mm, 494 mm, 363mm and 330 mm, respectively.

It seems that the 2A subbase layer experienced more active freezing phenomena than subgrade for the given climatic conditions. At deeper pavement layers, more time is required to reach the same level of frozen conditions. This is clearly observed for the subbase layer. As

92

higher levels of frozen state are reached, the freezing rate decreases through the entire subbase. Moreover, it is observed that the upper portion of the subbase experiences a higher rate of frost penetration compared to the lower portion. For the upper subbase interval from about a 330- to 400-mm depth, the averaged freezing rate could be obtained as 2 mm/hr, whereas for the lower subbase, the rate is 13 mm/hr.

It is difficult to evaluate freezing rate for the subgrade layer since at deeper points of this layer, measured resistivity did not reach 200 mV, a threshold for deciding ice formation. However, from Figure 70(a), there is evidence that subgrade layer responded to the freezing temperature. It is observed that deeper parts of subgrade reached the 150 mV level faster than the top part of the subgrade, possibly because of higher water content.
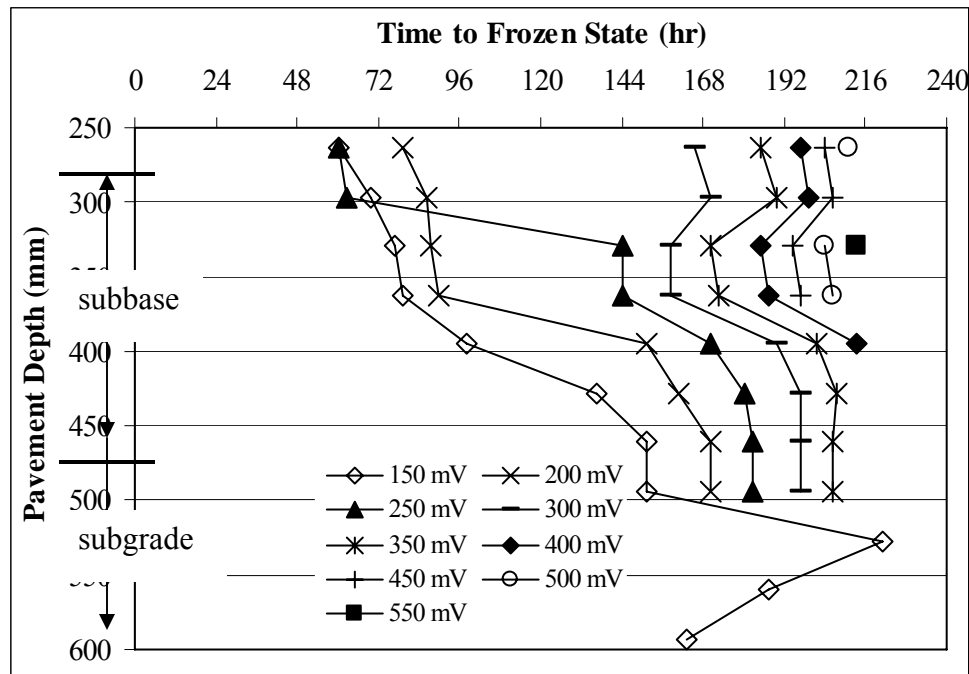
Figure 73. Time to each frozen state from January 15 to 24 in the 2005 winter season

Findings and Conclusions

Frost data from the Blair site was analyzed to determine the depth and rate of frost penetration. The probe used at the site emitted the electrical voltage, and interpretation of data is based on the difference of high voltage for frozen soil (high resistance) and low voltage of unfrozen soil (low resistance).

Data indicate that as the freezing period lasts longer, frost severity increases at various depths. Moreover, for the given temperature and site conditions, frost sensors closer to the pavement surface showed greater and sharper peak responses, implying a faster rate of frost formation and penetration. Overall, at deeper pavement layers, more time is required to reach a specific freezing condition. It was observed that the upper portion of the subbase at the site studied experienced a higher rate of frost penetration compared to the lower portion. For the

upper subbase interval from approximately a 330- to 400-mm depth, the averaged freezing rate could be obtained as 2 mm/hr, whereas for the lower section of the subbase, the rate was 13 mm/hr.

It was observed that there was some time delay between peak frost voltage measured at different depths. This was the basis for determination of the rate of frost penetration. It was also observed that the frost depth determined based on frost probe voltage read-out was less than that estimated based on only temperature; however, such a difference could be better interpreted if a relationship were established between the voltage level measured from the probe and the degree of frozen state in unbound material.

Frost Depth Evaluation Considering Freeze-Thaw Cycles at SISSI Sites

The freezing index has been the main factor for estimating pavement frost depth in cold regions. Many studies and researches have investigated the relationship between freezing index and frost depth, such as those by Hass and Bovid 1981, Chisholm and Phang, 1983, McKeown et al 1988, and Drumm and Meir 2003. Based on these studies and using analytical models and principles of thermal conductivity, it has been shown that frost depth has a linear relationship with the square root of the freezing index. Empirical models developed from observed data of frost penetration in these studies also involve the square root of freezing index as the main contributing factor.

In addition to the freezing index, characteristics of freeze-thaw cycles affect the depth of frost penetration. Sometimes, several low intensity freeze-thaw cycles can result in the same freezing index numerically, but with a less significant impact on frost depth. This is true for some areas of the Northeast region of the United States, where there are freezing cycles with relatively low temperature intensity that do not seem to significantly influence frost depth penetration. Summarized freezing index through the winter season in these regions might be considerably different from the net freezing index that predominantly contributes to frost penetration. Recent work by Jackson and Puccinelli (2006) focused on evaluating the impact of freeze-thaw cycles on pavement performance for 'moderate-frost' climatic conditions.

In analytical frost models, freezing index is evaluated for a single freeze-thaw cycle. On the other hand, the empirical models are practically derived by adopting the summarized freezing index from multiple freezing cycles through the whole period of the cold season. Thus, developing a proper relationship between the freeze-thaw cycles and the freezing index is an important step toward developing appropriate models to predict frost depth.

Freezing Index and Freeze-Thaw Cycle

For theoretical calculation of frost depth based on analytical models, Freezing Index (FI) needs to be obtained from pavement surface temperature within a single freeze-thaw cycle. However, in most cases, summarized FI from several freeze-thaw cycles through the whole cold season is used in empirical models. In addition, air temperature is usually used by multiplying n-factor (Eq. 9) that explains pavement surface temperature (Moulton and Schaub 1969). In this study, it was assumed that all SISSI sites had the same n-factor, and FI was obtained with daily mean air temperature.

$$n = \frac{\text{Freezing Index from Pavement Surface Temperature}}{\text{Freezing Index from Air Temperature}} \qquad (9)$$

An important question in determination of frost depth based on FI is whether one long single cycle of freeze (i.e., prolonged freeze) would provide the same impact as multiple freeze-thaw cycles providing the same magnitude of FI as the single cycle. Figure 74 explains this concept schematically. Both curves A and B deliver the same FI, 240°C-days. However, curve A represents six multiple cycles, and curve B displays one cycle of freeze. As shown in Figure 75, a single intensive cycle can generate deeper frost penetration than multiple moderate temperature cycles although the calculated FI is the same for both. Empirical models that have been developed for frost depths estimation so far do not distinguish between these two conditions.

For example, it can be seen from Figure 75 (a) that the maximum frost depth, 0.40 m, was caused by the first three cycles. Although the last four cycles lowered temperature in the deeper unbound layer, they did not affect the maximum frost depth. The same situation is observed from Figure 75 (b). The first longest cycle dominantly influenced the maximum frost depth, 0.27 m, and then, the freezing temperature could not penetrate more than 0.27 m by the following seven cycles. This observation implies that a large portion of the summarized FI from multiple cycles does not contribute to the maximum frost depth penetration in the regions that have multiple freeze-thaw cycles. In addition, this characteristic is generally found in other SISSI sites in Pennsylvania.
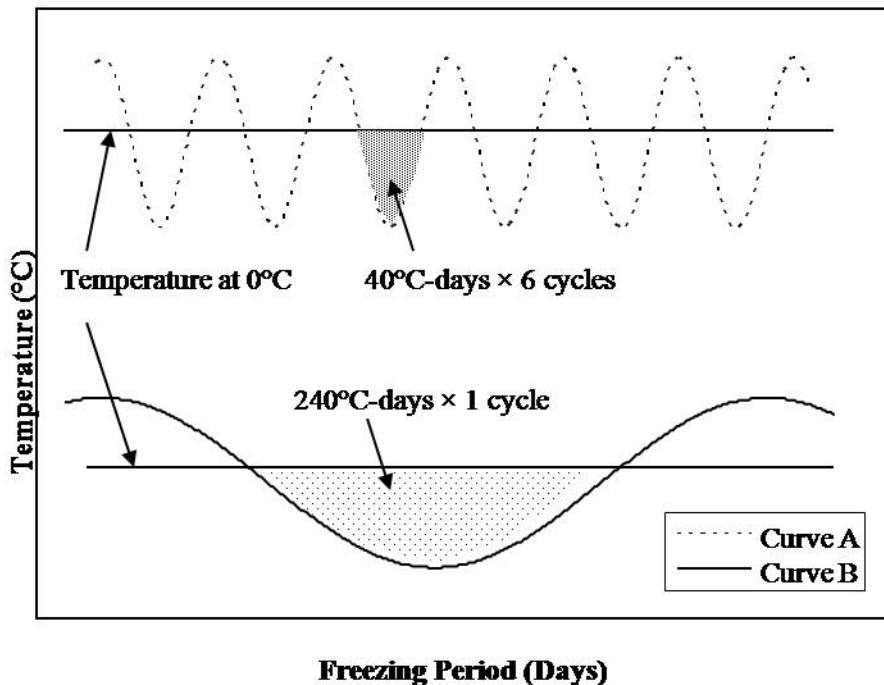
Figure 74. Two freezing cycles resulting in the same freezing index

95
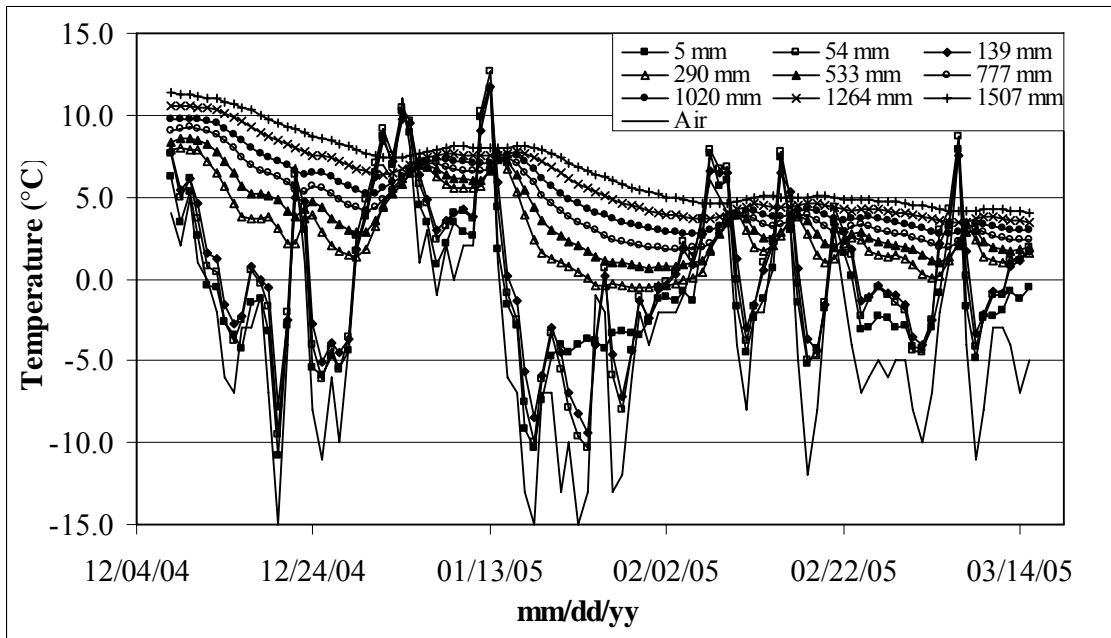
(a) 2005 winter
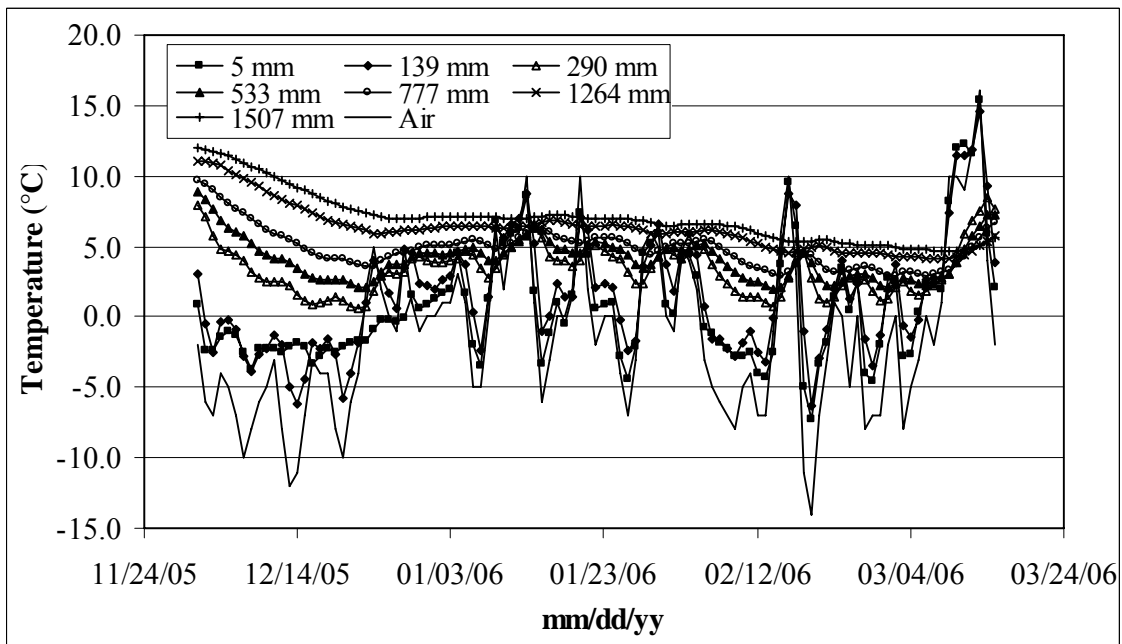
(b) 2006 winter

Figure 75. Temperature profiles at the Somerset location 1 for the 2005 and 2006 winters

Freezing Index and Freeze-Thaw Cycle at SISSI Sites

<u>*Relationship between Freezing index and Freeze-Thaw Cycles*</u>

To evaluate the impact of freeze cycles, FI was determined for a major (dominant) freeze-thaw cycle as well as for multiple cycles through the whole period of the cold season. Figure 76 shows the relationship between FI and the freeze-thaw cycle at the SISSI sites for the last 10 years. The freeze-thaw cycle was counted for fluctuation of mean daily air temperature above and below 0°C during the winter season. Ten data points are presented for multiple cycles, representing 10 years of data, and each data point represents the number of freeze-thaw cycles in a specific year. Each data point of multiple cycles is accompanied by one data point for a major cycle in a particular year. It was observed that, in relatively high FI sites (Figure 76 (a)-(d)), as freeze-thaw cycle increases, FI for a major cycle decreases. This phenomenon is more prominent in relatively severe winter regions, such as Warren site, which is in the northern part of Pennsylvania (Figure 6 (d)). Moreover, it should be noted that there is no significant correlation between freeze-thaw cycles with FI for multiple cycles. On the other hand, in the low FI sites (Figure 76 (f) and (g)), higher FI values are mostly associated with a greater number of freeze-thaw cycles.

Overall, each site has its own characteristics for the relationship between FI and the freeze-thaw cycle. This historical information in each region could be used to determine a net FI for a dominant freeze-thaw cycle for the considered region. Such FI could be a better predictor of the frost penetration depth.

<u>*Freeze-Thaw Cycle Distribution for the Last 10 Years*</u>

Figure 77 shows summarized distributions for periods of freeze-thaw cycles at SISSI sites for the last 10 years (1999 – 2008). It was a rare phenomenon to observe any freeze-thaw cycle exceeding 40 days; most freeze-thaw cycles had periods less than 10 days. Based on the temperature measured within the pavement layers of these sites, it could be observed that freeze-thaw cycles less than 10 days were mostly without a major freeze cycle and could not cause significant frost penetration. As shown in the distributions, the majority of cycles included freeze periods of less than 10 days in duration. Thus, it could be inferred that there were many ineffective cycles that did not directly contribute to the maximum frost penetration at these sites. The ways in which these ineffective cycles contributed to the summarized FI will be presented in the following section.

This study focused on investigating the difference between the impact of multiple freeze-thaw cycles and a single major cycle. The major freeze-thaw cycle was selected as a cycle with the longest freeze period in each year. FI was then computed based on only this cycle. Most major cycles were formed with over 15 days of continuous freeze at each site.
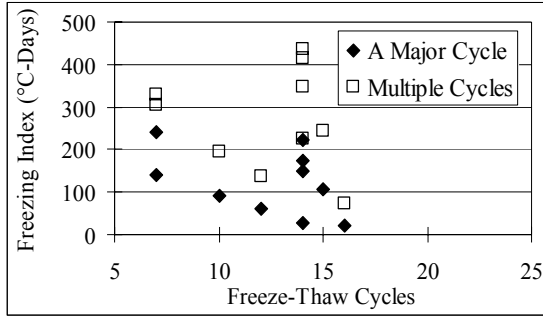
(a) Blair
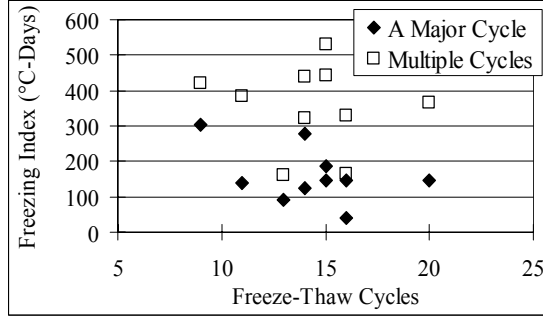
(b) Mercer East & West
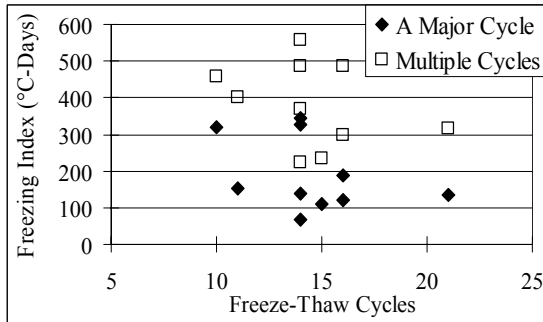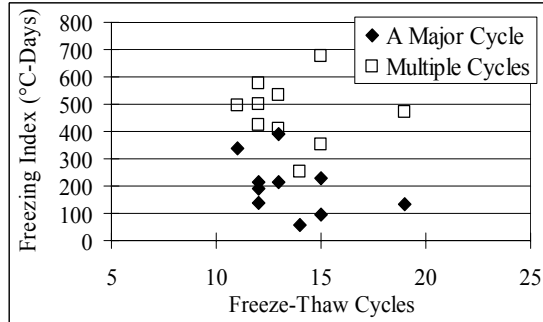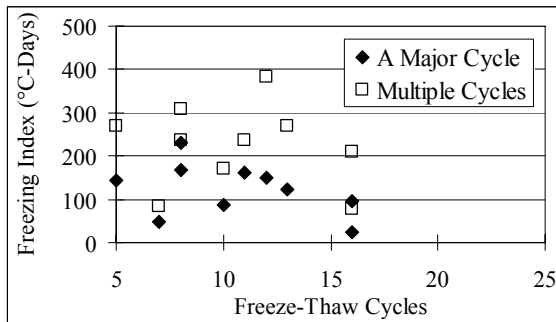
(c) Somerset
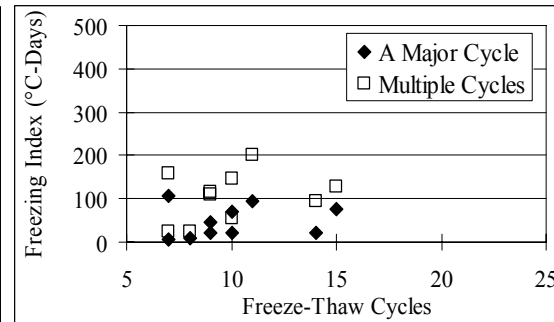
(d) Warren
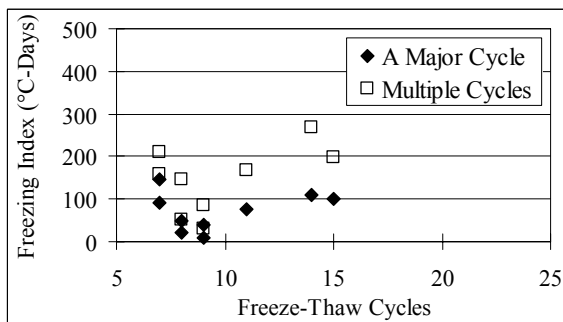
(e)Tioga

(f) Delaware

(g) Perry

Figure 76. Relationship between freezing index and freeze-thaw cycle at SISSI sites for the last 10 years (1999 – 2008)

98
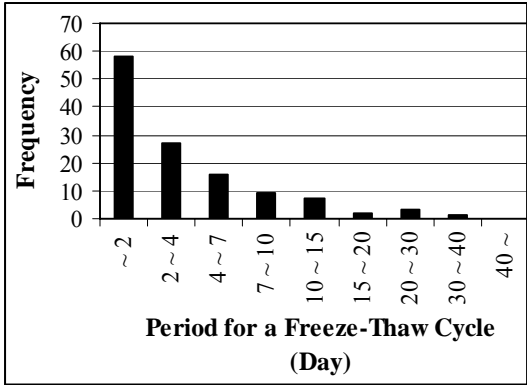
(a) Blair
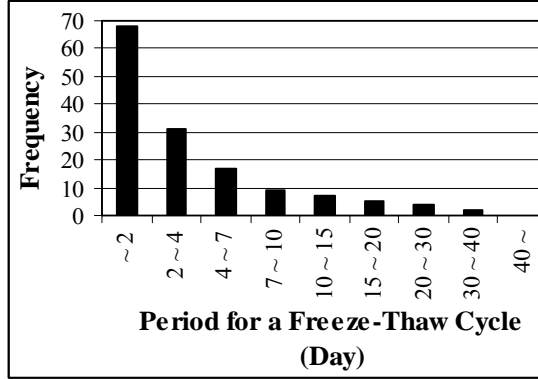
(b) Mercer East & West
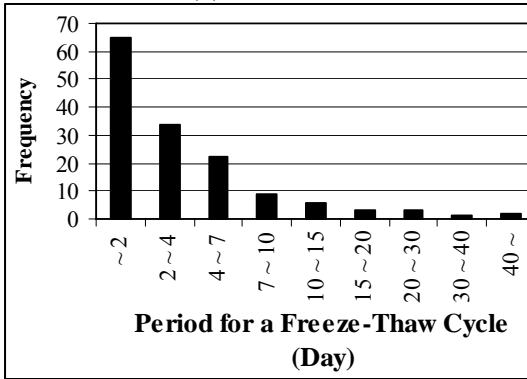
(c) Somerset
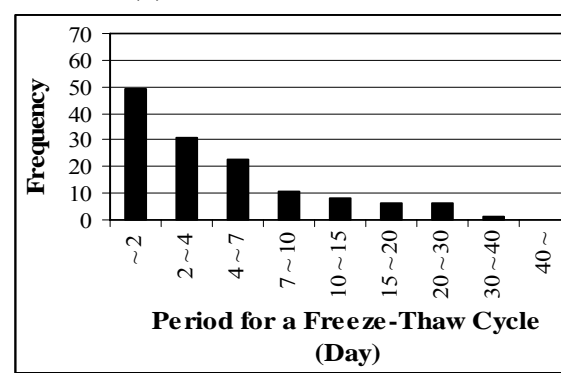
(d) Warren
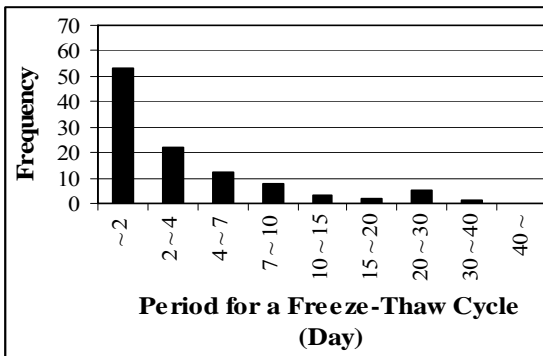
(e) Tioga
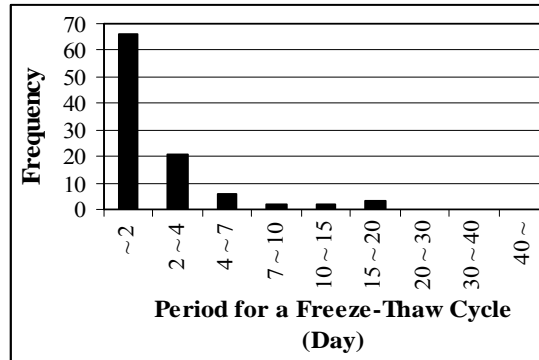
(f) Delaware
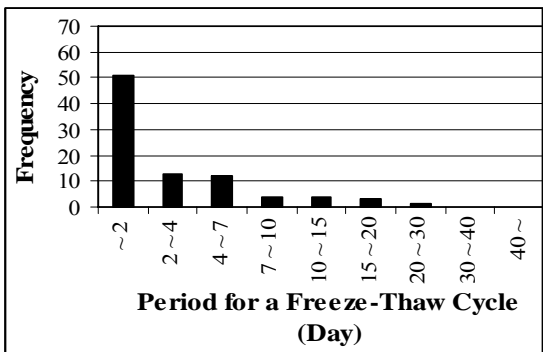
(g) Perry

Figure 77. Summarized distributions for periods of freeze-thaw cycle at SISSI sites for the last 10 years (1999 – 2008)

Freezing Index Difference due to Number of Freezing Cycles

Figure 78 shows how the ratio of FI from these two approaches (FI from multiple cycles over FI from the major cycle) correlates with the computed FI from a major freeze cycle. The graph also shows the relationship between the difference between FI from these two approaches and the computed FI from a major freeze cycle. For FI greater than 250 °C-days, it is noticed that the ratio does not exceed 2.0. In addition, for this range, the difference in FI does not exceed 170 °C-days. On the other hand, for FIs less than 100 °C-days, in spite of large FI ratios, it can be seen that the difference in FI from these two methods of computation is less than 200 °C-days.

The most critical range for FI is from 100 to 250 °C-days. Within this range, FI differences are mostly in the range of 200 to 300 °C-days, with the highest difference of 445 °C-days. Thus, it can be concluded that for the regions with a major cycle FI in the range of 100 to 250 °C-days, computed frost depth could be greatly larger than the measured depth if the multiple cycle FI through the whole period of the cold season is utilized. It will be shown how this overestimation occurs at the end of this study.
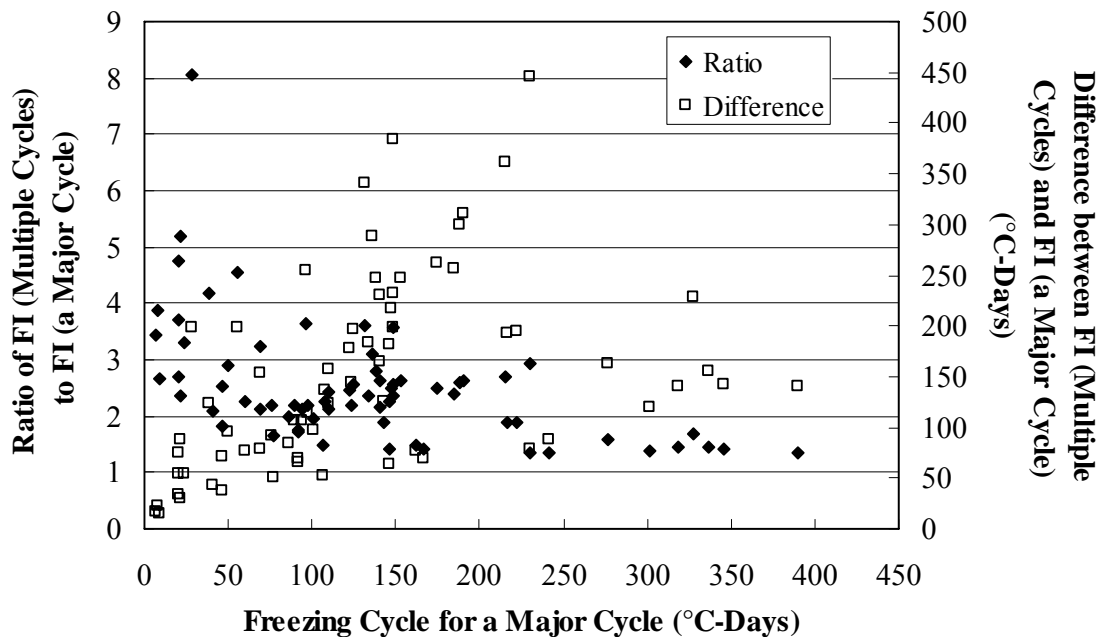
Figure 78. Relationships between the ratio and difference of FI (multiple cycles) to FI (a major cycle), and freezing index for a major cycle

Evaluation of Frost Depth Considering Freezing Index from a Major and Multiple Cycles(s)

One major objective of this study was to determine whether the FI based on one major freeze cycle or based on multiple cycles would be a better predictor of frost depth for a specific region. Therefore, the freezing indices determined based on these two approaches were used in currently available equations to determine the frost depth. The results were compared with measured freezing depths at SISSI sites to determine which approach was a better predictor.

Measured Frost Depth

For frost action in specifically unbound layers, penetration of freezing temperature, supply of moisture, and sufficient duration of freezing are dominant factors (Mitchell 1993). Frost action usually occurs at below 0°C, not at 0°C, due to soil mineral characteristics. To detect whether pavement layers are truly frozen, moisture and frost sensors are required in addition to the temperature sensors. However, this study focused on penetration of the freezing temperature, and as a result, only the temperature data are included in the analysis.

Maximum frost depth mostly lies at a point between the locations of temperature measurement by the thermocouples. As a result, the frost depth is interpolated based on available data. The measured frost depths from each site are summarized in Table 21.

Table 21. Measured and computed frost depths

	Year	Measured Depth of Freezing Temperature (m)	Computed Frost Depth Using Freezing Index for a Major Cycle (m)	Computed Frost Depth Using Freezing Index for Multiple Cycles (m)
	2007	0.69	0.72	0.82
Blair 1	2006	0.30	0.47	0.66
	2005	0.56	0.58	0.80
Blair 2	2006	0.19	0.51	0.67
	2005	0.30	0.59	0.79
Delaware 1	2005	0.39	0.42	0.48
Delaware 2	2005	0.49	0.43	0.48
	2007	0.77	0.86	1.02
Somerset 1	2006	0.27	0.62	0.89
	2005	0.40	0.68	0.92
	2007	1.34	0.76	0.81
Tioga 1	2006	0.92	0.54	0.71
	2004	1.49	0.87	0.93
	2007	1.28	0.75	0.82
Tioga 2	2006	0.87	0.52	0.72
	2004	1.30	0.84	0.91
	2007	1.17	0.91	1.01
Mercer E1	2006	0.55	0.66	0.86
	2005	1.02	0.69	0.94
Mercer E2	2005	1.02	0.69	0.96
	2007	1.03	0.99	1.09
Mercer W1	2006	0.59	0.75	0.92
	2005	0.87	0.78	0.99
	2007	1.05	0.98	1.05
Mercer W2	2006	0.40	0.76	0.94
	2005	0.77	0.78	0.98

Computed Frost Depth

Stefan established an analytical formula for frost depth computation in late 1800's. A more advanced formula was later introduced by Berggren (1943), which was further modified by Aldrich and Paynter (1956) to account for variability of the temperature in the field through introduction of the FI (Eq. 10). In the model, volumetric heat stored in soil was newly added for more accurate estimation of soil freezing. The modified Berggren model was incorporated into a multilayer system and was used for predicting frost depth in pavement (George and Berg 1968 and Zarling et al. 1989). In this study, the modified Berggren model for a multilayer system was adopted to compute frost depth at the SISSI sites.

$$\text{Frost Penetration Depth} = \lambda \cdot \sqrt{\frac{48 \cdot k_{ave} \cdot n \cdot FI}{L}} \tag{10}$$

where λ is a dimensionless coefficient that takes into consideration the effect of temperature changes in the soil mass, k_{ave} is thermal conductivity (W/m·K), n is the ratio of surface freezing index to air freezing index, and L is latent heat capacity (J/m^3).

The model requires thermal parameters such as thermal conductivity, specific heat, and latent heat capacity. The range of thermal conductivity of an asphalt mixture was found to be approximately in the range of 0.80 to 2.00 W/m·K (Highter and Wall 1984, Luca and Mrawira 2005). Recently, thermal conductivity of superpave mixes was examined to be in the range of 1.40 to 1.80 W/m·K (*14*). For the sites considered under this study, thermal conductivity was assigned a typical value, 1.60 W/m·K.

For other types of layers, typical thermal properties were reasonably selected from the information summarized and suggested from many historical research projects, such as those by Army Technical Manual (1988), Berg (1997), Tan et al. (1997), Andersland and Ladanyi (2004), and Mrawira and Luca (2006). Table 22 contains the thermal properties used in computing frost depth. Computed frost depths at all sites are summarized in Table 21.

Table 22. Thermal properties used in computing frost depth

	Thermal Conductivity k, (W/m·K)	Volumetric Heat Capacity c, (MJ/m^3·K)	Latent Heat L, (MJ/m^3)
HMA Wearing Course	1.6	1.8	0
HMA Binder Course	1.6	1.8	0
Leveling Course	1.3	1.5	0
Existed Concrete Pavement	1.3	1.5	0
BCBC	2.0	1.5	30
ATPB	2.0	1.5	30
Subbase	2.2	1.7	40
Subgrade	2.0	1.8	100

Comparison between Computed and Measured Frost Depths

Figure 79 presents a comparison between computed and measured frost depths. It is obvious that the magnitude of computed frost depth is dependent on adopted thermal properties and applied frost model (Berg 1997). Therefore, the analysis presented here is mostly concerned with the relationship between computed frost depth and measured frost depth rather than how accurately computed values compare with measured values. For frost penetrations deeper than approximately 0.8 m, it appears that underestimation occurs, and the computed frost depth based on the model used in this study is less than the measured frost depth. Overestimation occurs for frost depth less than about 0.8 m. However the focus here is to compare the effect of freeze cycles on frost depth computation, and in this regard, it was observed that FI calculated based on a major cycle of freeze provides a better prediction of frost penetration depth compared with FI based on multiple freeze cycles.
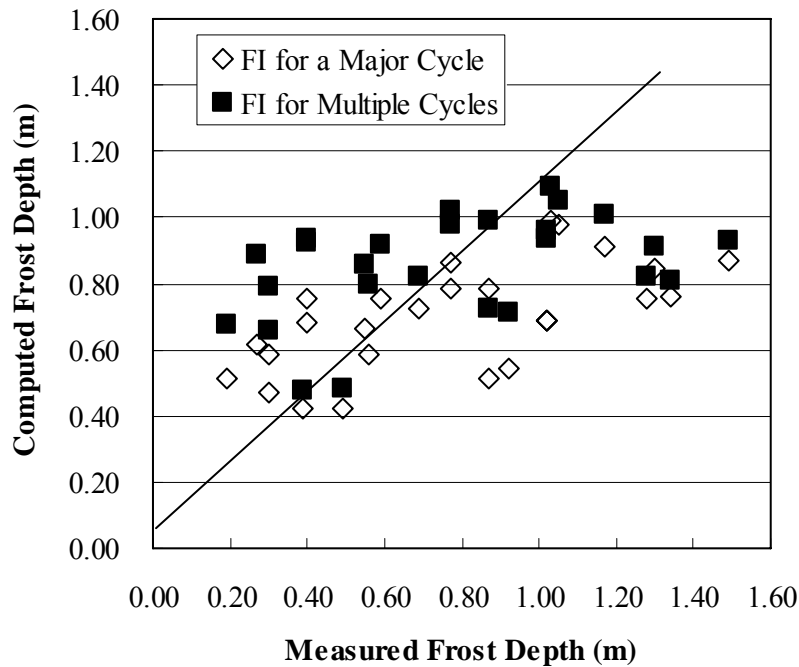
Figure 79. Comparison between computed and measured frost depths

Effects of Freezing Index Characteristics on Measured Frost Depth

The relationship between FI and measured frost depth is presented in Figure 80. FIs determined from multiple freeze cycles do not seem to correlate well with measured frost depth for the range of frost depths measured at various sites. Specifically, for FIs for multiple cycles within 300 to 450 °C-days, frost depth ranges from 0.25 to 1.49 m. However, FIs computed from temperature data associated with one major freeze cycle are relatively better correlated with measured frost depth. This implies that the frost depth is dominated by the major freeze cycle, and FI obtained from all freezing cycles throughout the cold season might not be a credible factor in predicting actual frost depth.
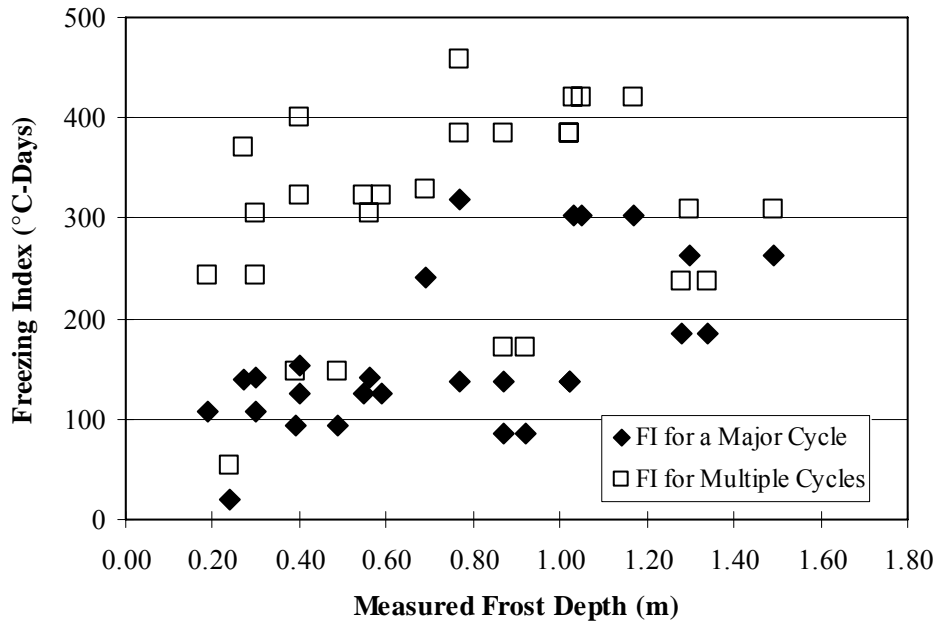
Figure 80. Relationship between measured frost depth and freezing indices for a major cycle and multiple cycles

Effects of FI Characteristics on Computed Frost Depth

In the previous section, it was shown that for cases of FI within 100 to 250 °C-days, there was a significant difference between FI from the two approaches (i.e., how freezing cycles are considered in determination of FI, a major cycle or multiple cycles). Figure 81 illustrates the effect of such difference in FI on computed frost depth. If the FI difference is less than 150 °C-days, it seems that variation of computed frost depth does not exceed 0.20 m. For an FI difference of approximately 200 °C-days, the change in computed frost depth could be from 0.15 to 0.25 m. It is obviously expected that a greater FI difference will produce greater variation in frost depth computation.
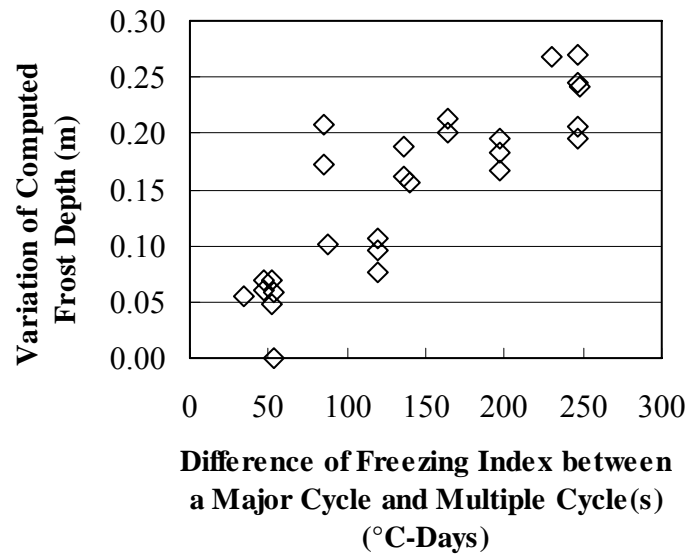
Figure 81. Variation of computed frost depth due to freezing index difference between a major cycle and multiple cycles

CHAPTER 8: SUMMARY AND CONCLUSIONS

As a result of the collection and analysis of the collected SISSI Phase 2 field data, a number of observations and conclusions have been obtained. Those are summarized briefly below. Further integrated analysis of the Phase I and Phase II SISSI data, focused on mechanistic analysis of the data, is presented in a separate volume.

At the time of the most recent distress surveys, the SISSI sites appeared to be in good shape except for those at Warren and Delaware. Rut depths continued to increase although the magnitude of increase was small at most sites. The Blair site exhibited the greatest percentage increase in rutting between 2004 and 2008.

The overall magnitudes of the Phase II dynamic data measurements are consistent with those from Phase I for approximately the same conditions of environment and testing. Measurements at very slow speeds resulted in considerably higher strain levels; increases in speeds above 20 mph do not produce further significant changes in response. The vertical stresses at the top of the subbase were significantly greater than those at the top of the subgrade. This demonstrates the protective role of the subbase layer.

Additional FWD testing at the Blair site, using additional load levels and collection of load-deflection history, indicated that the subgrade was behaving in a significantly nonlinear manner. Accounting for this nonlinearity explained much of the backcalculation difficulties encountered during Phase I for the Blair site.

The PSPA testing that was conducted demonstrated the variability over the area of the sites; the specific locations of the instrumentation did not differ significantly. The seismic moduli were consistently lower than the laboratory dynamic moduli; the laboratory complex modulus test always resulted in an elastic modulus approximately 4000 to 7000MPa higher than the corresponding in-situ seismic modulus. In the field, testing of cracked areas resulted in lower seismic moduli, as anticipated.

Traffic data during Phase II exhibited only small changes. The greatest change was at the Mercer sites, where the ADT dropped steadily from 2006 to 2008.

Collection of pavement temperature and solar radiation data continued during Phase II. Available temperature data could potentially play a major role in the calibration of MEPDG for local conditions. It is also useful in validation and calibration of integrated climatic models.

Different approaches in the determination of the freezing index and the impact of the freezing index on the computed frost depth were evaluated as part of the Phase-II SISSI research. Freezing index was calculated based on a major freeze cycle as well as multiple freeze-thaw cycles. It was observed that there was rarely a freeze-thaw cycle that was over 40 days in Pennsylvania. Most freeze-thaw cycles had periods less than 10 days. In the sites with a summarized freezing index 250 to 450 °C-days, as freeze-thaw cycle increases, freezing index for a major cycle decreases, but the summarized freezing index from multiple cycles did not exhibit any relationship to freeze-thaw cycles. It was also found that the freezing index difference due to number of freeze-thaw cycle is significantly great in the range from 100 to 250

°C-days of a major cycle freezing index. Within this range, the freezing index differences are mostly 200 to 300 °C-days, with the highest difference being around 445 °C-days. Thus, it was concluded that the summarized freezing index in the regions with this range of freezing index for a major cycle might be overestimated. Accordingly, a too conservative frost depth could be obtained.

Based on the modified Berggren model with assumed thermal properties, for deeper frost penetration than about 0.8 m, it was found that computed values are underestimated, whereas they are overestimated for frost depth less than about 0.8 m. For actual frost penetrations less than 0.8 m, it was observed that the freezing index for a major cycle has more relevance to measured values than the freezing index for multiple cycles. Freezing index within around 300 to 450 °C-days for multiple cycles seems not to have a significant relationship to measured frost depth. On the other hand, freezing index for a major cycle has relatively strong positive relationship to measured frost depth in the same range. For a freezing index difference less than 150 °C-days, variation of computed frost depth, in most cases, does not exceed 0.20 m; however, for a freezing index difference of approximately 200 °C-days, computed values vary from 0.15 to 0.25 m.

Frost data from the Blair site was analyzed to determine the depth and rate of frost penetration. Data indicate that as freezing period lasts longer, frost severity increases at various depths. Moreover, for the given temperature and site conditions, frost sensors closer to the pavement surface showed greater and sharper peak responses, implying faster rate of frost formation and penetration. Overall, at deeper pavement layers, more time is required to reach a specific freezing condition. For the upper subbase interval from about 330 to 400 mm depth, the averaged freezing rate could be obtained as 2 mm/hr, whereas for the lower section of the subbase, the rate was 13 mm/hr.

The additional collection of data during Phase II of the SISSI project contributed substantially to the overall contributions of the project. The data provided a firmer basis for mechanistic analysis of the pavement sections. The Phase II findings also directly improved the understanding of the long-term performance of the pavement sections.

REFERENCES

Aldrich, H. P. and H. M. Paynter. Derivation of a Rational Formula for the Prediction of Frost Penetration. *Highway Research Bulletin 135*, 1956, pp. 145-149.

Alexander, DR 1996, "In-situ Strength Measurements with Seismic Methods," Report from US Army Engineer Waterways Experiment Station, Vicksburg, Mississippi, for the US Air Force Civil Engineering Support Agency, Tyndall AFB, FL.

Andersland, O. B. and Ladanyi, B., "frozen ground engineering," 2nd Edition (Wiley, 2004), 256-257.

Army Technical Manual. Arctic and Subarctic Construction - Calculation Methods for Determination of Depths of Freeze and Thaw in Soils. Army TM 5-852-6, Departments of the Army and the Air Force, 1988.

Berg, R. L., "Calculating maximum frost depths at MnRoad winters 1993-94, 1994-95 and 1995-96", Final Report, MNRC - 97/21, Minnesota Department of Transportation, (1997).

Berggren, W. P. Prediction of Temperature-distribution in Frozen Soils. Transactions, American Geophysical Union, 1943, part 3:71-7.

Celaya, M and Nazarian, S 2006, "Seismic Testing to Determine Quality of Hot -Mix Asphalt." *Proceedings of the Transportation Research Board Annual Meeting, Washington, D.C.*

Chisholm, R. A. and Phang, W. A., "Measurement and prediction of frost penetration in highways," *Journal of the Transportation Research Board,* 918 (1983) 1-10.

Dempsey, B. and Thomson, M. R., "Effects of freeze-thaw parameters on the durability of stabilized materials," *Highway Research Record*, 379 (1972) 10-18.

Drumm, E. C., and R. Meier. LTPP Data Analysis: Daily and Seasonal Variations in In-situ Material Properties. Final Report, Project No. NCHRP 20-50 (7-12), 2003.

George, W. A. and R. L. Berg. Digital Solution of Modified Berggren Equation to Calculate Depths of Freeze or Thaw in Multilayered Systems. Special Report 122, USA CRREL, 1968.

Goel, A and Das, A 2006, "A Brief Review on Different Surface Wave Methods and Their Applicability for Non-Destructive Evaluation of Pavements." *Proceedings of Highway Geophysics – NDE, St. Louis, MO.*

Hass, W. M. and Bovid, G. C., "Frost depth prediction for highway subgrade soils, Northern community: A search for a quality environment," (1981) 719-733.

Highter, W. H. and D. J. Wall. Thermal Properties of Some Asphaltic Concrete Mixes. In *Transportation Research Record: Journal of the Transportation Research Board, No. 968*, 1984, pp. 38 – 45.

Irwin, L. H. MODCOMP. Cornell Local Roads Program, Ithaca, NY, 2000.

Jackson N. and J. Puccinelli. Long-Term Pavement Performance (LTPP) Data Analysis Support: National Pooled Fund Study TPF-5(013): Effects of Multiple Freeze Cycles and Deep Frost Penetration on Pavement Performance and Cost. Publication FHWA-HRT-06-121, FHWA, 2006.

Li, Y and Nazarian, S 1994, "Evaluation of Aging of Hot Mix Asphalt Using Wave Propagation Techniques." *In STP 1265*, *ASTM*, Philadelphia, PA.

Luca J. and D. Mrawira (2005). New Measurement of Thermal Properties of Superpave Asphalt Concrete. *Journal of Materials in Civil Engineering*, Vol. 17, No. 1, 2005, pp. 72-79.

McKeown, S., J. I. Clark and D. Matheson. Frost Penetration and Thermal Regime in Dry Gravel. *Journal of Cold Regions Engineering*, 1988, Vol. 2, No. 3, pp. 111-123.

Mitchell, J. K., "Fundamentals of soil behavior", 2nd Edn (Wiley, 1993).

Mrawira D. M. and J. Luca. Effect of Aggregate Type, Gradation, and Compaction Level on Thermal Properties of Hot-Mix Asphalts. *Canadian Journal of Civil Engineering*, Vol. 33, 2006, pp. 1410-1417.

Moulton L. K. and J. H. Schaub. Estimation of Pavement Surface Freezing Indices. *Proceedings of the American Society of Civil Engineers*, *Transportation Engineering Journal*, Vol. 95, No. TE 4, 1969, pp. 587-604.

Nazarian, S. and K. H. Stokoe 1984. "Nondestructive Testing of Pavements Using Surface Waves." *Transportation Research Record 993*, National Research Council, Washington, D.C.

Nazarian, S, Baker, MR, and Crain, K 1993, Fabrication and Testing of a Seismic Pavement Analyzer. SHRP Report H-375. National Research Council, Washington, D.C.

Saeed, A and Hall, J 1999, "*Determination of Moduli of Asphalt Concrete Cores with Ultrasonic methods*." Draft Report. NCHRP Project 10-44A, Geomedia Research and Development, El Paso, TX.

Saeed, A and Hall, J 2003, "Comparison of Non-Destructive Testing Devices To Determine In-situ Properties of Asphalt Concrete Pavement Layers." *Proceedings of the Transportation Research Board Annual Meeting,* Washington, D.C.

Solaimanian, M., Stoffels, S. M., Hunter, D. A., Morian, D. A., and Sadasivam, S., *Superpave in-situ/stress strain investigation.* Final Report, Publication FHWA-PA-2006-019-350R02, Pennsylvania Department of Transportation, (2006).

Stoffels, S. M., Solaimanian M., and Morian, D. (2006) *Seasonal Variations for Superpave In-Situ Stress/Strain Investigation*. Final Report, Pennsylvania Transportation Institute, University Park, PA.

Stolle, D., and Hein, D. "Parameter estimates of pavement structure layers and uniqueness of the solution." In Nondestructive testing of pavements and backcalculation of moduli. *Special Technical Publication (STP) 1026*, ASTM, Philadelphia, PA, 1989.

Tan, S. A., T. F. Fwa, C. T. Chuai, and B. H. Low. Determination of Thermal Properties of Pavement Materials and Unbound Aggregate by Transient Heat Conduction. *Journal of Testing and Evaluation*, Vol. 25, No. 1, 1997, pp. 15-22.

Tandon, T, Nazarian, S and Bai, X 2004, "Assessment of Relationship between Seismic and Dynamic Modulus of Hot Mix Asphalt Concrete." Submitted to *Road Materials and Pavement Design*.

Yin, H, Stoffels, S, and Antle, C 2006, "Profile Data Variability in Pavement Management: Findings and Tools from LTPP." *Proceedings of the Airfield and Highway Pavement Specialty Conference,* Atlantic City, NJ.

Zarling, J. P., A. Braely, and C. Pelz. The Modified Berggren Method. *Cold Regions Engineering: Proceedings of the Fifth International Conference*, 1989, pp. 262-273.

Appendix A

Photographs from the Most Recent Distress Surveys

Figure A-1. Condition survey photographs from Tioga site, 11/6/2007

Figure A-1. Condition survey photographs from Tioga site, 11/6/2007 (continued)

Figure A-1. Condition survey photographs from Tioga site, 11/6/2007 (continued)

Figure A-1. Condition survey photographs from Tioga site, 11/6/2007 (continued)

Figure A-1. Condition survey photographs from Tioga site, 11/6/2007 (continued)

Figure A-1. Condition survey photographs from Tioga site, 11/6/2007 (continued)

Figure A-1. Condition survey photographs from Tioga site, 11/6/2007 (continued)

Figure A-2. Condition survey photographs from Mercer East site, 11/1/2007

Figure A-2. Condition survey photographs from Mercer East site, 11/1/2007 (continued)
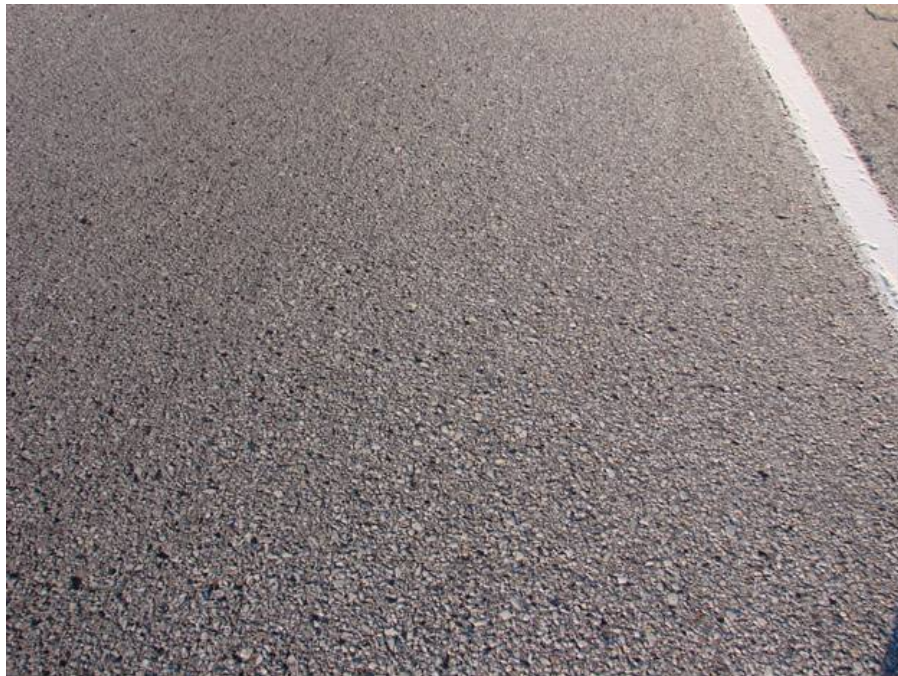
Figure A-2. Condition survey photographs from Mercer East site, 11/1/2007 (continued)

Figure A-2. Condition survey photographs from Mercer East site, 11/1/2007 (continued)

Figure A-2. Condition survey photographs from Mercer East site, 11/1/2007 (continued)

Figure A-2. Condition survey photographs from Mercer East site, 11/1/2007 (continued)

Figure A-2. Condition survey photographs from Mercer East site, 11/1/2007 (continued)

Figure A-3. Condition survey photographs from Mercer West site, 11/1/2007

Figure A-3. Condition survey photographs from Mercer West site, 11/1/2007 (continued)

Figure A-3. Condition survey photographs from Mercer West site, 11/1/2007 (continued)

Figure A-3. Condition survey photographs from Mercer West site, 11/1/2007 (continued)

Figure A-3. Condition survey photographs from Mercer West site, 11/1/2007 (continued)

Figure A-3. Condition survey photographs from Mercer West site, 11/1/2007 (continued)

Figure A-3. Condition survey photographs from Mercer West site, 11/1/2007 (continued)

Figure A-3. Condition survey photographs from Mercer West site, 11/1/2007 (continued)

Figure A-4. Condition survey photographs from Perry site, 7/17/2007

Figure A-4. Condition survey photographs from Perry site, 7/17/2007 (continued)

Figure A-4. Condition survey photographs from Perry site, 7/17/2007 (continued)

Figure A-4. Condition survey photographs from Perry site, 7/17/2007 (continued)

Figure A-4. Condition survey photographs from Perry site, 7/17/2007 (continued)

Figure A-4. Condition survey photographs from Perry site, 7/17/2007 (continued)

Figure A-4. Condition survey photographs from Perry site, 7/17/2007 (continued)

Figure A-4. Condition survey photographs from Perry site, 7/17/2007 (continued)

Figure A-4. Condition survey photographs from Perry site, 7/17/2007 (continued)

Figure A-4. Condition survey photographs from Perry site, 7/17/2007 (continued)

Figure A-4. Condition survey photographs from Perry site, 7/17/2007 (continued)

Figure A-4. Condition survey photographs from Perry site, 7/17/2007 (continued)

Figure A-4. Condition survey photographs from Perry site, 7/17/2007 (continued)

Figure A-4. Condition survey photographs from Perry site, 7/17/2007 (continued)

Figure A-4. Condition survey photographs from Perry site, 7/17/2007 (continued)

Figure A-4. Condition survey photographs from Perry site, 7/17/2007 (continued)

Figure A-4. Condition survey photographs from Perry site, 7/17/2007 (continued)

Figure A-4. Condition survey photographs from Perry site, 7/17/2007 (continued)

Figure A-4. Condition survey photographs from Perry site, 7/17/2007 (continued)

Figure A-5. Condition survey photographs from Delaware site, 10/07/2008

Figure A-5. Condition survey photographs from Delaware site, 10/07/2008 (continued)

Figure A-5. Condition survey photographs from Delaware site, 10/07/2008 (continued)

Figure A-5. Condition survey photographs from Delaware site, 10/07/2008 (continued)

Figure A-5. Condition survey photographs from Delaware site, 10/07/2008 (continued)

Figure A-5. Condition survey photographs from Delaware site, 10/07/2008 (continued)

Figure A-5. Condition survey photographs from Delaware site, 10/07/2008 (continued)

Figure A-5. Condition survey photographs from Delaware site, 10/07/2008 (continued)

Figure A-5. Condition survey photographs from Delaware site, 10/07/2008 (continued)

Figure A-5. Condition survey photographs from Delaware site, 10/07/2008 (continued)

Figure A-5. Condition survey photographs from Delaware site, 10/07/2008 (continued)

Figure A-5. Condition survey photographs from Delaware site, 10/07/2008 (continued)

Figure A-5. Condition survey photographs from Delaware site, 10/07/2008 (continued)

Figure A-5. Condition survey photographs from Delaware site, 10/07/2008 (continued)

Figure A-5. Condition survey photographs from Delaware site, 10/07/2008 (continued)

Figure A-5. Condition survey photographs from Delaware site, 10/07/2008 (continued)

Figure A-6. Condition survey photographs from Blair site, 6/24/2008 (continued)

Figure A-6. Condition survey photographs from Blair site, 6/24/2008 (continued)

Figure A-6. Condition survey photographs from Blair site, 6/24/2008 (continued)

Figure A-6. Condition survey photographs from Blair site, 6/24/2008 (continued)

Appendix B

Summary of Dynamic Data

Table B-1. Summary of dynamic data at Blair site (Location 1, Back Load, 03/27/2008)

Attempt Speed, mph	Actual Speed, mph	Load Configuration	Axle#	Vertical Stress, kPa		Tensile Strain, E-6		
				Top of Subbase	Top of Subgrade	Bottom of Wearing	Bottom of Binder	Bottom of BCBC
5	4.6	Back	Axle 1	9.4	5.0	32.3	22.4	14.1
			Axle 2	7.2	4.0	19.4	15.1	7.8
			Axle 3	8.1	4.0	18.7	14.4	8.0
			Axle 4	16.8	8.9	57.1	38.0	15.8
10	7.2	Back	Axle 1	9.6	5.6	29.7	20.8	2.0
			Axle 2	7.3	4.5	14.2	7.7	5.1
			Axle 3	8.0	4.5	12.7	7.3	4.8
			Axle 4	16.4	9.7	50.0	22.0	8.7
20 (Replicate 1)	14.9	Back	Axle 1	9.4	5.7	22.8	8.0	1.6
			Axle 2	7.4	4.8	11.3	5.3	3.3
			Axle 3	7.6	4.6	10.1	5.0	3.2
			Axle 4	16.8	9.6	41.1	15.4	8.2
20 (Replicate 2)	17.0	Back	Axle 1	8.9	5.8	21.9	7.8	1.6
			Axle 2	7.3	4.8	9.9	4.6	3.3
			Axle 3	7.4	4.5	9.4	4.6	3.7
			Axle 4	16.0	9.6	36.9	14.9	7.1
20 (Replicate 3)	17.7	Back	Axle 1	8.7	5.8	22.1	7.5	1.8
			Axle 2	7.1	4.7	9.8	4.5	3.2
			Axle 3	7.2	4.4	9.1	4.4	2.6
			Axle 4	15.4	9.2	36.0	14.3	5.2
40	37.5	Back	Axle 1	7.7	5.6	12.5	5.8	0.7
			Axle 2	7.1	5.0	5.9	2.3	1.7
			Axle 3	7.3	6.1	5.7	2.0	1.7
			Axle 4	14.1	9.7	24.7	10.3	5.6

Table B-2. Summary of dynamic data at Blair site (Location 1, Front Load, 03/27/2008)

Attempt Speed, mph	Actual Speed, mph	Load Configuration	Axle#	Vertical Stress, kPa		Tensile Strain, E-6		
				Top of Subbase	Top of Subgrade	Bottom of Wearing	Bottom of Binder	Bottom of BCBC
			Axle 3	7.6	4.6	10.1	5.0	3.2
			Axle 4	16.8	9.6	41.1	15.4	8.2
5	4.7	Front	Axle 1	9.8	5.8	33.2	25.6	7.8
			Axle 2	11.1	7.0	29.0	14.7	8.0
			Axle 3	9.1	6.9	28.6	15.3	7.5
			Axle 4	9.3	5.5	29.0	16.1	5.5
10	7.7	Front	Axle 1	9.5	5.4	30.3	21.1	2.3
			Axle 2	11.1	6.5	27.0	11.0	5.0
			Axle 3	11.8	6.8	26.7	12.2	4.7
			Axle 4	8.5	5.1	26.9	13.1	3.5
20 (Replicate 1)	14.1	Front	Axle 1	9.0	5.5	24.7	9.1	3.2
			Axle 2	10.7	6.8	21.7	6.8	3.9
			Axle 3	11.9	6.9	21.3	3.8	3.3
			Axle 4	8.6	5.2	21.1	7.6	3.7
20 (Replicate 2)	15.0	Front	Axle 1	9.0	5.6	23.6	7.7	2.6
			Axle 2	10.7	6.9	21.5	6.3	2.6
			Axle 3	11.5	6.8	20.6	3.9	3.0
			Axle 4	8.7	5.1	20.6	7.8	3.1
20 (Replicate 3)	16.3	Front	Axle 1	9.0	5.5	22.6	7.0	4.2
			Axle 2	10.4	6.7	20.6	6.1	2.0
			Axle 3	11.4	6.4	19.9	6.4	2.8
			Axle 4	8.5	5.4	20.4	7.5	3.0
40	37.6	Front	Axle 1	7.6	6.1	12.4	5.4	1.6
			Axle 2	10.2	9.2	7.8	3.6	2.9
			Axle 3	10.3	8.8	8.6	3.0	2.7
			Axle 4	8.1	5.4	13.5	5.3	2.2

Table B-3. Wander data at Blair site (Location 1, 03/27/2008)

Load Configuration	Replicate Runs at 20 mph	Wander, in			
		Downstream		Upstream	
		L	R	L	R
Front	1	0.0	0.0	0.0	0.0
Front	2	0.0	1.0	0.0	1.0
Front	3	0.0	0.0	0.0	0.0
Back	1	0.5	0.0	0.5	0.0
Back	2	0.0	0.0	0.0	0.0
Back	3	0.0	0.0	0.0	0.0

Table B-4. Summary of dynamic data at Blair site (Location 2, Back Load, 06/24/2008)

Attempt Speed, mph	Actual Speed, mph	Load Configuration	Axle#	Vertical Stress, kPa		Tensile Strain, E-6		
				Top of Subbase	Top of Subgrade	Bottom of Wearing	Bottom of Binder	Bottom of BCBC
5	6.7	Back	Axle 1	25.5	15.6	49.7	36.6	17.0
			Axle 2	16.3	9.9	30.9	23.0	10.9
			Axle 3	16.0	10.3	30.4	22.7	10.7
			Axle 4	39.3	25.6	76.5	56.0	26.2
10	10.5	Back	Axle 1	25.2	15.7	37.1	27.3	16.8
			Axle 2	17.9	10.2	26.1	19.3	11.9
			Axle 3	17.1	9.7	25.2	18.6	11.4
			Axle 4	43.5	27.4	65.5	47.8	29.0
20 (Replicate 1)	19.1	Back	Axle 1	23.2	15.1	34.3	24.8	15.5
			Axle 2	15.3	10.8	23.2	16.7	10.2
			Axle 3	15.3	11.1	22.9	16.5	10.2
			Axle 4	39.2	26.1	58.4	42.7	26.1
20 (Replicate 2)	17.7	Back	Axle 1	30.3	14.0	45.9	33.4	20.2
			Axle 2	18.8	10.2	27.8	20.4	12.5
			Axle 3	17.2	9.7	26.0	18.8	11.5
			Axle 4	42.1	23.5	63.0	45.9	28.0
20 (Replicate 3)	18.6	Back	Axle 1	27.5	14.6	41.3	30.1	18.4
			Axle 2	17.2	10.7	25.3	18.6	11.5
			Axle 3	15.4	10.0	23.4	16.8	10.3
			Axle 4	40.3	25.3	60.9	44.5	26.8
40	38.7	Back	Axle 1	20.7	11.8	30.8	22.8	13.8
			Axle 2	15.0	9.5	22.5	16.5	10.0
			Axle 3	13.6	5.2	20.5	15.0	9.1
			Axle 4	31.6	21.3	47.3	34.9	21.1

Table B-5. Summary of dynamic data at Blair site (Location 2, Front Load, 06/24/2008)

Attempt Speed, mph	Actual Speed, mph	Load Configuration	Axle#	Vertical Stress, kPa		Tensile Strain, E-6		
				Top of Subbase	Top of Subgrade	Bottom of Wearing	Bottom of Binder	Bottom of BCBC
			Axle 4	31.6	21.3	47.3	34.9	21.1
5	6.2	Front	Axle 1	26.3	12.9	49.9	37.4	17.5
			Axle 2	21.4	13.3	41.7	30.7	14.3
			Axle 3	22.6	14.7	43.1	31.9	15.1
			Axle 4	19.1	11.9	37.6	27.7	12.8
10	9.9	Front	Axle 1	27.5	13.0	41.2	30.1	18.3
			Axle 2	23.3	13.5	35.1	25.6	15.6
			Axle 3	25.1	14.4	38.2	27.8	16.8
			Axle 4	19.6	11.7	29.9	21.7	13.1
20 (Replicate 1)	19.5	Front	Axle 1	22.0	12.7	33.3	24.5	14.7
			Axle 2	19.4	12.8	28.4	21.1	13.0
			Axle 3	20.2	13.5	30.8	22.7	13.5
			Axle 4	17.1	12.1	26.0	19.0	11.4
20 (Replicate 2)	19.9	Front	Axle 1	21.8	11.2	36.8	27.6	14.6
			Axle 2	19.8	12.3	29.7	21.9	13.2
			Axle 3	20.7	12.7	30.3	22.5	13.8
			Axle 4	18.5	12.1	27.4	20.3	12.3
20 (Replicate 3)	20.4	Front	Axle 1	16.6	12.7	24.3	17.8	11.0
			Axle 2	16.5	12.5	24.7	18.2	11.0
			Axle 3	19.8	14.7	29.6	21.5	13.2
			Axle 4	15.7	12.2	23.8	17.3	10.4
40	41.3	Front	Axle 1	13.1	12.0	19.3	14.1	8.7
			Axle 2	15.6	14.3	23.1	16.9	10.4
			Axle 3	16.1	11.5	24.0	17.3	10.8
			Axle#	15.8	12.4	23.6	17.3	10.6

Table B-6. Wander data at Blair site (Location 2, 06/24/2008)

Load Configuration	Replicate Runs at 20 mph	Wander, in			
		Downstream		Upstream	
		L	R	L	R
Front	1	1.5	0.0	1.5	0.0
Front	2	0.0	0.0	0.0	1.0
Front	3	0.0	0.0	0.0	0.0
Back	1	1.0	0.0	1.5	0.0
Back	2	0.0	0.0	0.0	0.5
Back	3	0.0	0.0	0.0	0.0

Table B-7. Summary of dynamic data at Perry site (Location 2, 07/17/2008)

Attempt Speed, mph	Actual Speed, mph	Load Configuration	Axle#	Tensile Strain, E-6	
				Bottom of Wearing	Bottom of Binder
5	5.4	Back	Axle 1	111.7	97.3
			Axle 2	102.2	80.9
			Axle 3	77.4	66.1
			Axle 4	138.4	103.0
10	9.0	Back	Axle 1	99.9	87.1
			Axle 2	77.6	61.4
			Axle 3	63.1	53.9
			Axle 4	124.0	92.3
20 (Replicate 1)	16.7	Back	Axle 1	51.8	45.2
			Axle 2	44.3	35.0
			Axle 3	37.8	32.3
			Axle 4	90.8	67.5
20 (Replicate 2)	18.2	Back	Axle 1	49.5	43.2
			Axle 2	38.9	35.4
			Axle 3	35.4	30.3
			Axle 4	78.1	58.1
20 (Replicate 3)	19.1	Back	Axle 1	43.2	37.6
			Axle 2	31.0	24.5
			Axle 3	28.4	25.8
			Axle 4	62.5	46.5
40	36.3	Back	Axle 1	19.8	17.3
			Axle 2	14.8	11.7
			Axle 3	18.9	20.4
			Axle 4	32.6	31.7
60	63.5	Back	Axle 1	10.8	9.4
			Axle 2	8.7	14.8
			Axle 3	6.5	14.1
			Axle 4	17.5	20.5

Table B-8. Summary of dynamic data at Perry site (Location 2, 07/17/2008)

Attempt Speed, mph	Actual Speed, mph	Load Configuration	Axle#	Tensile Strain, E-6	
				Bottom of Wearing	Bottom of Binder
5	4.3	Front	Axle 1	96.3	88.2
			Axle 2	72.1	69.8
			Axle 3	83.4	73.6
			Axle 4	75.3	64.6
10	10.5	Front	Axle 1	60.4	55.3
			Axle 2	41.3	34.9
			Axle 3	55.3	42.5
			Axle 4	40.3	34.6
20 (Replicate 1)	22.6	Front	Axle 1	35.8	32.8
			Axle 2	28.0	23.7
			Axle 3	31.4	26.2
			Axle 4	29.4	25.2
20 (Replicate 2)	21.3	Front	Axle 1	41.0	37.5
			Axle 2	31.8	26.9
			Axle 3	35.1	29.2
			Axle 4	23.3	20.0
20 (Replicate 3)	22.2	Front	Axle 1	35.9	32.9
			Axle 2	28.5	24.2
			Axle 3	32.8	27.4
			Axle 4	28.4	24.3
40	37.3	Front	Axle 1	24.2	22.2
			Axle 2	18.1	15.3
			Axle 3	20.2	18.4
			Axle 4	17.4	14.9
60	58.4	Front	Axle 1	12.1	11.1
			Axle 2	9.6	8.1
			Axle 3	11.3	10.3
			Axle 4	7.4	6.4

Table B-9. Wander data at Perry site (Location 2, 7/17/2008)

Load Configuration	Replicate Runs at 20 mph	Wander, in			
		Downstream		Upstream	
		L	R	L	R
Front	1	0.5	0.0	0.0	0.0
Front	2	0.0	0.0	0.0	0.0
Front	3	0.0	0.0	0.0	0.0
Back	1	0.0	0.0	0.0	0.0
Back	2	0.0	0.0	0.0	0.0
Back	3	0.0	0.5	0.0	0.0

Appendix C

Summary of FWD Data from Blair Site

Table C-1. Summary of deflection data collection, Blair, 4/29/2008

Code	Blair	Testing Location	Repeated Measurements ID	Time	Surface Temp, °C	Air Temp, °C
B1-L2-R1	1	2	1	10:21	19.6	9.2
B1-L2-R2	1	2	2	10:24	20.4	9.8
B1-L2-R3	1	2	3	10:27	20.7	9.9
B1-L3-R1	1	3	1	10:33	17.8	9.9
B1-L3-R2	1	3	2	10:35	19.6	10.2
B1-L3-R3	1	3	3	10:37	18.7	9.9
B1-L1-R1	1	1	1	10:43	21.1	9.8
B1-L1-R2	1	1	2	10:44	21.1	9.8
B1-L1-R3	1	1	3	10:46	21.4	9.8
B1-L4-R1	1	4	1	10:56	17.8	10.1
B1-L4-R2	1	4	2	10:58	18.8	9.9
B1-L4-R3	1	4	3	11:00	19.5	10.1
B1-L5-R1	1	5	1	11:06	20.9	9.6
B1-L5-R2	1	5	2	11:09	22.8	9.9
B1-L5-R3	1	5	3	11:10	23.4	10.3
B1-L6-R1	1	6	1	11:13	21.2	10.5
B1-L6-R2	1	6	2	11:15	20.4	10.2
B1-L6-R3	1	6	3	11:18	21.5	10.3
B2-L2-R1	2	2	1	12:41	27.0	13.3
B2-L2-R2	2	2	2	12:43	26.7	13.4
B2-L2-R3	2	2	3	12:45	26.6	13.3
B2-L3-R1	2	3	1	12:49	26.5	13.4
B2-L3-R2	2	3	2	12:52	26.1	13.5
B2-L3-R3	2	3	3	12:54	24.3	13.3
B2-L1-R1	2	1	1	12:58	26.2	13.0
B2-L1-R2	2	1	2	13:00	24.8	12.8
B2-L1-R3	2	1	3	13:03	24.5	13.0
B2-L4-R1	2	4	1	13:06	23.3	13.4
B2-L4-R2	2	4	2	13:09	22.9	13.4
B2-L4-R3	2	4	3	13:10	22.8	13.4
B2-L5-R1	2	5	1	13:16	29.7	14.3
B2-L5-R2	2	5	2	13:17	29.3	14.1
B2-L5-R3	2	5	3	13:19	29.7	13.9
B2-L6-R1	2	6	1	13:22	28.2	14.0
B2-L6-R2	2	6	2	13:23	29.2	13.9
B2-L6-R3	2	6	3	13:25	29.8	13.9
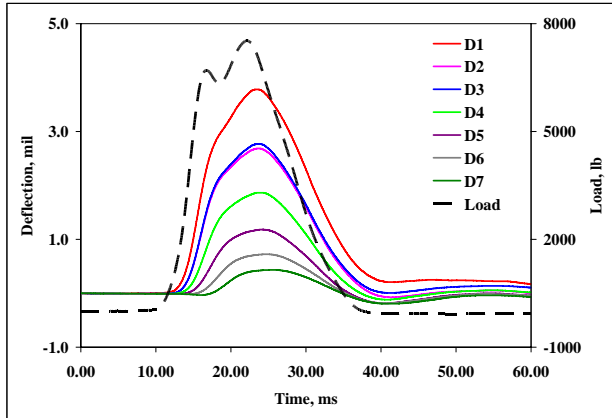
(a) 7500 lb
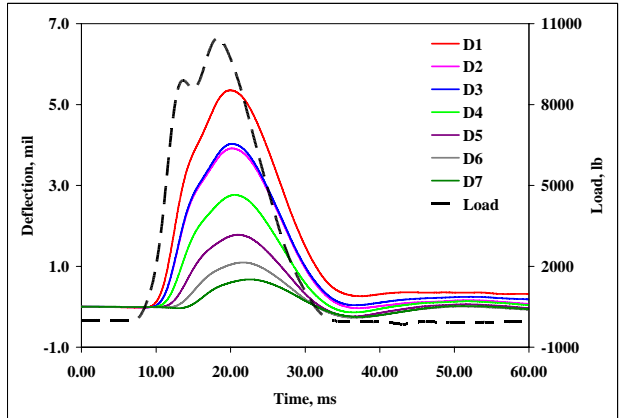
(b) 10500 lb
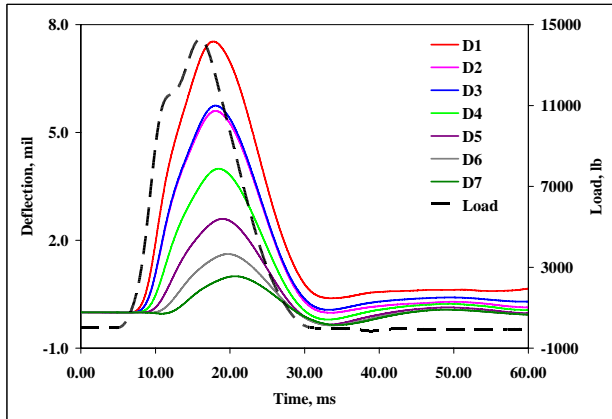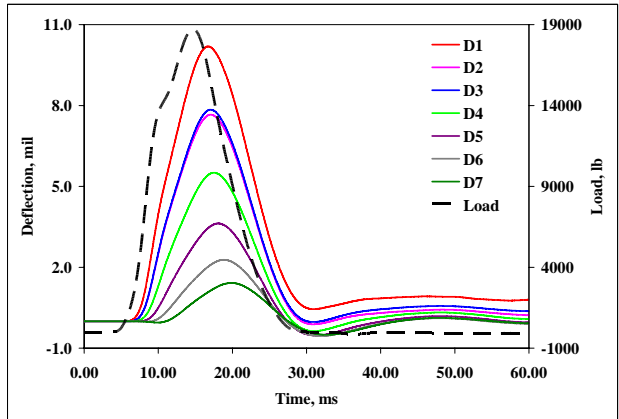
(c) 14500 lb

(b) 19000 lb

Figure C-1. Deflections at B1-L1-R1
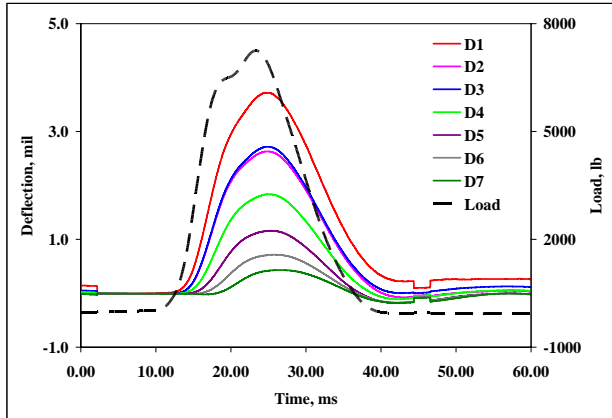
(a) 7500 lb
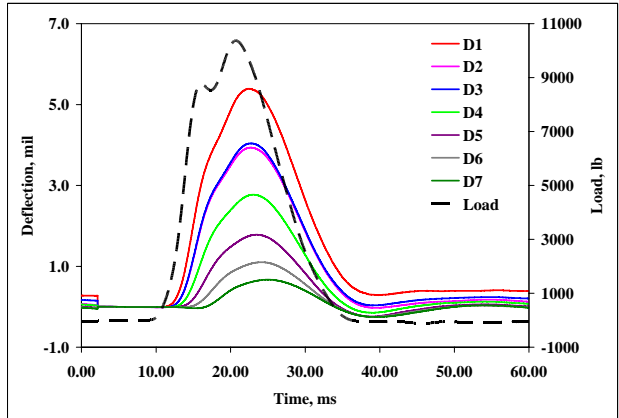
(b) 10500 lb
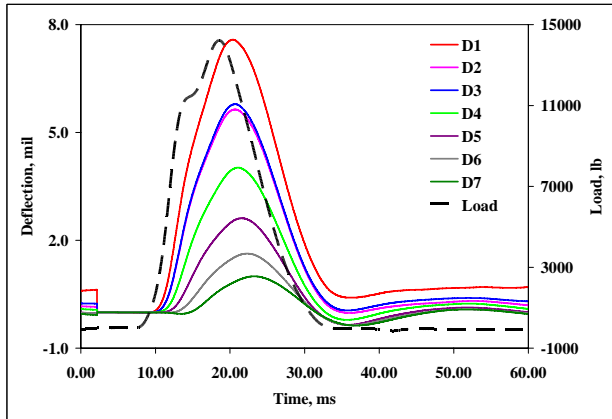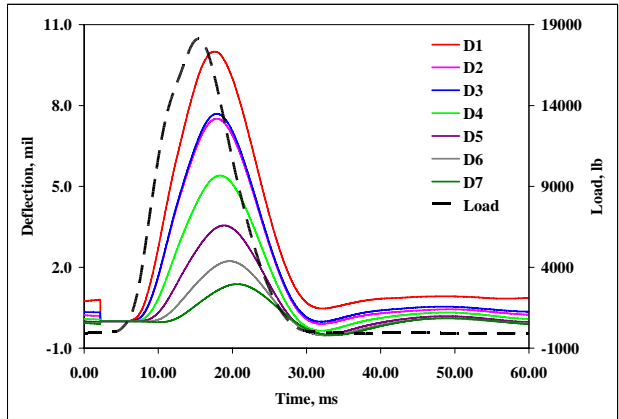
(c) 14500 lb

(b) 19000 lb

Figure C-2. Deflections at B1-L1-R2
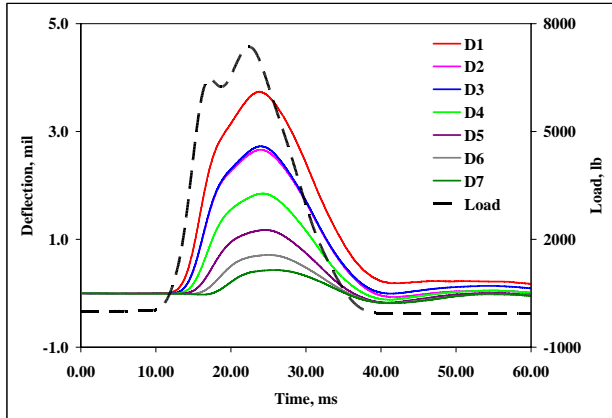
(a) 7500 lb
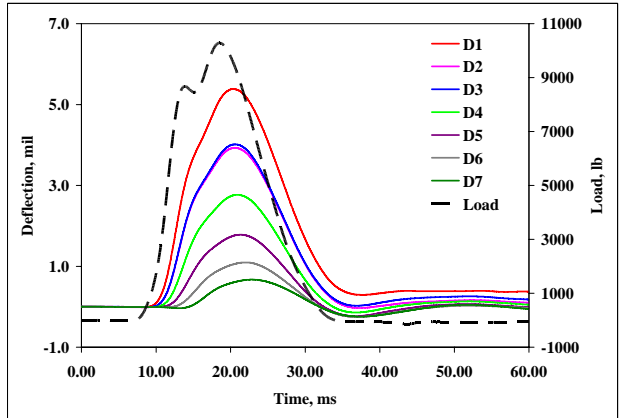
(b) 10500 lb
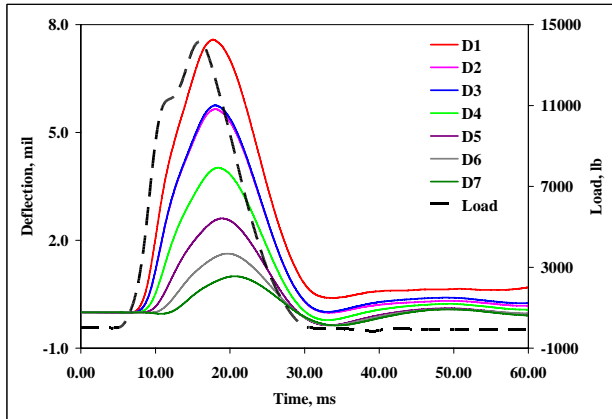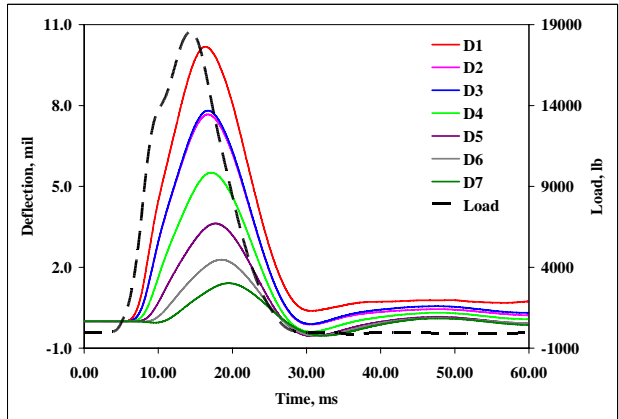
(c) 14500 lb

(b) 19000 lb

Figure C-3. Deflections at B1-L1-R3
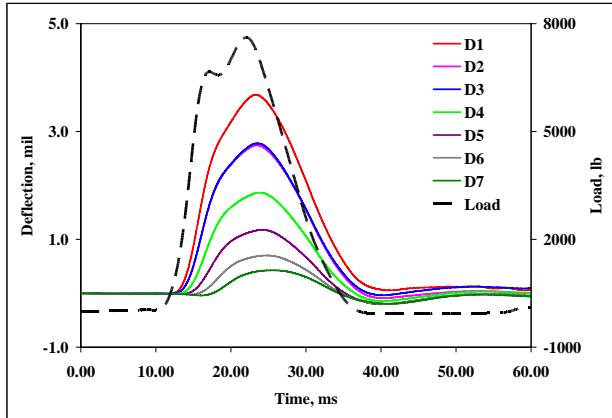
(a) 7500 lb
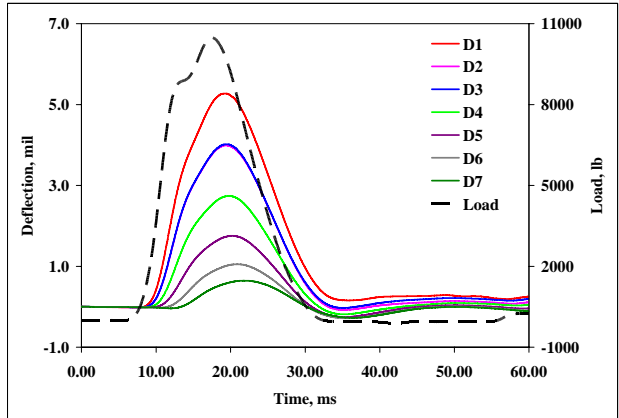
(b) 10500 lb
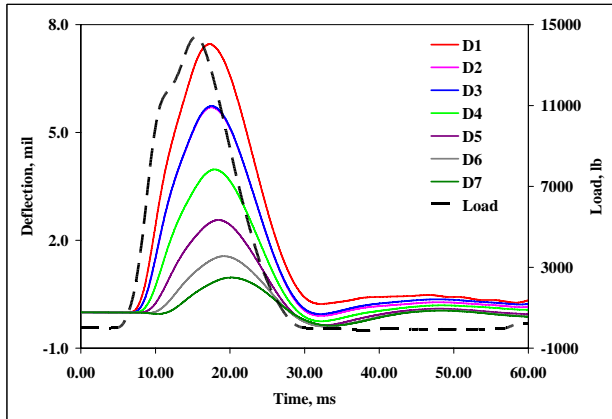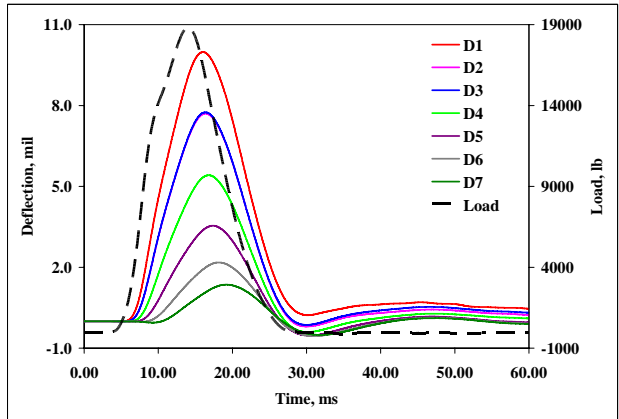
(c) 14500 lb

(b) 19000 lb

Figure C-4. Deflections at B1-L2-R1
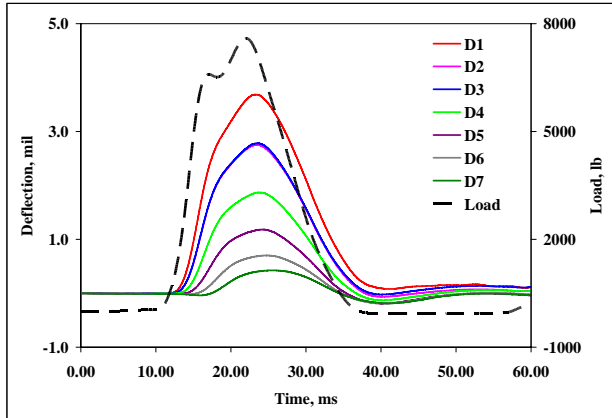
(a) 7500 lb
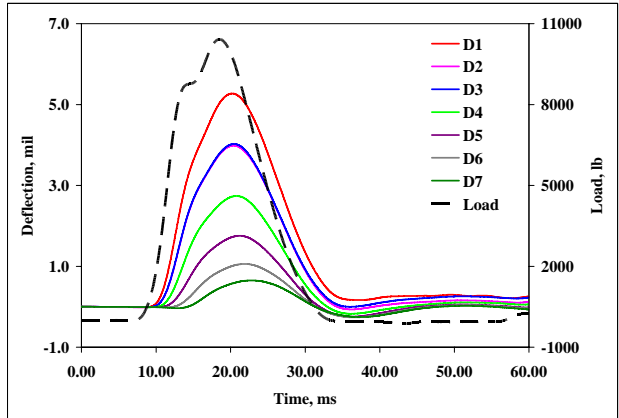
(b) 10500 lb
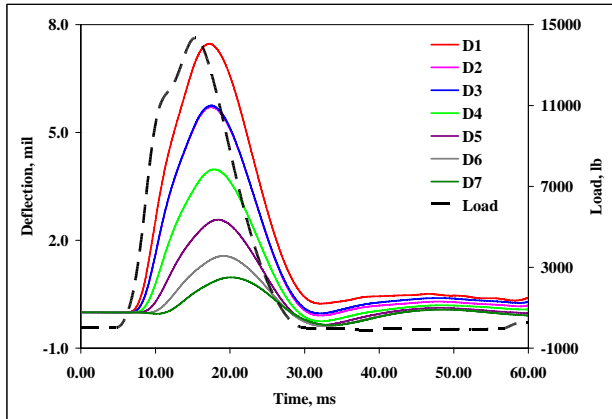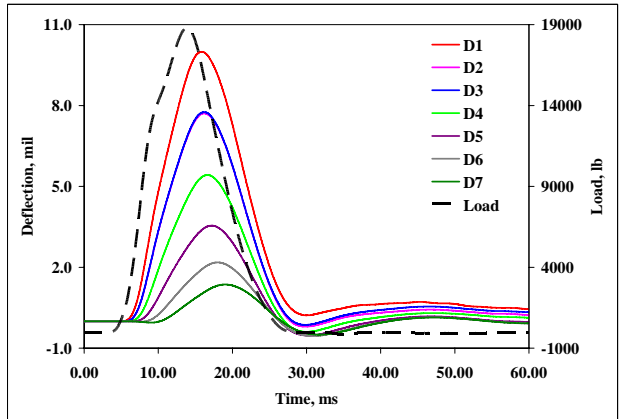
(c) 14500 lb

(b) 19000 lb

Figure C-5. Deflections at B1-L2-R2
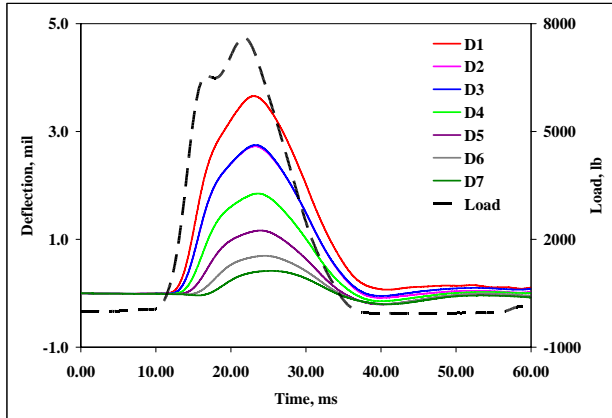
(a) 7500 lb
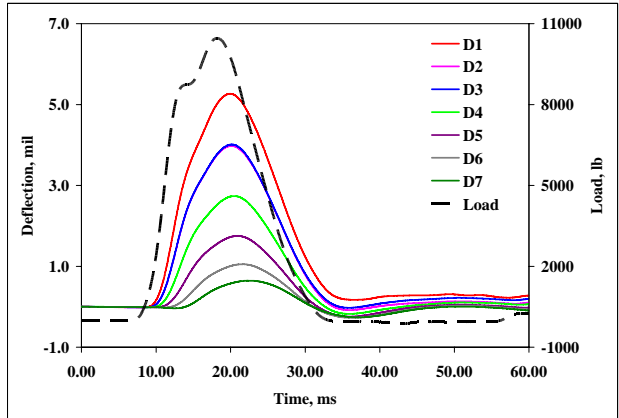
(b) 10500 lb
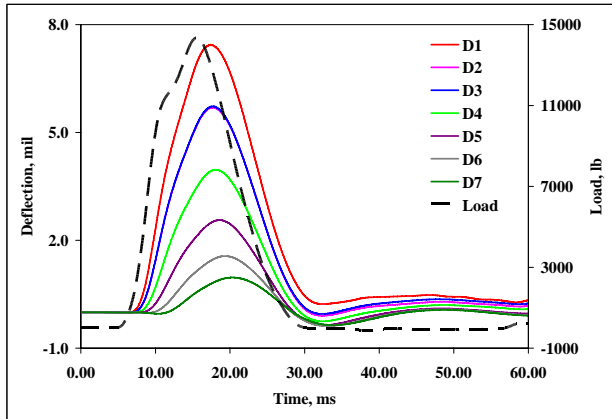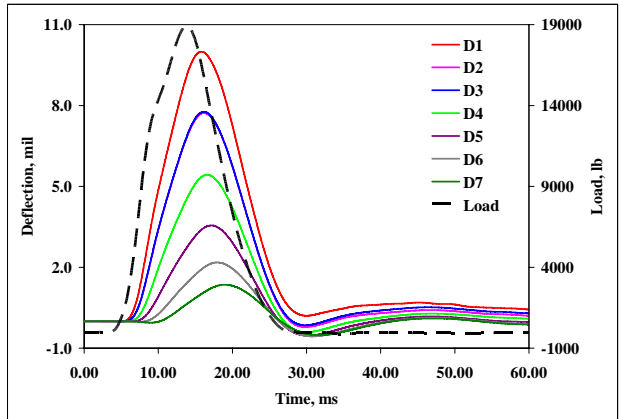
(c) 14500 lb

(b) 19000 lb

Figure C-6. Deflections at B1-L2-R3
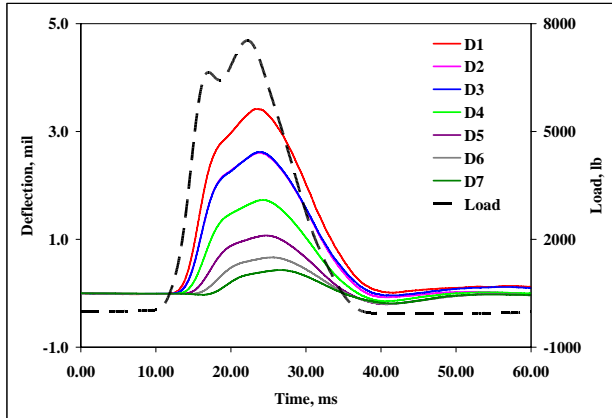
(a) 7500 lb
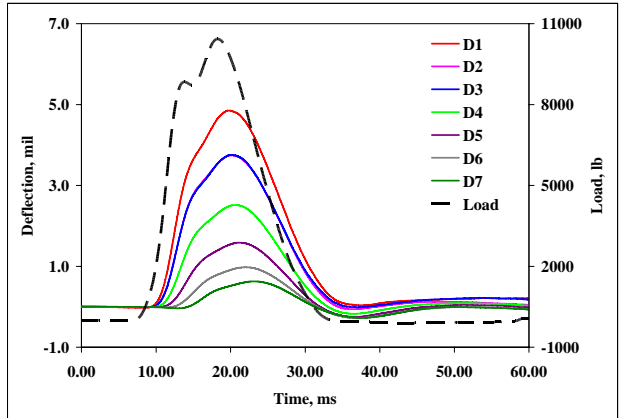
(b) 10500 lb
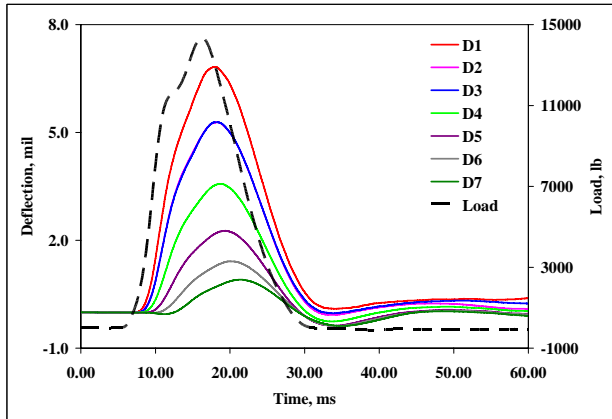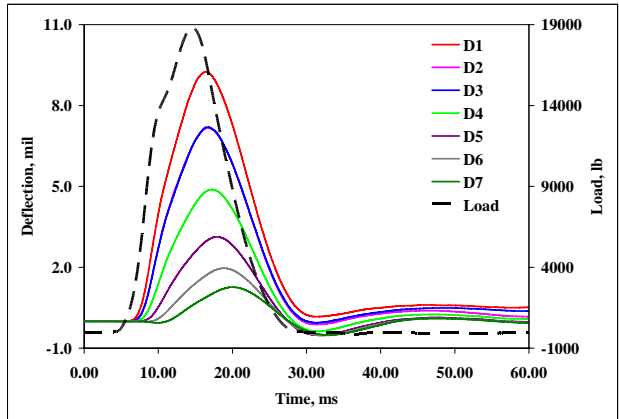
(c) 14500 lb

(b) 19000 lb

Figure C-7. Deflections at B1-L3-R1
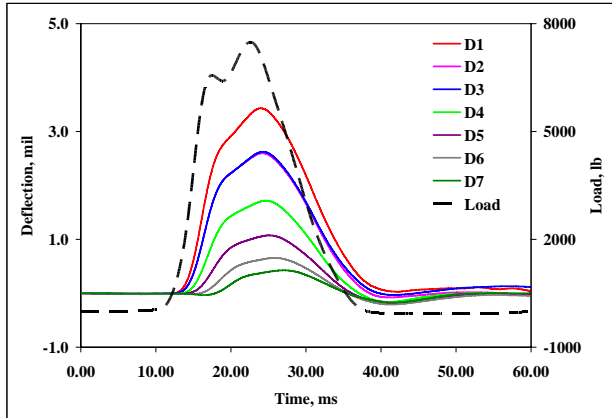
(a) 7500 lb
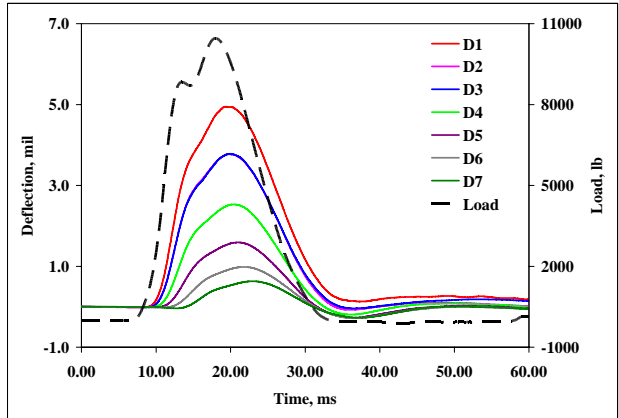
(b) 10500 lb
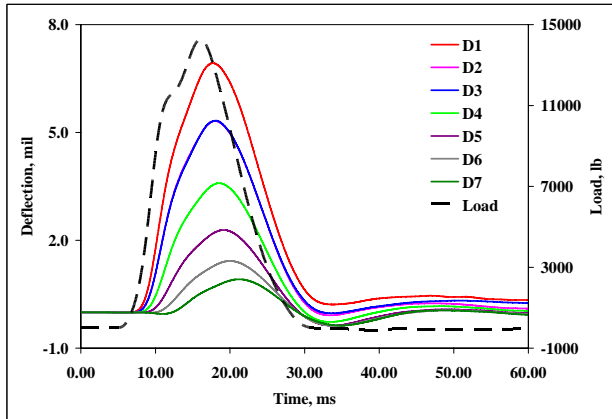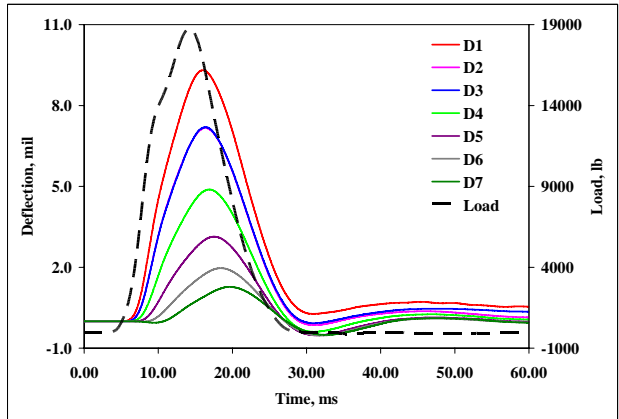
(c) 14500 lb

(b) 19000 lb

Figure C-8. Deflections at B1-L3-R2

C-10
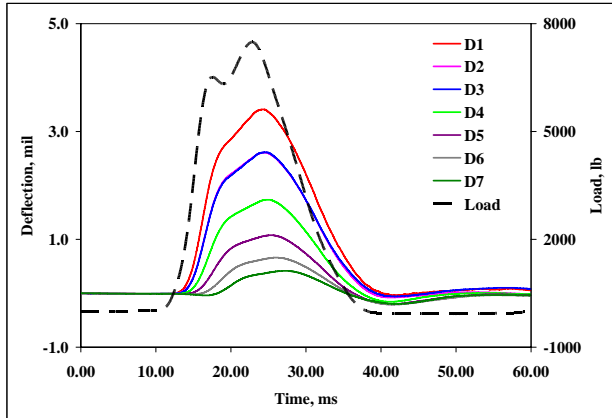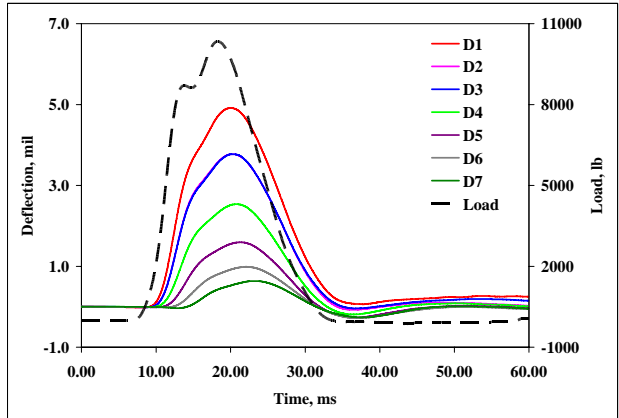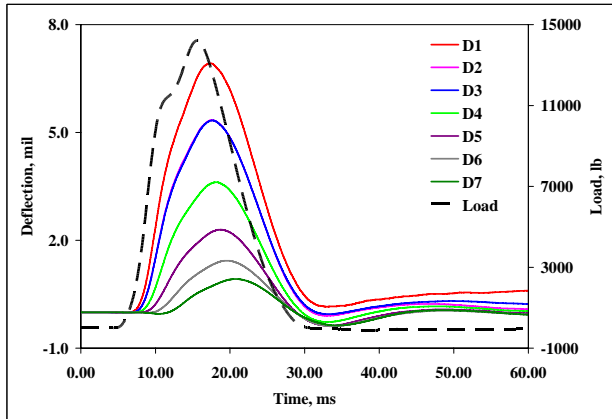
(a) 7500 lb
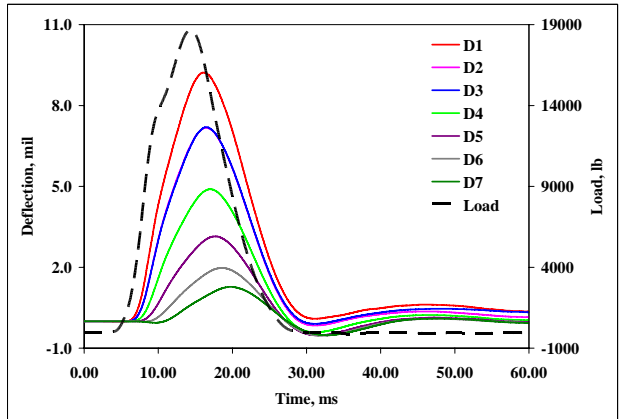
(b) 10500 lb

(c) 14500 lb

(b) 19000 lb

Figure C-9. Deflections at B1-L3-R3
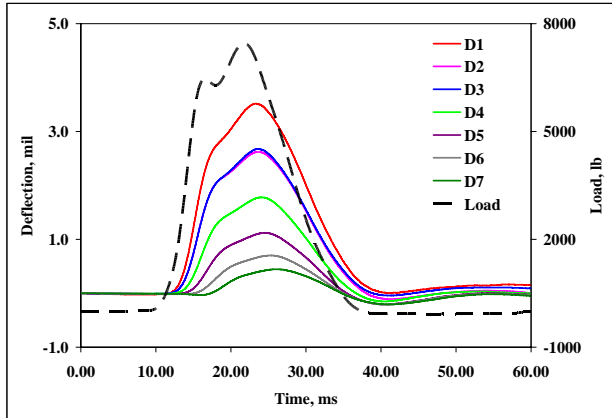
(a) 7500 lb
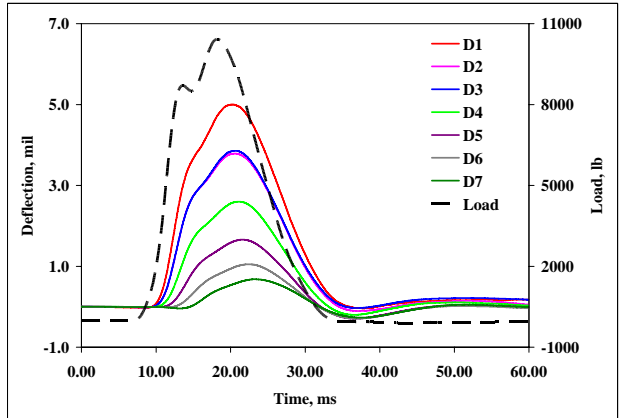
(b) 10500 lb
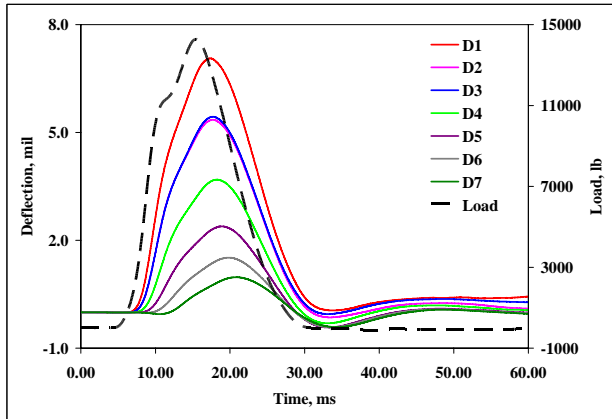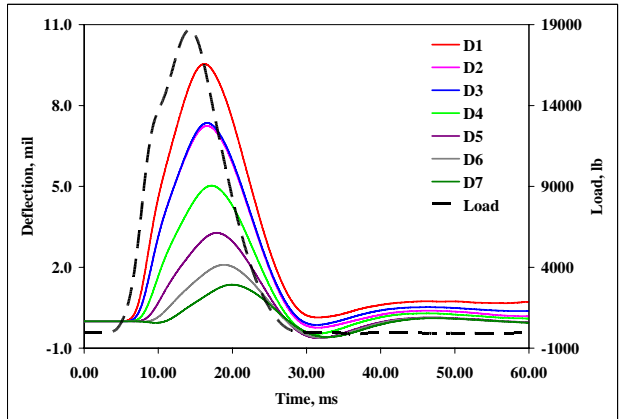
(c) 14500 lb

(b) 19000 lb

Figure C-10. Deflections at B1-L4-R1
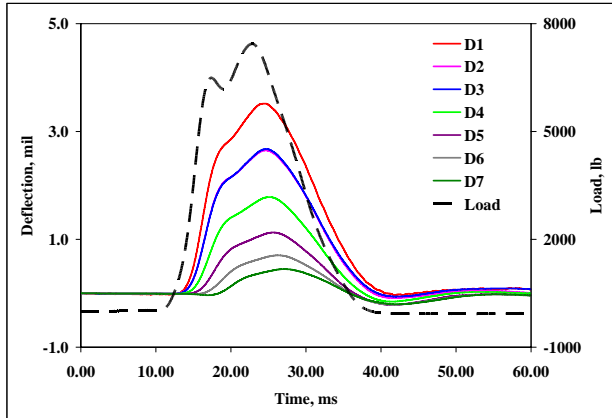
(a) 7500 lb
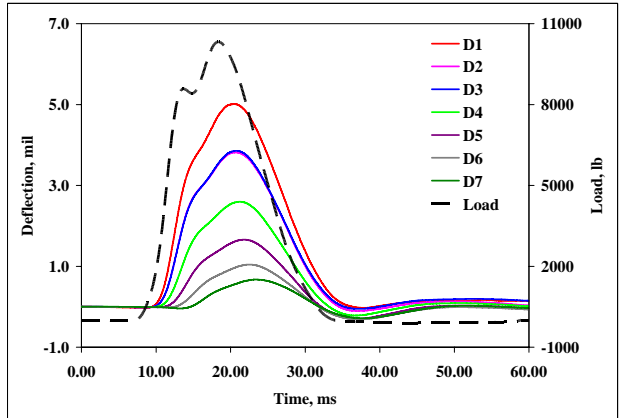
(b) 10500 lb
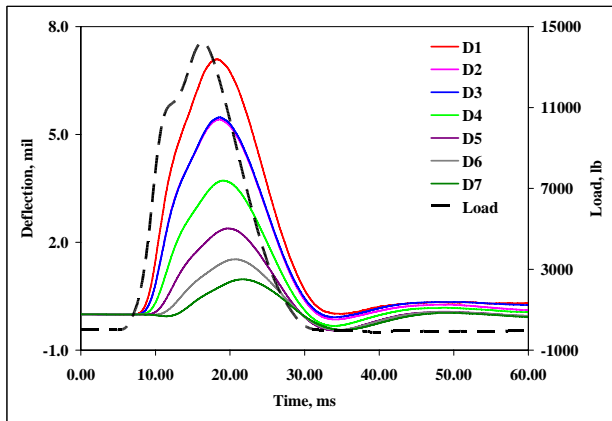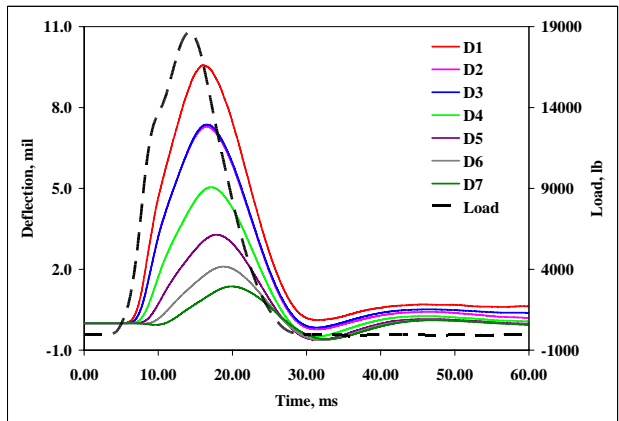
(c) 14500 lb

(b) 19000 lb

Figure C-11. Deflections at B1-L4-R2
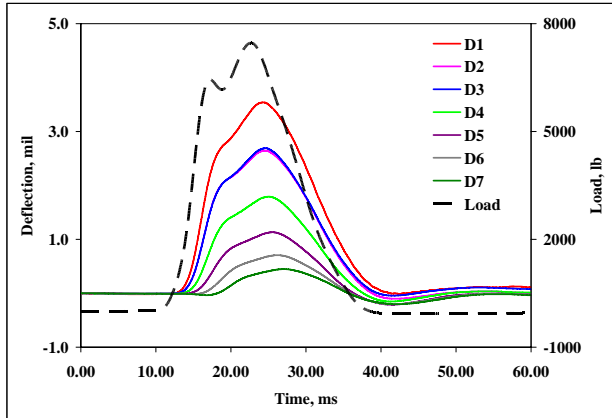
(a) 7500 lb
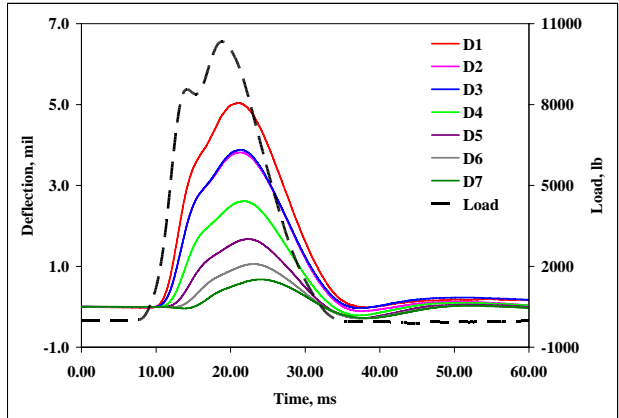
(b) 10500 lb
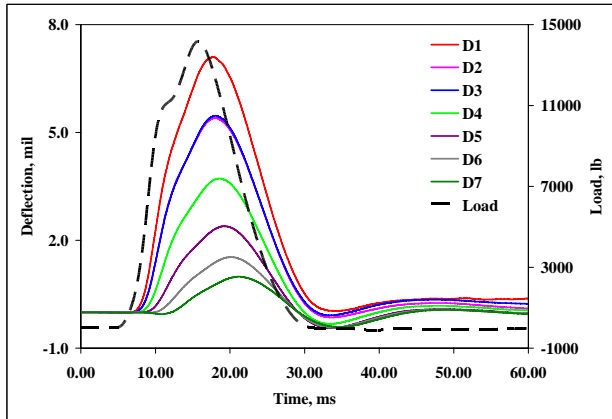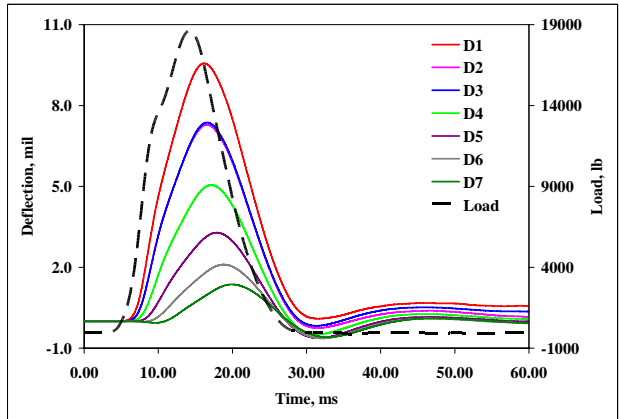
(c) 14500 lb

(b) 19000 lb

Figure C-12. Deflections at B1-L4-R3
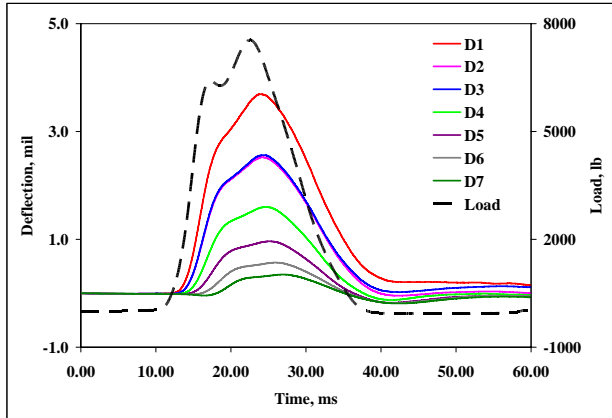
(a) 7500 lb
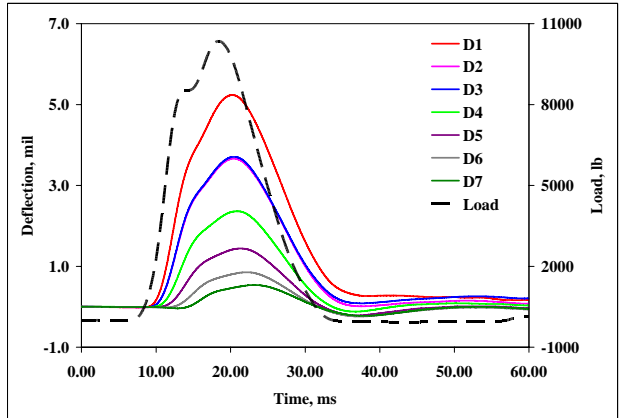
(b) 10500 lb
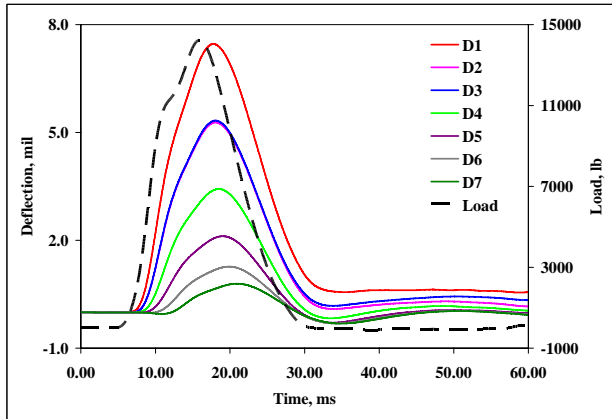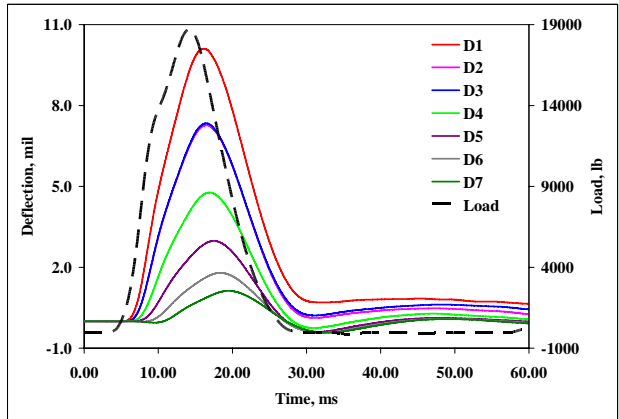
(c) 14500 lb

(b) 19000 lb

Figure C-13. Deflections at B1-L5-R1
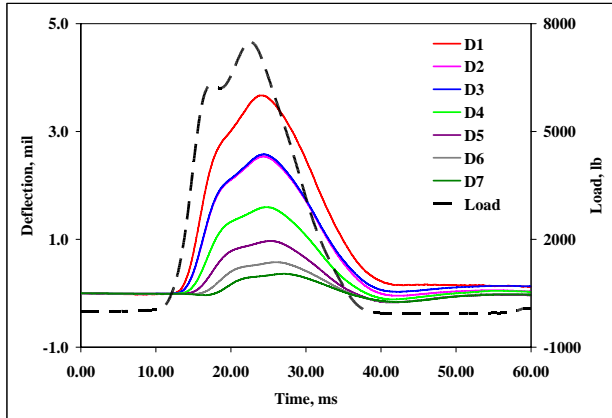
(a) 7500 lb
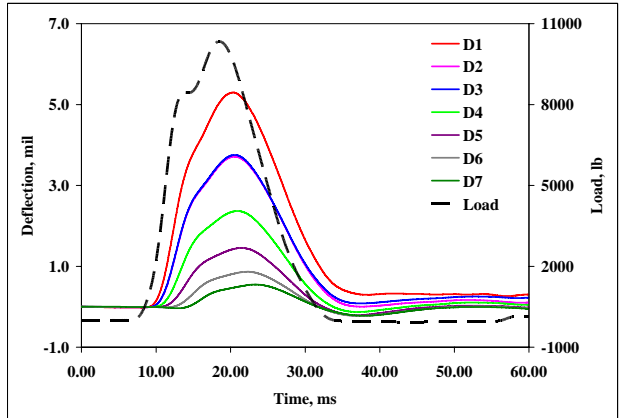
(b) 10500 lb
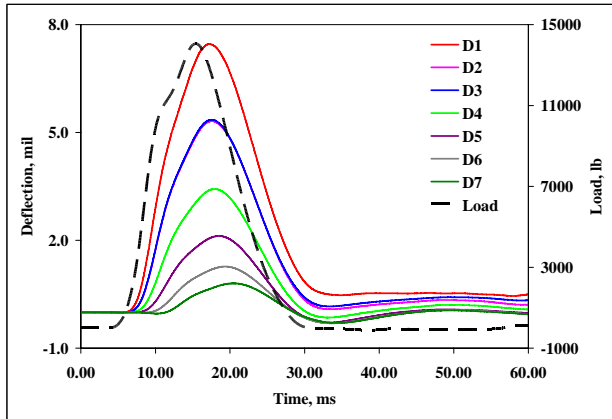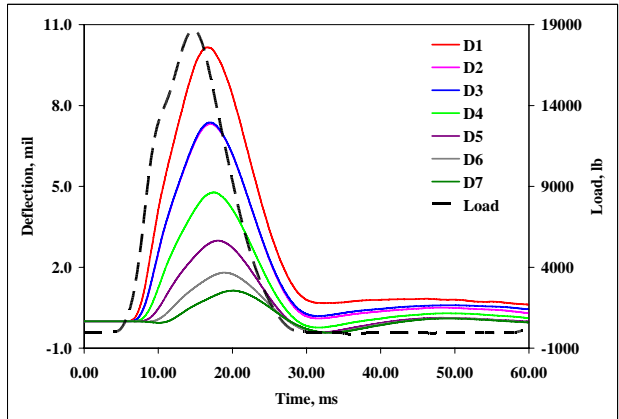
(c) 14500 lb

(b) 19000 lb

Figure C-14. Deflections at B1-L5-R2
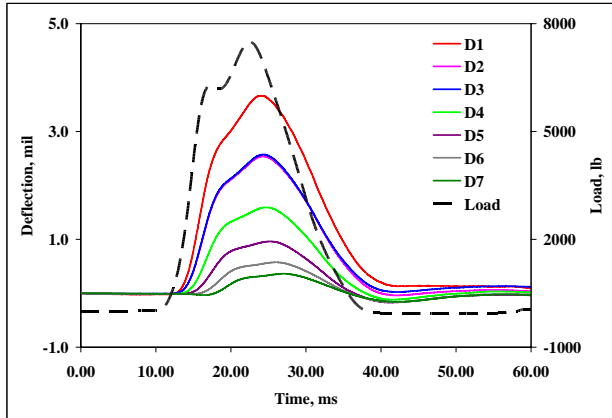
(a) 7500 lb
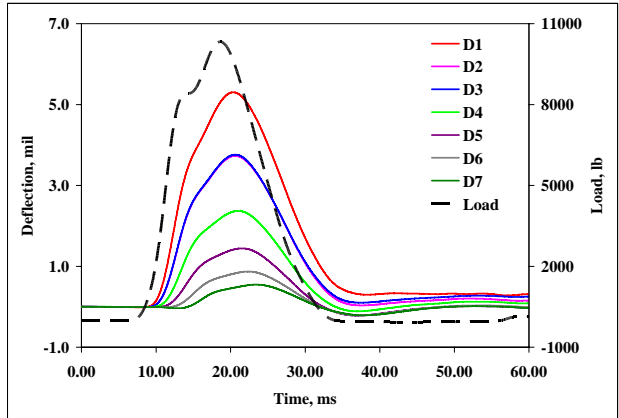
(b) 10500 lb
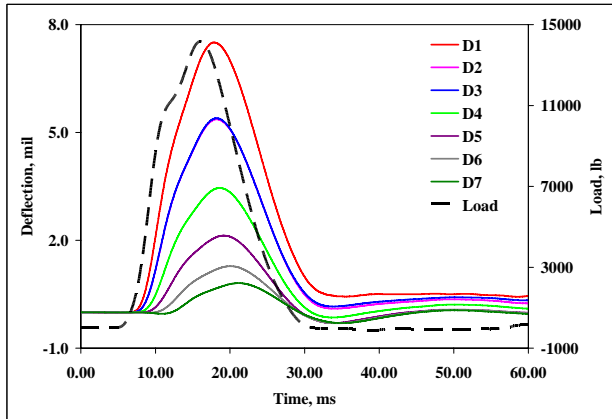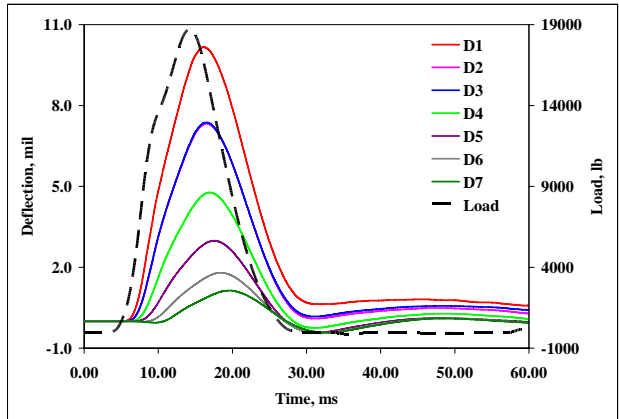
(c) 14500 lb

(b) 19000 lb

Figure C-15. Deflections at B1-L5-R3
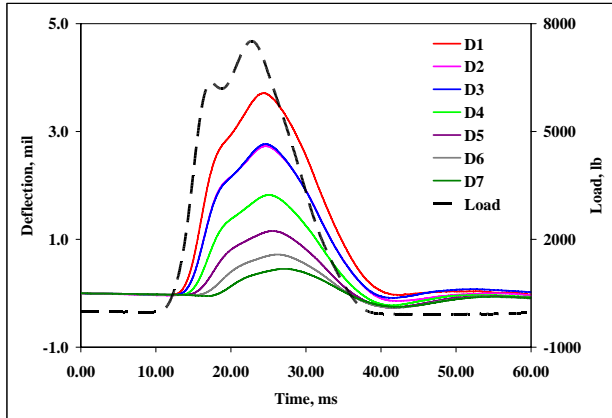
(a) 7500 lb
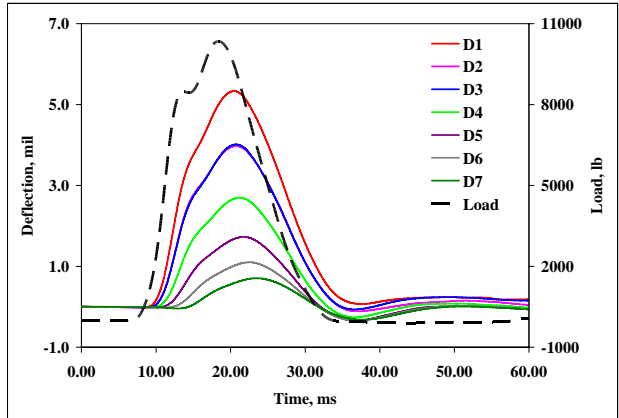
(b) 10500 lb
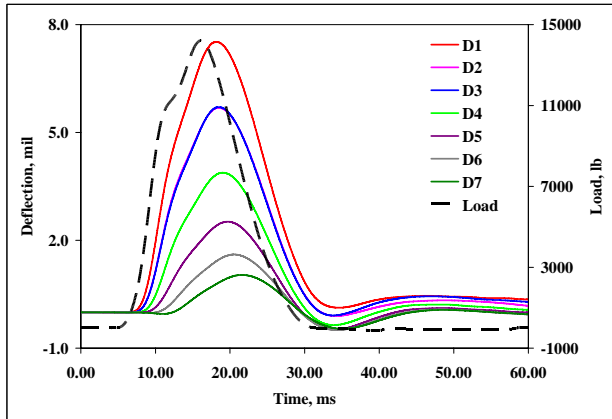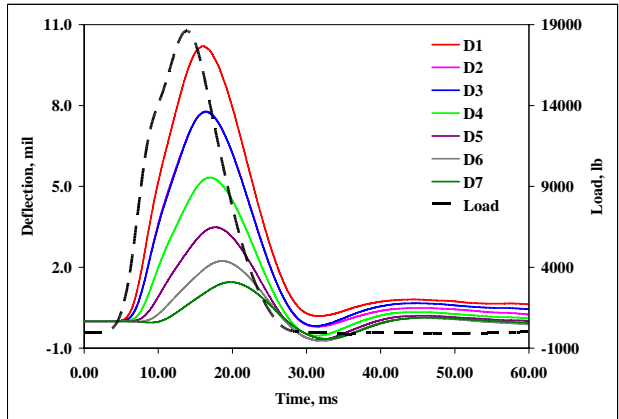
(c) 14500 lb

(b) 19000 lb

Figure C-16. Deflections at B1-L6-R1
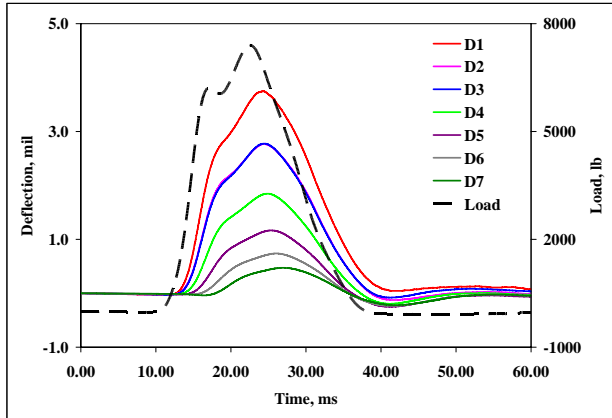
(a) 7500 lb
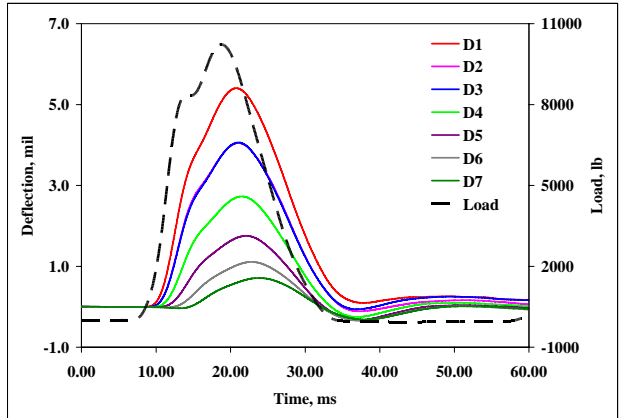
(b) 10500 lb
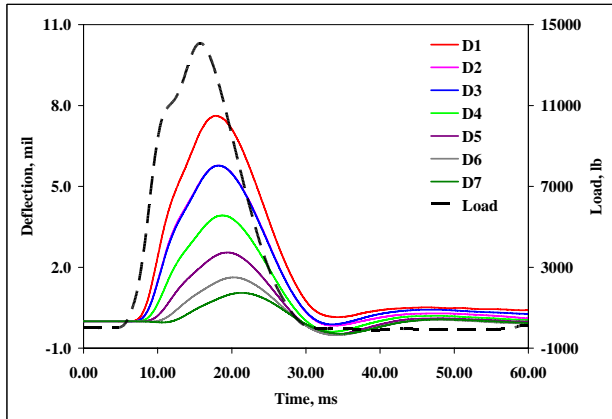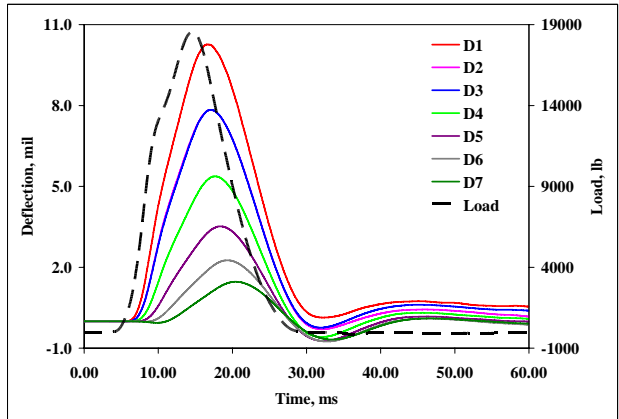
(c) 14500 lb

(b) 19000 lb

Figure C-17. Deflections at B1-L6-R2
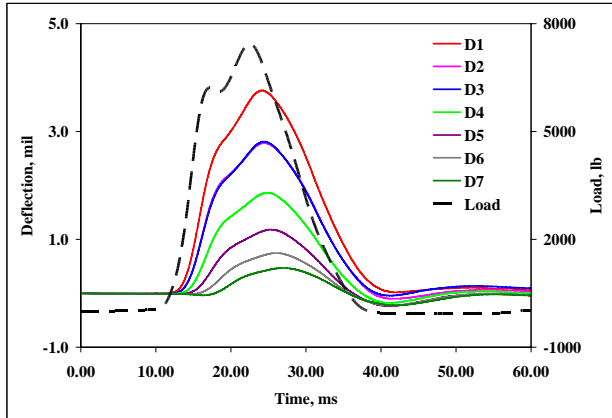
(a) 7500 lb
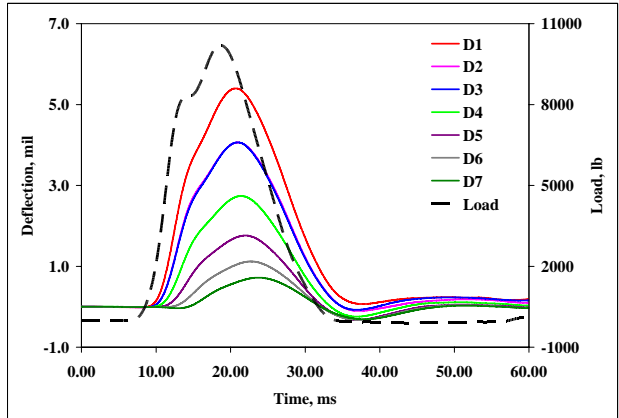
(b) 10500 lb
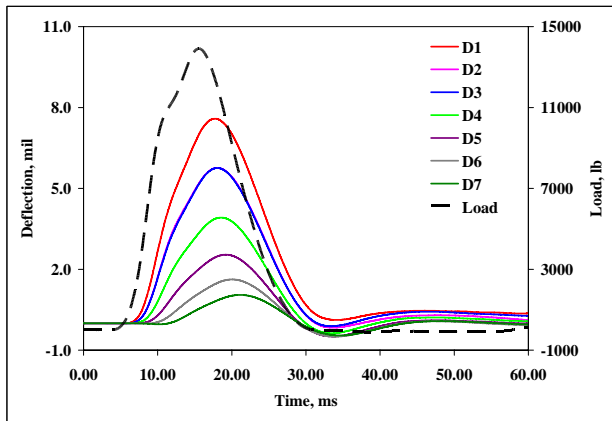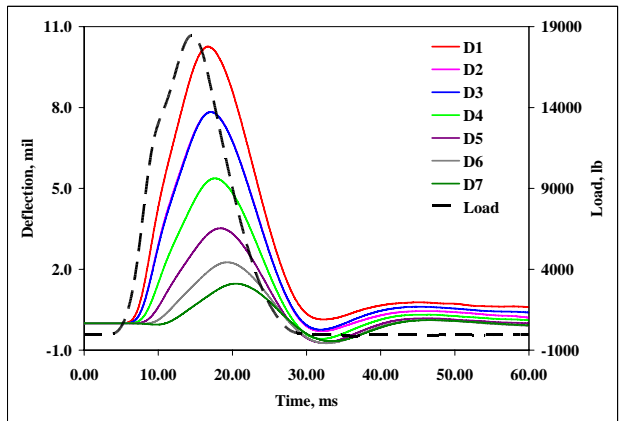
(c) 14500 lb

(b) 19000 lb

Figure C-18. Deflections at B1-L6-R3
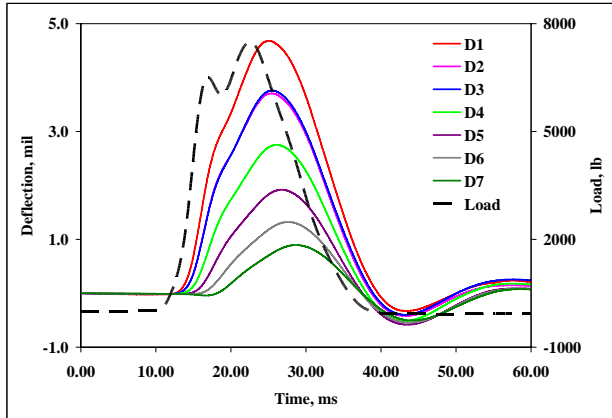
(a) 7500 lb
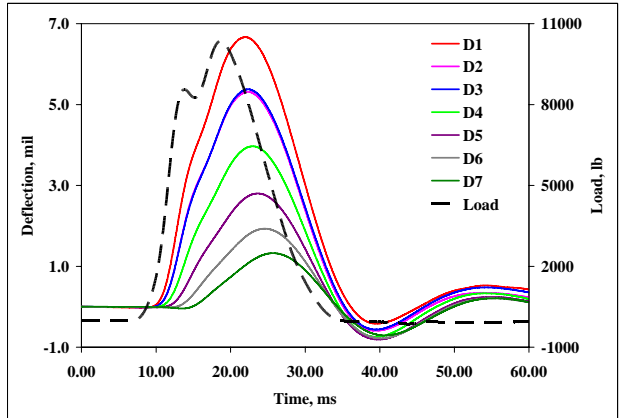
(b) 10500 lb
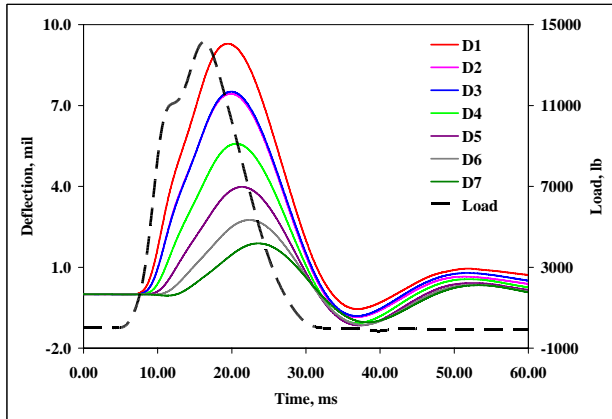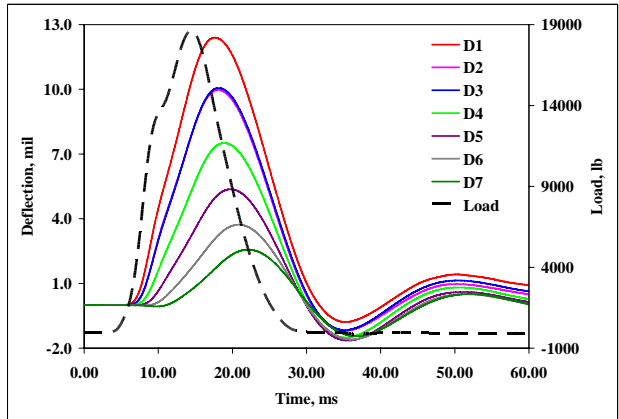
(c) 14500 lb

(b) 19000 lb

Figure C-19. Deflections at B2-L1-R1
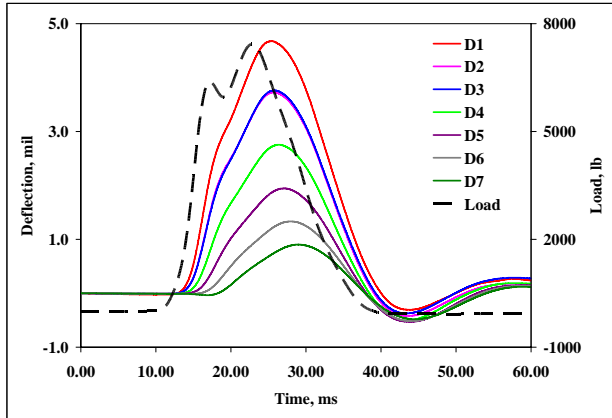
(a) 7500 lb
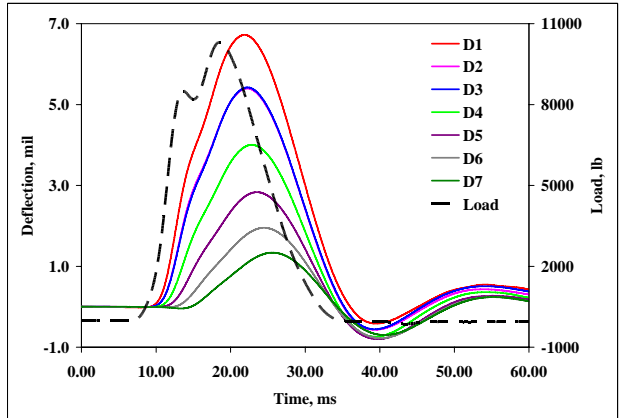
(b) 10500 lb
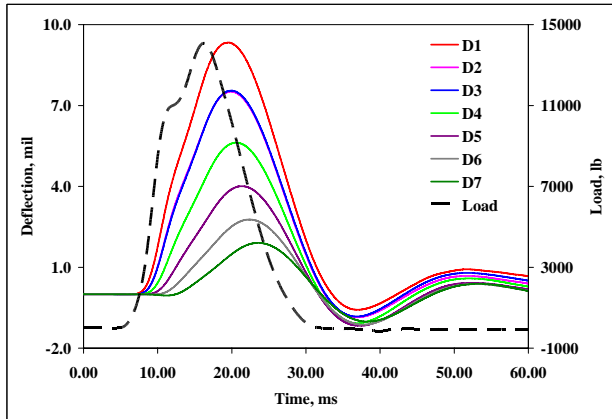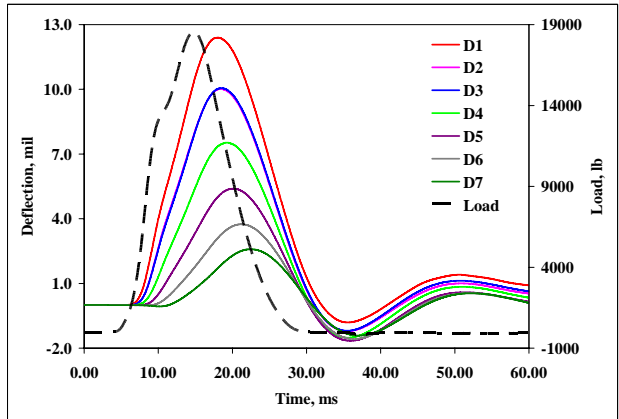
(c) 14500 lb

(b) 19000 lb

Figure C-20. Deflections at B2-L1-R2
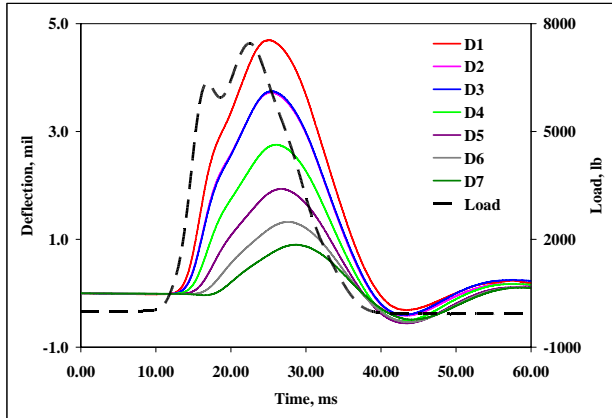
(a) 7500 lb
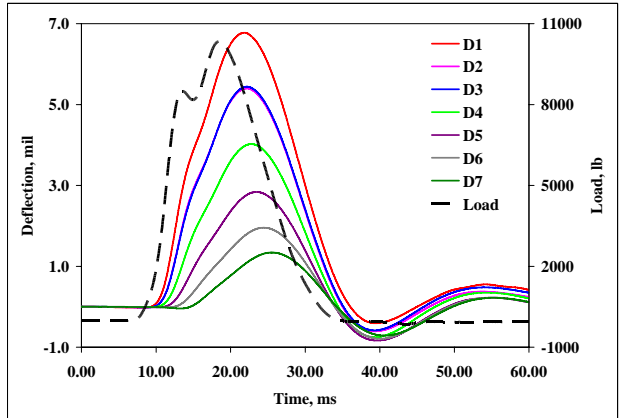
(b) 10500 lb
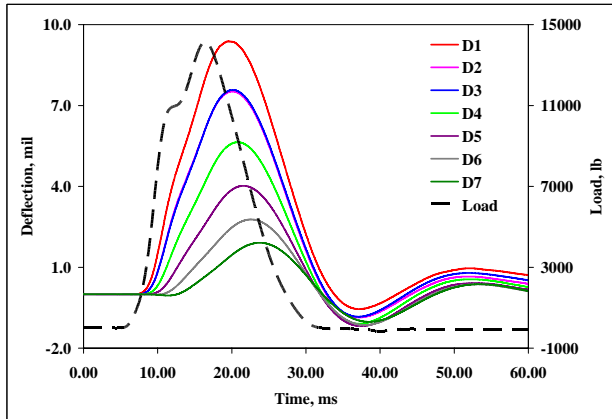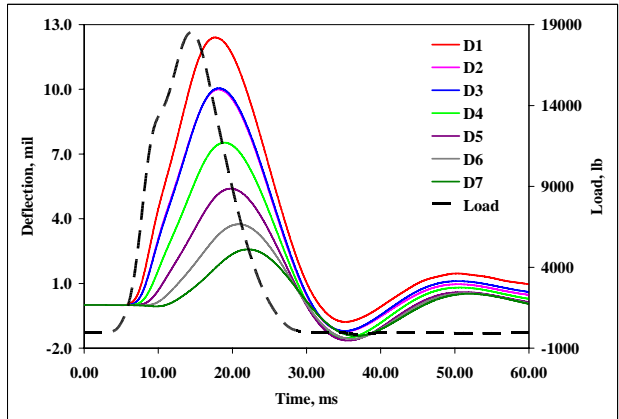
(c) 14500 lb

(b) 19000 lb

Figure C-21. Deflections at B2-L1-R3

C-23
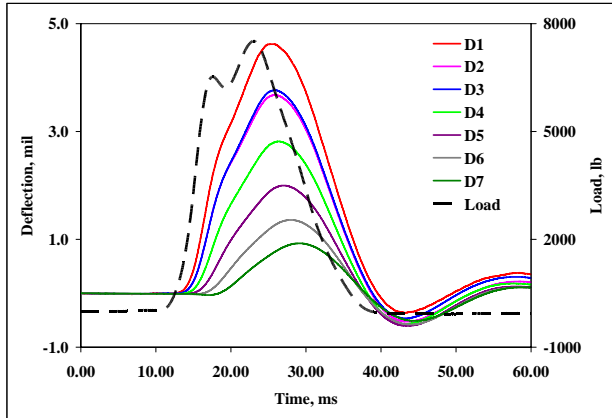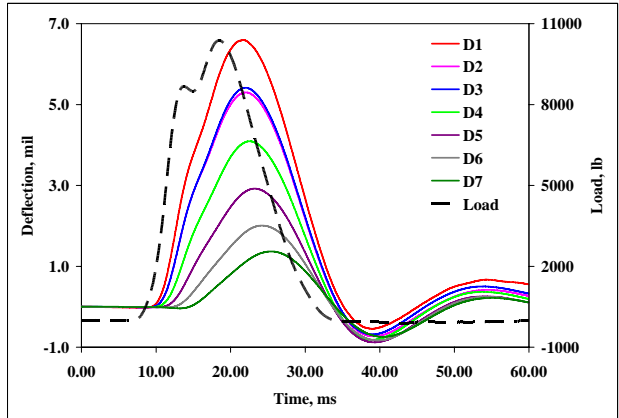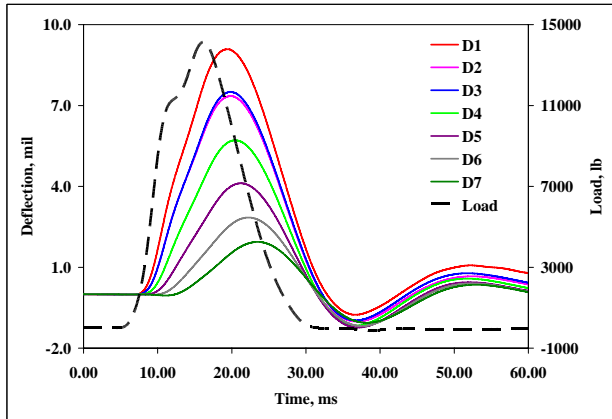
(a) 7500 lb
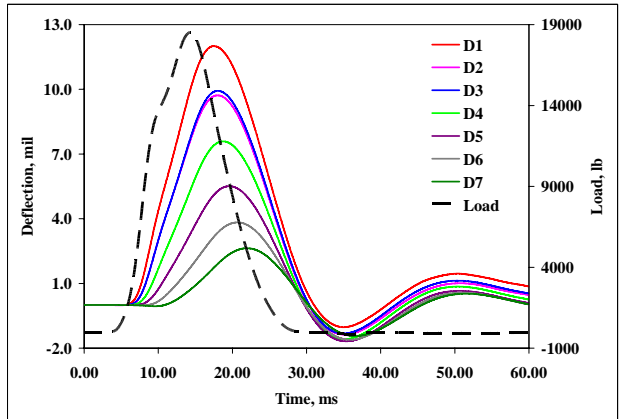
(b) 10500 lb

(c) 14500 lb

(b) 19000 lb

Figure C-22. Deflections at B2-L2-R2
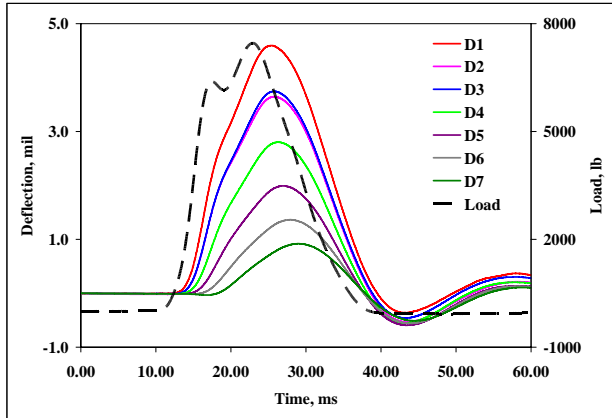
(a) 7500 lb
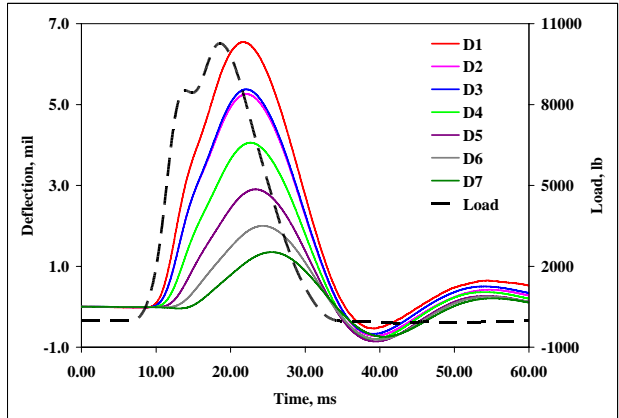
(b) 10500 lb
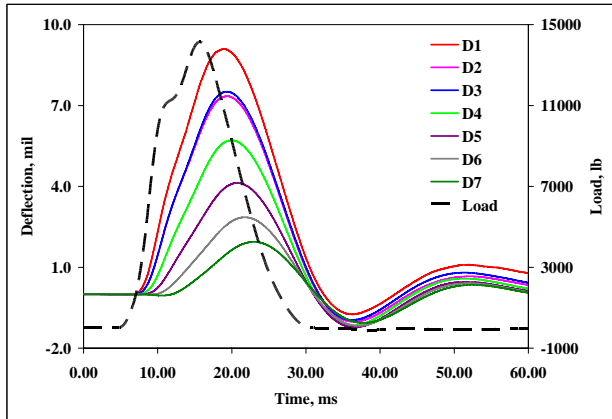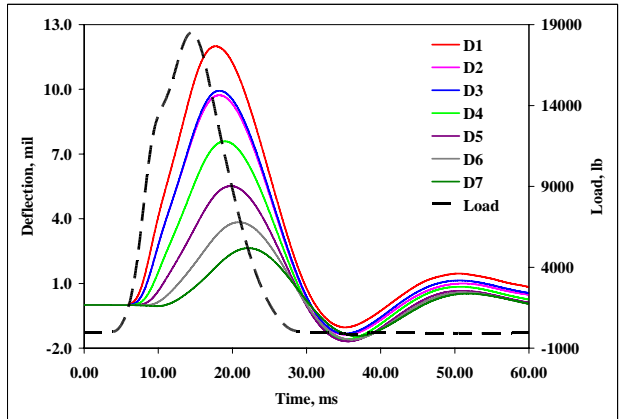
(c) 14500 lb

(b) 19000 lb

Figure C-23. Deflections at B2-L2-R3
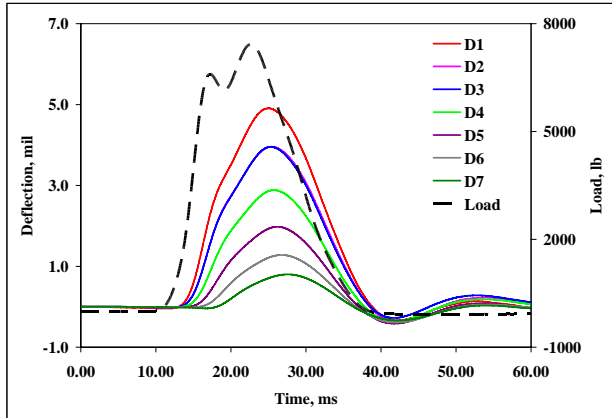
(a) 7500 lb
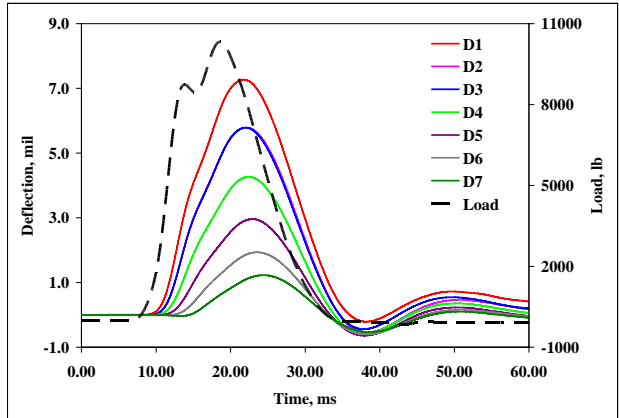
(b) 10500 lb
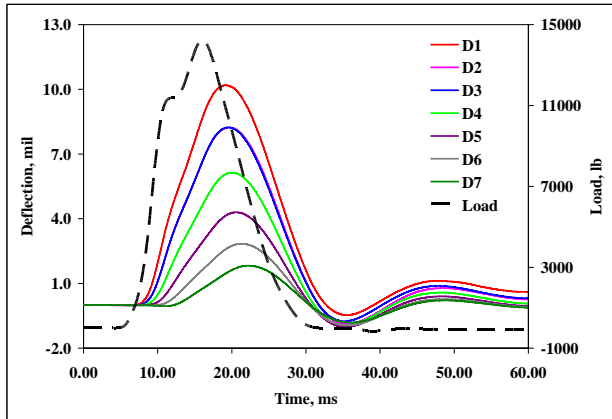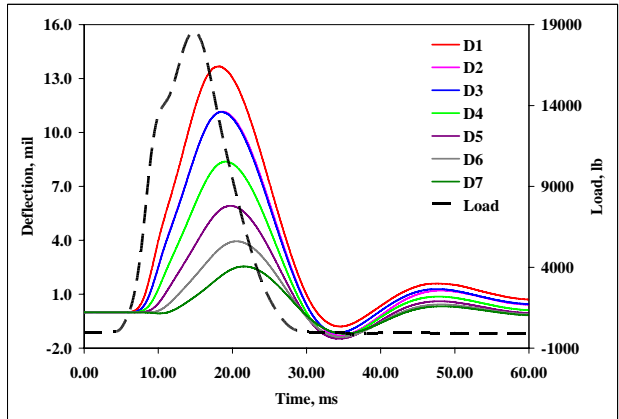
(c) 14500 lb

(b) 19000 lb

Figure C-24. Deflections at B2-L3-R1
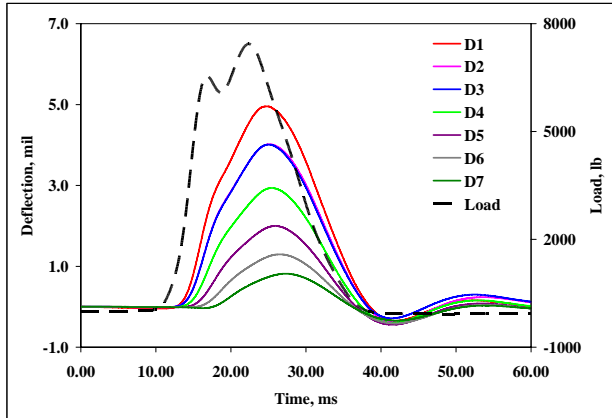
(a) 7500 lb
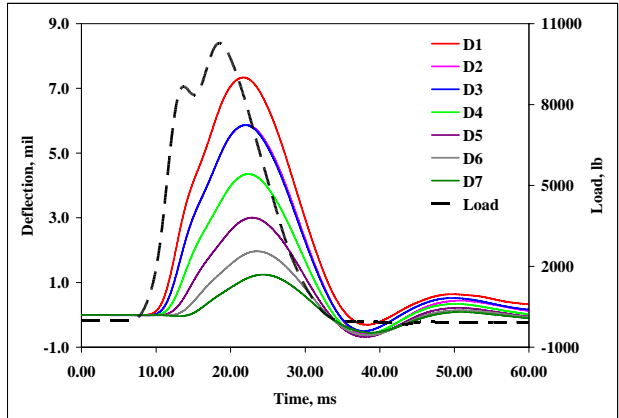
(b) 10500 lb
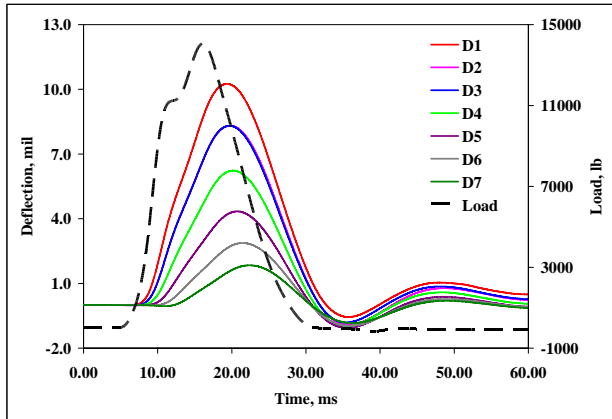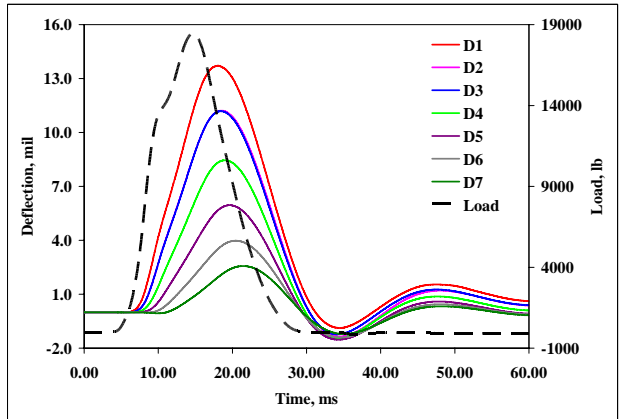
(c) 14500 lb

(b) 19000 lb

Figure C-25. Deflections at B2-L3-R2
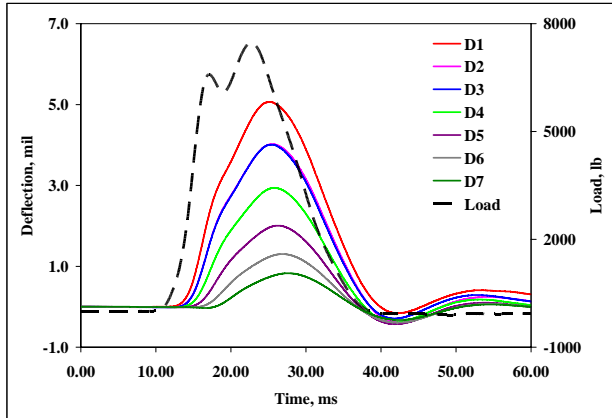
(a) 7500 lb
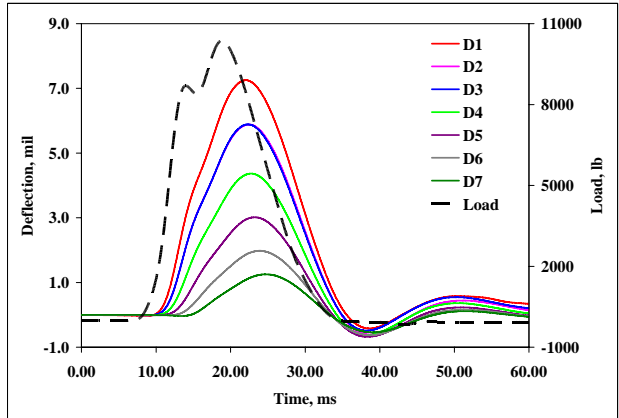
(b) 10500 lb
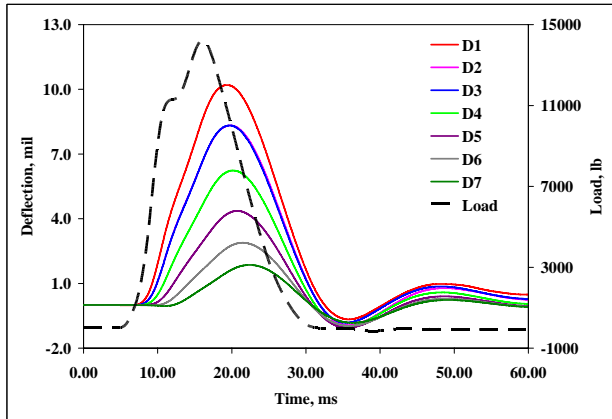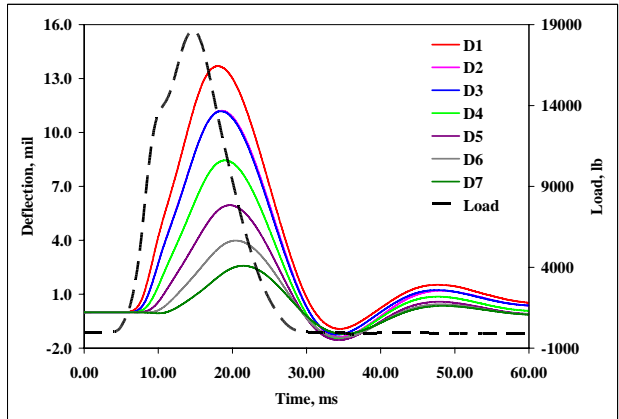
(c) 14500 lb

(b) 19000 lb

Figure C-26. Deflections at B2-L3-R3
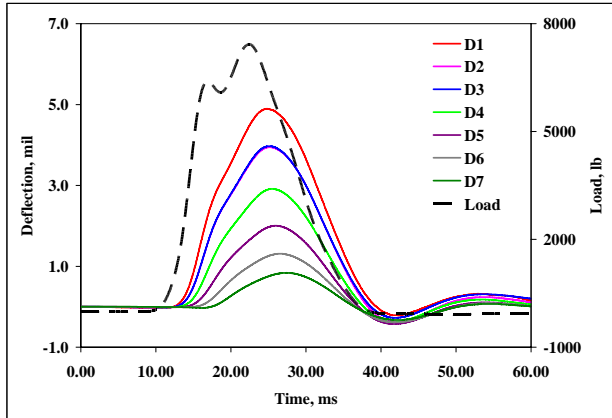
(a) 7500 lb
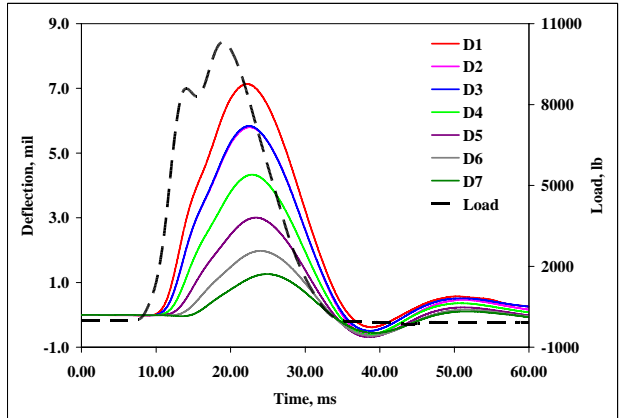
(b) 10500 lb
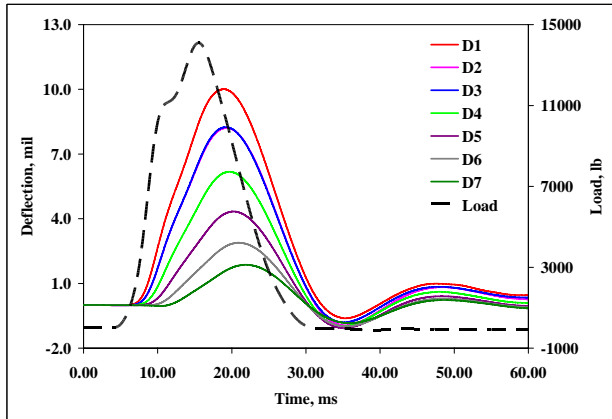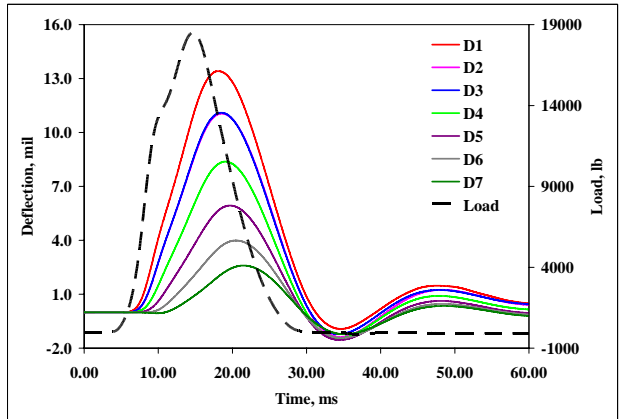
(c) 14500 lb

(b) 19000 lb

Figure C-27. Deflections at B2-L4-R1
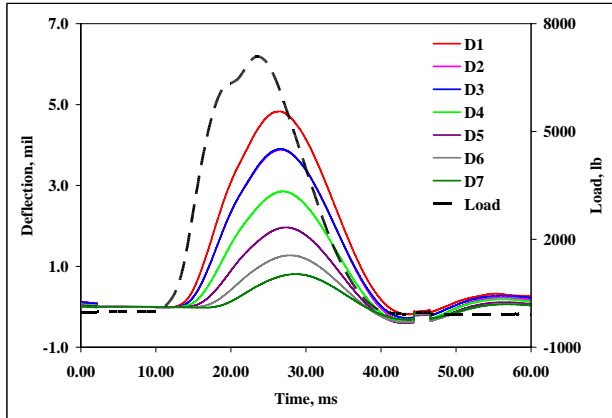
(a) 7500 lb
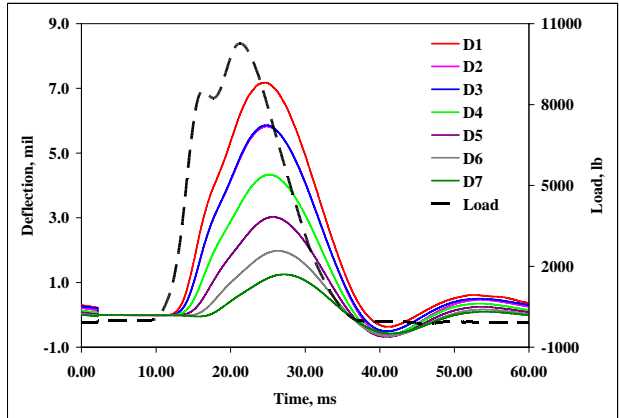
(b) 10500 lb
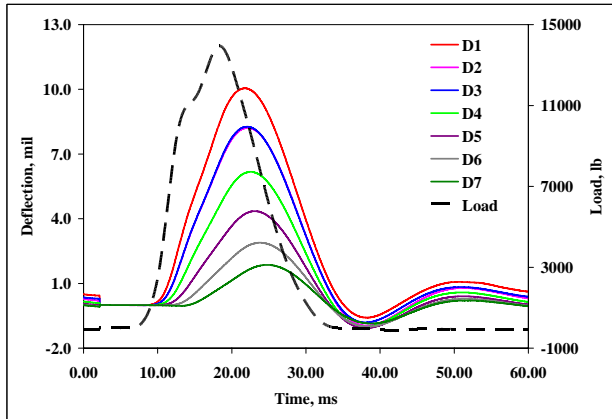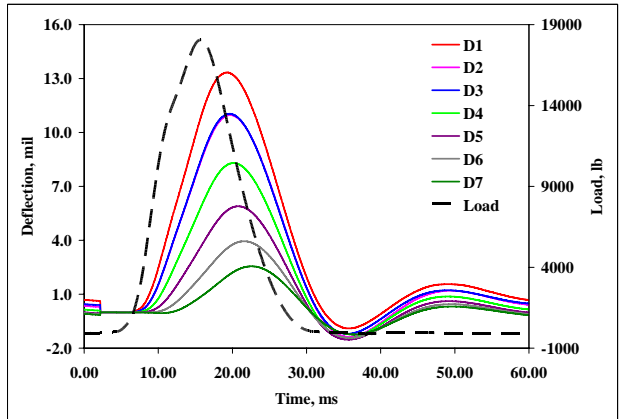
(c) 14500 lb

(b) 19000 lb

Figure C-28. Deflections at B2-L4-R2
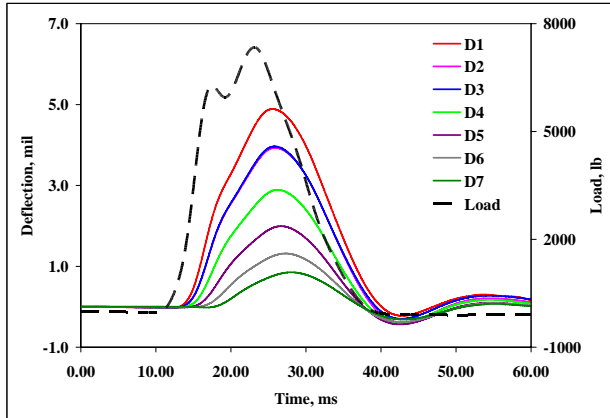
(a) 7500 lb
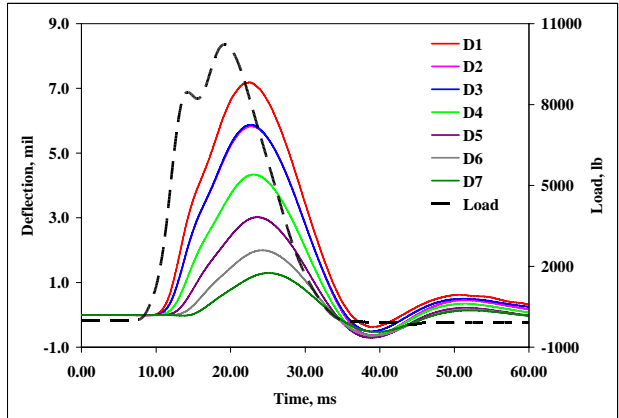
(b) 10500 lb
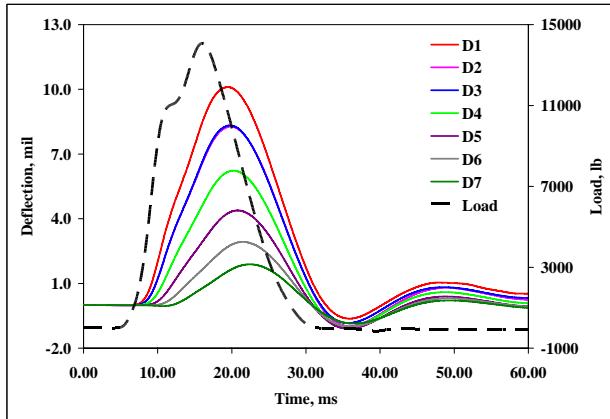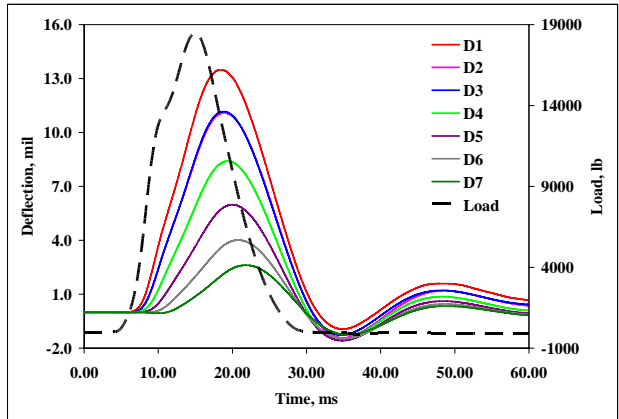
(c) 14500 lb

(b) 19000 lb

Figure C-29. Deflections at B2-L4-R3
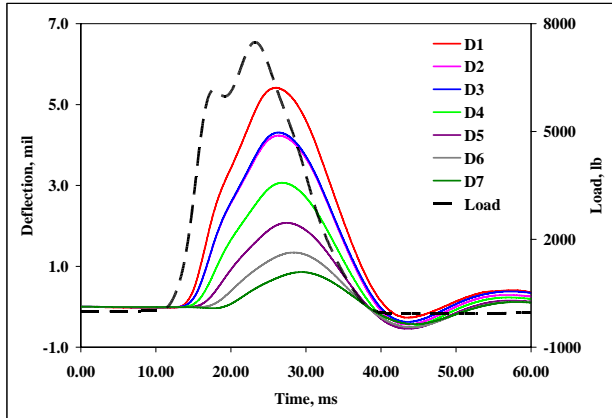
(a) 7500 lb
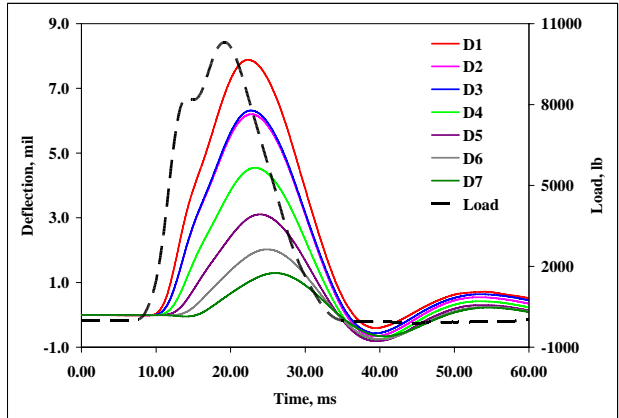
(b) 10500 lb
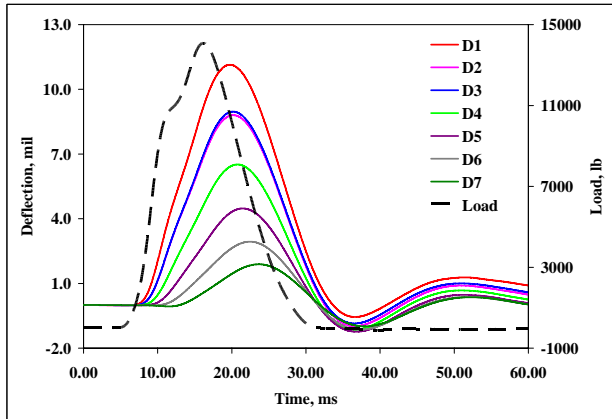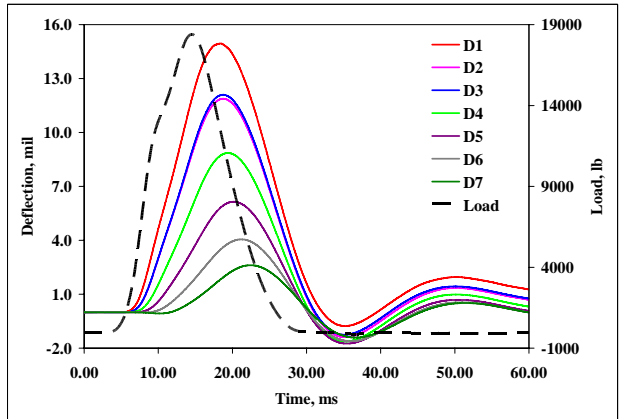
(c) 14500 lb

(b) 19000 lb

Figure C-30. Deflections at B2-L5-R1
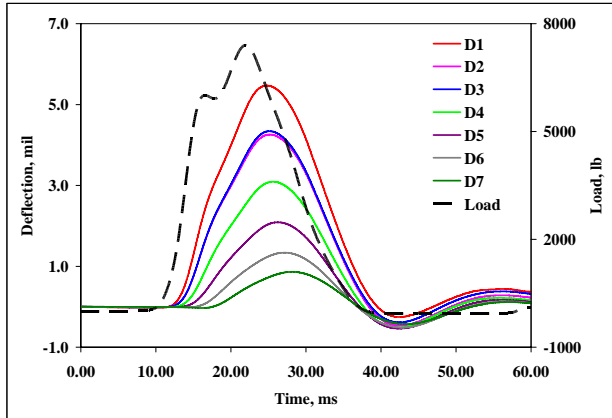
(a) 7500 lb
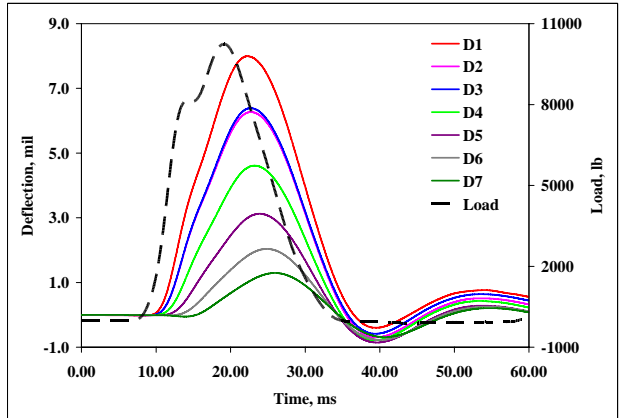
(b) 10500 lb
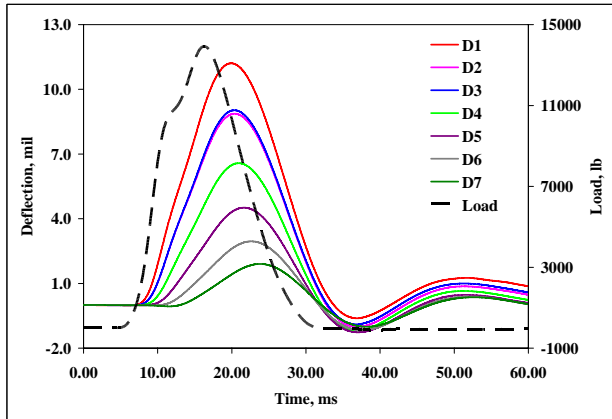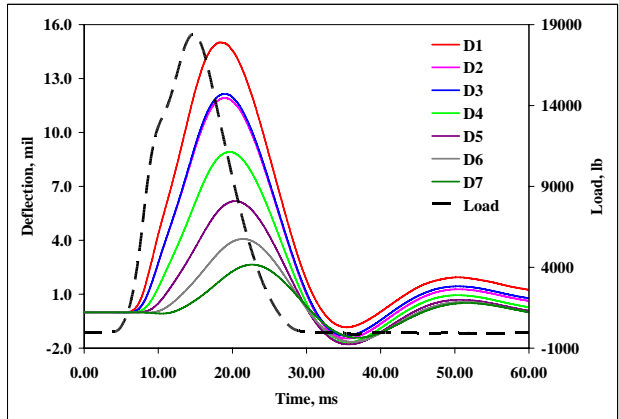
(c) 14500 lb

(b) 19000 lb

Figure C-31. Deflections at B2-L5-R2
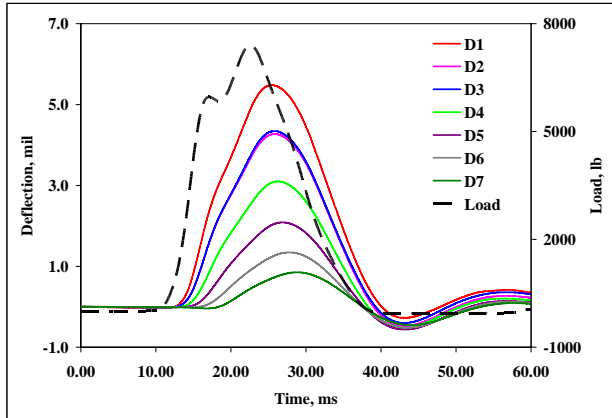
(a) 7500 lb
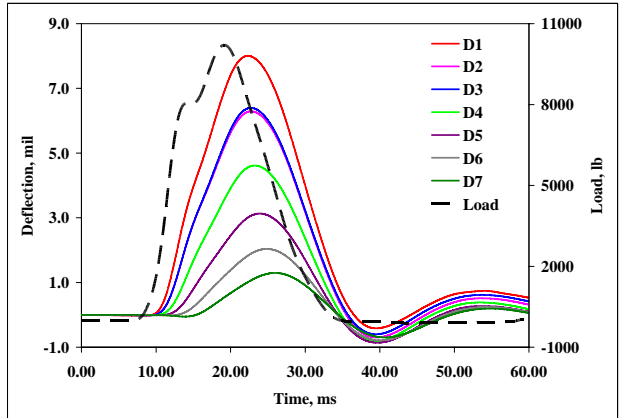
(b) 10500 lb
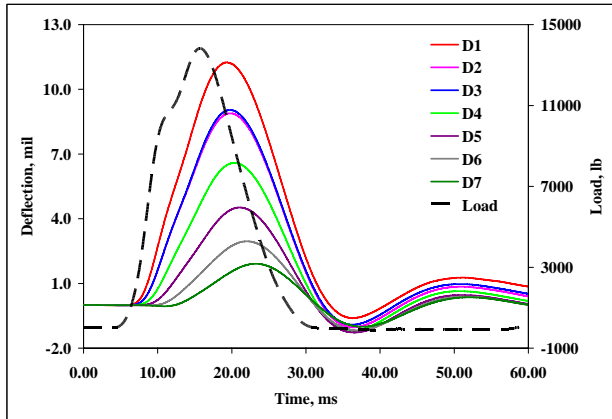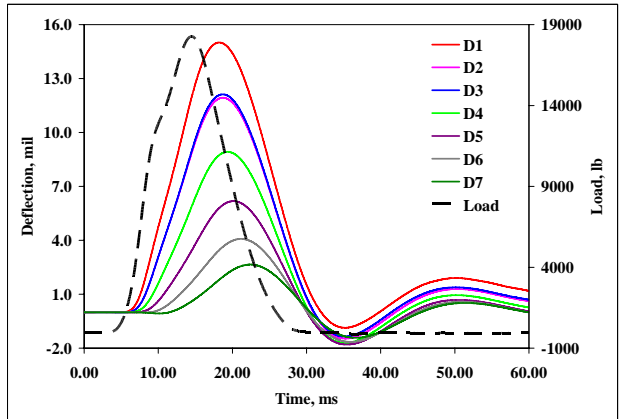
(c) 14500 lb

(b) 19000 lb

Figure C-32. Deflections at B2-L5-R3
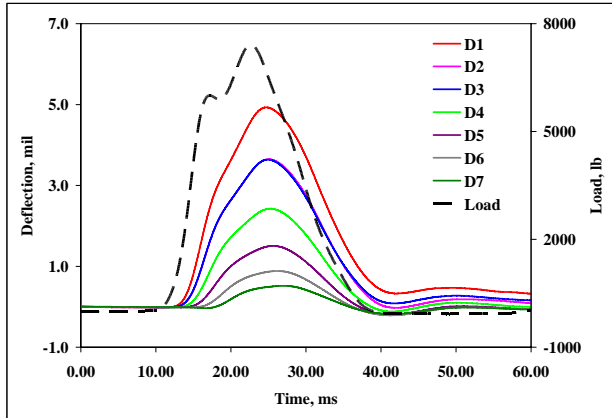
(a) 7500 lb
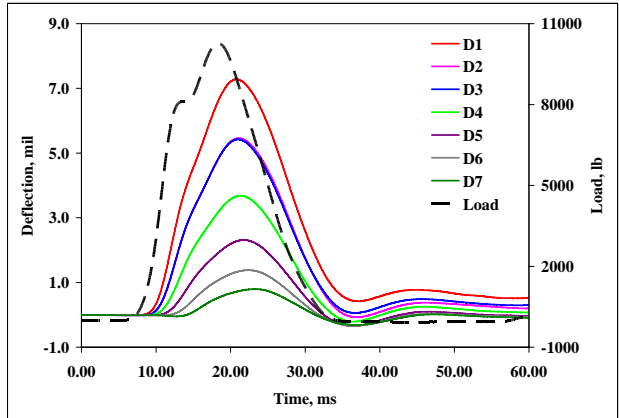
(b) 10500 lb
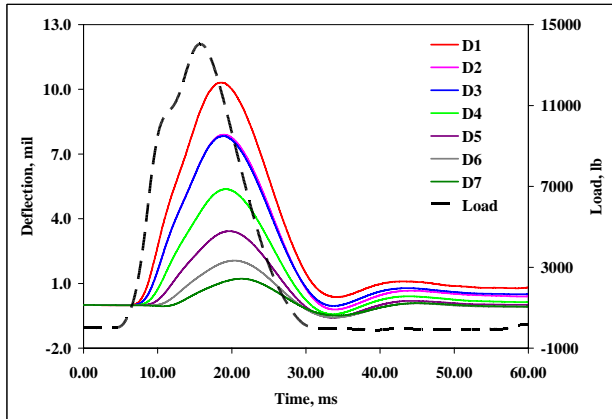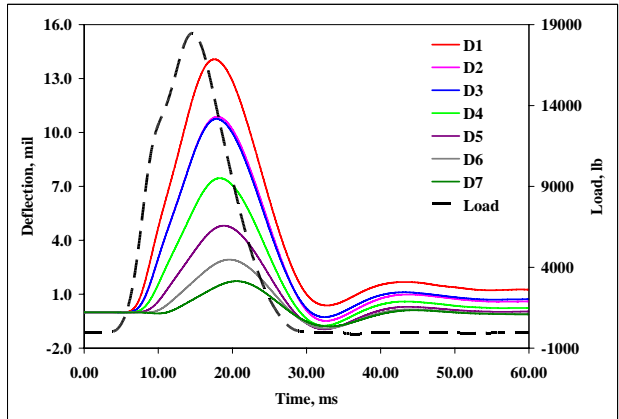
(c) 14500 lb

(b) 19000 lb

Figure C-33. Deflections at B2-L6-R1
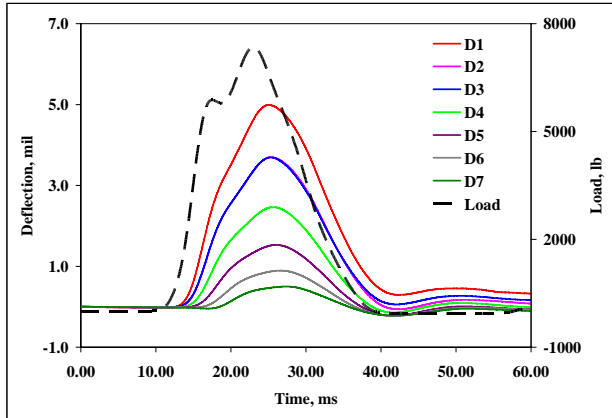
(a) 7500 lb
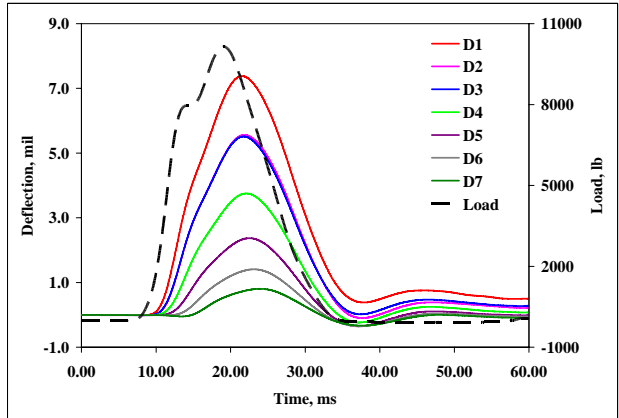
(b) 10500 lb
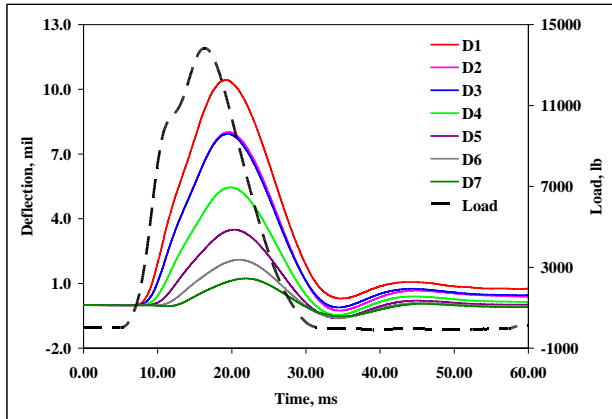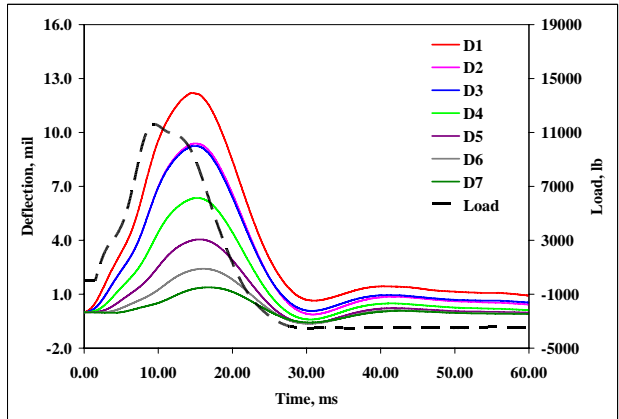
(c) 14500 lb

(b) 19000 lb

Figure C-34. Deflections at B2-L6-R2
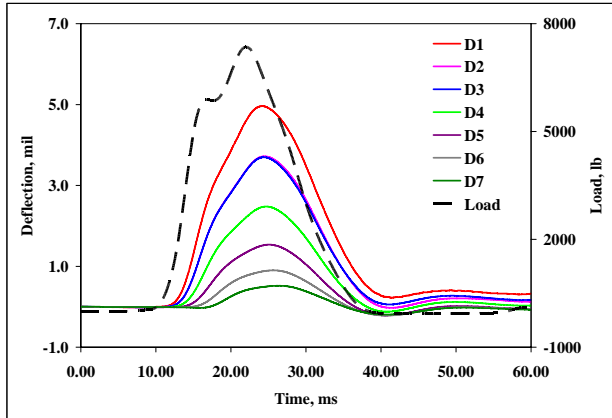
(a) 7500 lb
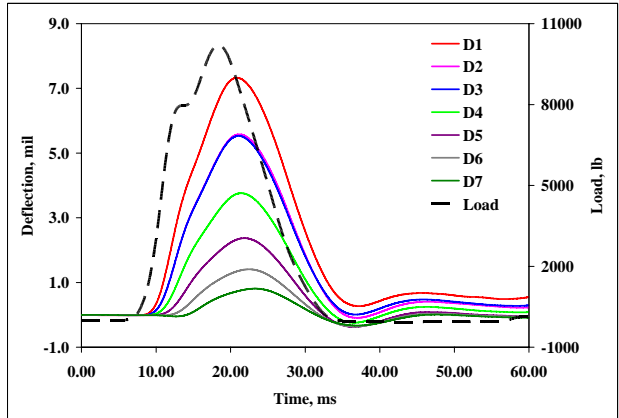
(b) 10500 lb
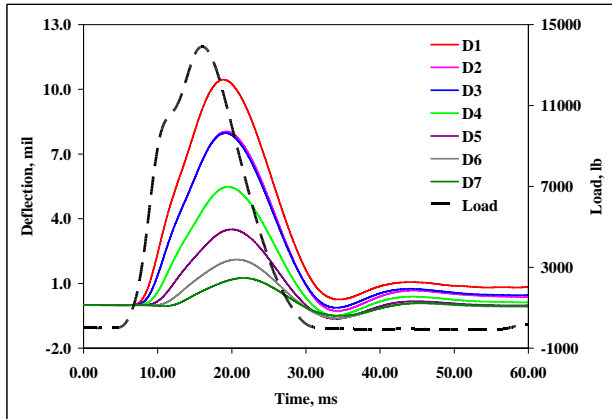
(c) 14500 lb
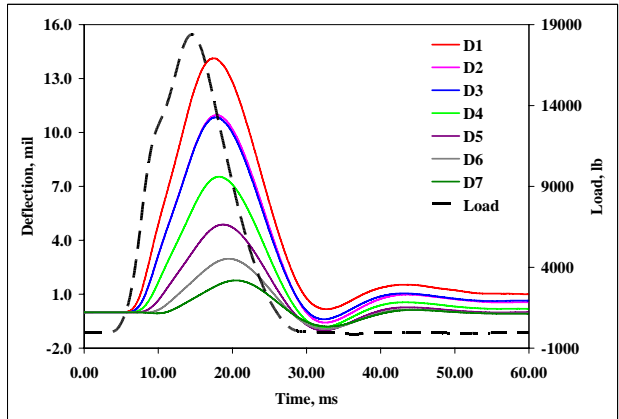
(b) 19000 lb

Figure C-35. Deflections at B2-L6-R3

Appendix D

Seismic Data Collection Procedure

The following procedure is recommended when operating the PSPA in the field.

1. Preparation

◆ Make sure the computer is turned off and the power switch on the PSPA electronics box is off (in the "off" position, the toggle switch points toward the outer edge of the electronics box). Make sure the batteries of the PSPA and the laptop are charged.

◆ The PSPA power switch should be turned on only after connecting the PSPA to the laptop.

◆ Turn on the laptop and the PSPA. Open the PSPA manager in the laptop and start a new application or the last project.

◆ Check the PSPA to make sure the correct instrument is connected to the computer (sensor spacing and serial number).

◆ The most effective thickness range of measurement with PSPA is between 1/2 the spacing to twice the spacing of the two receivers. Adjust the receiver spacing according to the thickness of the layer being measured. (This step is only for advanced users.)

◆ Place the PSPA on the pavement surface, and push the source cylinder (the one that is farthest from the electronics box) down gently. If it bounces back instead of staying in place, open the two end knobs and the let trapped air out.

2. Field operation

◆ At each test point, pull the receivers 1/8 inch down (not more than that), and then set the electronics box down and gently push the source down. Make sure there is good contact between the sensors (source and receivers) and the pavement surface.

◆ Run the test, look at the signals, and make sure that the black and green records contain a quiet period at the beginning followed by a sine-wave-shaped record. If the signal is bad, that means that contact between the PSPA and the pavement surface is not good.

Move the PSPA a little (or find a smoother surface), and set it down as in the previous step. Run the test again, and check the signal. Repeat the process until the signal is good.

◆ Run the test at least two times at one point. PSPA is parallel to the traffic in the first test and perpendicular to the traffic in the second test. The average of the two test results is considered to be the final result of the point. The test results include pavement temperature and the modulus of the top layer.

3. Test Signal Examples (good and bad)

◆ Examples of good signals and bad signals are shown in Figures D-1 and D-2, respectively. The good signal has a sine-wave-shaped record for the two receivers (green and black curves), and the bad signal has two spikes at the beginning and the end of record for the source (red curve), which means the source is not in good contact with the pavement. The corresponding dispersion curve in the data reduction is smooth for the good signal and jagged for the bad signal.
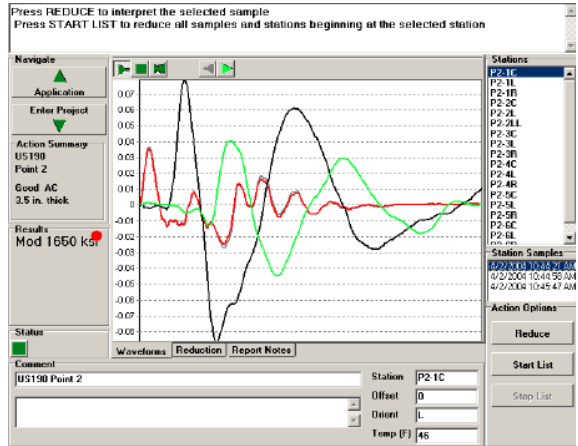
(a) signal
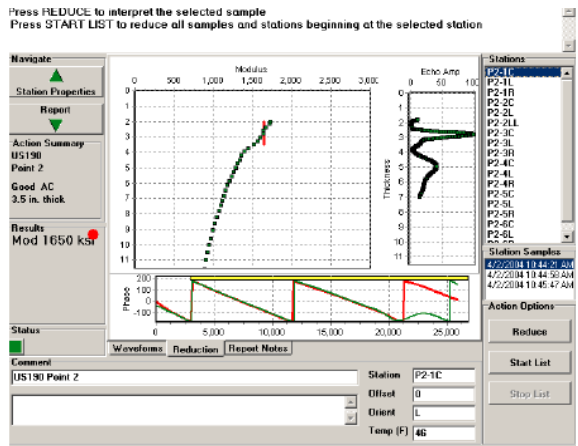
(b) data reduction

Figure D-1. Good PSPA data
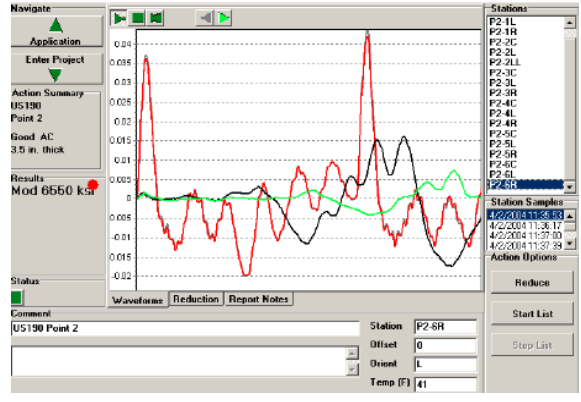
(a) signal
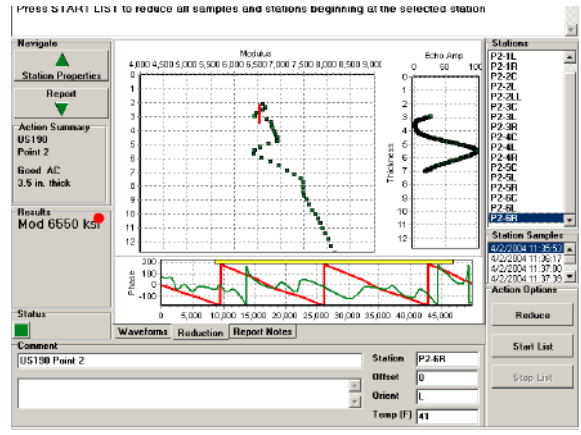
(b) data reduction

Figure D-2. Bad PSPA data

Appendix E

Summary of Traffic Data

Table E-1. WIM data for Mercer East and Mercer West sites

Lane Information

Site	Lane Number	Direction	Lane
	Lane 1	West	Travel
	Lane 2	West	Passing
Mercer	Lane 3	East	Passing
	Lane 4	East	Travel

Annual Average Daily Traffic

Year	AASHTO Method			
	Lane 1	Lane 2	Lane 3	Lane 4
2001	9124	3291	3097	9211
2002	9658	3787	3640	9753
2003	9387	3755	3629	9608
2004	9036	3560	3489	8189
2005	9001	3763	3482	9336
2006	9175	3469	3386	9312
2007	8865	3340	3205	8894

Year	Simple Method			
	Lane 1	Lane 2	Lane 3	Lane 4
2001	9105	3242	3053	9184
2002	9859	3896	3778	9958
2003	9431	3788	3674	9666
2004	9081	3538	3468	8091
2005	8983	3714	3461	9322
2006	9220	3505	3428	9353
2007	8721	3204	3124	8775

Table E-1. WIM data for Mercer East and Mercer West sites (cont'd)

Annual Average Daily Truck Traffic

Year	AASHTO Method			
	Lane 1	Lane 2	Lane 3	Lane 4
2001	3484	820	761	4795
2002	3953	824	786	4415
2003	4209	823	779	4508
2004	2948	598	589	3187
2005	4317	870	799	4621
2006	4376	807	798	4772
2007	4228	770	752	4531
Year	Simple Method			
	Lane 1	Lane 2	Lane 3	Lane 4
2001	3484	801	746	4810
2002	4137	863	826	4566
2003	4229	833	791	4564
2004	2841	580	576	3093
2005	4332	870	804	4654
2006	4377	809	801	4761
2007	4198	758	752	4509

Traffic Volume in 2008

Parameter	Method	Year	Lane 1	Lane 2	Lane 3	Lane 4
AADT	AASHTO	2008	8366	2932	2369	8471
AADT	Simple	2008	8425	2977	2376	8532
AADTT	AASHTO	2008	4202	736	380	4533
AADTT	Simple	2008	4221	740	361	4564

*Based on WIM data collected from January to May 2008

Table E-1. WIM data for Mercer East and Mercer West sites (cont'd)

Vehicle Class Distribution

Year 2006

Vehicle	Lane 1	Lane 2	Lane 3	Lane 4	Average
Class 4	0.73	0.76	1.28	0.81	0.90
Class 5	0.02	0.02	0.02	6.03	1.52
Class 6	3.49	2.98	3.54	2	3.00
Class 7	0.51	0.54	0.73	0.95	0.68
Class 8	3.56	4.39	3.66	1.9	3.38
Class 9	83.57	87.46	86.94	80.6	84.64
Class 10	0.67	0.8	0.63	0.69	0.70
Class 11	5.76	1.74	1.82	5.28	3.65
Class 12	1.58	1.25	1.28	1.63	1.44
Class 13	0.1	0.06	0.09	0.12	0.09
Class 14	0	0	0	0	0.00
Class 15	1.39	1.72	2.53	1.53	1.79
Total	209.65	430.06	424.22	195.15	314.77
Truck	100	100	100	100	100.00

Vehicle Class Distribution

Year 2007

Vehicle	Lane 1	Lane 2	Lane 3	Lane 4	Average
Class 4	0.79	0.77	1.38	0.82	0.94
Class 5	0.02	0.02	0.02	5.85	1.48
Class 6	3.37	2.79	4.2	2.26	3.16
Class 7	0.59	0.62	0.77	0.86	0.71
Class 8	3.12	3.85	3.37	1.87	3.05
Class 9	84.54	87.59	86.07	81.11	84.83
Class 10	0.61	0.66	0.53	0.62	0.61
Class 11	5.34	2.22	2.25	4.91	3.68
Class 12	1.52	1.29	1.35	1.57	1.43
Class 13	0.1	0.19	0.06	0.12	0.12
Class 14	0	0	0	0	0.00
Class 15	2.9	5.84	3.69	2.03	3.62
Total	209.68	433.56	426.47	196.28	316.50
Truck	100	100	100	100	100.00

Table E-1. WIM data for Mercer East and Mercer West sites (cont'd)

Vehicle Class Distribution

Year 2008

Vehicle	Lane 1	Lane 2	Lane 3	Lane 4	Average
Class 4	0.79	0.85	1.45	0.88	0.99
Class 5	0.01	0.02	0.02	5.97	1.51
Class 6	3.33	2.93	4.74	2.35	3.34
Class 7	0.56	0.69	0.73	0.89	0.72
Class 8	2.89	3.52	2.99	1.93	2.83
Class 9	84.93	87.15	85.37	80.83	84.57
Class 10	0.69	0.8	0.52	0.65	0.67
Class 11	5.12	2.45	2.54	4.76	3.72
Class 12	1.58	1.5	1.56	1.62	1.57
Class 13	0.1	0.08	0.08	0.12	0.10
Class 14	0	0	0	0	0.00
Class 15	3.33	5.28	23.98	2.59	8.80
Total	199.09	398.66	623.85	186.87	352.12
Truck	100	100	100	100	100.00

*Based on WIM data collected from January to May 2008

Number of Axles Per Truck

Year 2006

Vehicle Type	Single Axle/ Truck	Tandem Axle/ Truck	Tridem Axle/ Truck	Quad Axle/ Truck	# Trucks
Class 4	1.61	0.39	0.00	0.00	8757
Class 5	2.02	0.11	0.00	0.00	64402
Class 6	1.00	1.00	0.00	0.00	21397
Class 7	1.01	0.01	0.99	0.00	10046
Class 8	2.36	0.69	0.00	0.00	20207
Class 9	1.31	1.85	0.00	0.00	859927
Class 10	1.02	1.01	0.98	0.00	7354
Class 11	5.00	0.00	0.00	0.00	56247
Class 12	4.00	1.00	0.00	0.00	17415
Class 13	1.24	0.89	0.89	0.31	1175

Table E-1. WIM data for Mercer East and Mercer West sites (cont'd)

Number of Axles Per Truck

Year 2007

Vehicle Type	Single Axle/ Truck	Tandem Axle/ Truck	Tridem Axle/ Truck	Quad Axle/ Truck	# Trucks
Class 4	1.62	0.38	0.00	0.00	6151
Class 5	2.01	0.09	0.00	0.00	44123
Class 6	1.00	1.00	0.00	0.00	17403
Class 7	1.01	0.01	0.99	0.00	6630
Class 8	2.30	0.72	0.00	0.00	14546
Class 9	1.30	1.85	0.00	0.00	623487
Class 10	1.03	1.01	0.98	0.00	4929
Class 11	5.00	0.00	0.00	0.00	37587
Class 12	4.00	1.00	0.00	0.00	11958
Class 13	1.22	0.90	0.93	0.36	843

Number of Axles Per Truck

Year 2008

Vehicle Type	Single Axle/ Truck	Tandem Axle/ Truck	Tridem Axle/ Truck	Quad Axle/ Truck	# Trucks
Class 4	1.60	0.40	0.00	0.00	5717
Class 5	2.01	0.08	0.00	0.00	38914
Class 6	1.00	1.00	0.00	0.00	15294
Class 7	1.01	0.01	0.99	0.00	5921
Class 8	2.28	0.74	0.00	0.00	12546
Class 9	1.31	1.84	0.00	0.00	527786
Class 10	1.04	1.02	0.97	0.00	4238
Class 11	5.00	0.00	0.00	0.00	31183
Class 12	4.00	1.00	0.00	0.00	10611
Class 13	1.22	0.87	1.03	0.33	716

*Based on WIM data collected from January to May 2008

Table E-1. WIM data for Mercer East and Mercer West sites (cont'd)

Monthly Adjustment Factors

Year 2006-Lane 1

Month	Class 4	Class 5	Class 6	Class 7	Class 8	Class 9	Class 10	Class 11	Class 12	Class 13
January	0.76	0.38	0.95	0.62	0.82	0.96	0.91	0.96	0.9	0.75
February	0.89	0.36	0.96	1.07	0.85	1	0.96	1.04	1.01	0.72
March	1.02	0.59	0.97	1.08	0.95	1.05	0.99	1.03	1.11	1.08
April	1.15	0.83	1.04	1.17	1.06	1.05	1.04	1.05	1.08	0.98
May	1.14	1.43	1.04	0.96	1.13	1.02	1.03	1.01	1.02	1.08
June	1.19	1.65	1.09	1.01	1.2	1.04	1.17	1.06	1.02	1.28
July	1.02	1.94	1.12	1.02	1.18	0.97	1.02	0.98	0.9	1.26
August	N.A.	N.A.	N.A.	N.A.	N.A.	N.A.	N.A.	N.A.	N.A.	N.A.
September	N.A.	N.A.	N.A.	N.A.	N.A.	N.A.	N.A.	N.A.	N.A.	N.A.
October	N.A.	N.A.	N.A.	N.A.	N.A.	N.A.	N.A.	N.A.	N.A.	N.A.
November	N.A.	N.A.	N.A.	N.A.	N.A.	N.A.	N.A.	N.A.	N.A.	N.A.
December	0.83	0.81	0.84	1.08	0.83	0.91	0.87	0.88	0.96	0.85

Monthly Adjustment Factors

Year 2006-Lane 2

Month	Class 4	Class 5	Class 6	Class 7	Class 8	Class 9	Class 10	Class 11	Class 12	Class 13
January	0.57	0.57	0.84	0.57	0.67	0.88	0.8	0.85	0.84	0.73
February	0.73	0.25	0.87	1.28	0.67	0.92	0.74	0.87	0.9	0.66
March	0.92	1.28	0.91	1.24	0.84	0.99	0.99	1.08	0.94	0.8
April	1.19	0.44	1.13	1	1.09	1.06	1.16	0.99	1.09	1.07
May	1.33	1.96	1.13	0.86	1.2	1.07	1.11	1.07	1.09	1.14
June	1.36	1.47	1.14	0.99	1.33	1.16	1.35	1.2	1.1	1.75
July	1.21	1.37	1.22	1.06	1.46	1.09	1.26	1.08	1.19	0.98
August	N.A.	N.A.	N.A.	N.A.	N.A.	N.A.	N.A.	N.A.	N.A.	N.A.
September	N.A.	N.A.	N.A.	N.A.	N.A.	N.A.	N.A.	N.A.	N.A.	N.A.
October	N.A.	N.A.	N.A.	N.A.	N.A.	N.A.	N.A.	N.A.	N.A.	N.A.
November	N.A.	N.A.	N.A.	N.A.	N.A.	N.A.	N.A.	N.A.	N.A.	N.A.
December	0.69	0.65	0.78	1	0.74	0.85	0.58	0.86	0.84	0.88

Table E-1. WIM data for Mercer East and Mercer West sites (cont'd)

Monthly Adjustment Factors

Year 2006-Lane 3

Month	Class 4	Class 5	Class 6	Class 7	Class 8	Class 9	Class 10	Class 11	Class 12	Class 13
January	0.68	0.68	0.82	0.99	0.59	0.9	0.82	0.79	0.74	0.34
February	0.77	0.74	0.91	0.92	0.66	0.9	0.87	0.9	0.77	0.7
March	0.77	0.48	1.03	0.9	0.78	0.97	1.04	0.86	1	0.65
April	1.06	0.74	1.06	1.04	0.92	1.04	1.17	0.9	1.05	1.27
May	1.42	2.16	1.14	1.41	1.45	1.17	1.42	1.46	1.18	2.22
June	1.27	0.97	1.09	0.99	1.33	1.11	1.2	1.06	1.17	0.96
July	1.27	1.04	1.08	0.92	1.58	1.05	0.97	1.14	1.16	1.03
August	N.A.	N.A.	N.A.	N.A.	N.A.	N.A.	N.A.	N.A.	N.A.	N.A.
September	N.A.	N.A.	N.A.	N.A.	N.A.	N.A.	N.A.	N.A.	N.A.	N.A.
October	N.A.	N.A.	N.A.	N.A.	N.A.	N.A.	N.A.	N.A.	N.A.	N.A.
November	N.A.	N.A.	N.A.	N.A.	N.A.	N.A.	N.A.	N.A.	N.A.	N.A.
December	0.75	1.18	0.88	0.82	0.69	0.87	0.52	0.89	0.93	0.84

Monthly Adjustment Factors

Year 2006-Lane 4

Month	Class 4	Class 5	Class 6	Class 7	Class 8	Class 9	Class 10	Class 11	Class 12	Class 13
January	0.78	0.97	0.88	0.93	0.91	0.98	1.01	0.96	0.89	0.92
February	0.77	0.97	0.98	0.99	0.92	1	0.96	1.02	1.01	1.02
March	1.02	0.99	1.04	0.85	0.98	1.05	0.98	1.05	1.09	1.07
April	1.24	1.03	1.12	1.1	1.02	1.05	1.11	1.06	1.09	1.32
May	1.09	1.03	1.01	1.07	1.01	1	1.06	0.99	1.01	1.05
June	1.23	1.14	1.05	1.14	1.12	1.05	1.2	1.07	1.03	0.98
July	1.02	1.11	1.01	1.14	1.09	0.96	1.01	0.98	0.94	0.9
August	N.A.	N.A.	N.A.	N.A.	N.A.	N.A.	N.A.	N.A.	N.A.	N.A.
September	N.A.	N.A.	N.A.	N.A.	N.A.	N.A.	N.A.	N.A.	N.A.	N.A.
October	N.A.	N.A.	N.A.	N.A.	N.A.	N.A.	N.A.	N.A.	N.A.	N.A.
November	N.A.	N.A.	N.A.	N.A.	N.A.	N.A.	N.A.	N.A.	N.A.	N.A.
December	0.85	0.76	0.9	0.77	0.94	0.92	0.66	0.87	0.95	0.74

Table E-1. WIM data for Mercer East and Mercer West sites (cont'd)

Monthly Adjustment Factors

Year 2007-Lane 1

Month	Class 4	Class 5	Class 6	Class 7	Class 8	Class 9	Class 10	Class 11	Class 12	Class 13
January	0.68	0.59	0.94	0.61	0.93	0.96	0.87	0.97	0.96	0.81
February	0.88	0.44	0.94	0.78	0.98	0.98	0.92	0.97	0.89	0.98
March	0.82	1.11	0.89	0.69	0.95	0.98	1.04	1.02	0.91	0.94
April	1.25	0.44	1.04	1.05	0.97	1.02	1.07	1.04	1.04	1.07
May	1.17	1.36	1.09	1.87	1.17	1.05	1.08	1.06	1.02	1.09
June	1.24	2.58	1.16	1.21	1.14	1.04	1.06	1.04	1.08	1.26
July	N.A.	N.A.	N.A.	N.A.	N.A.	N.A.	N.A.	N.A.	N.A.	N.A.
August	1.13	1.81	1.3	1.36	1.27	1.14	1.13	1.11	1.12	1.12
September	N.A.	N.A.	N.A.	N.A.	N.A.	N.A.	N.A.	N.A.	N.A.	N.A.
October	N.A.	N.A.	N.A.	N.A.	N.A.	N.A.	N.A.	N.A.	N.A.	N.A.
November	1.01	0.48	0.91	0.67	0.9	0.98	0.86	0.94	1.07	0.92
December	0.91	0.56	0.83	0.86	0.78	0.91	1.02	0.88	0.93	0.91

Monthly Adjustment Factors

Year 2007-Lane 2

Month	Class 4	Class 5	Class 6	Class 7	Class 8	Class 9	Class 10	Class 11	Class 12	Class 13
January	0.63	0.8	0.88	0.7	0.78	0.93	0.9	0.84	0.94	0.31
February	0.65	0.85	0.95	0.96	0.88	0.92	0.9	0.89	0.83	0.32
March	0.84	0.57	0.86	0.89	0.74	0.96	1.05	0.94	0.87	0.25
April	1.23	0	0.98	1.24	1	1.04	1.1	0.96	0.95	0.85
May	1.27	1.82	1.14	1.46	1.21	1.07	1.23	0.94	1.08	1.36
June	1.45	1.33	1.12	0.9	1.15	0.99	0.98	1.02	1.3	3.38
July	N.A.	N.A.	N.A.	N.A.	N.A.	N.A.	N.A.	N.A.	N.A.	N.A.
August	1.04	2.65	1.48	0.97	1.79	1.29	0.98	1.49	1.07	2.56
September	N.A.	N.A.	N.A.	N.A.	N.A.	N.A.	N.A.	N.A.	N.A.	N.A.
October	N.A.	N.A.	N.A.	N.A.	N.A.	N.A.	N.A.	N.A.	N.A.	N.A.
November	1.15	1.14	0.97	0.94	0.96	0.98	0.95	0.96	0.96	0.38
December	0.88	0.23	0.76	0.94	0.67	0.88	0.93	1.03	1.06	0.29

Table E-1. WIM data for Mercer East and Mercer West sites (cont'd)

Monthly Adjustment Factors

Year 2007-Lane 3

Month	Class 4	Class 5	Class 6	Class 7	Class 8	Class 9	Class 10	Class 11	Class 12	Class 13
January	0.74	0.95	0.76	0.94	0.77	0.97	0.83	0.9	0.88	0.77
February	0.96	0.92	0.89	0.62	0.81	0.95	0.94	1.06	0.76	1.71
March	0.62	2.3	0.8	0.48	0.79	0.92	0.7	0.95	0.8	0.34
April	1.17	1.84	1.16	1.43	1.06	1.07	0.87	1.13	1.03	1.37
May	1.24	0.55	1.26	1.15	1.31	1.07	1.11	0.91	1.08	1.23
June	1.41	0.54	1.14	1.21	1.26	1.02	1.31	0.86	1.09	1.79
July	N.A.	N.A.	N.A.	N.A.	N.A.	N.A.	N.A.	N.A.	N.A.	N.A.
August	1.32	1.07	1.1	1.5	1.22	1.16	1.46	1.18	1.18	0.8
September	N.A.	N.A.	N.A.	N.A.	N.A.	N.A.	N.A.	N.A.	N.A.	N.A.
October	N.A.	N.A.	N.A.	N.A.	N.A.	N.A.	N.A.	N.A.	N.A.	N.A.
November	0.91	0.61	0.97	0.96	1.12	0.95	1.01	0.97	1.07	0.57
December	0.77	0.23	0.97	0.83	0.74	0.92	0.93	1.03	1.09	0.65

Monthly Adjustment Factors

Year 2007-Lane 4

Month	Class 4	Class 5	Class 6	Class 7	Class 8	Class 9	Class 10	Class 11	Class 12	Class 13
January	0.87	0.81	0.83	0.73	0.97	0.98	1.13	0.95	0.93	0.87
February	0.79	0.76	0.84	0.68	0.95	0.98	0.75	1.02	0.92	1.06
March	1.11	0.97	1	0.93	0.96	0.94	0.87	0.93	0.91	1.14
April	1.14	1.23	1.3	1.43	1.06	1.06	0.98	1.07	1.03	1.19
May	1.3	1.34	1.14	1.4	1.09	1.04	1.1	1.05	1.09	1.27
June	N.A.	N.A.	N.A.	N.A.	N.A.	N.A.	N.A.	N.A.	N.A.	N.A.
July	1.2	1.42	1.33	1.4	1.19	1.14	1.31	1.13	1.12	0.98
August	N.A.	N.A.	N.A.	N.A.	N.A.	N.A.	N.A.	N.A.	N.A.	N.A.
September	N.A.	N.A.	N.A.	N.A.	N.A.	N.A.	N.A.	N.A.	N.A.	N.A.
October	1.02	0.94	0.92	0.87	0.95	0.96	0.96	0.95	1.02	0.89
November	0.88	0.86	0.92	0.73	0.98	0.93	0.87	0.9	0.97	0.91
December	0.77	0.81	0.8	0.97	0.93	0.98	1.13	0.99	0.99	0.73

Table E-1. WIM data for Mercer East and Mercer West sites (cont'd)

Wheelbase of Vehicles

Distance (ft)	Percent
0	0.0001%
2	0.0431%
4	0.9301%
6	0.0782%
8	0.0212%
10	1.2814%
12	10.4721%
14	4.8529%
16	29.6754%
18	37.7236%
20	13.7680%
22	0.9051%
24	0.1704%
26	0.0405%
28	0.0176%
30	0.0058%
32	0.0048%
34	0.0027%
36	0.0010%
38	0.0014%
40	0.0046%

Table E-1. WIM data for Mercer East and Mercer West sites (cont'd)

Axle Load Distribution Factors
Single Axle Load Distributions for various FHWA Vehicle Classes

Axle Weight	4	5	6	7	8	9	10	11	12	13
3000	0.0	9.0	0.3	0.8	1.2	1.1	0.5	0.1	0.2	2.2
4000	0.0	19.2	1.6	0.3	1.8	2.4	0.4	0.4	0.5	1.8
5000	0.3	13.7	1.4	0.2	1.5	1.7	0.3	1.7	2.8	1.6
6000	1.1	10.2	0.8	0.2	3.1	1.0	0.3	5.6	10.3	1.4
7000	4.3	10.6	1.7	0.5	7.1	1.0	1.1	3.9	7.5	3.2
8000	8.5	9.2	4.5	0.7	10.0	2.3	6.9	4.4	8.3	5.7
9000	11.9	6.8	11.6	1.1	17.1	7.8	19.1	9.3	11.3	15.6
10000	14.4	5.3	23.0	2.6	16.3	24.6	32.9	14.8	13.3	18.2
11000	14.7	4.2	19.8	5.3	9.5	31.8	24.3	9.3	11.5	14.9
12000	11.5	3.0	13.6	7.6	5.5	10.8	8.9	8.5	9.9	9.9
13000	10.0	2.4	8.8	9.3	5.1	1.8	2.8	9.0	8.9	10.6
14000	8.0	1.7	5.1	11.6	5.0	1.2	1.1	9.0	7.0	4.6
15000	5.6	1.3	3.1	12.4	5.1	1.8	0.4	7.9	4.0	3.2
16000	3.4	1.0	1.8	11.9	3.6	2.6	0.2	6.2	2.2	1.7
17000	2.3	0.8	1.0	11.4	2.6	3.0	0.2	4.5	1.2	1.5
18000	1.7	0.6	0.6	8.5	2.0	2.3	0.1	2.9	0.6	1.2
19000	1.1	0.4	0.6	6.5	1.4	1.4	0.2	1.6	0.3	1.0
20000	0.5	0.3	0.3	3.8	0.9	0.7	0.1	0.7	0.1	0.3
21000	0.4	0.1	0.3	1.9	0.5	0.4	0.1	0.3	0.1	0.3
22000	0.2	0.1	0.1	1.7	0.3	0.2	0.0	0.1	0.0	0.2
23000	0.1	0.1	0.0	1.3	0.2	0.1	0.0	0.0	0.0	0.1
24000	0.0	0.0	0.0	0.3	0.1	0.1	0.0	0.0	0.0	0.0
25000	0.1	0.0	0.0	0.0	0.1	0.0	0.0	0.0	0.0	0.0
26000	0.0	0.0	0.0	0.0	0.0	0.0	0.0	0.0	0.0	0.1
27000	0.0	0.0	0.0	0.0	0.0	0.0	0.0	0.0	0.0	0.0
28000	0.0	0.0	0.0	0.0	0.0	0.0	0.0	0.0	0.0	0.1
29000	0.0	0.0	0.0	0.0	0.0	0.0	0.0	0.0	0.0	0.1
30000	0.0	0.0	0.0	0.0	0.0	0.0	0.0	0.0	0.0	0.0
31000	0.0	0.0	0.0	0.0	0.0	0.0	0.0	0.0	0.0	0.1
32000	0.0	0.0	0.0	0.0	0.0	0.0	0.0	0.0	0.0	0.0
33000	0.0	0.0	0.0	0.0	0.0	0.0	0.0	0.0	0.0	0.0
34000	0.0	0.0	0.0	0.0	0.0	0.0	0.0	0.0	0.0	0.1
35000	0.0	0.0	0.0	0.0	0.0	0.0	0.0	0.0	0.0	0.0
36000	0.0	0.0	0.0	0.0	0.0	0.0	0.0	0.0	0.0	0.0
37000	0.0	0.0	0.0	0.0	0.0	0.0	0.0	0.0	0.0	0.1
38000	0.0	0.0	0.0	0.0	0.0	0.0	0.0	0.0	0.0	0.0
39000	0.0	0.0	0.0	0.0	0.0	0.0	0.0	0.0	0.0	0.0
40000	0.0	0.0	0.0	0.0	0.0	0.0	0.0	0.0	0.0	0.1
41000	0.0	0.0	0.0	0.0	0.0	0.0	0.0	0.0	0.0	0.1

Tandem Axle Load Distributions for various FHWA Vehicle Classes

Axle Weight	4	5	6	7	8	9	10	11	12	13
6000	0.0	71.7	1.2	2.3	1.2	0.4	0.3	0.0	0.1	1.2
8000	0.1	23.3	17.4	9.6	3.7	1.7	0.1	0.0	0.3	2.3
10000	0.9	4.8	14.2	39.6	13.9	4.6	0.7	0.0	3.0	0.9
12000	1.6	0.2	7.8	24.6	17.1	6.6	2.2	0.0	11.9	3.7
14000	1.9	0.0	10.0	6.3	14.6	6.7	3.8	0.0	7.2	3.4
16000	2.0	0.0	8.0	5.7	11.6	5.9	3.9	0.0	10.7	3.1
18000	2.9	0.0	5.7	1.0	9.6	5.8	3.9	0.0	21.0	5.0
20000	3.9	0.0	6.5	0.0	7.1	6.0	4.5	0.0	23.9	7.7
22000	4.5	0.0	5.7	1.9	6.3	6.3	3.9	25.0	13.0	4.4
24000	5.8	0.0	4.6	4.3	4.8	6.2	6.0	50.0	6.3	4.3
26000	9.3	0.0	3.4	0.0	4.0	6.5	10.1	25.0	2.0	6.6
28000	16.0	0.0	3.4	0.0	2.4	7.9	14.3	0.0	0.4	8.4
30000	21.2	0.0	3.0	0.0	1.7	11.0	19.0	0.0	0.1	8.3
32000	19.7	0.0	3.5	0.0	1.2	12.6	11.9	0.0	0.0	8.9
34000	7.3	0.0	2.5	4.7	0.4	7.7	7.0	0.0	0.0	8.5
36000	2.1	0.0	1.1	0.0	0.3	2.8	3.7	0.0	0.0	7.9
38000	0.6	0.0	0.8	0.0	0.1	0.9	2.1	0.0	0.0	6.9
40000	0.0	0.0	0.5	0.0	0.1	0.3	1.1	0.0	0.0	3.0
42000	0.0	0.0	0.2	0.0	0.0	0.1	0.7	0.0	0.0	2.5
44000	0.0	0.0	0.2	0.0	0.0	0.0	0.4	0.0	0.0	1.4
46000	0.0	0.0	0.1	0.0	0.0	0.0	0.2	0.0	0.0	0.5
48000	0.0	0.0	0.2	0.0	0.0	0.0	0.1	0.0	0.0	0.5
50000	0.0	0.0	0.1	0.0	0.0	0.0	0.0	0.0	0.0	0.1
52000	0.0	0.0	0.1	0.0	0.0	0.0	0.1	0.0	0.0	0.1
54000	0.0	0.0	0.0	0.0	0.0	0.0	0.0	0.0	0.0	0.3
56000	0.0	0.0	0.0	0.0	0.0	0.0	0.0	0.0	0.0	0.1
58000	0.0	0.0	0.0	0.0	0.0	0.0	0.0	0.0	0.0	0.0
60000	0.0	0.0	0.0	0.0	0.0	0.0	0.0	0.0	0.0	0.0
62000	0.0	0.0	0.0	0.0	0.0	0.0	0.0	0.0	0.0	0.0
64000	0.0	0.0	0.0	0.0	0.0	0.0	0.0	0.0	0.0	0.0
66000	0.0	0.0	0.0	0.0	0.0	0.0	0.0	0.0	0.0	0.0
68000	0.0	0.0	0.0	0.0	0.0	0.0	0.0	0.0	0.0	0.0
70000	0.0	0.0	0.0	0.0	0.0	0.0	0.0	0.0	0.0	0.0
72000	0.0	0.0	0.0	0.0	0.0	0.0	0.0	0.0	0.0	0.0
74000	0.0	0.0	0.0	0.0	0.0	0.0	0.0	0.0	0.0	0.0
76000	0.0	0.0	0.0	0.0	0.0	0.0	0.0	0.0	0.0	0.0
78000	0.0	0.0	0.0	0.0	0.0	0.0	0.0	0.0	0.0	0.0
80000	0.0	0.0	0.0	0.0	0.0	0.0	0.0	0.0	0.0	0.0
82000	0.0	0.0	0.0	0.0	0.0	0.0	0.0	0.0	0.0	0.0

Table E-1. WIM data for Mercer East and Mercer West sites (cont'd)

Tridem Axle Load Distributions for various FHWA Vehicle Classes

Axle Weight	4	5	6	7	8	9	10	11	12	13
12000	N.A.	N.A.	N.A.	100	N.A.	N.A.	100	N.A.	N.A.	100
15000	N.A.	N.A.	N.A.	0.2	N.A.	N.A.	9.4	N.A.	N.A.	0.6
18000	N.A.	N.A.	N.A.	0.1	N.A.	N.A.	5.2	N.A.	N.A.	0.6
21000	N.A.	N.A.	N.A.	0.3	N.A.	N.A.	3.4	N.A.	N.A.	1.8
24000	N.A.	N.A.	N.A.	0.5	N.A.	N.A.	2.8	N.A.	N.A.	1.5
27000	N.A.	N.A.	N.A.	0.5	N.A.	N.A.	2.8	N.A.	N.A.	1.3
30000	N.A.	N.A.	N.A.	0.7	N.A.	N.A.	2.8	N.A.	N.A.	1.6
33000	N.A.	N.A.	N.A.	0.6	N.A.	N.A.	4.2	N.A.	N.A.	2.5
36000	N.A.	N.A.	N.A.	1.9	N.A.	N.A.	7.3	N.A.	N.A.	3.1
39000	N.A.	N.A.	N.A.	2.5	N.A.	N.A.	14.0	N.A.	N.A.	3.4
42000	N.A.	N.A.	N.A.	3.8	N.A.	N.A.	20.3	N.A.	N.A.	6.5
45000	N.A.	N.A.	N.A.	4.3	N.A.	N.A.	14.8	N.A.	N.A.	12.5
48000	N.A.	N.A.	N.A.	7.0	N.A.	N.A.	7.5	N.A.	N.A.	15.0
51000	N.A.	N.A.	N.A.	11.8	N.A.	N.A.	2.9	N.A.	N.A.	14.4
54000	N.A.	N.A.	N.A.	18.6	N.A.	N.A.	1.2	N.A.	N.A.	10.7
57000	N.A.	N.A.	N.A.	21.2	N.A.	N.A.	0.9	N.A.	N.A.	9.9
60000	N.A.	N.A.	N.A.	17.1	N.A.	N.A.	0.2	N.A.	N.A.	6.2
63000	N.A.	N.A.	N.A.	6.7	N.A.	N.A.	0.2	N.A.	N.A.	4.2
66000	N.A.	N.A.	N.A.	1.7	N.A.	N.A.	0.1	N.A.	N.A.	1.8
69000	N.A.	N.A.	N.A.	0.5	N.A.	N.A.	0.0	N.A.	N.A.	0.8
72000	N.A.	N.A.	N.A.	0.1	N.A.	N.A.	0.0	N.A.	N.A.	0.7
75000	N.A.	N.A.	N.A.	0.0	N.A.	N.A.	0.0	N.A.	N.A.	0.4
78000	N.A.	N.A.	N.A.	0.0	N.A.	N.A.	0.0	N.A.	N.A.	0.2
81000	N.A.	N.A.	N.A.	0.0	N.A.	N.A.	0.0	N.A.	N.A.	0.1
84000	N.A.	N.A.	N.A.	0.0	N.A.	N.A.	0.0	N.A.	N.A.	0.0
87000	N.A.	N.A.	N.A.	0.0	N.A.	N.A.	0.0	N.A.	N.A.	0.0
90000	N.A.	N.A.	N.A.	0.0	N.A.	N.A.	0.0	N.A.	N.A.	0.1
93000	N.A.	N.A.	N.A.	0.0	N.A.	N.A.	0.0	N.A.	N.A.	0.0
96000	N.A.	N.A.	N.A.	0.0	N.A.	N.A.	0.0	N.A.	N.A.	0.1
99000	N.A.	N.A.	N.A.	0.0	N.A.	N.A.	0.0	N.A.	N.A.	0.0
102000	N.A.	N.A.	N.A.	0.0	N.A.	N.A.	0.0	N.A.	N.A.	0.0
105000	N.A.	N.A.	N.A.	0.0	N.A.	N.A.	0.0	N.A.	N.A.	0.1

Table E-1. WIM data for Mercer East and Mercer West sites (cont'd)

Quad Axle Load Distributions for various FHWA Vehicle Classes

Axle Weight	4	5	6	7	8	9	10	11	12	13
12000	N.A.	N.A.	N.A.	N.A.	N.A.	100	N.A.	N.A.	N.A.	100
15000	N.A.	N.A.	N.A.	N.A.	N.A.	0.0	N.A.	N.A.	N.A.	7.6
18000	N.A.	N.A.	N.A.	N.A.	N.A.	0.0	N.A.	N.A.	N.A.	16.2
21000	N.A.	N.A.	N.A.	N.A.	N.A.	0.0	N.A.	N.A.	N.A.	5.4
24000	N.A.	N.A.	N.A.	N.A.	N.A.	0.0	N.A.	N.A.	N.A.	2.5
27000	N.A.	N.A.	N.A.	N.A.	N.A.	0.0	N.A.	N.A.	N.A.	1.9
30000	N.A.	N.A.	N.A.	N.A.	N.A.	0.0	N.A.	N.A.	N.A.	4.0
33000	N.A.	N.A.	N.A.	N.A.	N.A.	0.0	N.A.	N.A.	N.A.	0.9
36000	N.A.	N.A.	N.A.	N.A.	N.A.	0.0	N.A.	N.A.	N.A.	1.5
39000	N.A.	N.A.	N.A.	N.A.	N.A.	0.0	N.A.	N.A.	N.A.	1.2
42000	N.A.	N.A.	N.A.	N.A.	N.A.	0.0	N.A.	N.A.	N.A.	1.3
45000	N.A.	N.A.	N.A.	N.A.	N.A.	0.0	N.A.	N.A.	N.A.	8.7
48000	N.A.	N.A.	N.A.	N.A.	N.A.	0.0	N.A.	N.A.	N.A.	4.2
51000	N.A.	N.A.	N.A.	N.A.	N.A.	0.0	N.A.	N.A.	N.A.	5.8
54000	N.A.	N.A.	N.A.	N.A.	N.A.	0.0	N.A.	N.A.	N.A.	14.2
57000	N.A.	N.A.	N.A.	N.A.	N.A.	0.0	N.A.	N.A.	N.A.	5.0
60000	N.A.	N.A.	N.A.	N.A.	N.A.	100.0	N.A.	N.A.	N.A.	1.8
63000	N.A.	N.A.	N.A.	N.A.	N.A.	0.0	N.A.	N.A.	N.A.	4.4
66000	N.A.	N.A.	N.A.	N.A.	N.A.	0.0	N.A.	N.A.	N.A.	1.4
69000	N.A.	N.A.	N.A.	N.A.	N.A.	0.0	N.A.	N.A.	N.A.	2.5
72000	N.A.	N.A.	N.A.	N.A.	N.A.	0.0	N.A.	N.A.	N.A.	1.8
75000	N.A.	N.A.	N.A.	N.A.	N.A.	0.0	N.A.	N.A.	N.A.	4.5
78000	N.A.	N.A.	N.A.	N.A.	N.A.	0.0	N.A.	N.A.	N.A.	2.4
81000	N.A.	N.A.	N.A.	N.A.	N.A.	0.0	N.A.	N.A.	N.A.	0.5
84000	N.A.	N.A.	N.A.	N.A.	N.A.	0.0	N.A.	N.A.	N.A.	0.3
87000	N.A.	N.A.	N.A.	N.A.	N.A.	0.0	N.A.	N.A.	N.A.	0.0
90000	N.A.	N.A.	N.A.	N.A.	N.A.	0.0	N.A.	N.A.	N.A.	0.0
93000	N.A.	N.A.	N.A.	N.A.	N.A.	0.0	N.A.	N.A.	N.A.	0.0
96000	N.A.	N.A.	N.A.	N.A.	N.A.	0.0	N.A.	N.A.	N.A.	0.0
99000	N.A.	N.A.	N.A.	N.A.	N.A.	0.0	N.A.	N.A.	N.A.	0.0
102000	N.A.	N.A.	N.A.	N.A.	N.A.	0.0	N.A.	N.A.	N.A.	0.0
105000	N.A.	N.A.	N.A.	N.A.	N.A.	0.0	N.A.	N.A.	N.A.	0.0

Table E-1. WIM data for Mercer East and Mercer West sites (cont'd)

Hourly Truck Distribution

<u>Year 2006</u>

Hour	Percent Trucks			
	Lane 1	Lane 2	Lane 3	Lane 4
0	2.84	1.64	1.85	2.91
1	2.38	1.16	1.44	2.52
2	2.18	0.96	1.24	2.36
3	2.13	0.88	1.29	2.44
4	2.23	0.90	1.59	2.70
5	2.38	1.21	2.33	3.20
6	2.81	1.55	3.08	3.73
7	3.11	2.01	3.69	4.12
8	3.72	2.96	4.53	4.51
9	4.42	4.22	4.95	4.72
10	4.81	4.80	5.49	4.91
11	5.16	5.44	5.74	5.14
12	5.39	5.87	5.39	5.03
13	5.60	6.56	5.38	5.01
14	5.80	7.23	5.38	4.80
15	5.78	7.74	5.78	5.03
16	5.80	7.77	6.09	5.11
17	5.63	7.30	6.40	5.14
18	5.38	6.77	6.25	5.02
19	5.16	6.00	5.82	4.88
20	4.96	5.53	5.43	4.82
21	4.63	4.97	4.79	4.51
22	4.27	3.96	3.51	3.96
23	3.43	2.58	2.56	3.41

Table E-1. WIM data for Mercer East and Mercer West sites (cont'd)

Hourly Truck Distribution

Year 2007

Hour	Percent Trucks			
	Lane 1	Lane 2	Lane 3	Lane 4
0	3.00	1.90	1.97	2.86
1	2.43	1.26	1.48	2.48
2	2.19	1.03	1.28	2.29
3	2.11	0.90	1.33	2.35
4	2.12	0.90	1.54	2.51
5	2.30	1.11	2.18	2.94
6	2.67	1.56	2.96	3.46
7	3.06	2.11	3.79	3.94
8	3.59	2.68	4.55	4.44
9	4.27	3.80	4.79	4.76
10	4.82	4.60	5.16	5.01
11	5.27	5.43	5.61	5.18
12	5.43	5.82	5.59	5.29
13	5.63	6.26	5.54	5.24
14	5.90	6.97	5.17	5.04
15	5.90	7.52	5.62	5.12
16	5.91	7.84	6.07	5.32
17	5.76	7.63	6.32	5.16
18	5.38	7.09	6.34	5.10
19	5.15	6.29	5.73	4.95
20	4.89	5.64	5.41	4.74
21	4.52	5.02	5.00	4.46
22	4.16	3.87	3.87	4.00
23	3.55	2.76	2.71	3.37

Table E-1. WIM data for Mercer East and Mercer West sites (cont'd)

Hourly Truck Distribution

Year 2008

Hour	Percent Trucks			
	Lane 1	Lane 2	Lane 3	Lane 4
0	2.78	1.55	1.67	2.70
1	2.31	1.12	1.45	2.31
2	2.10	0.87	1.15	2.13
3	2.03	0.80	1.18	2.17
4	2.10	0.84	1.64	2.46
5	2.33	1.10	2.28	2.93
6	2.76	1.71	3.01	3.57
7	3.10	2.20	3.78	4.03
8	3.65	3.12	4.38	4.51
9	4.32	4.34	4.58	4.70
10	4.88	5.10	5.14	5.04
11	5.20	5.78	5.75	5.30
12	5.32	5.90	5.48	5.28
13	5.60	6.54	5.53	5.20
14	5.86	7.34	5.45	5.11
15	5.98	7.60	5.66	5.15
16	6.07	7.81	6.40	5.34
17	5.79	7.48	6.74	5.40
18	5.56	6.47	7.28	5.39
19	5.22	5.93	6.26	5.09
20	5.00	5.62	5.38	4.84
21	4.54	4.76	4.26	4.36
22	4.09	3.60	3.23	3.77
23	3.43	2.43	2.32	3.23

*Based on WIM data collected from January to May 2008

Table E-1. WIM data for Mercer East and Mercer West sites (cont'd

Average Speed, Gross Weight and Length of Trucks

Month	Average Speed, mph	Gross Weight (kips)	Length (ft)
Jan-06	67.52	59.73	63.47
Feb-06	67.55	59.72	63.55
Mar-06	67.97	58.29	63.73
Apr-06	68.11	54.55	63.57
May-06	67.94	53.83	63.55
Jun-06	68.08	52.56	63.55
Jul-06	67.92	51.51	63.47
Aug-06	N.A.	N.A.	N.A.
Sep-06	N.A.	N.A.	N.A.
Oct-06	N.A.	N.A.	N.A.
Nov-06	N.A.	N.A.	N.A.
Dec-06	67.48	57.11	64.17
Jan-07	66.59	59.09	64.14
Feb-07	66.40	57.49	64.16
Mar-07	67.10	57.00	64.38
Apr-07	67.08	53.71	62.39
May-07	67.20	54.19	62.11
Jun-07	67.04	53.70	61.93
Jul-07	N.A.	N.A.	N.A.
Aug-07	67.11	53.21	62.11
Sep-07	N.A.	N.A.	N.A.
Oct-07	N.A.	N.A.	N.A.
Nov-07	66.41	53.06	62.74
Dec-07	65.58	52.88	62.69
Jan-08	65.83	53.79	62.71
Feb-08	65.12	53.69	62.73
Mar-08	65.74	53.93	62.74
Apr-08	66.30	54.49	62.47
May-08	66.03	55.37	61.45

Table E-2. WIM data for Perry site

Lane Information

Site	Lane Number	Direction	Lane
Perry	Lane 1	West	Travel
	Lane 2	West	Passing
	Lane 3	East	Passing
	Lane 4	East	Travel

Annual Average Daily Traffic

Year	AASHTO Method			
	Lane 1	Lane 2	Lane 3	Lane 4
2003	7823	2527	2414	8253
2004	7496	2374	2276	8005
2005	7505	2364	2228	8028
2006	7606	2429	2281	8101
2007	7715	2561	2432	8223

Year	Simple Method			
	Lane 1	Lane 2	Lane 3	Lane 4
2003	7868	2563	2436	8325
2004	7523	2398	2304	8032
2005	7487	2353	2219	8005
2006	7606	2436	2281	8094
2007	7729	2564	2410	8220

Table E-2. WIM data for Perry site (cont'd)

Annual Average Daily Truck Traffic

Year	AASHTO Method			
	Lane 1	Lane 2	Lane 3	Lane 4
2003	1090	170	205	1383
2004	1099	174	213	1408
2005	1207	184	228	1425
2006	1062	177	212	1437
2007	1046	184	215	1443

Year	Simple Method			
	Lane 1	Lane 2	Lane 3	Lane 4
2003	1094	171	203	1391
2004	1106	176	215	1416
2005	1203	183	228	1420
2006	1060	177	212	1436
2007	1065	185	216	1452

Traffic Volume in 2008

Parameter	Method	Year	Lane 1	Lane 2	Lane 3	Lane 4
AADT	AASHTO	2008	7222	2306	2081	7784
AADT	Simple	2008	7188	2277	2077	7766
AADTT	AASHTO	2008	850	155	129	1436
AADTT	Simple	2008	858	154	121	1426

*Based on WIM data collected from January to May 2008

Table E-2. WIM data for Perry site (cont'd)

Vehicle Class Distribution

Year 2006

Vehicle	Lane 1	Lane 2	Lane 3	Lane 4	Average
Class 4	3.16	1.91	2.09	1.41	2.14
Class 5	8.25	6.17	4.26	17.17	8.96
Class 6	5.36	5.83	2.92	3.65	4.44
Class 7	1.48	1.27	2.31	1.92	1.75
Class 8	16.2	10.33	11.26	3.25	10.26
Class 9	62.38	72.08	75.12	69.67	69.81
Class 10	0.55	0.7	0.61	0.59	0.61
Class 11	1.94	0.82	0.48	1.62	1.22
Class 12	0.61	0.79	0.66	0.65	0.68
Class 13	0.06	0.09	0.29	0.08	0.13
Class 14	0	0	0	0	0.00
Class 15	7.85	2.38	2.57	4.52	4.33
Total	716.14	1371.51	1078.4	563.63	932.42
Truck	100	100	100	100	100

Vehicle Class Distribution

Year 2007

Vehicle	Lane 1	Lane 2	Lane 3	Lane 4	Average
Class 4	4.58	2.04	2.41	1.51	2.64
Class 5	8.01	6.58	4.73	17.85	9.29
Class 6	5.41	4.92	3.07	3.88	4.32
Class 7	1.43	1.44	2	1.62	1.62
Class 8	16.06	12.36	11.86	2.98	10.82
Class 9	61.71	70.25	74.02	69.24	68.81
Class 10	0.59	0.73	0.5	0.57	0.60
Class 11	1.56	0.84	0.53	1.54	1.12
Class 12	0.59	0.74	0.66	0.71	0.68
Class 13	0.06	0.1	0.21	0.1	0.12
Class 14	0	0	0	0	0.00
Class 15	9.48	3.25	2.8	4.93	5.12
Total	737.91	1395.68	1133.42	569.95	959.24
Truck	100	100	100	100	100

Table E-2. WIM data for Perry site (cont'd)

Vehicle Class Distribution

Year 2008

Vehicle	Lane 1	Lane 2	Lane 3	Lane 4	Average
Class 4	10.66	2.68	3.09	1.47	4.48
Class 5	0.11	0.08	0.02	18.2	4.60
Class 6	5.04	4.79	4.16	7.67	5.42
Class 7	0.80	1.41	1.87	1.4	1.37
Class 8	33.25	20.97	8.96	2.86	16.51
Class 9	47.50	67.30	79.87	65.59	65.07
Class 10	0.49	0.86	0.64	0.56	0.64
Class 11	1.52	0.93	0.49	1.51	1.11
Class 12	0.51	0.88	0.76	0.67	0.71
Class 13	0.11	0.12	0.13	0.08	0.11
Class 14	0.00	0.00	0	0	0.00
Class 15	25.84	6.84	4.36	6.68	10.93
Total	849.28	1487.64	1614.49	542.14	1123.39
Truck	100.00	100.00	100	100	100.00

*Based on WIM data collected from January to May 2008

Number of Axles Per Truck

Year 2006

Vehicle Type	Single Axle/ Truck	Tandem Axle/ Truck	Tridem Axle/ Truck	Quad Axle/ Truck	# Trucks
Class 4	1.41	0.59	0.00	0.00	7281
Class 5	2.00	0.01	0.00	0.00	81261
Class 6	1.00	1.00	0.00	0.00	18903
Class 7	1.00	0.00	1.00	0.00	9937
Class 8	2.22	0.80	0.00	0.00	16770
Class 9	1.39	1.81	0.00	0.00	359760
Class 10	1.04	1.03	0.97	0.00	3075
Class 11	5.00	0.00	0.00	0.00	8351
Class 12	4.00	1.00	0.00	0.00	3338
Class 13	1.52	0.82	1.00	0.23	312

Table E-2. WIM data for Perry site (cont'd)

Vehicle Class Distribution

<u>Year 2007</u>

Vehicle Type	Single Axle/ Truck	Tandem Axle/ Truck	Tridem Axle/ Truck	Quad Axle/ Truck	# Trucks
Class 4	1.48	0.52	0.00	0.00	6918
Class 5	2.00	0.01	0.00	0.00	75458
Class 6	1.00	1.00	0.00	0.00	17873
Class 7	1.01	0.01	0.99	0.00	7372
Class 8	2.21	0.81	0.00	0.00	13713
Class 9	1.38	1.81	0.00	0.00	317913
Class 10	1.04	1.03	0.97	0.00	2636
Class 11	5.00	0.00	0.00	0.00	7060
Class 12	4.00	1.00	0.00	0.00	3256
Class 13	1.57	0.95	0.96	0.25	317

Vehicle Class Distribution

<u>Year 2008</u>

Vehicle Type	Single Axle/ Truck	Tandem Axle/ Truck	Tridem Axle/ Truck	Quad Axle/ Truck	# Trucks
Class 4	1.48	0.52	0.00	0.00	2796
Class 5	2.01	0.07	0.00	0.00	34609
Class 6	1.00	1.00	0.00	0.00	14503
Class 7	1.01	0.01	0.99	0.00	2681
Class 8	2.25	0.78	0.00	0.00	5377
Class 9	1.42	1.79	0.00	0.00	123997
Class 10	1.07	1.04	0.95	0.00	1065
Class 11	5.00	0.00	0.00	0.00	2887
Class 12	4.00	1.00	0.00	0.00	1292
Class 13	1.32	0.69	1.07	0.28	145

*Based on WIM data collected from January to May 2008

Table E-2. WIM data for Perry site (cont'd)

Monthly Adjustment Factors

<u>Year 2006-Lane 1</u>

Month	Class 4	Class 5	Class 6	Class 7	Class 8	Class 9	Class 10	Class 11	Class 12	Class 13
January	0.63	0.83	0.96	1.06	0.38	1.27	1.45	1.08	1.39	1.13
February	0.62	0.85	0.93	0.85	0.37	1.31	1.17	1.09	1.35	0.95
March	0.71	0.9	0.93	1.19	0.45	1.39	1.47	1.15	1.41	1.3
April	0.79	0.96	1.06	1.5	0.73	1.27	1.44	1.12	1.2	0.85
May	0.86	0.97	1.08	1.96	0.8	1.22	1.3	1.09	1.01	0.96
June	0.76	0.98	1.05	1.5	0.59	1.28	1.32	1.08	1.13	1.21
July	0.93	1.11	1.23	1.08	0.93	1.12	1.39	1.05	1.12	2.22
August	1.64	1.14	0.54	0.16	2.7	0.16	0.13	0.86	0.26	0.69
September	1.8	1.09	0.7	0.15	1.98	0.22	0.11	0.64	0.36	0.2
October	1.44	1.3	1.23	0.73	1.68	0.75	0.52	0.96	0.73	0.76
November	0.87	0.99	1.2	1.01	0.61	1.12	0.89	1.09	1.08	0.8
December	0.93	0.89	1.08	0.83	0.77	0.89	0.81	0.78	0.96	0.93

Monthly Adjustment Factors

<u>Year 2006-Lane 2</u>

Month	Class 4	Class 5	Class 6	Class 7	Class 8	Class 9	Class 10	Class 11	Class 12	Class 13
January	0.78	0.84	0.82	0.64	0.5	0.94	1.17	0.89	0.79	0.43
February	0.69	0.87	0.88	0.94	0.56	0.96	1	1.15	1.1	1.28
March	0.82	0.91	0.81	1.08	0.57	1.03	1.23	0.64	0.82	0.77
April	1	0.99	0.83	1.64	0.83	1.09	1.13	0.86	0.81	0.64
May	1	1.06	0.83	1.23	1.16	1.03	0.97	0.99	1.05	1.96
June	0.89	0.98	0.94	0.69	1.4	0.93	1	0.85	1.04	1.17
July	0.86	1.07	1.14	0.68	1.96	0.91	0.85	0.94	0.92	0.94
August	1.18	1.15	1.04	0.58	1.92	1.03	1.02	1.44	1.25	1.32
September	1.4	1.11	0.82	1.2	1.04	1.08	1.06	1.23	0.97	0.43
October	1.16	1.26	1.47	1.11	0.83	1.09	0.96	1.24	1.02	0.38
November	1.32	0.91	1.56	0.98	0.76	0.96	0.68	0.89	1.23	1.15
December	0.89	0.85	0.85	1.23	0.47	0.93	0.92	0.87	1.02	1.54

Table E-2. WIM data for Perry site (cont'd)

Monthly Adjustment Factors

Year 2006-Lane 3

Month	Class 4	Class 5	Class 6	Class 7	Class 8	Class 9	Class 10	Class 11	Class 12	Class 13
January	0.68	0.86	0.78	0.88	0.75	0.9	0.93	0.77	0.89	0.78
February	0.79	0.78	0.71	0.74	0.9	0.91	0.86	0.52	0.67	0.94
March	0.96	0.92	0.85	0.81	0.9	0.99	1.3	0.68	0.8	0.9
April	1.07	0.98	1.05	1.09	0.97	1.07	1.24	1.02	0.71	1.06
May	1.15	0.95	1.19	0.96	1.33	1.08	1.02	1.17	1.14	1.32
June	1.1	0.97	0.99	0.93	1.29	1.01	0.95	1	1	1.1
July	0.99	1.09	1.01	1.05	1.26	1	1.27	1.43	1.49	1.41
August	1.12	1.08	1.18	1.13	1.14	1.15	1.15	1.1	1.08	1.14
September	1.17	1.25	1.08	0.79	1.06	1.04	0.92	1.13	1.23	0.92
October	1.13	1.38	1.15	1.42	0.98	1.06	0.88	1.1	1.04	1.08
November	1.04	0.99	0.99	1.48	0.82	0.91	0.76	0.8	1.07	0.49
December	0.81	0.75	1.02	0.71	0.61	0.9	0.7	1.27	0.87	0.86

Monthly Adjustment Factors

Year 2006-Lane 4

Month	Class 4	Class 5	Class 6	Class 7	Class 8	Class 9	Class 10	Class 11	Class 12	Class 13
January	0.64	0.85	0.87	0.93	0.97	0.98	1.18	0.94	0.95	0.92
February	0.61	0.91	0.82	1.05	1.02	1.02	1.06	0.97	1.02	0.58
March	0.88	0.94	0.98	0.79	1.08	1.07	1.28	1.08	1.03	0.94
April	1.12	1	1.05	0.91	1.06	1.07	1.12	1.07	1.08	1.31
May	1.3	1.02	1.26	0.93	1.04	1.04	1.15	1.07	0.91	1.66
June	1.13	1.04	1.08	0.92	0.98	1	1.04	0.99	0.88	1.32
July	0.96	1.05	0.95	1.15	0.96	0.96	0.98	1	0.89	1.84
August	0.91	1.17	1.05	1.07	1.07	1.02	1.12	1.03	1.07	0.97
September	1.26	1.13	1.04	0.77	0.98	1	0.75	0.97	0.96	0.61
October	1.23	1.11	1.04	1.46	1.02	1.01	0.82	1.06	1.06	0.57
November	1.05	0.95	0.91	1.38	0.89	0.91	0.74	0.95	1.02	0.68
December	0.91	0.82	0.96	0.64	0.93	0.91	0.75	0.89	1.13	0.62

Table E-2. WIM data for Perry site (cont'd)

Monthly Adjustment Factors

Year 2007-Lane 1

Month	Class 4	Class 5	Class 6	Class 7	Class 8	Class 9	Class 10	Class 11	Class 12	Class 13
January	0.77	0.84	1.09	0.7	0.75	0.74	0.66	0.72	0.8	0.85
February	0.55	0.58	0.8	0.33	0.51	0.51	0.51	0.5	0.56	0.71
March	0.62	0.98	1.25	0.94	0.67	1.18	1.11	1.13	1.04	0.91
April	0.7	1.06	1.35	1.45	0.71	1.24	1.07	1.11	1.09	1.11
May	1.77	1.01	0.94	1.24	0.96	1.07	1.07	0.94	1.13	0.85
June	1.34	1.05	1.02	1.14	1.21	1.08	1.14	1.08	1.13	1.66
July	0.53	1.06	0.96	1.65	1.01	1.25	1.43	1.32	1.1	0.93
August	0.51	1.05	0.97	1.36	1.01	1.29	1.42	1.3	1.35	1.67
September	0.68	1.23	1.06	1.2	0.99	1.25	1.32	1.23	1.21	1.28
October	1.16	1.25	0.92	0.78	1.41	1.04	0.99	1.21	1.14	0.88
November	2.37	0.9	0.64	0.21	1.76	0.36	0.29	0.46	0.45	0.16
December	N.A.	N.A.	N.A.	N.A.	N.A.	N.A.	N.A.	N.A.	N.A.	N.A.

Monthly Adjustment Factors

Year 2007-Lane 2

Month	Class 4	Class 5	Class 6	Class 7	Class 8	Class 9	Class 10	Class 11	Class 12	Class 13
January	0.65	0.87	1.01	0.76	0.4	0.95	1.08	0.95	0.9	0.58
February	0.68	0.84	0.88	0.71	0.43	0.93	0.9	0.89	0.72	0.7
March	0.71	0.85	1.03	0.71	0.49	1.05	1.11	1.35	1.12	0.58
April	0.81	0.86	1.03	1.05	0.53	1.04	0.86	0.87	0.76	1.27
May	1.29	0.98	1.05	1.17	1.11	1.07	1.07	0.86	1.13	0.69
June	1.25	0.95	1.02	1.24	1.19	1.06	0.96	0.96	1.09	1.28
July	1.17	0.98	0.85	1.5	1.17	1.02	0.84	0.72	1.03	1.53
August	1.05	1.13	1.02	1.16	1.38	1.09	1.1	0.86	1.09	0.77
September	0.96	1.2	1.08	1.04	1.3	1.06	1.1	1.29	1.16	1.34
October	1.19	1.37	1.06	1.15	1.47	1.06	1.29	1.34	1.08	1.11
November	1.23	0.96	0.96	0.5	1.52	0.68	0.67	0.91	0.93	1.15
December	N.A.	N.A.	N.A.	N.A.	N.A.	N.A.	N.A.	N.A.	N.A.	N.A.

Table E-2. WIM data for Perry site (cont'd)

Monthly Adjustment Factors

Year 2007-Lane 3

Month	Class 4	Class 5	Class 6	Class 7	Class 8	Class 9	Class 10	Class 11	Class 12	Class 13
January	0.61	0.71	0.76	0.93	0.71	0.85	0.67	0.83	0.59	0.9
February	0.73	0.61	0.75	0.79	0.56	0.9	1.12	0.44	0.78	0.83
March	0.91	0.81	0.91	1.14	0.55	0.99	0.87	1.23	0.82	0.88
April	0.77	0.91	1	1.28	0.8	0.99	0.63	0.84	0.85	1.12
May	1.21	0.95	1.2	1.2	1	1.11	0.9	1	1.07	1.4
June	1.11	1	1.16	1.28	0.98	1.14	1.33	1.62	1.18	1.14
July	1.01	0.97	1.18	0.83	1.33	1.01	1.24	0.93	0.99	0.99
August	1.16	1.23	1.12	0.95	1.34	1.11	0.74	1.05	1.28	1.29
September	1.05	1.31	1.08	0.85	1.38	0.99	1.35	1.37	1.13	0.91
October	1.37	1.48	0.9	0.87	1.39	1.07	1.28	1.08	1.25	0.82
November	1.07	1.03	0.93	0.88	0.96	0.83	0.88	0.63	1.04	0.72
December	N.A.	N.A.	N.A.	N.A.	N.A.	N.A.	N.A.	N.A.	N.A.	N.A.

Monthly Adjustment Factors

Year 2007-Lane 4

Month	Class 4	Class 5	Class 6	Class 7	Class 8	Class 9	Class 10	Class 11	Class 12	Class 13
January	0.82	0.8	0.84	0.86	1.03	0.97	0.93	0.94	1.04	0.68
February	0.8	0.8	0.74	0.8	0.88	0.88	0.78	0.83	0.76	0.57
March	0.91	0.87	0.92	0.9	1.07	1.03	0.91	1.01	0.94	0.75
April	1.11	0.94	1.02	1.08	1.01	1.04	0.96	1.02	0.93	0.86
May	1.14	1.01	1.08	1.07	1.03	1.06	1.08	1.06	1.03	1.26
June	0.97	1.09	1.2	1.14	1.08	1.06	1.21	1.11	1.14	2.36
July	0.93	1.07	1.16	1.01	1.05	1	1.11	1.09	0.97	0.96
August	0.89	1.16	1.16	0.9	1.04	1.03	1.11	1.02	1.07	0.87
September	1.21	1.16	1.06	1.15	0.96	1.02	1.11	0.94	0.98	1.17
October	1.26	1.17	1	1.03	1.06	1.04	1.02	1.09	1.11	0.82
November	0.95	0.94	0.83	1.07	0.79	0.87	0.8	0.89	1.02	0.7
December	N.A.	N.A.	N.A.	N.A.	N.A.	N.A.	N.A.	N.A.	N.A.	N.A.

Table E-2. WIM data for Perry site (cont'd)

Single Axle Load Distributions for various FHWA Vehicle Classes

Axle Weight	4	5	6	7	8	9	10	11	12	13
3000	0.0	3.0	0.0	0.2	0.6	2.3	0.3	0.3	0.6	18.4
4000	0.1	22.7	0.2	0.0	1.0	3.6	0.4	1.5	3.4	4.5
5000	0.2	18.6	0.4	0.0	2.1	1.9	0.3	7.5	12.8	2.6
6000	0.9	8.7	0.7	0.1	2.9	1.2	0.5	5.5	13.9	2.8
7000	6.3	10.3	1.1	0.2	6.1	0.9	1.0	3.1	3.2	3.6
8000	10.0	9.3	3.1	0.4	11.6	1.4	2.8	4.3	4.5	4.2
9000	7.8	7.3	8.5	0.7	19.1	4.8	9.3	6.9	7.7	6.7
10000	9.9	5.2	17.9	1.6	20.1	15.1	27.8	14.9	13.6	9.5
11000	13.7	4.0	24.4	2.8	10.4	29.4	31.4	13.8	12.9	14.8
12000	13.1	2.8	19.2	4.5	6.2	20.2	17.9	8.2	10.5	11.5
13000	11.4	1.9	10.0	6.9	4.1	4.3	5.0	7.3	7.6	6.0
14000	8.8	1.6	5.5	10.1	3.4	1.5	2.0	6.7	4.7	5.0
15000	6.9	1.2	3.7	13.8	3.0	2.0	0.7	5.7	2.1	1.8
16000	4.1	0.8	2.0	13.6	2.6	2.9	0.2	5.0	1.3	3.5
17000	1.7	0.7	1.0	12.0	1.9	3.3	0.2	3.7	0.7	1.2
18000	1.5	0.5	0.6	10.0	1.5	2.5	0.2	2.7	0.3	0.7
19000	1.4	0.4	0.5	9.8	1.2	1.5	0.1	1.8	0.2	1.2
20000	0.7	0.3	0.3	8.2	0.7	0.7	0.0	0.8	0.0	0.4
21000	0.6	0.3	0.3	3.1	0.5	0.3	0.0	0.3	0.0	0.1
22000	0.4	0.2	0.2	1.4	0.3	0.1	0.0	0.1	0.0	0.2
23000	0.3	0.1	0.2	0.6	0.1	0.1	0.0	0.1	0.0	0.4
24000	0.1	0.1	0.1	0.1	0.1	0.0	0.0	0.0	0.0	0.0
25000	0.1	0.0	0.1	0.0	0.0	0.0	0.0	0.0	0.0	0.3
26000	0.0	0.0	0.0	0.0	0.0	0.0	0.0	0.0	0.0	0.2
27000	0.0	0.0	0.0	0.0	0.0	0.0	0.0	0.0	0.0	0.0
28000	0.0	0.0	0.0	0.0	0.0	0.0	0.0	0.0	0.0	0.0
29000	0.0	0.0	0.0	0.0	0.0	0.0	0.0	0.0	0.0	0.0
30000	0.0	0.0	0.0	0.0	0.0	0.0	0.0	0.0	0.0	0.0
31000	0.0	0.0	0.0	0.0	0.0	0.0	0.0	0.0	0.0	0.0
32000	0.0	0.0	0.0	0.0	0.0	0.0	0.0	0.0	0.0	0.2
33000	0.0	0.0	0.0	0.0	0.0	0.0	0.0	0.0	0.0	0.2
34000	0.0	0.0	0.0	0.0	0.0	0.0	0.0	0.0	0.0	0.0
35000	0.0	0.0	0.0	0.0	0.0	0.0	0.0	0.0	0.0	0.3
36000	0.0	0.0	0.0	0.0	0.0	0.0	0.0	0.0	0.0	0.0
37000	0.0	0.0	0.0	0.0	0.0	0.0	0.0	0.0	0.0	0.2
38000	0.0	0.0	0.0	0.0	0.0	0.0	0.0	0.0	0.0	0.0
39000	0.0	0.0	0.0	0.0	0.0	0.0	0.0	0.0	0.0	0.0
40000	0.0	0.0	0.0	0.0	0.0	0.0	0.0	0.0	0.0	0.0
41000	0.0	0.0	0.0	0.0	0.0	0.0	0.0	0.0	0.0	0.0

Tandem Axle Load Distributions for various FHWA Vehicle Classes

Axle Weight	4	5	6	7	8	9	10	11	12	13
6000	0.0	84.2	5.2	1.5	2.5	1.2	0.2	N.A.	0.1	3.2
8000	0.0	15.0	22.6	16.4	6.9	4.3	0.4	N.A.	0.7	4.5
10000	0.5	0.8	7.8	27.0	18.0	9.9	2.1	N.A.	5.9	6.7
12000	0.8	0.0	6.8	7.6	21.8	11.2	5.9	N.A.	18.1	7.2
14000	2.3	0.0	8.3	0.0	17.3	7.2	6.0	N.A.	5.7	5.6
16000	1.4	0.0	7.6	0.0	10.0	4.8	7.4	N.A.	10.7	3.6
18000	3.1	0.0	7.3	0.0	7.1	4.6	6.8	N.A.	26.4	5.2
20000	6.7	0.0	6.6	1.8	5.7	4.8	4.8	N.A.	21.6	4.9
22000	12.3	0.0	5.1	0.0	3.9	4.4	5.1	N.A.	8.0	5.8
24000	11.5	0.0	4.2	6.1	3.0	4.4	5.8	N.A.	2.2	2.4
26000	13.7	0.0	3.3	4.1	1.7	4.7	10.3	N.A.	0.6	4.4
28000	15.5	0.0	2.4	11.2	0.8	6.1	11.4	N.A.	0.0	4.5
30000	14.4	0.0	2.5	2.3	0.5	8.8	12.2	N.A.	0.0	4.5
32000	10.9	0.0	2.3	0.0	0.3	10.9	8.1	N.A.	0.0	6.6
34000	5.7	0.0	1.8	3.0	0.2	8.1	3.8	N.A.	0.0	8.2
36000	0.9	0.0	1.5	13.5	0.1	3.3	2.2	N.A.	0.0	6.9
38000	0.2	0.0	1.5	0.0	0.1	1.0	2.3	N.A.	0.0	6.5
40000	0.1	0.0	1.0	3.8	0.1	0.3	1.5	N.A.	0.0	3.2
42000	0.0	0.0	0.8	0.0	0.1	0.1	1.4	N.A.	0.0	1.9
44000	0.0	0.0	0.6	0.0	0.0	0.0	0.6	N.A.	0.0	1.7
46000	0.1	0.0	0.3	1.8	0.0	0.0	0.6	N.A.	0.0	0.5
48000	0.0	0.0	0.1	0.0	0.0	0.0	0.4	N.A.	0.0	1.0
50000	0.0	0.0	0.2	0.0	0.0	0.0	0.2	N.A.	0.0	0.0
52000	0.0	0.0	0.1	0.0	0.0	0.0	0.2	N.A.	0.0	0.0
54000	0.0	0.0	0.1	0.0	0.0	0.0	0.1	N.A.	0.0	0.0
56000	0.0	0.0	0.0	0.0	0.0	0.0	0.1	N.A.	0.0	0.5
58000	0.0	0.0	0.0	0.0	0.0	0.0	0.0	N.A.	0.0	0.5
60000	0.0	0.0	0.0	0.0	0.0	0.0	0.0	N.A.	0.0	0.0
62000	0.0	0.0	0.0	0.0	0.0	0.0	0.0	N.A.	0.0	0.0
64000	0.0	0.0	0.0	0.0	0.0	0.0	0.0	N.A.	0.0	0.0
66000	0.0	0.0	0.0	0.0	0.0	0.0	0.0	N.A.	0.0	0.0
68000	0.0	0.0	0.0	0.0	0.0	0.0	0.0	N.A.	0.0	0.0
70000	0.0	0.0	0.0	0.0	0.0	0.0	0.0	N.A.	0.0	0.0
72000	0.0	0.0	0.0	0.0	0.0	0.0	0.0	N.A.	0.0	0.0
74000	0.0	0.0	0.0	0.0	0.0	0.0	0.0	N.A.	0.0	0.0
76000	0.0	0.0	0.0	0.0	0.0	0.0	0.0	N.A.	0.0	0.0
78000	0.0	0.0	0.0	0.0	0.0	0.0	0.0	N.A.	0.0	0.0
80000	0.0	0.0	0.0	0.0	0.0	0.0	0.0	N.A.	0.0	0.0
82000	0.0	0.0	0.0	0.0	0.0	0.0	0.0	N.A.	0.0	0.0

Table E-2. WIM data for Perry site (cont'd)

Tridem Axle Load Distributions for various FHWA Vehicle Classes

Axle Weight	4	5	6	7	8	9	10	11	12	13
12000	N.A.	N.A.	N.A.	100	N.A.	N.A.	100	N.A.	N.A.	100
15000	N.A.	N.A.	N.A.	0.1	N.A.	N.A.	13.8	N.A.	N.A.	1.8
18000	N.A.	N.A.	N.A.	0.2	N.A.	N.A.	10.1	N.A.	N.A.	1.3
21000	N.A.	N.A.	N.A.	0.2	N.A.	N.A.	3.8	N.A.	N.A.	2.2
24000	N.A.	N.A.	N.A.	0.2	N.A.	N.A.	3.3	N.A.	N.A.	0.9
27000	N.A.	N.A.	N.A.	0.4	N.A.	N.A.	4.0	N.A.	N.A.	1.3
30000	N.A.	N.A.	N.A.	0.5	N.A.	N.A.	4.3	N.A.	N.A.	1.2
33000	N.A.	N.A.	N.A.	0.8	N.A.	N.A.	5.2	N.A.	N.A.	2.8
36000	N.A.	N.A.	N.A.	1.0	N.A.	N.A.	7.7	N.A.	N.A.	1.4
39000	N.A.	N.A.	N.A.	1.4	N.A.	N.A.	13.6	N.A.	N.A.	3.8
42000	N.A.	N.A.	N.A.	1.6	N.A.	N.A.	16.1	N.A.	N.A.	6.8
45000	N.A.	N.A.	N.A.	2.8	N.A.	N.A.	7.8	N.A.	N.A.	7.0
48000	N.A.	N.A.	N.A.	3.8	N.A.	N.A.	3.2	N.A.	N.A.	10.2
51000	N.A.	N.A.	N.A.	7.6	N.A.	N.A.	2.2	N.A.	N.A.	11.8
54000	N.A.	N.A.	N.A.	15.7	N.A.	N.A.	2.2	N.A.	N.A.	11.6
57000	N.A.	N.A.	N.A.	23.0	N.A.	N.A.	1.0	N.A.	N.A.	11.5
60000	N.A.	N.A.	N.A.	24.7	N.A.	N.A.	0.7	N.A.	N.A.	8.2
63000	N.A.	N.A.	N.A.	12.8	N.A.	N.A.	0.4	N.A.	N.A.	7.1
66000	N.A.	N.A.	N.A.	2.9	N.A.	N.A.	0.3	N.A.	N.A.	6.0
69000	N.A.	N.A.	N.A.	0.4	N.A.	N.A.	0.0	N.A.	N.A.	2.1
72000	N.A.	N.A.	N.A.	0.0	N.A.	N.A.	0.0	N.A.	N.A.	1.0
75000	N.A.	N.A.	N.A.	0.0	N.A.	N.A.	0.0	N.A.	N.A.	0.0
78000	N.A.	N.A.	N.A.	0.0	N.A.	N.A.	0.0	N.A.	N.A.	0.0
81000	N.A.	N.A.	N.A.	0.0	N.A.	N.A.	0.0	N.A.	N.A.	0.0
84000	N.A.	N.A.	N.A.	0.0	N.A.	N.A.	0.0	N.A.	N.A.	0.0
87000	N.A.	N.A.	N.A.	0.0	N.A.	N.A.	0.0	N.A.	N.A.	0.0
90000	N.A.	N.A.	N.A.	0.0	N.A.	N.A.	0.0	N.A.	N.A.	0.0
93000	N.A.	N.A.	N.A.	0.0	N.A.	N.A.	0.0	N.A.	N.A.	0.0
96000	N.A.	N.A.	N.A.	0.0	N.A.	N.A.	0.0	N.A.	N.A.	0.0
99000	N.A.	N.A.	N.A.	0.0	N.A.	N.A.	0.0	N.A.	N.A.	0.0
102000	N.A.	N.A.	N.A.	0.0	N.A.	N.A.	0.0	N.A.	N.A.	0.0
105000	N.A.	N.A.	N.A.	0.0	N.A.	N.A.	0.0	N.A.	N.A.	0.0

Table E-2. WIM data for Perry site (cont'd)

Quad Axle Load Distributions for various FHWA Vehicle Classes

Axle Weight	4	5	6	7	8	9	10	11	12	13
12000	N.A.	N.A.	N.A.	N.A.	N.A.	100	N.A.	N.A.	N.A.	100
15000	N.A.	N.A.	N.A.	N.A.	N.A.	0.0	N.A.	N.A.	N.A.	4.2
18000	N.A.	N.A.	N.A.	N.A.	N.A.	0.0	N.A.	N.A.	N.A.	18.7
21000	N.A.	N.A.	N.A.	N.A.	N.A.	0.0	N.A.	N.A.	N.A.	19.5
24000	N.A.	N.A.	N.A.	N.A.	N.A.	0.0	N.A.	N.A.	N.A.	9.4
27000	N.A.	N.A.	N.A.	N.A.	N.A.	0.0	N.A.	N.A.	N.A.	1.8
30000	N.A.	N.A.	N.A.	N.A.	N.A.	0.0	N.A.	N.A.	N.A.	0.8
33000	N.A.	N.A.	N.A.	N.A.	N.A.	0.0	N.A.	N.A.	N.A.	0.0
36000	N.A.	N.A.	N.A.	N.A.	N.A.	0.0	N.A.	N.A.	N.A.	0.0
39000	N.A.	N.A.	N.A.	N.A.	N.A.	0.0	N.A.	N.A.	N.A.	0.0
42000	N.A.	N.A.	N.A.	N.A.	N.A.	0.0	N.A.	N.A.	N.A.	1.8
45000	N.A.	N.A.	N.A.	N.A.	N.A.	0.0	N.A.	N.A.	N.A.	3.3
48000	N.A.	N.A.	N.A.	N.A.	N.A.	0.0	N.A.	N.A.	N.A.	1.3
51000	N.A.	N.A.	N.A.	N.A.	N.A.	0.0	N.A.	N.A.	N.A.	0.0
54000	N.A.	N.A.	N.A.	N.A.	N.A.	0.0	N.A.	N.A.	N.A.	0.8
57000	N.A.	N.A.	N.A.	N.A.	N.A.	0.0	N.A.	N.A.	N.A.	2.3
60000	N.A.	N.A.	N.A.	N.A.	N.A.	0.0	N.A.	N.A.	N.A.	3.9
63000	N.A.	N.A.	N.A.	N.A.	N.A.	0.0	N.A.	N.A.	N.A.	3.9
66000	N.A.	N.A.	N.A.	N.A.	N.A.	0.0	N.A.	N.A.	N.A.	5.0
69000	N.A.	N.A.	N.A.	N.A.	N.A.	0.0	N.A.	N.A.	N.A.	2.4
72000	N.A.	N.A.	N.A.	N.A.	N.A.	0.0	N.A.	N.A.	N.A.	3.6
75000	N.A.	N.A.	N.A.	N.A.	N.A.	0.0	N.A.	N.A.	N.A.	5.2
78000	N.A.	N.A.	N.A.	N.A.	N.A.	0.0	N.A.	N.A.	N.A.	2.0
81000	N.A.	N.A.	N.A.	N.A.	N.A.	16.7	N.A.	N.A.	N.A.	5.8
84000	N.A.	N.A.	N.A.	N.A.	N.A.	0.0	N.A.	N.A.	N.A.	2.0
87000	N.A.	N.A.	N.A.	N.A.	N.A.	16.7	N.A.	N.A.	N.A.	2.1
90000	N.A.	N.A.	N.A.	N.A.	N.A.	0.0	N.A.	N.A.	N.A.	0.0
93000	N.A.	N.A.	N.A.	N.A.	N.A.	0.0	N.A.	N.A.	N.A.	0.0
96000	N.A.	N.A.	N.A.	N.A.	N.A.	0.0	N.A.	N.A.	N.A.	0.0
99000	N.A.	N.A.	N.A.	N.A.	N.A.	0.0	N.A.	N.A.	N.A.	0.0
102000	N.A.	N.A.	N.A.	N.A.	N.A.	50.0	N.A.	N.A.	N.A.	0.0
105000	N.A.	N.A.	N.A.	N.A.	N.A.	16.7	N.A.	N.A.	N.A.	0.0

Table E-2. WIM data for Perry site (cont'd)

Hourly Truck Distribution

<u>Year 2006</u>

Hour	Percent Trucks			
	Lane 1	Lane 2	Lane 3	Lane 4
0	3.14	2.26	0.67	1.81
1	2.72	2.36	0.48	1.74
2	3.11	3.00	0.48	1.87
3	3.56	3.44	0.66	2.20
4	3.88	4.75	0.77	2.57
5	3.91	6.49	1.39	3.46
6	4.16	7.83	2.36	4.02
7	4.56	6.94	2.63	4.42
8	5.15	5.75	4.13	5.19
9	5.25	5.40	5.57	5.76
10	5.07	5.06	6.60	6.13
11	5.08	5.05	6.92	6.43
12	4.98	4.90	7.26	6.45
13	4.79	4.67	7.76	6.45
14	4.58	4.22	8.55	6.42
15	4.13	3.82	8.70	5.75
16	3.91	3.10	8.83	5.25
17	4.04	3.48	7.96	4.81
18	4.32	3.20	5.60	4.37
19	4.19	3.03	4.04	3.85
20	3.97	3.15	3.24	3.32
21	4.09	3.19	2.50	3.00
22	3.92	2.67	1.81	2.65
23	3.49	2.24	1.10	2.08

Table E-2. WIM data for Perry site (cont'd)

Hourly Truck Distribution

<u>Year 2007</u>

Hour	Percent Trucks			
	Lane 1	Lane 2	Lane 3	Lane 4
0	2.90	2.55	0.68	1.73
1	2.58	2.35	0.46	1.70
2	2.71	2.89	0.50	1.80
3	3.20	3.93	0.60	2.22
4	3.38	4.72	0.82	2.65
5	3.65	6.32	1.49	3.54
6	3.88	7.50	2.16	4.06
7	4.20	6.71	2.63	4.31
8	5.00	5.52	4.29	5.12
9	5.38	5.13	5.38	5.68
10	5.28	4.97	6.57	6.16
11	5.43	4.96	6.82	6.57
12	5.32	4.80	7.39	6.58
13	5.19	4.78	7.98	6.49
14	4.96	4.28	8.73	6.36
15	4.55	3.86	8.77	5.80
16	4.30	3.33	8.66	5.19
17	4.26	3.39	7.51	4.72
18	4.45	3.43	5.70	4.45
19	4.27	3.10	4.08	3.89
20	4.13	3.10	3.30	3.32
21	3.86	3.03	2.58	3.01
22	3.76	2.70	1.80	2.60
23	3.34	2.65	1.09	2.07

Table E-2. WIM data for Perry site (cont'd)

Hourly Truck Distribution

Year 2008

Hour	Percent Trucks			
	Lane 1	Lane 2	Lane 3	Lane 4
0	3.30	2.31	0.53	1.64
1	2.97	2.55	0.54	1.59
2	3.14	2.93	0.39	1.67
3	3.52	3.82	0.49	2.14
4	3.84	4.56	0.63	2.62
5	3.91	6.51	1.31	3.37
6	4.13	7.90	1.93	4.18
7	4.19	7.18	2.62	4.47
8	4.73	6.09	3.95	5.20
9	5.02	5.31	4.65	5.64
10	5.06	5.09	5.76	5.92
11	5.06	5.04	6.94	6.51
12	5.14	4.87	7.08	6.66
13	4.86	4.48	8.25	6.66
14	4.61	3.89	8.63	6.47
15	4.26	3.48	9.94	5.90
16	4.15	3.09	9.16	5.34
17	4.04	2.90	9.08	4.76
18	4.39	3.54	6.58	4.54
19	4.39	3.09	3.86	3.94
20	4.13	3.20	2.98	3.44
21	4.00	2.86	2.26	2.86
22	3.64	2.61	1.31	2.48
23	3.52	2.68	1.11	1.98

*Based on WIM data collected from January to May 2008

Table E-2. WIM data for Perry site (cont'd)

Average Speed, Gross Weight and Length of Trucks

Month	Average Speed, mph	Gross Weight (kips)	Length (ft)
Jan-06	66.35	47.20	56.13
Feb-06	66.24	47.56	56.00
Mar-06	66.65	47.64	56.24
Apr-06	67.03	47.88	56.16
May-06	67.05	47.62	55.61
Jun-06	66.93	47.83	55.61
Jul-06	66.97	47.65	55.28
Aug-06	67.00	47.38	55.08
Sep-06	66.70	46.25	55.12
Oct-06	66.61	46.64	55.16
Nov-06	66.90	46.02	55.39
Dec-06	66.78	45.65	56.36
Jan-07	66.51	46.32	56.69
Feb-07	65.76	46.83	55.92
Mar-07	66.61	46.97	56.61
Apr-07	66.70	46.51	56.14
May-07	66.86	47.46	55.82
Jun-07	66.85	47.31	55.50
Jul-07	66.95	47.03	55.44
Aug-07	66.78	46.55	55.06
Sep-07	66.60	46.52	54.88
Oct-07	66.46	46.29	55.43
Nov-07	66.42	45.87	55.58
Dec-07	N.A.	N.A.	N.A.
Jan-08	66.37	45.17	52.98
Feb-08	65.55	44.76	52.92
Mar-08	66.32	45.15	52.92
Apr-08	66.28	45.29	52.45
May-08	65.85	44.99	52.24

Table E-2. WIM data for Perry site (cont'd)

Wheelbase of Vehicles

Distance (ft)	Percent
0	0.0319%
2	0.0019%
4	1.1752%
6	0.2028%
8	0.0644%
10	1.5345%
12	11.7082%
14	12.9706%
16	22.6306%
18	33.3571%
20	14.8284%
22	1.1820%
24	0.2496%
26	0.0443%
28	0.0072%
30	0.0028%
32	0.0033%
34	0.0017%
36	0.0008%
38	0.0008%
40	0.0019%

Lane Information

Site	Lane Number	Direction	Lane
Blair	Lane 1	South	Travel
	Lane 2	South	Passing
	Lane 3	North	Passing
	Lane 4	North	Travel

Table E-3. WIM data for Blair site

Annual Average Daily Traffic

Year	AASHTO Method			
	Lane 1	Lane 2	Lane 3	Lane 4
2004	5609	2711	3356	4920
2005	5894	2623	3560	4866
2006	5980	2735	3751	4932
2007	6049	2718	3824	4925

Year	Simple Method			
	Lane 1	Lane 2	Lane 3	Lane 4
2004	5635	2695	3362	4920
2005	5911	2635	3576	4873
2006	5982	2738	3754	4943
2007	6059	2729	3834	4937

Annual Average Daily Truck Traffic

Year	AASHTO Method			
	Lane 1	Lane 2	Lane 3	Lane 4
2004	172	78	103	88
2005	141	56	81	122
2006	118	40	66	134
2007	70	12	27	137

Year	Simple Method			
	Lane 1	Lane 2	Lane 3	Lane 4
2004	177	84	109	89
2005	144	59	84	123
2006	120	43	70	133
2007	70	13	27	137

Traffic Volume in 2008

Parameter	Method	Year	Lane 1	Lane 2	Lane 3	Lane 4
AADT	AASHTO	2008	5962	2631	3781	4755
AADT	Simple	2008	6000	2675	3826	4793
AADTT	AASHTO	2008	72	N.A.	33	131
AADTT	Simple	2008	73	N.A.	33	131

*Based on WIM data collected from January to May 2008

Table E-3. WIM data for Blair site (cont'd)

Vehicle Class Distribution

<u>Year 2006</u>

Vehicle	Lane 1	Lane 2	Lane 3	Lane 4	Average
Class 4	5.84	5.91	10.75	3.75	6.56
Class 5	30.45	23.94	29.06	63.32	36.69
Class 6	11.21	6.11	6.39	7.18	7.72
Class 7	1.83	0.11	0.22	0.39	0.64
Class 8	16.18	9.45	6.72	7.46	9.95
Class 9	22.09	17.18	9.72	17.53	16.63
Class 10	0.41	0.05	0.32	0.17	0.24
Class 11	0.09	0.19	0.06	0.13	0.12
Class 12	0.11	0.09	0.03	0.05	0.07
Class 13	11.78	36.97	36.75	0.03	21.38
Class 14	3.38	10.65	7.83	0	5.47
Class 15	1.16	8.66	4.21	5.84	4.97
Total	5078	6801	5690	3693	5315
Truck	100	100	100	100	100

Vehicle Class Distribution

<u>Year 2007</u>

Vehicle	Lane 1	Lane 2	Lane 3	Lane 4	Average
Class 4	11.11	12.87	31.24	3.22	14.61
Class 5	0.13	0.07	0.06	66.31	16.64
Class 6	20.29	17.74	19.43	7.34	16.20
Class 7	3.04	0.7	1.64	0.3	1.42
Class 8	26.61	26.93	19.61	7.09	20.06
Class 9	37.71	41.07	27.44	15.43	30.41
Class 10	0.69	0.15	0.52	0.2	0.39
Class 11	0.21	0.37	0.04	0.07	0.17
Class 12	0.07	0.05	0	0.02	0.04
Class 13	0.14	0.04	0.02	0.02	0.06
Class 14	0	0	0	0	0.00
Class 15	2.89	20.1	9.26	5.56	9.45
Total	8697	22378	14010	3606	12173
Truck	100	100	100	100	100

Table E-3. WIM data for Blair site (cont'd)

Vehicle Class Distribution

Year 2008

Vehicle	Lane 1	Lane 2	Lane 3	Lane 4	Average
Class 4	13.55	N.A.	36.67	3.35	17.86
Class 5	0.01	N.A.	0.09	65.21	21.77
Class 6	20.43	N.A.	19.48	7.52	15.81
Class 7	1.83	N.A.	0.43	0.28	0.85
Class 8	26.27	N.A.	15.92	7.97	16.72
Class 9	36.78	N.A.	26.5	15.33	26.20
Class 10	0.86	N.A.	0.73	0.19	0.59
Class 11	0.17	N.A.	0	0.14	0.10
Class 12	0.08	N.A.	0	0.01	0.03
Class 13	0.01	N.A.	0.19	0.01	0.07
Class 14	0	N.A.	0	0	0.00
Class 15	1.65	N.A.	6.52	4.83	4.33
Total	8306	N.A.	411	30	2916
Truck	100	N.A.	100	100	100

*Based on WIM data collected from January to May 2008

Number of Axles Per Truck

Year 2006

Vehicle Type	Single Axle/ Truck	Tandem Axle/ Truck	Tridem Axle/ Truck	Quad Axle/ Truck	# Trucks
Class 4	1.83	0.17	0.00	0.00	1559
Class 5	2.00	0.00	0.00	0.00	24361
Class 6	1.00	1.00	0.00	0.00	3104
Class 7	1.03	0.03	0.97	0.00	162
Class 8	2.41	0.59	0.00	0.00	3205
Class 9	1.11	1.95	0.00	0.00	7488
Class 10	1.00	1.00	1.00	0.00	72
Class 11	5.00	0.00	0.00	0.00	32
Class 12	4.00	1.00	0.00	0.00	19
Class 13	1.70	1.10	0.50	0.40	10

Table E-3. WIM data for Blair site (cont'd)

Number of Axles Per Truck

Year 2007

Vehicle Type	Single Axle/ Truck	Tandem Axle/ Truck	Tridem Axle/ Truck	Quad Axle/ Truck	# Trucks
Class 4	1.82	0.18	0.00	0.00	1389
Class 5	2.00	0.01	0.00	0.00	28517
Class 6	1.00	1.00	0.00	0.00	3215
Class 7	1.04	0.04	0.96	0.00	136
Class 8	2.35	0.66	0.00	0.00	3077
Class 9	1.15	1.93	0.00	0.00	6674
Class 10	1.03	1.03	0.97	0.00	88
Class 11	5.00	0.00	0.00	0.00	30
Class 12	4.00	1.00	0.00	0.00	10
Class 13	1.38	1.13	1.25	0.13	8

Number of Axles Per Truck

Year 2008

Vehicle Type	Single Axle/ Truck	Tandem Axle/ Truck	Tridem Axle/ Truck	Quad Axle/ Truck	# Trucks
Class 4	1.81	0.19	0.00	0.00	393
Class 5	2.00	0.01	0.00	0.00	7845
Class 6	1.00	1.00	0.00	0.00	979
Class 7	1.03	0.03	0.97	0.00	32
Class 8	2.28	0.72	0.00	0.00	970
Class 9	1.14	1.93	0.00	0.00	1914
Class 10	1.05	1.05	0.95	0.00	22
Class 11	5.00	0.00	0.00	0.00	13
Class 12	4.00	1.00	0.00	0.00	1
Class 13	1.00	0.50	1.00	0.50	2

*Based on WIM data collected from January to May 2008

Table E-3. WIM data for Blair site (cont'd)

Monthly Adjustment Factors

Year 2006-Lane 1

Month	Class 4	Class 5	Class 6	Class 7	Class 8	Class 9	Class 10	Class 11	Class 12	Class 13
January	1.18	1.26	0.93	0.44	0.71	0.92	0.67	0	0.28	0
February	1.23	1.23	0.99	0.61	0.94	0.95	0.89	1.29	1.93	0
March	1.19	1.21	0.94	1.11	0.92	0.94	0.84	1.23	2.64	4.08
April	1.16	1.26	1.08	1.29	1.1	1.01	1.56	2.78	0.5	0
May	1.19	1.27	1.13	1.85	1.09	0.91	1.94	0.32	1.38	0.46
June	0.53	1.11	1.13	1.92	1.16	1.09	1.79	1.27	0.5	2.11
July	0.28	1	1.23	1.01	1.08	0.98	0.77	0	0.22	0
August	0.45	1.1	0.99	1	1.1	1.01	0.76	1.42	2.92	5.34
September	1.3	1.24	0.99	1.21	1.14	1.02	0.81	1.29	1.38	0.01
October	1.27	1.31	1	0.71	1.03	1.19	0.64	0.43	0	0
November	1.13	0	0.81	0.55	0.92	1.05	1.04	1.29	0	0
December	1.11	0	0.78	0.31	0.79	0.92	0.3	0.65	0.28	0.01

Monthly Adjustment Factors

Year 2006-Lane 2

Month	Class 4	Class 5	Class 6	Class 7	Class 8	Class 9	Class 10	Class 11	Class 12	Class 13
January	0.64	0.95	0.92	0.8	0.83	0.81	0	0	1.3	0
February	1.02	0.94	0.89	1.6	1.05	0.91	0	0.46	0	0
March	0.98	1.2	0.96	0	0.93	0.86	0	2.12	1.56	3.37
April	1	1.09	1.12	0.8	1.12	1.05	0	0.92	0	0
May	1.04	1.27	1.05	0	1.23	1.04	0	2.22	2.34	1.08
June	1.09	1.12	0.95	0.8	1.26	1.07	1.89	0.92	0.78	2.42
July	1.01	1.35	1.02	0	1.04	0.93	0	0.46	0.97	0
August	0.97	1.43	1.07	0.8	1.06	1.1	1.89	3.05	3.11	5.12
September	1.31	1.28	1.26	1.6	1.03	1.12	1.89	0.92	0.97	0
October	1.16	1.37	1.15	3.2	0.91	1.03	3.79	0	0	0
November	0.88	0	0.68	0	0.81	1.13	2.53	0	0	0
December	0.9	0	0.93	2.4	0.71	0.95	0	0.92	0.97	0

Table E-3. WIM data for Blair site (cont'd)

Monthly Adjustment Factors

Year 2006-Lane 3

Month	Class 4	Class 5	Class 6	Class 7	Class 8	Class 9	Class 10	Class 11	Class 12	Class 13
January	1.1	1.04	0.99	0.66	0.68	0.93	0	0	0	0
February	1.21	1.19	1.07	0.75	0.8	1.03	0.85	0	0	0
March	1.3	1.28	1.3	0.65	0.9	1.04	1.26	1.91	6.43	4.11
April	1.26	1.38	0.99	0.5	1.18	1.35	1.19	0	0	0
May	1.35	1.26	1.54	5.63	1.27	1.17	1.7	0.77	1.71	1.69
June	0.64	1.31	1.42	1.05	1.21	1.16	1.73	3.96	2.14	2.53
July	0.31	1.24	1.11	0.5	1.22	1.01	0.65	0	0	0
August	0.35	1.19	1	0.7	1.15	1.05	1.16	5.36	1.71	3.67
September	1.1	1.06	0.89	0.25	0.98	0.8	0.68	0	0	0
October	1.15	1.05	0.51	1	1.05	0.79	1.25	0	0	0
November	1.01	0	0.46	0.33	0.73	0.63	0.68	0	0	0
December	1.21	0	0.72	0	0.82	1.04	0.85	0	0	0

Monthly Adjustment Factors

Year 2006-Lane 4

Month	Class 4	Class 5	Class 6	Class 7	Class 8	Class 9	Class 10	Class 11	Class 12	Class 13
January	0.93	0.93	0.75	0.23	0.96	0.95	1.23	1.48	2.69	0
February	1.14	1.02	0.86	0.82	0.99	0.94	0.64	1.26	0.54	1.9
March	1.07	0.93	0.79	0.76	1.09	0.91	1.13	1.26	1.4	1.9
April	1.23	0.93	1.2	1.57	1.08	0.96	0.8	0.84	0.54	1.9
May	1.41	0.99	1.09	1.16	0.99	1.01	1.86	1.85	0.97	0.76
June	0.87	1.02	1.14	1.76	1.02	1.1	0.51	1.39	1.5	0
July	0.71	0.99	1.32	0.26	1.01	1.1	0.39	0.21	1.07	0.95
August	0.82	1.02	1.05	0.67	1.04	1.05	1.41	2.36	0.43	0.76
September	1.09	1.05	1.11	1.02	1	1.05	1.45	0.84	0	0
October	0.99	1.05	1	2.18	0.93	1.08	1.07	0.28	2.15	0
November	0.93	1.03	0.88	0.82	0.93	1	1.18	0	0.72	3.81
December	0.81	1.03	0.82	0.75	0.95	0.84	0.32	0.21	0	0

Table E-3. WIM data for Blair site (cont'd)

Monthly Adjustment Factors

<u>Year 2007-Lane 1</u>

Month	Class 4	Class 5	Class 6	Class 7	Class 8	Class 9	Class 10	Class 11	Class 12	Class 13
January	N.A.	N.A.	N.A.	N.A.	N.A.	N.A.	N.A.	N.A.	N.A.	N.A.
February	1.17	0	1.1	0.15	0.76	0.96	0.47	0.33	1.67	0
March	1.05	0	1.05	0.53	0.93	1.09	0.79	0.59	0	1.57
April	1.26	0.79	1.06	4.03	0.97	1.09	1.22	1.38	0	2.5
May	1.07	1.73	0.97	0.93	1.2	0.99	0.91	0.59	1.29	2.21
June	0.53	2.75	0.97	0.76	1.2	1.02	1.51	1.48	0	0.71
July	0.23	1.65	0.9	0.38	1.14	0.94	1.85	1.18	1.29	0.57
August	0.42	0.63	0.89	0.45	1.17	0.99	0.97	1.68	2.87	1.21
September	1.36	1.18	0.89	0.67	1.06	1.04	0.72	0.39	2.15	0.36
October	1.39	0.39	1.06	0.86	1	1.03	1.81	1.33	1.15	1.86
November	1.01	1.89	0.88	1.27	0.88	0.89	0.49	0.89	0.57	0
December	1.51	0	1.22	0.96	0.69	0.97	0.25	1.15	0	0

Monthly Adjustment Factors

<u>Year 2007-Lane 2</u>

Month	Class 4	Class 5	Class 6	Class 7	Class 8	Class 9	Class 10	Class 11	Class 12	Class 13
January	N.A.	N.A.	N.A.	N.A.	N.A.	N.A.	N.A.	N.A.	N.A.	N.A.
February	1.28	0	1.08	0	0.64	1.07	0	2.12	0	0
March	1.22	3.14	1.01	0.42	0.71	1.23	1.96	0.63	0	5.5
April	1.5	0	1.19	1.18	1.11	1.3	0	0	0	0
May	1.6	0	1.53	2.02	1.43	1.28	1.96	0.63	0	5.5
June	1.04	0	1.39	1.18	1.75	1.48	1.57	0.79	0	0
July	0.93	0	1.44	1.68	1.72	1.27	3.93	1.43	0	0
August	1.37	0	1.56	0.76	1.68	1.38	1.57	0.79	11	0
September	1.39	0	1.3	3.78	1.4	1.41	0	3.97	0	0
October	0.67	7.86	0.5	0	0.55	0.58	0	0.63	0	0
November	N.A.	N.A.	N.A.	N.A.	N.A.	N.A.	N.A.	N.A.	N.A.	N.A.
December	N.A.	N.A.	N.A.	N.A.	N.A.	N.A.	N.A.	N.A.	N.A.	N.A.

Table E-3. WIM data for Blair site (cont'd)

Monthly Adjustment Factors

Year 2007-Lane 3

Month	Class 4	Class 5	Class 6	Class 7	Class 8	Class 9	Class 10	Class 11	Class 12	Class 13
January	N.A.	N.A.	N.A.	N.A.	N.A.	N.A.	N.A.	N.A.	N.A.	N.A.
February	1.21	0	1.19	4.98	0.68	1.07	1.25	0	N.A.	0
March	1.03	0	1.01	2.91	0.76	1.08	0.4	3.24	N.A.	0
April	1.2	0	1.18	0.24	0.91	1.1	1.6	2.59	N.A.	0
May	1.26	0	0.93	0.8	1.05	1.29	0.25	0	N.A.	0
June	0.41	4.4	0.89	0.4	1.25	0.99	1.9	5.18	N.A.	0
July	0.28	2.2	0.69	0.24	1.1	0.89	1.7	0	N.A.	6.11
August	0.46	0	0.72	0.16	1.3	0.81	0.9	0	N.A.	0
September	1.38	2.2	0.63	0.27	1.08	0.9	0.45	0	N.A.	0
October	1.33	2.2	0.99	0.32	1.08	0.93	1.05	0	N.A.	4.89
November	1.02	0	0.9	0.48	1.1	0.88	0.5	0	N.A.	0
December	1.41	0	1.87	0.21	0.69	1.05	1	0	N.A.	0

Monthly Adjustment Factors

Year 2007-Lane 4

Month	Class 4	Class 5	Class 6	Class 7	Class 8	Class 9	Class 10	Class 11	Class 12	Class 13
January	N.A.	N.A.	N.A.	N.A.	N.A.	N.A.	N.A.	N.A.	N.A.	N.A.
February	1	1.04	0.77	0.2	0.94	1.04	0.53	0.89	1.51	0
March	1.23	1.02	0.9	0.98	0.99	1.05	0.5	0.69	0	0
April	1	0.89	1.07	0.72	1.25	1.03	1.03	1.45	2.26	0
May	1.06	1.05	1.22	1.47	1.02	0.96	1.03	0.99	0	1.41
June	0.81	1.05	1.03	1	1.03	1.05	1.17	1.15	1.13	1.41
July	0.79	0.98	1.03	1.62	0.82	0.97	1.75	1.38	3.16	1.41
August	0.75	1	1.02	0.9	1.05	0.96	1.06	0.76	0.9	3.95
September	1.07	0.95	1.05	1.45	0.96	0.99	0.66	1.38	1.13	0
October	1.17	0.96	1.14	0.98	1.03	1.05	2.09	0.38	0.9	2.82
November	0.9	0.94	0.89	0.98	0.92	0.92	0.56	0.92	0	0
December	1.21	1.12	0.89	0.69	1.01	0.98	0.62	1.02	0	0

Axle Load Distribution Factors

Single Axle Load Distributions for various FHWA Vehicle Classes

Axle Weight	4	5	6	7	8	9	10	11	12	13
3000	0.1	9.1	0.1	1.5	0.7	0.7	0.0	2.3	1.2	0.0
4000	0.0	20.3	0.2	0.8	0.7	2.2	0.0	6.8	1.2	0.0
5000	0.7	23.5	0.1	0.0	1.6	1.4	0.0	6.8	4.2	0.0
6000	2.7	13.7	0.7	0.0	3.2	1.2	0.0	10.2	11.9	0.0
7000	8.4	8.7	1.2	0.0	6.5	1.0	0.0	22.9	14.3	20.0
8000	18.6	7.2	3.9	0.4	12.2	3.3	0.0	13.6	8.3	0.0
9000	15.2	5.2	10.0	2.5	19.3	16.2	5.9	8.8	11.9	0.0
10000	10.2	3.3	18.1	0.4	17.8	26.0	16.1	10.0	13.7	20.0
11000	11.1	2.3	15.6	5.3	9.4	25.4	19.9	8.2	10.1	0.0
12000	10.5	1.5	8.8	3.8	6.5	13.5	26.8	3.8	12.5	0.0
13000	7.9	1.0	10.3	7.3	5.5	3.4	24.0	1.8	0.0	0.0
14000	6.4	0.8	8.1	6.8	5.1	1.1	4.2	1.4	0.0	18.7
15000	4.0	0.6	4.8	7.6	3.3	0.9	1.0	0.9	7.1	4.0
16000	2.2	0.5	3.4	9.6	2.2	1.1	0.5	0.9	3.6	20.0
17000	0.8	0.4	2.5	10.9	1.6	1.1	0.6	0.5	0.0	17.3
18000	0.2	0.3	1.8	19.9	1.5	0.8	0.0	0.6	0.0	0.0
19000	0.3	0.4	2.5	11.1	1.2	0.5	0.5	0.0	0.0	0.0
20000	0.2	0.4	3.2	5.2	0.6	0.2	0.0	0.0	0.0	0.0
21000	0.0	0.2	2.8	2.2	0.5	0.0	0.0	0.6	0.0	0.0
22000	0.1	0.1	1.2	0.5	0.2	0.0	0.0	0.0	0.0	0.0
23000	0.1	0.1	0.4	1.3	0.2	0.0	0.0	0.0	0.0	0.0
24000	0.0	0.0	0.1	1.5	0.1	0.0	0.0	0.0	0.0	0.0
25000	0.0	0.0	0.2	0.0	0.0	0.1	0.0	0.0	0.0	0.0
26000	0.0	0.0	0.0	1.2	0.0	0.0	0.6	0.0	0.0	0.0
27000	0.0	0.0	0.0	0.0	0.0	0.0	0.0	0.0	0.0	0.0
28000	0.1	0.0	0.0	0.0	0.0	0.0	0.0	0.0	0.0	0.0
29000	0.0	0.0	0.0	0.0	0.0	0.0	0.0	0.0	0.0	0.0
30000	0.0	0.0	0.0	0.0	0.0	0.0	0.0	0.0	0.0	0.0
31000	0.0	0.0	0.0	0.0	0.0	0.0	0.0	0.0	0.0	0.0
32000	0.0	0.0	0.0	0.0	0.0	0.0	0.0	0.0	0.0	0.0
33000	0.0	0.0	0.0	0.0	0.0	0.0	0.0	0.0	0.0	0.0
34000	0.0	0.0	0.0	0.0	0.0	0.0	0.0	0.0	0.0	0.0
35000	0.0	0.0	0.0	0.0	0.0	0.0	0.0	0.0	0.0	0.0
36000	0.0	0.0	0.0	0.0	0.0	0.0	0.0	0.0	0.0	0.0
37000	0.0	0.0	0.0	0.0	0.0	0.0	0.0	0.0	0.0	0.0
38000	0.0	0.0	0.0	0.0	0.0	0.0	0.0	0.0	0.0	0.0
39000	0.0	0.0	0.0	0.0	0.0	0.0	0.0	0.0	0.0	0.0
40000	0.0	0.0	0.0	0.0	0.0	0.0	0.0	0.0	0.0	0.0
41000	0.0	0.0	0.0	0.0	0.1	0.0	0.0	0.0	0.0	0.0

Table E-3. WIM data for Blair site (cont'd)

Tandem Axle Load Distributions for various FHWA Vehicle Classes

Axle Weight	4	5	6	7	8	9	10	11	12	13
6000	0.0	65.6	2.7	0.0	1.3	1.2	0.0	N.A.	0.0	0.0
8000	0.0	25.6	10.7	0.0	3.3	2.9	0.0	N.A.	4.8	0.0
10000	0.6	8.8	13.9	25.0	13.6	8.0	0.0	N.A.	0.0	0.0
12000	1.1	0.0	5.3	0.0	25.7	15.6	0.0	N.A.	14.3	0.0
14000	1.2	0.0	7.2	0.0	20.9	14.8	0.0	N.A.	28.6	0.0
16000	1.1	0.0	8.3	0.0	11.6	10.0	4.3	N.A.	7.1	0.0
18000	3.6	0.0	6.0	0.0	8.3	8.3	11.0	N.A.	31.0	0.0
20000	8.8	0.0	5.7	0.0	5.0	6.6	7.4	N.A.	14.3	0.0
22000	15.0	0.0	6.1	0.0	2.6	5.0	3.4	N.A.	0.0	0.0
24000	9.7	0.0	5.6	0.0	1.2	4.6	3.0	N.A.	0.0	16.7
26000	12.5	0.0	5.1	12.5	0.7	3.6	6.2	N.A.	0.0	8.3
28000	14.5	0.0	5.0	0.0	1.2	3.8	3.2	N.A.	0.0	0.0
30000	17.9	0.0	4.2	25.0	0.9	4.2	15.1	N.A.	0.0	0.0
32000	8.7	0.0	4.3	12.5	1.4	4.2	18.9	N.A.	0.0	12.5
34000	3.2	0.0	3.0	0.0	1.2	3.8	4.3	N.A.	0.0	0.0
36000	1.9	0.0	2.1	0.0	0.7	2.3	7.2	N.A.	0.0	37.5
38000	0.3	0.0	1.2	0.0	0.2	0.9	3.3	N.A.	0.0	16.7
40000	0.0	0.0	1.0	0.0	0.0	0.2	5.1	N.A.	0.0	0.0
42000	0.0	0.0	0.8	0.0	0.0	0.1	1.0	N.A.	0.0	8.3
44000	0.0	0.0	0.3	0.0	0.0	0.0	2.6	N.A.	0.0	0.0
46000	0.0	0.0	0.5	0.0	0.1	0.0	1.0	N.A.	0.0	0.0
48000	0.0	0.0	0.3	25.0	0.0	0.0	0.0	N.A.	0.0	0.0
50000	0.0	0.0	0.1	0.0	0.0	0.0	0.0	N.A.	0.0	0.0
52000	0.0	0.0	0.2	0.0	0.0	0.0	0.0	N.A.	0.0	0.0
54000	0.0	0.0	0.0	0.0	0.0	0.0	0.0	N.A.	0.0	0.0
56000	0.0	0.0	0.1	0.0	0.0	0.0	0.6	N.A.	0.0	0.0
58000	0.0	0.0	0.1	0.0	0.0	0.0	1.8	N.A.	0.0	0.0
60000	0.0	0.0	0.0	0.0	0.0	0.0	0.6	N.A.	0.0	0.0
62000	0.0	0.0	0.0	0.0	0.0	0.0	0.0	N.A.	0.0	0.0
64000	0.0	0.0	0.0	0.0	0.0	0.0	0.0	N.A.	0.0	0.0
66000	0.0	0.0	0.0	0.0	0.0	0.0	0.0	N.A.	0.0	0.0
68000	0.0	0.0	0.0	0.0	0.0	0.0	0.0	N.A.	0.0	0.0
70000	0.0	0.0	0.0	0.0	0.0	0.0	0.0	N.A.	0.0	0.0
72000	0.0	0.0	0.0	0.0	0.0	0.0	0.0	N.A.	0.0	0.0
74000	0.0	0.0	0.0	0.0	0.0	0.0	0.0	N.A.	0.0	0.0
76000	0.0	0.0	0.0	0.0	0.0	0.0	0.0	N.A.	0.0	0.0
78000	0.0	0.0	0.0	0.0	0.0	0.0	0.0	N.A.	0.0	0.0
80000	0.0	0.0	0.0	0.0	0.0	0.0	0.0	N.A.	0.0	0.0
82000	0.0	0.0	0.0	0.0	0.0	0.0	0.0	N.A.	0.0	0.0

Table E-3. WIM data for Blair site (cont'd)

Tridem Axle Load Distributions for various FHWA Vehicle Classes

Axle Weight	4	5	6	7	8	9	10	11	12	13
12000	N.A.	N.A.	N.A.	100	N.A.	N.A.	100	N.A.	N.A.	100
15000	N.A.	N.A.	N.A.	0.5	N.A.	N.A.	5.3	N.A.	N.A.	0.0
18000	N.A.	N.A.	N.A.	0.0	N.A.	N.A.	9.6	N.A.	N.A.	0.0
21000	N.A.	N.A.	N.A.	1.2	N.A.	N.A.	6.0	N.A.	N.A.	0.0
24000	N.A.	N.A.	N.A.	0.7	N.A.	N.A.	1.8	N.A.	N.A.	0.0
27000	N.A.	N.A.	N.A.	2.7	N.A.	N.A.	4.0	N.A.	N.A.	0.0
30000	N.A.	N.A.	N.A.	0.8	N.A.	N.A.	1.2	N.A.	N.A.	0.0
33000	N.A.	N.A.	N.A.	1.7	N.A.	N.A.	3.2	N.A.	N.A.	0.0
36000	N.A.	N.A.	N.A.	2.8	N.A.	N.A.	6.5	N.A.	N.A.	0.0
39000	N.A.	N.A.	N.A.	2.2	N.A.	N.A.	6.7	N.A.	N.A.	0.0
42000	N.A.	N.A.	N.A.	4.8	N.A.	N.A.	8.0	N.A.	N.A.	0.0
45000	N.A.	N.A.	N.A.	10.4	N.A.	N.A.	23.4	N.A.	N.A.	0.0
48000	N.A.	N.A.	N.A.	7.0	N.A.	N.A.	12.0	N.A.	N.A.	0.0
51000	N.A.	N.A.	N.A.	7.2	N.A.	N.A.	4.7	N.A.	N.A.	0.0
54000	N.A.	N.A.	N.A.	9.0	N.A.	N.A.	1.0	N.A.	N.A.	0.0
57000	N.A.	N.A.	N.A.	14.3	N.A.	N.A.	4.0	N.A.	N.A.	6.3
60000	N.A.	N.A.	N.A.	22.3	N.A.	N.A.	0.0	N.A.	N.A.	0.0
63000	N.A.	N.A.	N.A.	8.0	N.A.	N.A.	0.0	N.A.	N.A.	43.8
66000	N.A.	N.A.	N.A.	4.6	N.A.	N.A.	2.5	N.A.	N.A.	0.0
69000	N.A.	N.A.	N.A.	0.0	N.A.	N.A.	0.0	N.A.	N.A.	18.8
72000	N.A.	N.A.	N.A.	0.0	N.A.	N.A.	0.0	N.A.	N.A.	0.0
75000	N.A.	N.A.	N.A.	0.0	N.A.	N.A.	0.0	N.A.	N.A.	18.8
78000	N.A.	N.A.	N.A.	0.0	N.A.	N.A.	0.0	N.A.	N.A.	12.5
81000	N.A.	N.A.	N.A.	0.0	N.A.	N.A.	0.0	N.A.	N.A.	0.0
84000	N.A.	N.A.	N.A.	0.0	N.A.	N.A.	0.0	N.A.	N.A.	0.0
87000	N.A.	N.A.	N.A.	0.0	N.A.	N.A.	0.0	N.A.	N.A.	0.0
90000	N.A.	N.A.	N.A.	0.0	N.A.	N.A.	0.0	N.A.	N.A.	0.0
93000	N.A.	N.A.	N.A.	0.0	N.A.	N.A.	0.0	N.A.	N.A.	0.0
96000	N.A.	N.A.	N.A.	0.0	N.A.	N.A.	0.0	N.A.	N.A.	0.0
99000	N.A.	N.A.	N.A.	0.0	N.A.	N.A.	0.0	N.A.	N.A.	0.0
102000	N.A.	N.A.	N.A.	0.0	N.A.	N.A.	0.0	N.A.	N.A.	0.0
105000	N.A.	N.A.	N.A.	0.0	N.A.	N.A.	0.0	N.A.	N.A.	0.0

Table E-3. WIM data for Blair site (cont'd)

Quad Axle Load Distributions for various FHWA Vehicle Classes

Axle Weight	4	5	6	7	8	9	10	11	12	13
12000	N.A.	N.A.	N.A.	N.A.	N.A.	N.A.	N.A.	N.A.	N.A.	100
15000	N.A.	N.A.	N.A.	N.A.	N.A.	N.A.	N.A.	N.A.	N.A.	0.0
18000	N.A.	N.A.	N.A.	N.A.	N.A.	N.A.	N.A.	N.A.	N.A.	0.0
21000	N.A.	N.A.	N.A.	N.A.	N.A.	N.A.	N.A.	N.A.	N.A.	0.0
24000	N.A.	N.A.	N.A.	N.A.	N.A.	N.A.	N.A.	N.A.	N.A.	100.0
27000	N.A.	N.A.	N.A.	N.A.	N.A.	N.A.	N.A.	N.A.	N.A.	0.0
30000	N.A.	N.A.	N.A.	N.A.	N.A.	N.A.	N.A.	N.A.	N.A.	0.0
33000	N.A.	N.A.	N.A.	N.A.	N.A.	N.A.	N.A.	N.A.	N.A.	0.0
36000	N.A.	N.A.	N.A.	N.A.	N.A.	N.A.	N.A.	N.A.	N.A.	0.0
39000	N.A.	N.A.	N.A.	N.A.	N.A.	N.A.	N.A.	N.A.	N.A.	0.0
42000	N.A.	N.A.	N.A.	N.A.	N.A.	N.A.	N.A.	N.A.	N.A.	0.0
45000	N.A.	N.A.	N.A.	N.A.	N.A.	N.A.	N.A.	N.A.	N.A.	0.0
48000	N.A.	N.A.	N.A.	N.A.	N.A.	N.A.	N.A.	N.A.	N.A.	0.0
51000	N.A.	N.A.	N.A.	N.A.	N.A.	N.A.	N.A.	N.A.	N.A.	0.0
54000	N.A.	N.A.	N.A.	N.A.	N.A.	N.A.	N.A.	N.A.	N.A.	0.0
57000	N.A.	N.A.	N.A.	N.A.	N.A.	N.A.	N.A.	N.A.	N.A.	0.0
60000	N.A.	N.A.	N.A.	N.A.	N.A.	N.A.	N.A.	N.A.	N.A.	0.0
63000	N.A.	N.A.	N.A.	N.A.	N.A.	N.A.	N.A.	N.A.	N.A.	0.0
66000	N.A.	N.A.	N.A.	N.A.	N.A.	N.A.	N.A.	N.A.	N.A.	0.0
69000	N.A.	N.A.	N.A.	N.A.	N.A.	N.A.	N.A.	N.A.	N.A.	0.0
72000	N.A.	N.A.	N.A.	N.A.	N.A.	N.A.	N.A.	N.A.	N.A.	0.0
75000	N.A.	N.A.	N.A.	N.A.	N.A.	N.A.	N.A.	N.A.	N.A.	0.0
78000	N.A.	N.A.	N.A.	N.A.	N.A.	N.A.	N.A.	N.A.	N.A.	0.0
81000	N.A.	N.A.	N.A.	N.A.	N.A.	N.A.	N.A.	N.A.	N.A.	0.0
84000	N.A.	N.A.	N.A.	N.A.	N.A.	N.A.	N.A.	N.A.	N.A.	0.0
87000	N.A.	N.A.	N.A.	N.A.	N.A.	N.A.	N.A.	N.A.	N.A.	0.0
90000	N.A.	N.A.	N.A.	N.A.	N.A.	N.A.	N.A.	N.A.	N.A.	0.0
93000	N.A.	N.A.	N.A.	N.A.	N.A.	N.A.	N.A.	N.A.	N.A.	0.0
96000	N.A.	N.A.	N.A.	N.A.	N.A.	N.A.	N.A.	N.A.	N.A.	0.0
99000	N.A.	N.A.	N.A.	N.A.	N.A.	N.A.	N.A.	N.A.	N.A.	0.0
102000	N.A.	N.A.	N.A.	N.A.	N.A.	N.A.	N.A.	N.A.	N.A.	0.0
105000	N.A.	N.A.	N.A.	N.A.	N.A.	N.A.	N.A.	N.A.	N.A.	0.0

Table E-3. WIM data for Blair site (cont'd)

Hourly Truck Distribution

Year 2006

Hour	Percent Trucks			
	Lane 1	Lane 2	Lane 3	Lane 4
0	1.26	1.49	0.58	1.00
1	2.01	1.48	1.46	1.63
2	2.08	1.55	1.56	2.10
3	1.62	1.67	3.25	3.01
4	5.81	2.45	4.99	3.31
5	3.79	2.49	2.67	2.13
6	5.16	4.22	5.49	3.56
7	7.87	4.86	7.06	6.10
8	7.95	6.76	9.44	8.71
9	7.84	6.64	4.76	8.77
10	7.95	6.54	6.03	8.11
11	6.34	6.50	4.46	7.99
12	5.34	6.90	5.28	7.01
13	6.39	7.15	5.82	6.86
14	6.99	8.02	7.67	6.34
15	5.09	5.87	6.52	5.81
16	3.67	4.95	5.40	3.87
17	3.10	7.48	5.65	3.10
18	2.38	5.46	7.00	2.91
19	1.64	1.85	1.65	2.03
20	1.51	1.22	0.72	1.71
21	0.97	0.99	0.86	1.76
22	1.35	2.18	0.53	1.05
23	1.90	1.30	1.14	1.12

Table E-3. WIM data for Blair site (cont'd)

Year 2007

Hour	Percent Trucks			
	Lane 1	Lane 2	Lane 3	Lane 4
0	1.29	1.00	0.89	1.04
1	1.89	0.83	1.08	1.15
2	2.25	0.88	1.17	1.74
3	1.40	1.05	1.13	2.70
4	1.42	1.31	1.05	3.63
5	2.51	2.31	1.56	2.60
6	5.02	3.12	4.10	3.95
7	7.42	4.10	6.72	6.22
8	8.41	8.46	12.81	8.36
9	8.17	7.13	6.92	8.38
10	9.18	8.68	8.89	8.04
11	7.47	7.61	5.99	7.20
12	6.75	6.94	7.22	7.31
13	6.55	6.94	6.37	6.99
14	7.33	7.38	7.62	6.58
15	5.32	6.29	6.97	5.41
16	5.06	5.64	5.40	4.09
17	3.30	3.65	3.58	3.47
18	2.23	6.80	3.38	3.06
19	1.73	2.73	2.62	2.19
20	1.25	1.88	1.70	1.94
21	1.20	1.78	1.05	1.79
22	1.50	1.23	0.95	1.14
23	1.34	2.28	0.82	1.02

Table E-3. WIM data for Blair site (cont'd)

Year 2008

Hour	Percent Trucks			
	Lane 1	Lane 2	Lane 3	Lane 4
0	0.77	N.A.	0.79	1.28
1	2.21	N.A.	0.88	1.15
2	2.70	N.A.	1.16	1.95
3	0.78	N.A.	0.79	3.14
4	1.40	N.A.	1.42	5.16
5	2.49	N.A.	2.36	2.27
6	5.44	N.A.	5.19	4.08
7	8.06	N.A.	7.21	5.54
8	8.27	N.A.	14.98	8.42
9	8.09	N.A.	4.72	8.39
10	10.34	N.A.	10.65	7.91
11	6.86	N.A.	5.16	7.55
12	6.19	N.A.	6.76	6.61
13	6.28	N.A.	6.23	6.95
14	7.75	N.A.	8.62	6.23
15	5.53	N.A.	7.99	5.10
16	4.56	N.A.	4.66	3.69
17	3.17	N.A.	2.17	3.79
18	2.30	N.A.	2.39	3.59
19	1.63	N.A.	1.76	2.34
20	1.95	N.A.	1.86	1.98
21	0.84	N.A.	0.75	1.07
22	1.06	N.A.	0.69	0.82
23	1.35	N.A.	0.82	0.97

*Based on WIM data collected from January to May 2008

Table E-3. WIM data for Blair site (cont'd)

Average Speed, Gross Weight and Length of Trucks

Month	Average Speed, mph	Gross Weight (kips)	Length (ft)
Jan-06	42.89	23.72	33.48
Feb-06	43.18	23.30	32.91
Mar-06	43.22	23.96	33.91
Apr-06	43.02	24.13	34.06
May-06	43.55	23.84	34.06
Jun-06	43.15	24.45	34.00
Jul-06	43.25	24.53	34.10
Aug-06	43.60	24.82	34.50
Sep-06	43.45	23.90	33.93
Oct-06	43.17	24.51	34.01
Nov-06	43.69	23.47	34.51
Dec-06	43.65	22.57	33.04
Jan-07	N.A.	N.A.	N.A.
Feb-07	42.91	22.15	32.44
Mar-07	43.46	21.71	32.34
Apr-07	43.97	22.37	33.70
May-07	43.29	21.56	31.74
Jun-07	43.51	21.80	32.18
Jul-07	43.94	22.30	32.32
Aug-07	43.69	22.28	32.36
Sep-07	44.10	21.97	32.47
Oct-07	43.65	22.64	33.16
Nov-07	43.92	21.82	32.11
Dec-07	42.47	21.44	31.63
Jan-08	N.A.	N.A.	N.A.
Feb-08	43.66	22.77	31.69
Mar-08	43.56	22.33	32.33
Apr-08	43.37	23.11	32.89
May-08	43.86	22.09	33.47

Table E-3. WIM data for Blair site (cont'd)

Wheelbase of Vehicles

Distance (ft)	Percent
0	0.0530%
2	0.3089%
4	1.6858%
6	1.3504%
8	0.3089%
10	4.2189%
12	37.7935%
14	13.7952%
16	12.6478%
18	14.9603%
20	6.2754%
22	0.2824%
24	0.6620%
26	0.6531%
28	0.5472%
30	0.3707%
32	0.3619%
34	0.3266%
36	0.3266%
38	0.2913%
40	2.7802%

Appendix F

Environmental Data

County: Mercer East   Highway: SR 80-A04   Location 1
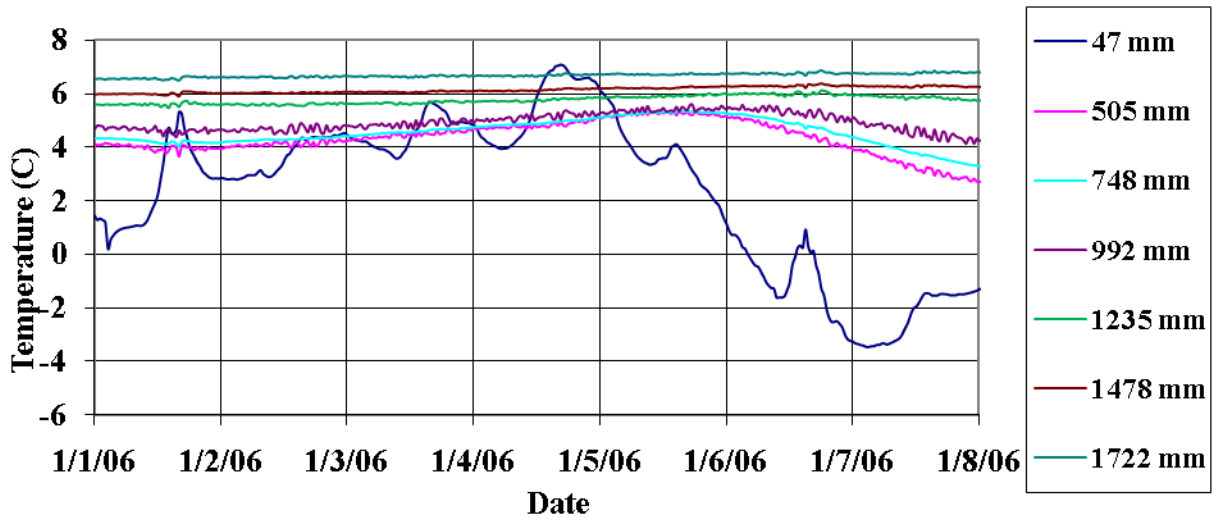
County: Mercer East   Highway: SR 80-A04   Location 1

County: Mercer East   Highway: SR 80-A04   Location 1

County: Mercer East   Highway: SR 80-A04   Location 1

County: Mercer East   Highway: SR 80-A04   Location 1

Legend: 47 mm, 505 mm, 748 mm, 992 mm, 1235 mm, 1478 mm, 1722 mm

County: Mercer West   Highway: SR 80-A04   Location 2

Legend: 5 mm, 40 mm, 404 mm, 647 mm, 891 mm, 1134 mm, 1378 mm, 1621 mm

County: Mercer West   Highway: SR 80-A04   Location 2

County: Mercer West   Highway: SR 80-A04   Location 2

County: Mercer West   Highway: SR 80-A04   Location 2

Legend: 5 mm, 40 mm, 404 mm, 647 mm, 891 mm, 1134 mm, 1378 mm, 1621 mm

County: Tioga   Highway SR 6015   Location 1

Legend: Pedestal, Air, 5 mm, 52 mm, 367 mm, 610 mm, 854 mm, 1097 mm, 1341 mm, 1584 mm
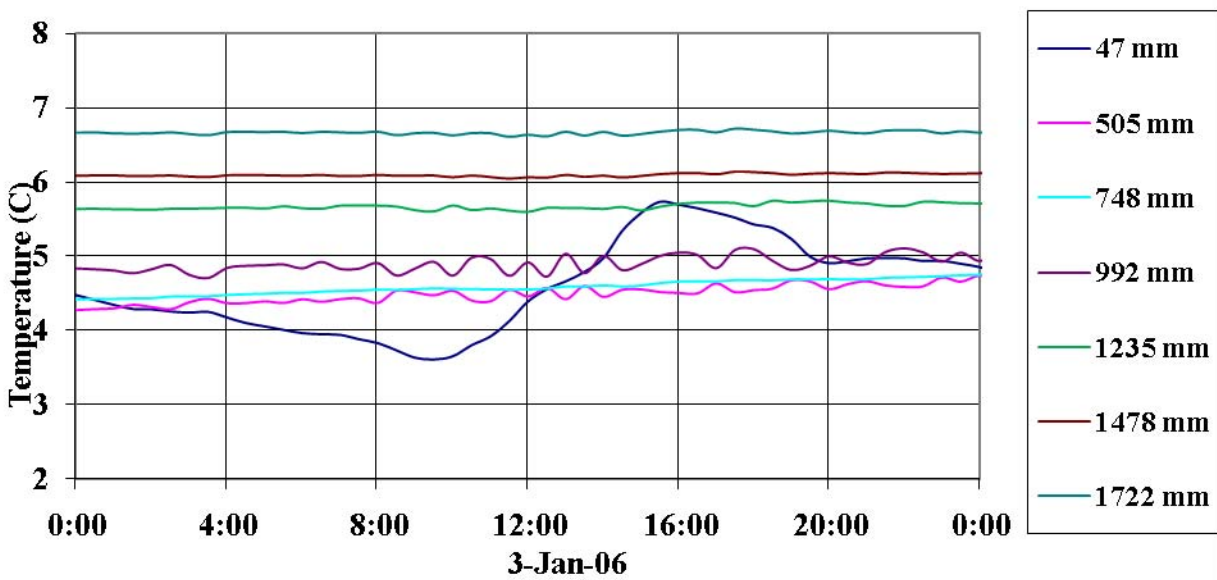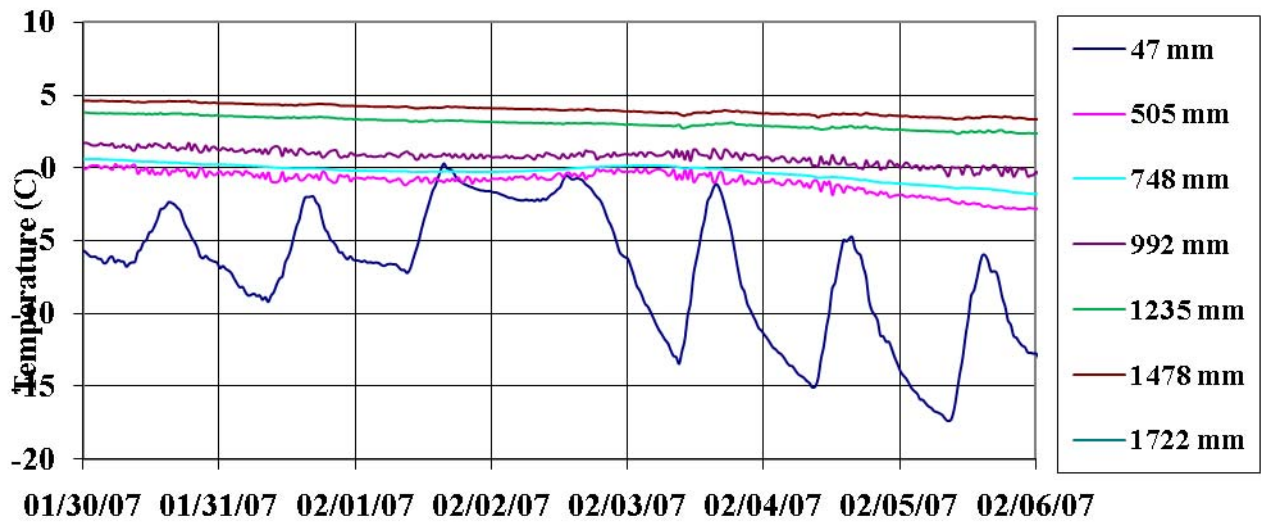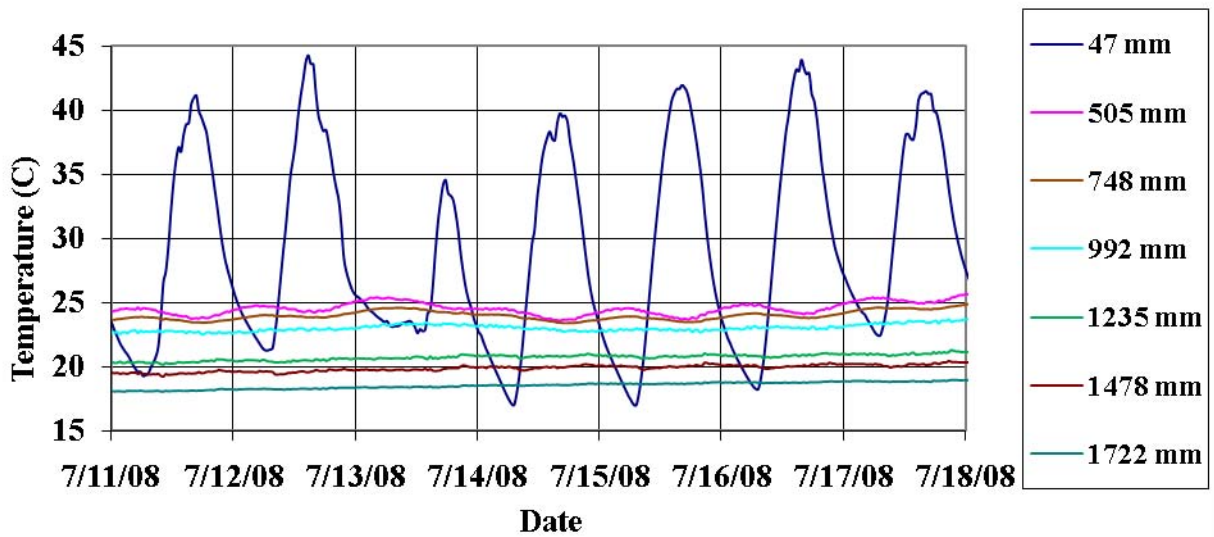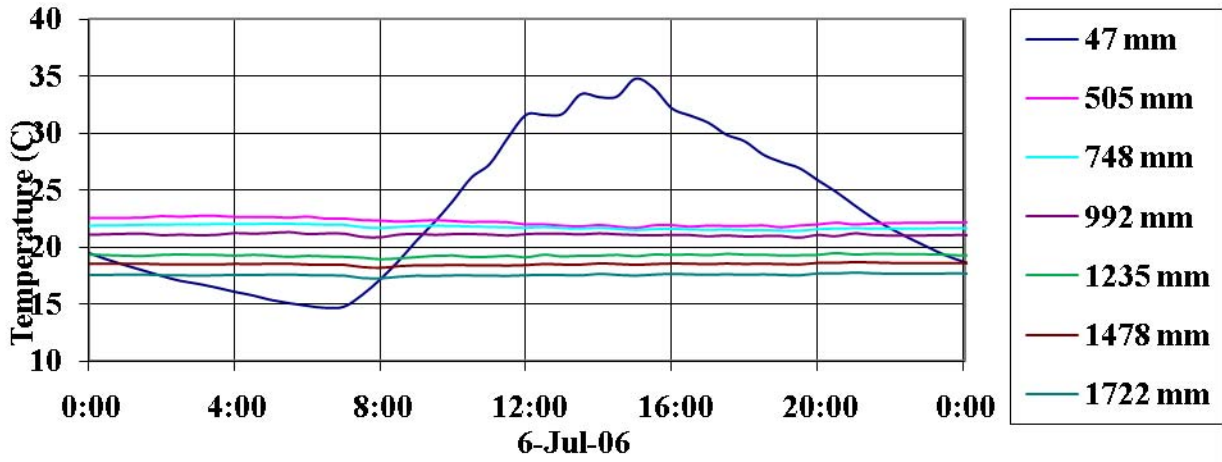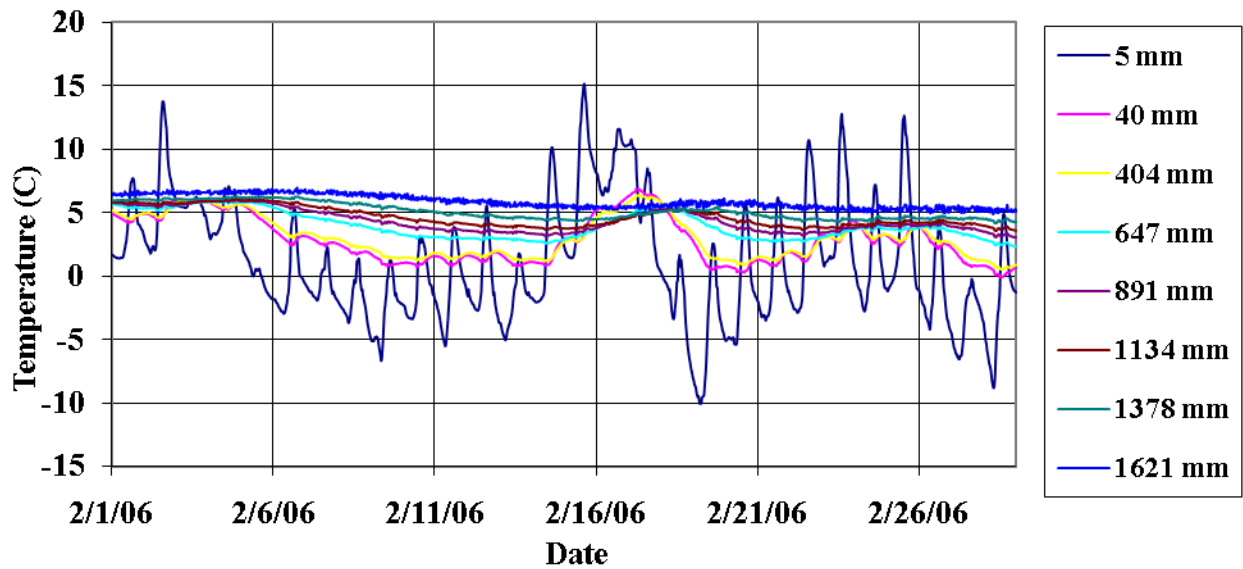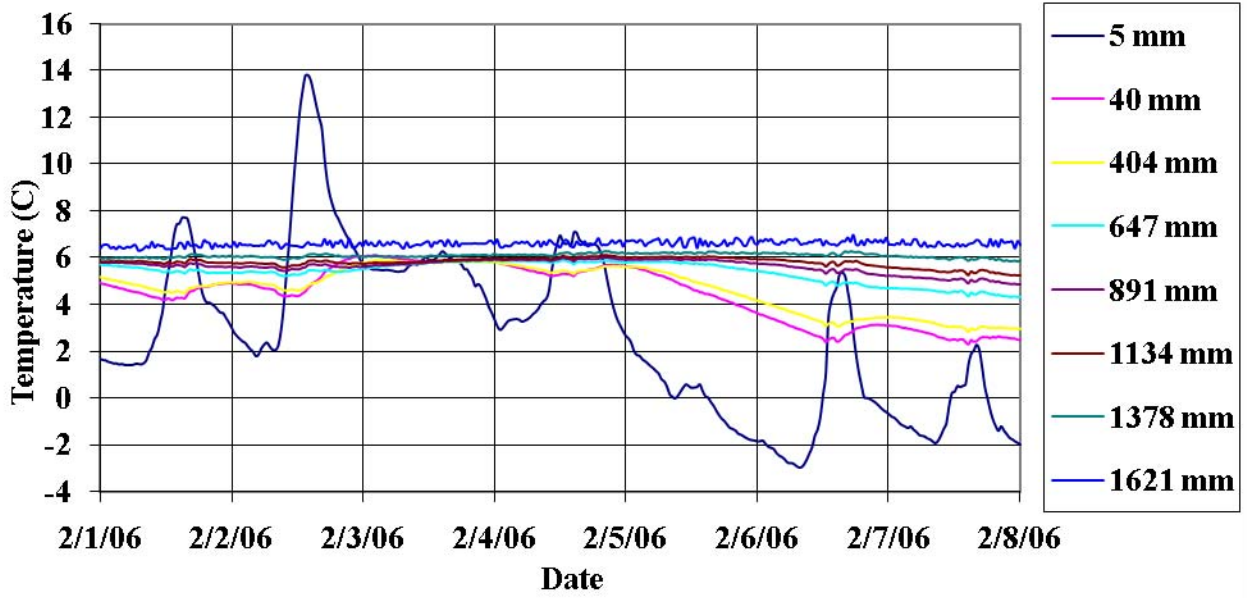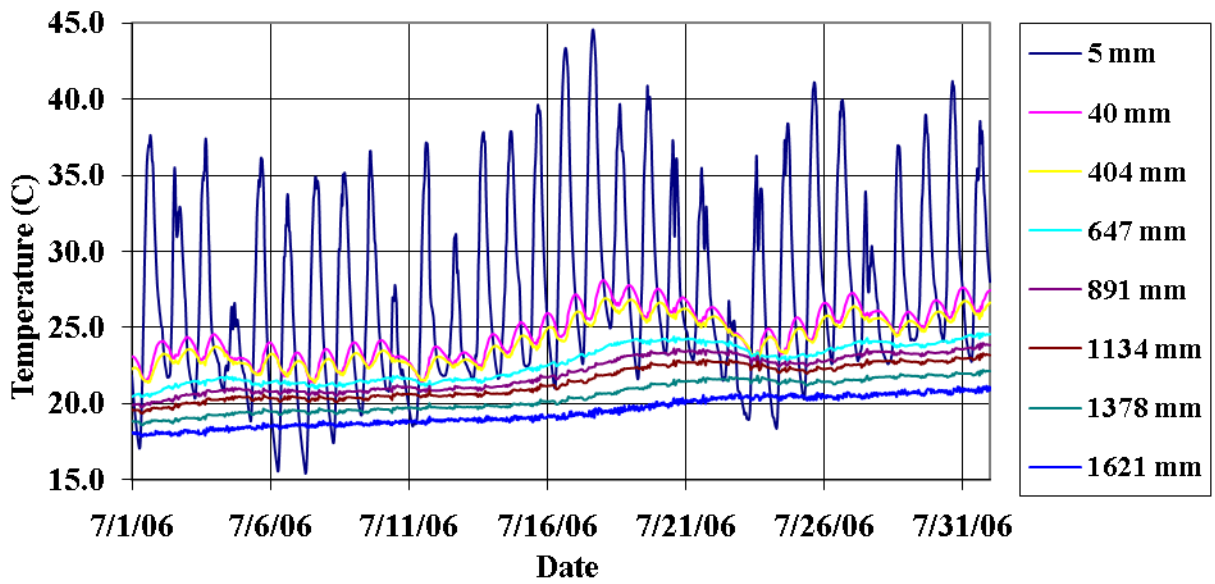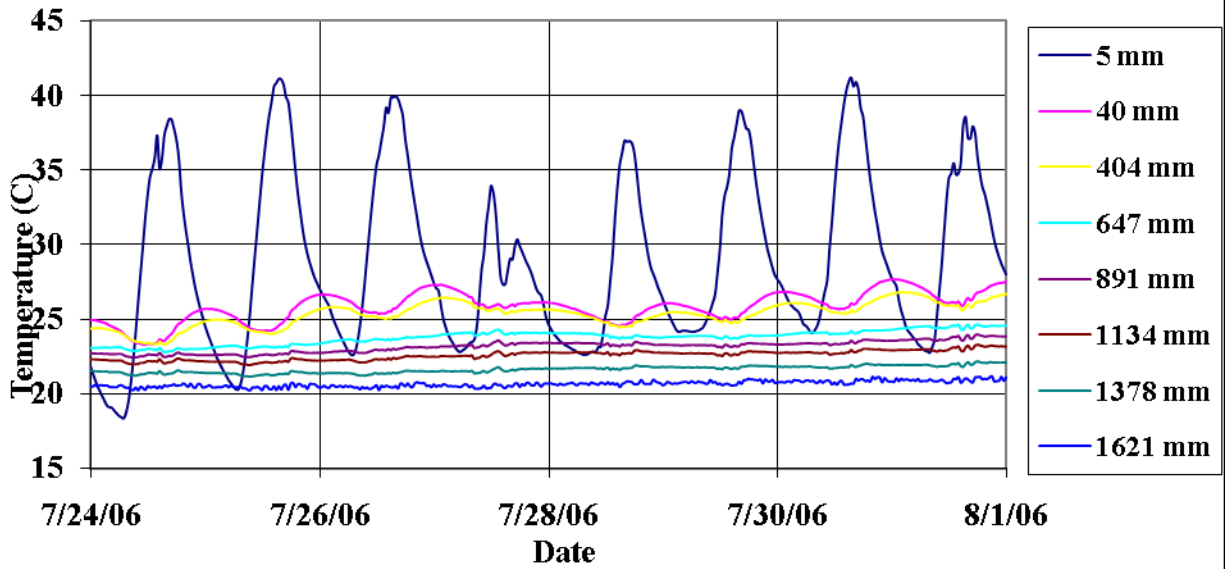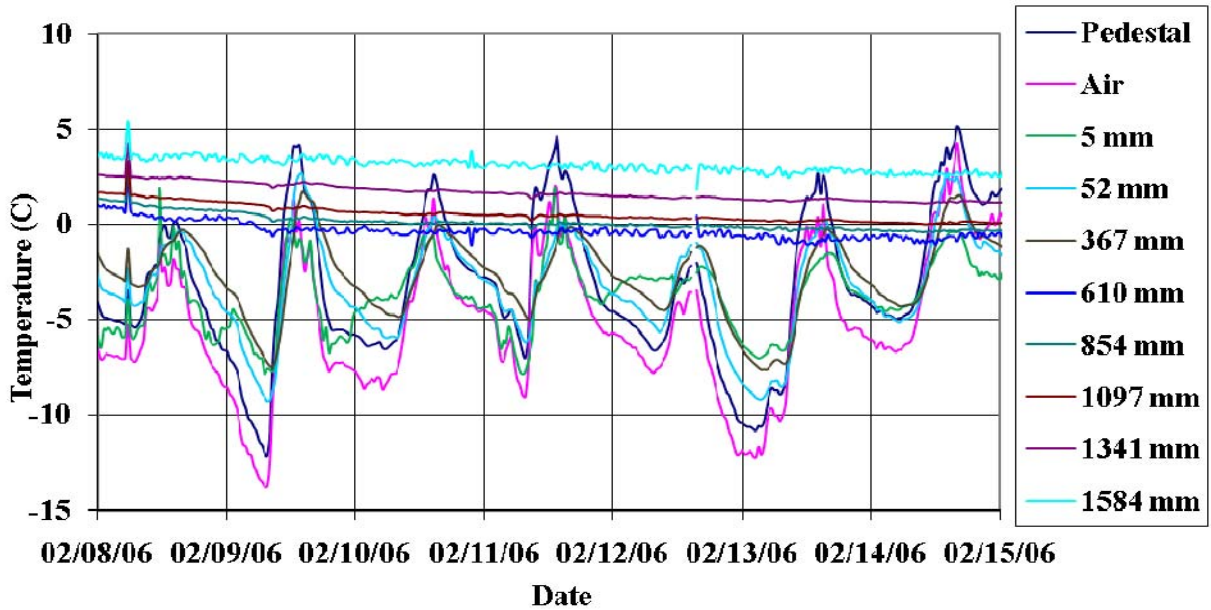
County: Tioga   Highway: SR 6015   Location 1

County: Tioga   Highway: SR 6015   Location 2
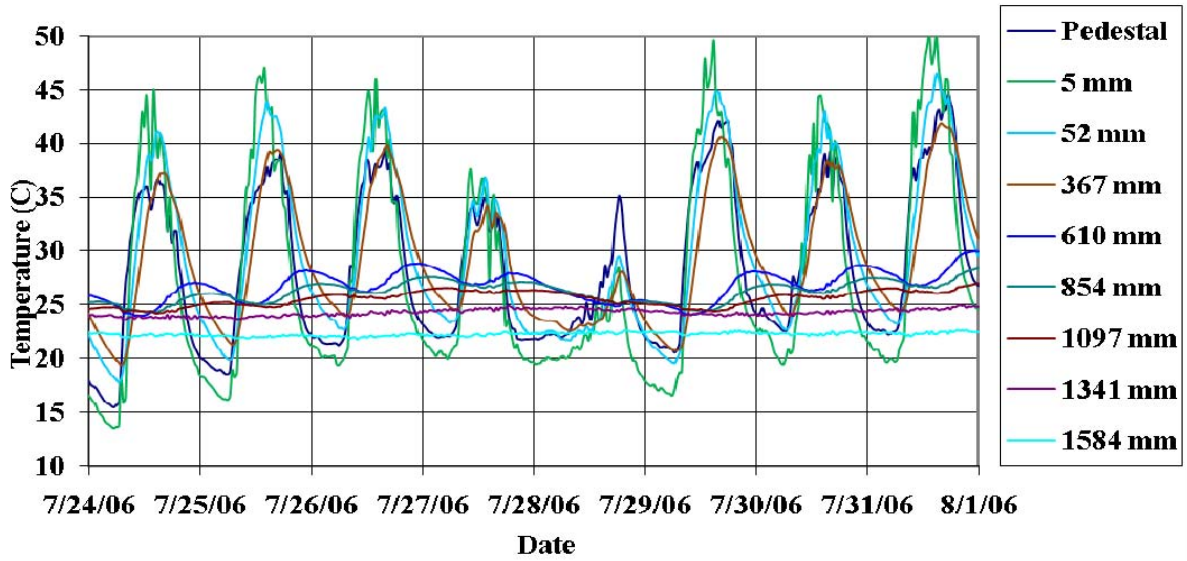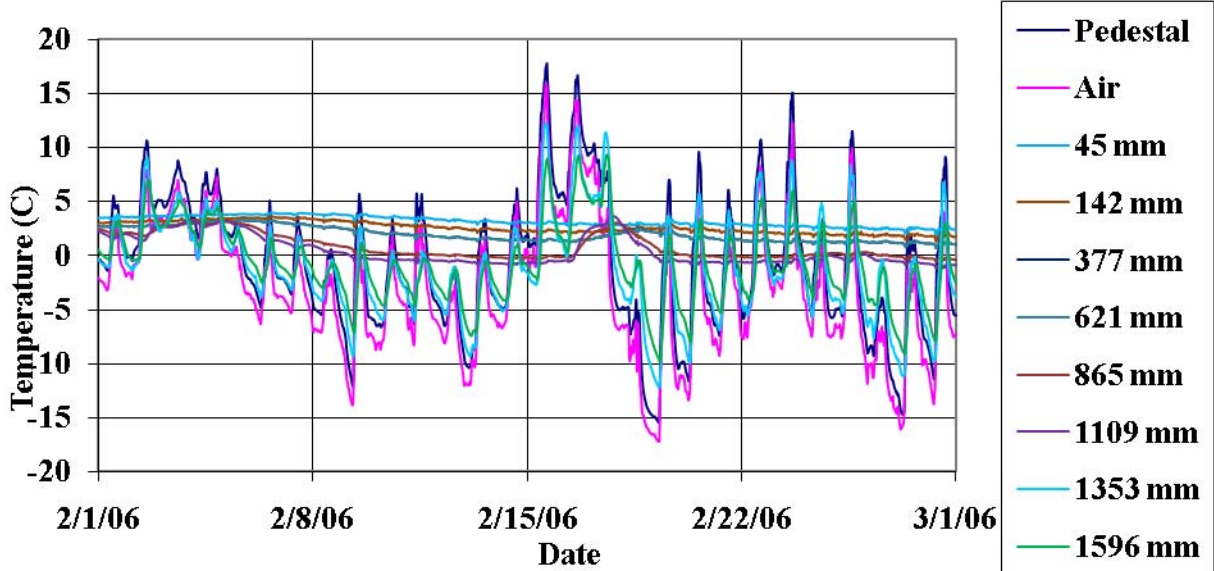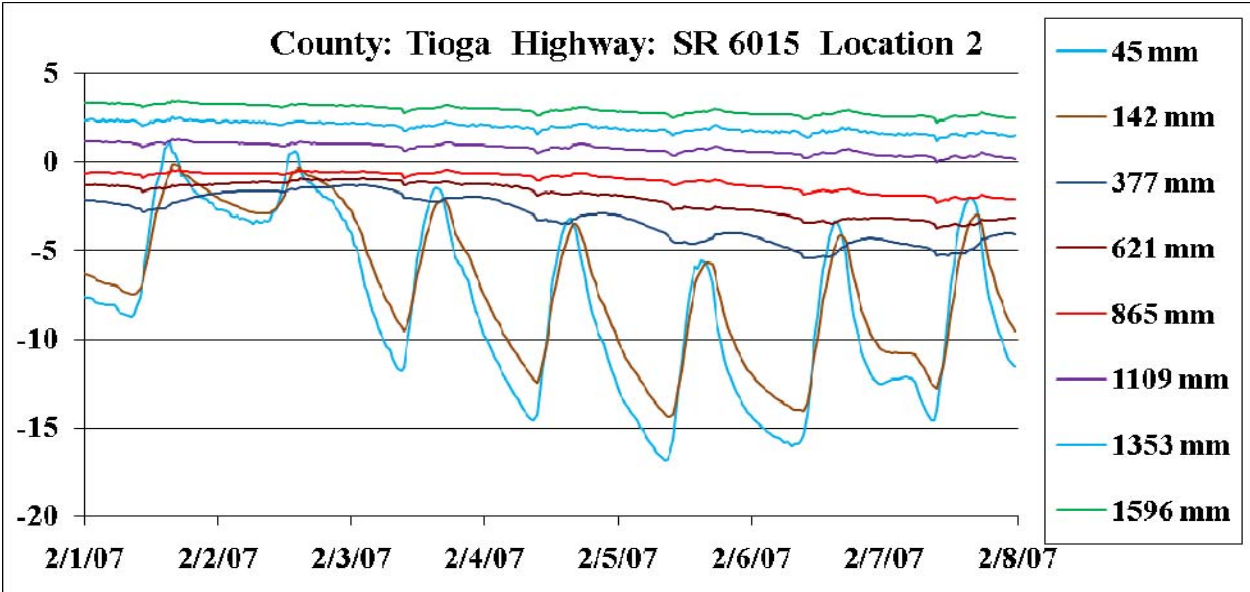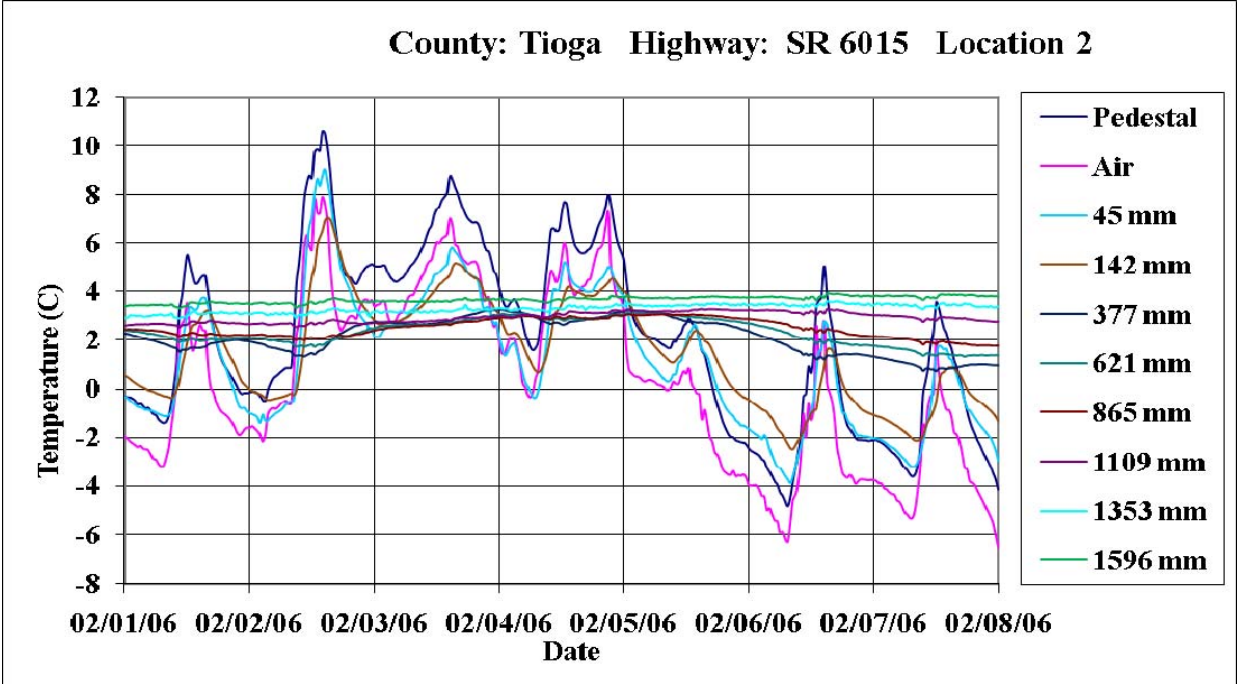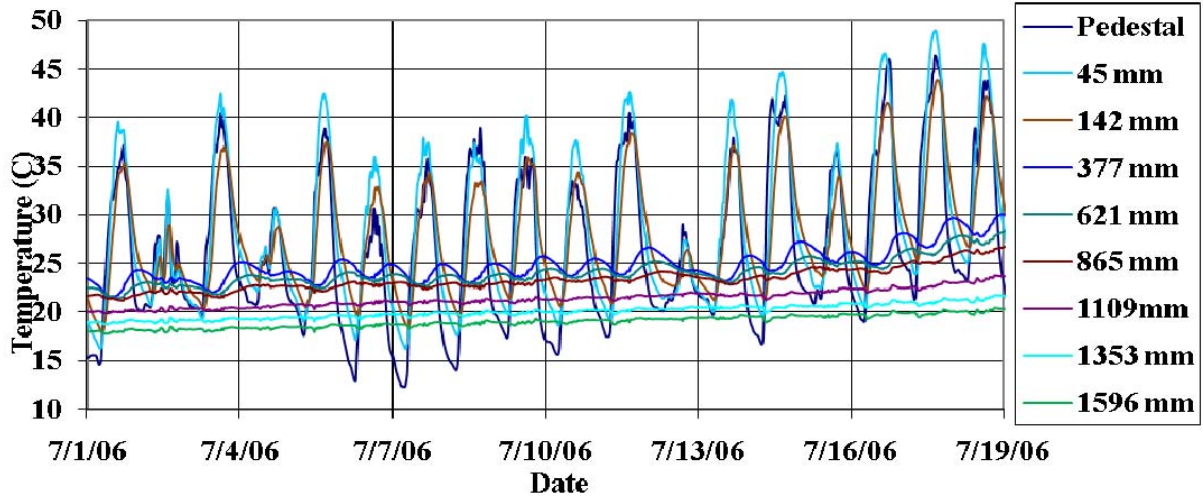
County: Tioga   Highway: SR 6015   Location 2

County: Tioga   Highway: SR 6015   Location 2

F-8

County: Tioga   Highway: SR 6015   Location 2

County: Tioga   Highway: SR 6015   Location 2

County: Warren   Highway: SR 6   Location 2

County: Warren   Highway: SR 6   Location 2
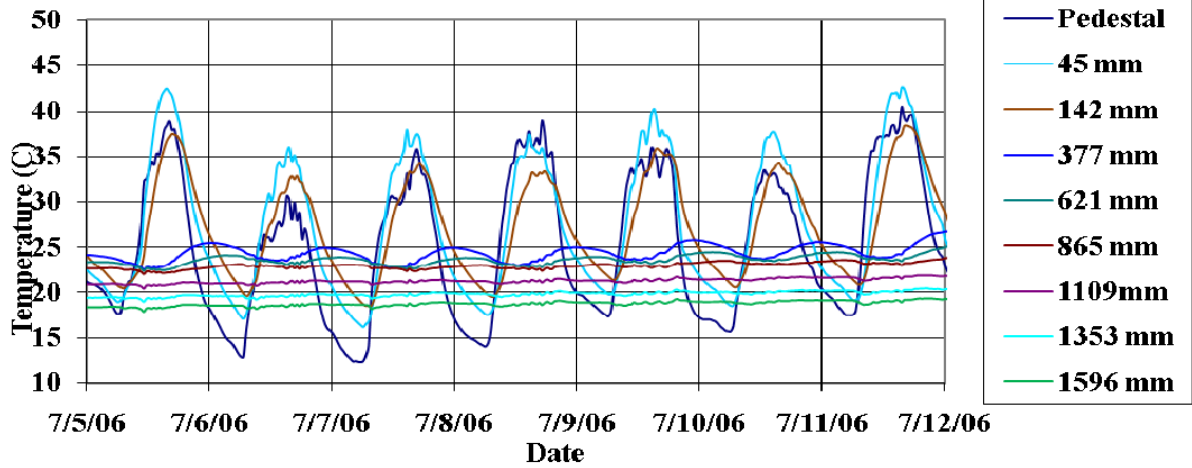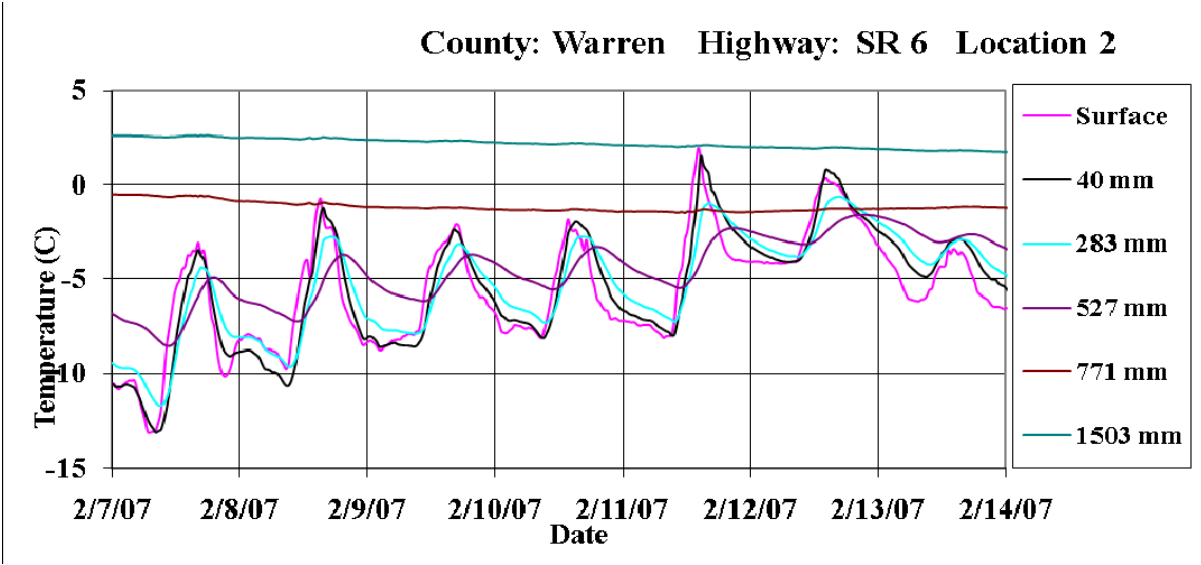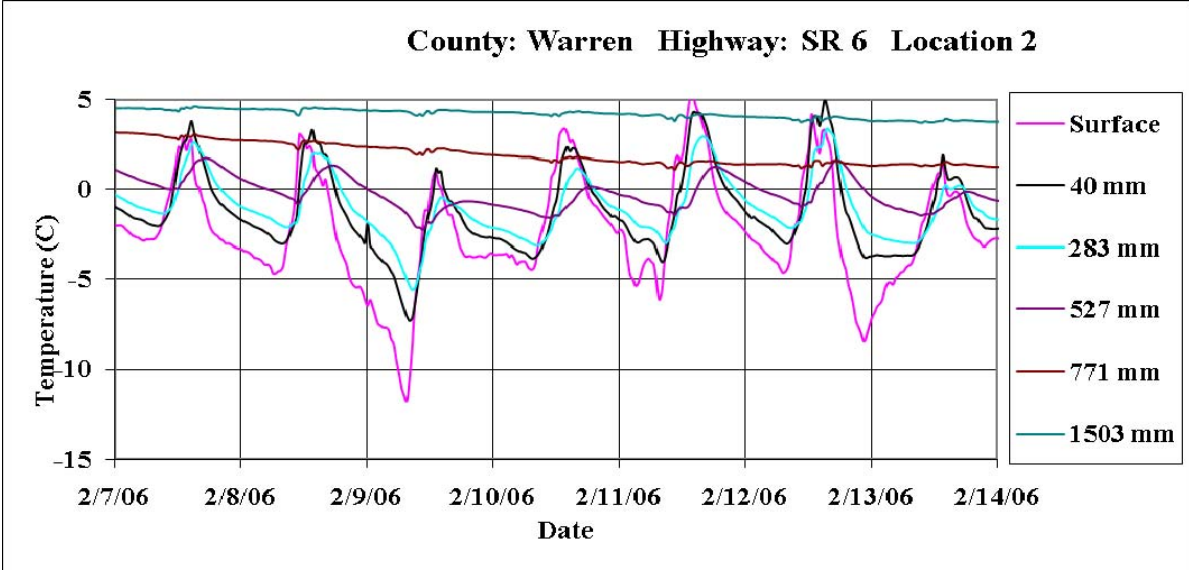
County: Warren   Highway: SR 6   Location 2
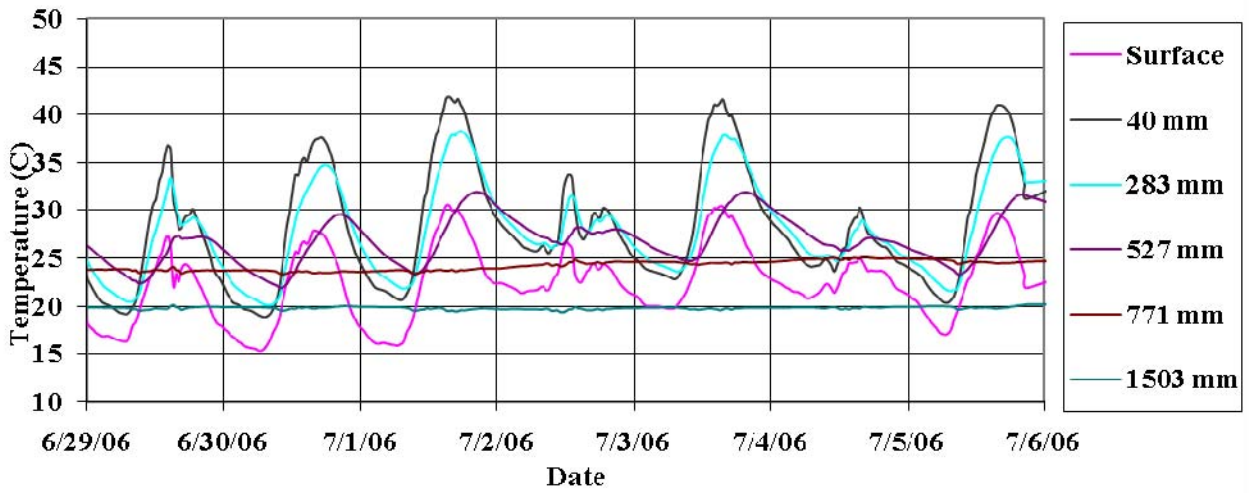
County: Warren   Highway: SR 6   Location 2

Mercer County East - SR 0080, Location 1
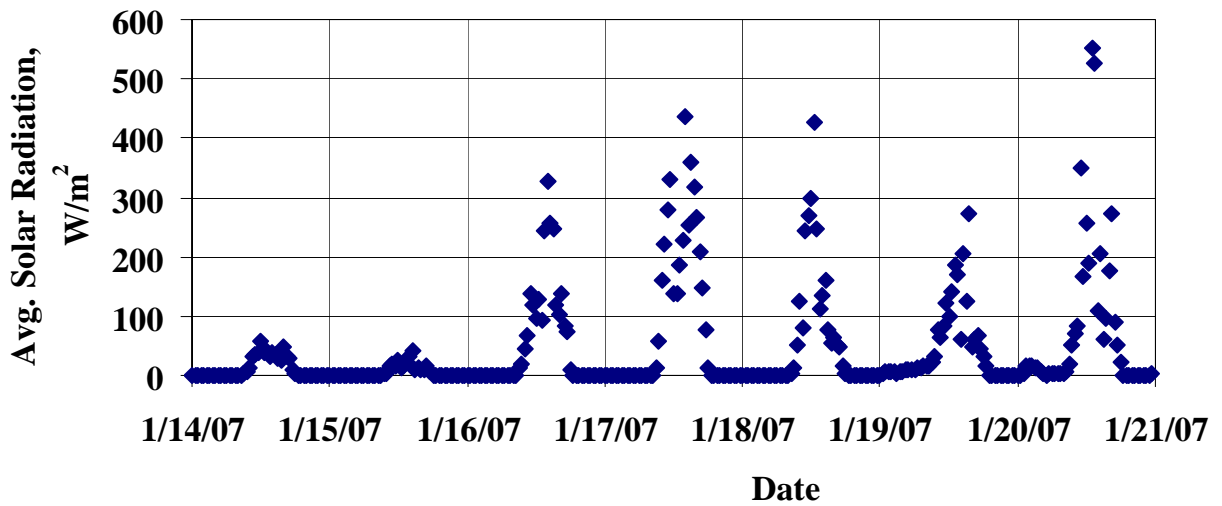
Mercer County East - SR 0080, Location 1

Mercer County East - SR 0080, Location 1

Mercer County West - SR 0080, Location 1

Mercer County West - SR 0080, Location 1

Mercer County West - SR 0080, Location 1

Y-axis: Avg. Solar Radiation, W/m^2; X-axis: January 17, 2007
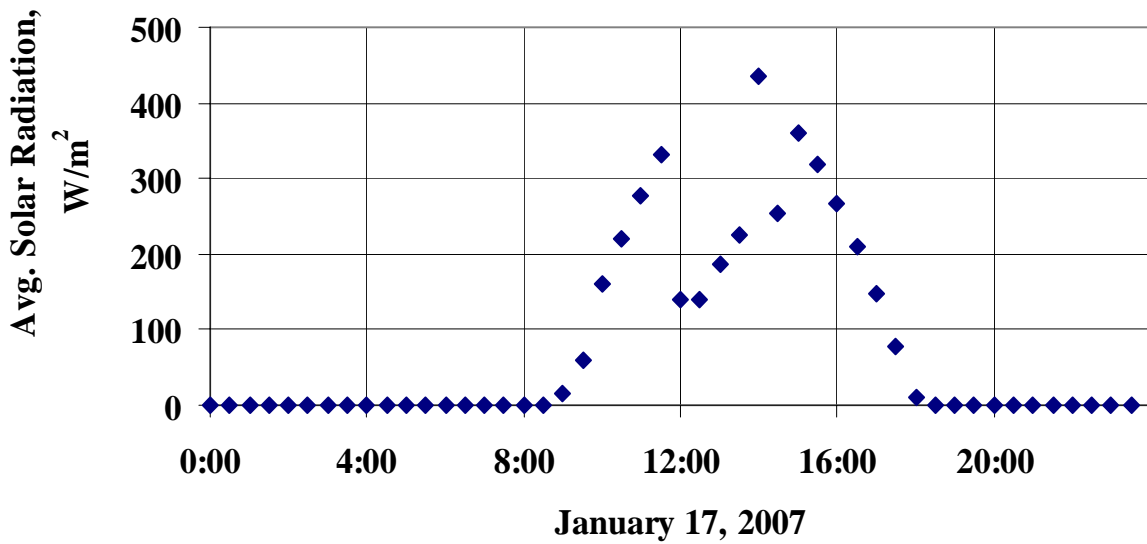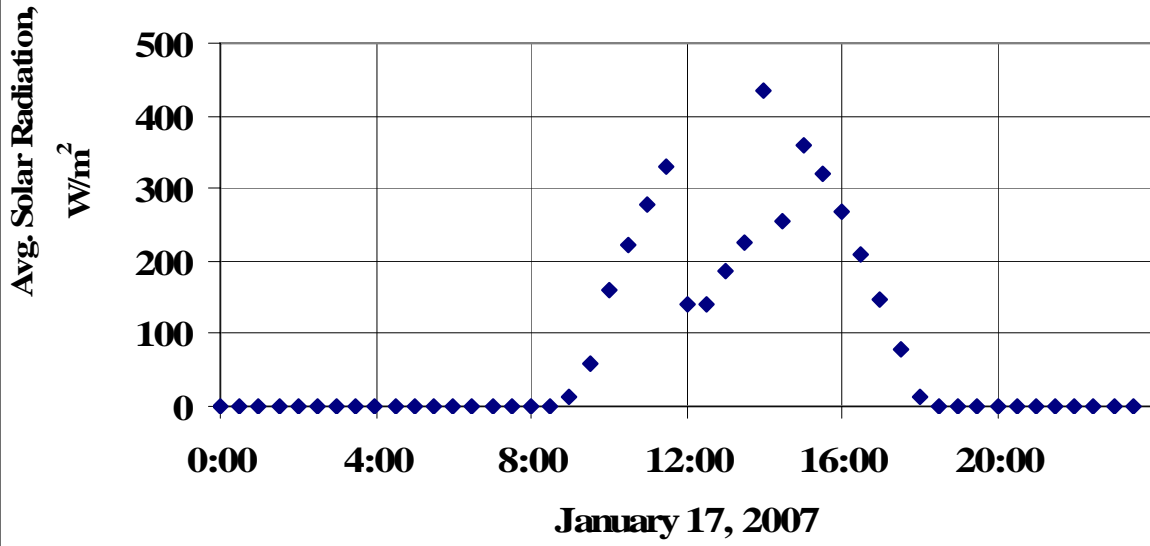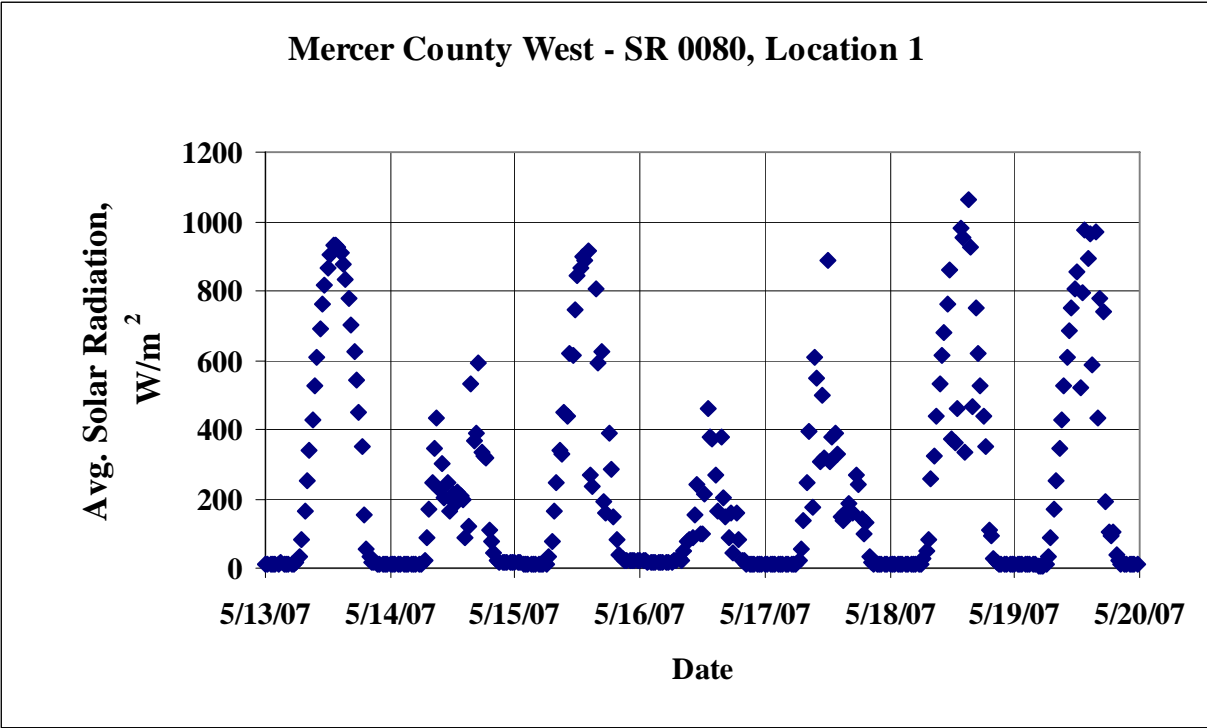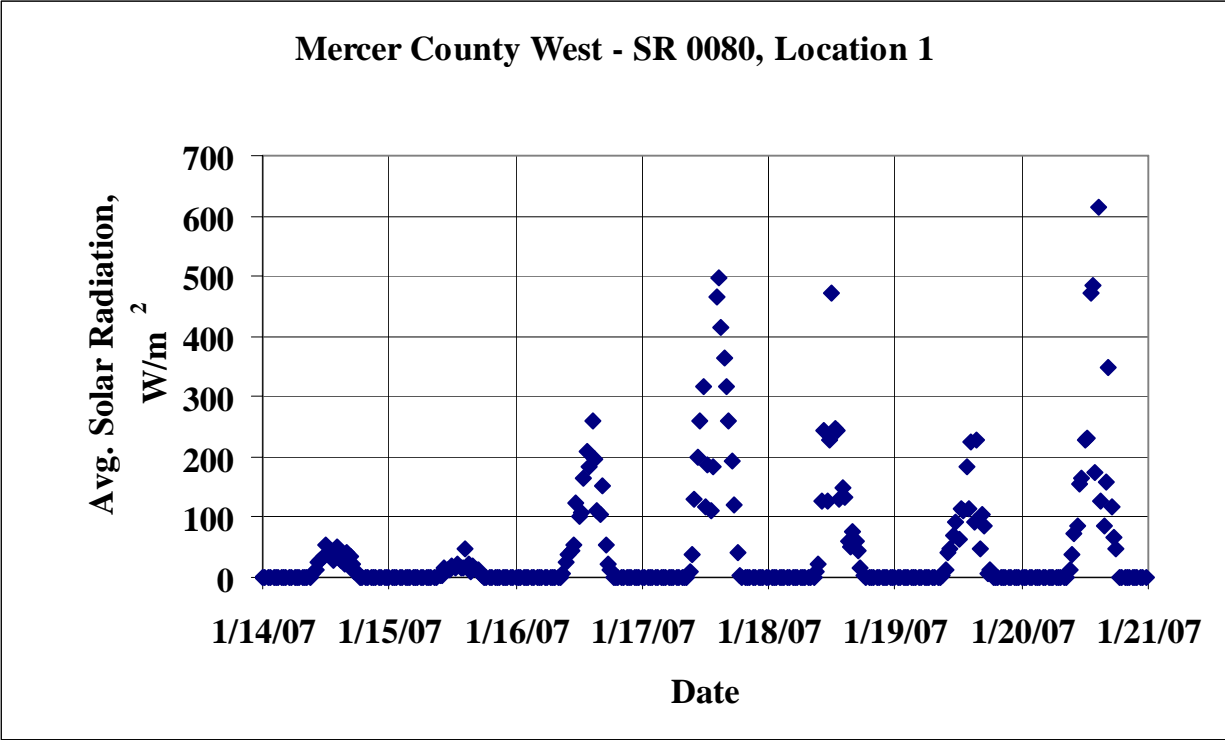
Mercer County West - SR 0080, Location 1

Warren County - SR 0006, Location 2

F-16

Warren County - SR 0006, Location 2

Warren County - SR 0006, Location 2

Warren County - SR 0006, Location 2

June 18, 2008

Warren County - SR 0006, Location 2

September 10, 2008

Delaware County - SR 0202, Location 1

Delaware County - SR 0202, Location 1

Delaware County - SR 0202, Location 1

December 19, 2007

Delaware County - SR 0202, Location 1

June 18, 2008

F-20

Delaware County - SR 0202, Location 1

September 9, 2008

Somerset County - I-76, Location 1

Date

Somerset County - I-76, Location 1

Somerset County - I-76, Location 1

Somerset County - I-76, Location 1

Avg. Solar Radiation, W/m^2

December 20, 2007

Somerset County - I-76, Location 1

Avg. Hourly Radiation, W/m^2

September 17-2007